Regional-scale Modelling of the Occurrence and Dynamics of Rockglaciers and the Distribution of Paleopermafrost

Dissertation
zur
Erlangung der naturwissenschaftlichen Doktorwürde
(Dr. sc. nat.)
vorgelegt der
Mathematisch-naturwissenschaftlichen Fakultät
der
Universität Zürich
von
Regula Frauenfelder
von
Henggart ZH

Promotionskomitee
Prof. Dr. Wilfried Haeberli (Vorsitz & Leitung)
Dr. Martin Hoelzle
Dr. Bernhard Schneider
Dr. Bernd Etzelmüller

Zürich 2004

Abstract

Approximately 5% of the land surface of Switzerland is characterized by mountain permafrost. The most prominent landforms in these areas are, beyond doubt, the numerous rockglaciers[1], i.e. forms of creeping mountain permafrost. In spite of the great advances achieved in permafrost and rockglacier research in recent decades, and the important, detailed knowledge now available on individual rockglaciers, the understanding of intra-regional variability of rockglacier distribution is still rather limited.

This thesis deals, therefore, with issues related to the regional distribution patterns of rockglaciers, in particular talus-derived ones. Special focus is on the process chain that extends from weathering in scree slopes, to rockfall, to accumulation of talus slopes, and finally, to debris displacement by permafrost creep, i.e. to the formation of rockglaciers. Other aspects investigated include relative surface ages of rockglaciers, the exploration of different approaches to modelling regional spatio-temporal rockglacier distribution patterns, and the reconstruction of paleopermafrost distributions at the end of the Lateglacial and the Holocene.

The following four items summarize the investigations carried out:

- Relative age chronologies of six rockglaciers were investigated by photogrammetry, and measurements of Schmidt-hammer rebound values and weathering rind thicknesses on surface boulders. Based on these analyses, conclusions were drawn about the age of contemporaneous Alpine rockglaciers.
- Relationships between terrain parameters and rockglacier parameters were investigated for a sample of 84 rockglaciers by means of statistics in order to answer two main questions: (a) is there a connection between source headwall area (a proxy for debris supply) and rockglacier size, and (b) is rockglacier speed dependent on topographic and/or climatic conditions?
- Potential rockglacier occurrence was modelled using an approach based on the geomorphometric signature of rockglaciers, and a dynamic model was created that allows a 4D simulation of talus-derived rockglacier occurrence, i.e. the modelling of their spatio-temporal development and distribution.

[1] In this thesis, the term "rockglacier" will be written as one word, following the suggestion by Barsch (1988: p. 71) to use the term "rockglacier" as a single word instead of two, as in "rock glacier", in order to emphasize the fact that an independent phenomenon is being dealt with and to clearly make a distinction from (true) glaciers: "[...] the term rockglacier (expressed as one word) is preferred for this feature since, [...], it is part of the periglacial rather than the glacial realm."

– Finally, data obtained from the analysis of relict rockglaciers were used to estimate the depression of the permafrost limit during the Younger Dryas and the 'Little Ice Age' relative to present-day permafrost distribution.

The thesis consists of a manuscript and a collection of five papers; the studies reported on were carried out, for the most part, in a periglacial area of the eastern Swiss Alps.

Zusammenfassung

Ungefähr 5% der schweizerischen Landesfläche befinden sich im Verbreitungsgebiet des alpinen Dauerfrostbodens. Zu den auffälligsten Landschaftsformen in diesen Regionen zählen zweifelsohne die zahlreich vorkommenden Blockgletscher, d.h. Formen des kriechenden Permafrosts. Obwohl in den letzten Jahrzehnten grosse Fortschritte in der Blockgletscher- und Permafrostforschung erzielt wurden und heute wichtiges und detailliertes Wissen über einzelne Blockgletscher vorliegt, ist das Verständnis der intra-regionalen Variabilität des Blockgletscherauftretens immer noch eingeschränkt.

Die vorliegende Dissertation beschäftigt sich daher mit Aspekten, die in Zusammenhang mit dem regionalen Verbreitungsmuster von Blockgletschern stehen, insbesondere derer von Schutthalden-Blockgletschern (sogen. talus-derived Blockgletschern). Ein spezielles Augenmerk gilt dabei der Prozesskette, die mit der Verwitterung von Felswänden beginnt und über Steinschlag und Akkumulation von Schutthalden zur Schuttdislokation durch Permafrostkriechen führt, also zur Bildung von Blockgletschern. Ebenfalls untersucht worden sind das Relativalter von Blockgletscher(oberfläche)n, verschiedene numerische Ansätze zur Modellierung der räumlichen Blockgletscherverbreitung und die Rekonstruktion der Paläo-Permafrostverbreitung am Ende des Spätglazials sowie während des Holozäns.

Konkret wurden folgende Arbeiten durchgeführt:

- Mittels photogrammetrischer Methoden sowie der Messung von Schmidt-Hammer Rückprallwerten und Verwitterungsrinden-Dicken wurde eine relative Alterschronologie von sechs Blockgletschern ermittelt. Anhand der dabei erlangten Resultate konnte das Alter alpiner Blockgletscher abgeleitet werden.
- Die Zusammenhänge zwischen Gelände- und Blockgletscherparametern wurden statistisch an einer Stichprobe von 84 Blockgletschern untersucht. Dabei standen zwei Hauptfragestellungen im Mittelpunkt: (a) Gibt es einen Zusammenhang zwischen der Grösse schuttliefernder Felswände, stellvertretend für die Menge des gelieferten Schutts, und der Blockgletschergrösse? (b) Ist die Geschwindigkeit eines Blockgletschers abhängig von klimatischen und/oder topographischen Faktoren?
- Die potentielle Verbreitung von Blockgletschern wurde mit einem geomorphometrischen Ansatz berechnet und es wurde ein Modell entwickelt, das die Simulation der raum-zeitlichen Entwicklung und Verbreitung von Schutthalden-Blockgletschern erlaubt.
- Schliesslich wurde die Depression der Untergrenze des Permafrosts während der Jüngeren Dryas und der kleinen Eiszeit (in Bezug auf die Höhe der heutigen

Permafrost-Untergrenze) anhand von Messungen an relikten Blockgletschern abgeschätzt.

Die Dissertation setzt sich aus einem Manuskript und fünf Publikationen zusammen. Die Studien, über die berichtet wird, wurden mehrheitlich im Gebiet der östlichen Schweizer Alpen durchgeführt.

Contents

Part I Overview

Part II Papers

The thesis is based on five papers and one chapter containing work unpublished to date. The papers will be referred to in the text by Roman numerals. Please note that they are ordered according to thematic considerations, starting with papers reporting measurements on selected rockglaciers and statistical analyses, followed by papers incorporating the outcome of the former in numerical modelling approaches.

I. **Frauenfelder, R.**, Laustela, M. & Kääb, A. 2005. Relative age dating of Alpine rockglacier surfaces. *Zeitschrift für Geomorphologie N.F.* 49 (2): 145–166.

II. **Frauenfelder, R.**, Haeberli, W. & Hoelzle, M. 2003. Rockglacier occurrence and related terrain parameters in a study area of the Eastern Swiss Alps. *In* Phillips, M., Springman, S. & Arenson, L. (eds.), *8th International Conference on Permafrost, Proceedings* 1, Zürich. Swets & Zeitlinger, Lisse: 275–280.

III. **Frauenfelder, R.**, Schneider, B. & Etzelmüller, B. submitted. Morphometric modelling of rockglaciers – A case study from the Alps. *Earth Surface Processes and Landforms*.

IV. **Frauenfelder, R.** & Kääb, A. 2000. Towards a palaeoclimatic model of rock glacier formation in the Swiss Alps. *Annals of Glaciology* 31: 281–286.

V. **Frauenfelder, R.**, Haeberli, W., Hoelzle, M. & Maisch, M. 2001. Using relict rock-glaciers in GIS-based modelling to reconstruct Younger Dryas permafrost distribution patterns in the Err-Julier area, Swiss Alps. *Norwegian Journal of Geography* 55 (4): 195–202.

A complete list of publications with contributions by the PhD candidate is given on pages 64–67.

List of Figures

List of Symbols

A	rate factor; parameter in Glen's glacier flow law for pure ice
α	slope angle
$\dot{\varepsilon}$	strain rate
F	shape factor; parameter in Glen's glacier flow law for pure ice
g	acceleration due to gravity
ρ	density of rockglacier matrix
h	thickness of rockglacier
n	parameter in Glen's glacier flow law for pure ice
τ	basal shear stress
v	flow velocity
$\overline{v}$	average velocity
$v_{adv.}$	advance rate
C_{melt}	correction term accounting for the reduction of the advance rate due to ice melt at the front of the rockglacier

List of Abbreviations

2D, 3D, 4D	2-dimensional, 3-dimensional, 4-dimensional
a.s.l.	above sea level
BTS	Bottom Temperature of the Snow cover
DEM	Digital Elevation Model
ELA	Equilibrium Line Altitude on glaciers
GIS	Geographical Information Systems / Science
LIA	Litte Ice Age; period of major Holocene glacier re-advances, peaking around the year 1850
RADAR	Radio Detection And Ranging (in radar interferometry)
RRZ	Rockglacier Root Zone
TM	Thematic Mapper (in Landsat TM)
y BP	years Before Present: conventional ^{14}C, uncalibrated
YD	Younger Dryas

Part I: Overview

Chapter 1

Introduction

1.1 Motivation

Many processes in high alpine regions are governed by climate and its variations. The spatial extent of glaciers and of permafrost are two particularly sensitive indicators of climatic change. If atmospheric warming continues as anticipated, it will likely be accompanied by further striking changes in the extent of glaciers and permafrost (cf. Anisimov & Nelson 1996, Haeberli *et al.* 1999a, McCarthy *et al.* 2001).

Alpine glaciers and permafrost react in a sensitive way to atmospheric warming due to their proximity to melting conditions. Glaciers react directly to temperature increases, converting each energy surplus into melting, for example, whereas the response of permafrost to climatic warming is filtered. The reaction occurs through the increase in active layer thickness and melting at the top of the permafrost over periods of years. A warming of the temperature profile within permafrost occurs over the span of decades to centuries. Upward displacement of the base of permafrost to reach a new equilibrium thickness takes centuries to millennia (Osterkamp & Gosink 1991, Burn 1998).

Approximately 5% of the land surface of Switzerland is characterized by mountain permafrost (Keller *et al.* 1998). A better understanding of the impacts of climatic change on high mountain environments has become increasingly important, in particular for the densely populated Alpine region. The thawing of frozen soil and rocks enhances the risk of intensified rockfall activity, debris flows, and landslides that threaten infrastructure, cultivated land and inhabited places. In order to be able to anticipate and quantify the possible impact of forecast climatic change on these mountain regions, it is important to know the current conditions and dominant active processes in these areas. In this context, the study of active, inactive, and relict rockglaciers should help to promote a better understanding of both the paleoclimatic conditions in high alpine regions and the present state of permafrost in general, and rockglaciers in particular.

Rockglaciers are common landforms in alpine periglacial areas, since they are a phenomenon of mountain permafrost creeping (Haeberli 1985). As such, their evolution and existence is controlled mainly by climatic conditions (temperature, precipitation, snow cover) and other additional factors such as, for example, topography and geology. Rockglaciers are composed of an ice-debris matrix, usually with a high debris content of up to 70 % by volume or even more (cf. Arenson 2002). As a consequence, rockglaciers do not disappear completely because their maximum extent is always manifested in the landscape by its remaining debris body, even after complete melt-out of the ice (e.g. during extreme warm phases), unless the rockglacier material was evacuated by glaciers. This latter

situation, however, did not occur in the Alps during the Holocene, since during this period glaciers were, and are, confined to the maximum extents of their Little Ice Age (LIA) re-advances.

Based on results from absolute and relative dating, the surface age of the active rockglacier Murtèl is estimated at 5 to 6 ka (Haeberli *et al.* 1999b). Relative age dating on several other active and relict rockglaciers indicate ages in the same order. This shows that the investigation of these landforms enables the analysis of time periods in the range of centuries to millennia (e.g. Ivy-Ochs *et al.* 1996, and *Papers I, IV, V*). Thus, the topography of a rockglacier reflects the cumulative expression of its entire Holocene history and is a key to its past and present environment. In this way, the decoding of present-day dynamics, morphology and distribution of rockglaciers can provide important information on Holocene climate conditions.

In general, glaciers can be seen as most characteristic of moist-cold environments, while rockglaciers represent rather dry-cold conditions. This is, of course, a simplification because some rockglacier observations are reported from relatively maritime arctic areas as well (Humlum 1998) and glaciers are known to exist also in dry-cold regions (e.g. Tien Shan), but it is true on a global scale. This leads in many places to a spatial separation of rockglaciers and glaciers, enabling the completion of paleoinformation from glacier reconstructions with data derived from rockglacier interpretation. In addition, in areas with fewer glaciers (e.g. dry continental areas) periglacial landforms are often essential for obtaining paleoinformation.

Numerous inventory studies on rockglaciers have yielded valuable information about their characteristics, such as form, geology, extent, location, etc. (e.g. Kirkbride & Brazier 1995, IPA 1998, Lehmkuhl *et al.* 2003). In addition, detailed studies on individual rockglaciers helped to build up a profound knowledge base about these examples (e.g. Humlum 1997, Kääb *et al.* 1997, Berthling *et al.* 1998, Haeberli *et al.* 1999b, Konrad *et al.* 1999, Arenson 2002). Nevertheless, the topographic and climatic controls on rockglacier initiation and growth are still far from being known in detail, and a comprehensive understanding of intra-regional variability of rockglacier distribution is largely lacking.

In the present study, the rockglaciers dealt with are mainly of the talus-derived type (for definitions, cf. *Chapter 2*, p. 8). Thus most explanations in the text refer, by implication, to talus-derived rockglaciers, even if this is not specially mentioned. In passages that relate solely to moraine-derived rockglaciers, the rockglaciers are referred to specifically as such.

1.2 Objectives

The objectives of this study are (a) the investigation and modelling of regional-scale rockglacier distribution and dynamics, in order to better understand rockglacier evolution in general, and (b) the analysis of the implications of the findings relating to the distribution of paleopermafrost. The focus of the study is on:

- the investigation of the regional effects that cause rockglacier abundance or rockglacier scarcity,
- the investigation of the (relative) age structure of rockglaciers,

– the exploration of different approaches to modelling regional spatio-temporal rockglacier distribution patterns, and
– the tentative reconstruction of paleopermafrost distributions for different stages of the ending Lateglacial and the Holocene from rockglacier data.

1.3 Outline of the thesis

The thesis is divided into two parts (see Figure 1.1):

Part I provides an overview of the presented research and consists of six major chapters; this introduction constitutes *Chapter 1*. *Chapter 2* gives an overview of the scientific background of the study, with an outline of the current state of research on rockglaciers (i.e. creeping mountain permafrost), and focuses on the aspects relevant to this thesis. In *Chapter 3*, the methods applied are presented briefly. *Chapter 4* consists of a summary of the main results derived from the publications on which this thesis is based, and one subchapter outlining the results obtained during the project which are not yet ready for submission. All results are discussed in *Chapter 5*; concluding remarks and proposals for future research are formulated in *Chapter 6*.

Part II of this thesis contains a full version of the five papers which comprise the main scientific work.

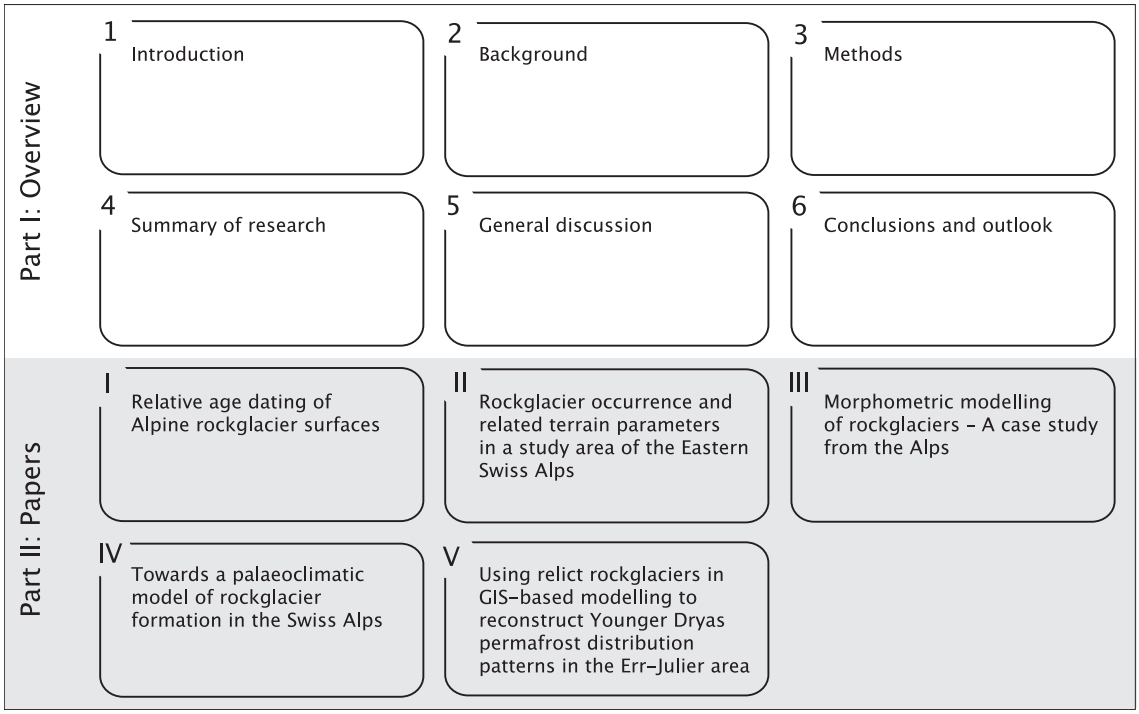

Figure 1.1 *Schematic structure of the thesis, showing the contents of the two main parts 'Overview' and 'Papers'.*

Chapter 2

Background

2.1 Creeping mountain permafrost

Rockglaciers are characteristic and conspicuous large-scale phenomena of creeping frozen material in periglacial high-relief alpine and polar landscapes (see Figure 2.1). They originate from periglacial talus and/or glacier-transported debris, mostly from lateral and terminal moraines.

Rockglaciers result from the internal deformation of interstitial ice, ice lenses or an ice core within coarse debris under the influence of gravity (Payne 1998). Depending on their ice content and their movement, i.e. their activity as debris transport systems, rockglaciers are usually classified into active, inactive and relict forms. According to Barsch (1996): "active rockglaciers are lobate or tongue-shaped bodies of perennially frozen unconsolidated material supersaturated with ice and ice lenses that move downslope [...]." Humlum (2000b) defines them as 20–100 m thick tongue- or lobe-shaped bodies with cascading frontal slopes standing at the angle of repose. The length of rockglaciers may be as much as several kilometres, but the typical length is 200–800 m (Barsch 1996).

Active rockglaciers creep downslope with velocities in the order of cm to dm per year and are thus several orders of magnitude slower than glaciers. Nevertheless, due to their (relatively) large extents they can be seen as efficient debris transport agents (Humlum 2000a). Jäckli (1957) estimated the mass turnover by active rockglaciers in the catchment area of the Rhine river to be in the order of $18*10^6$ m^3a^{-1}, or in horizontally shifted mass: $8.5*10^9$ $mkga^{-1}$. Barsch (1977) estimated the horizontal mass transport by active rockglaciers for the entire Swiss Alps to be in the order of 400 to $650*10^9$ $mkga^{-1}$.

Inactive rockglaciers have a form similar to active rockglaciers and contain an ice core as well. However, this ice is not in equilibrium with the prevailing climatic conditions, it is melting. As a consequence, the total volume of the rockglacier decreases, the inner friction of the ice-debris matrix rises, and movement diminishes towards zero (Imhof 1994).

Relict rockglaciers are free of ice and, therefore, no longer creep. Their forms often show signs of collapsing, their fronts and sides are flatter than the angle of repose, and they may have some alpine vegetation, sometimes including dwarf shrubs and even small trees.

Due to their peculiar appearance, rockglaciers were described already in the first decades of the 20th century (e.g. Capps 1910, Chaix 1919, Brown 1925). With the exception of the seminal work by Wahrhaftig & Cox (1959) the systematic investigation of rockglaciers and permafrost did not start until the mid-1970s, however. During this period the interest in rockglaciers grew steadily and the number of papers dealing with this phenomenon

increased significantly (e.g. Osborn 1975, Fisch sen. *et al.* 1977, Barsch *et al.* 1979, Johnson & Nickling 1979, White 1979).

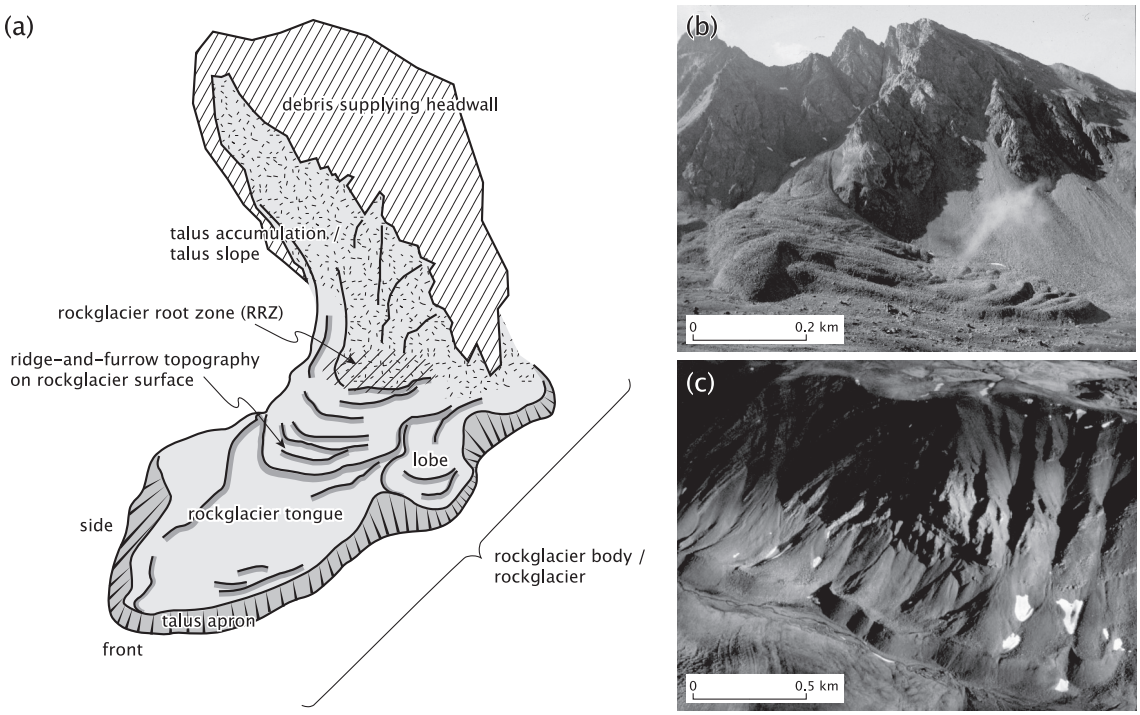

Figure 2.1 *(a) Schematic plot of a talus-derived rockglacier, using the main expressions found in the following chapters, (b, c) two examples of active rockglaciers: (b) Muragl rockglacier in the Upper Engadine, Eastern Swiss Alps (photograph by R. Frauenfelder), (c) rockglaciers at Nordenskiöldkysten, Svalbard Archipelago (photograph by A. Kääb).*

The origin of rockglaciers is the subject of intense debate. Some authors claim a general periglacial origin for rockglaciers, and attribute flow mainly to the internal deformation of ice-rich lenses within permafrost (e.g. Jäckli 1957, Wahrhaftig & Cox 1959, Barsch 1996). Other authors argue that many rockglaciers contain a significant core of glacier ice, and have been formed through its deformation (e.g. Outcalt & Benedict 1965, Humlum 1982, Whalley & Martin 1992). And some authors provide explanations involving gradual changes, a continuum of forms or two (perhaps more) alternative models according to different formative conditions (e.g. Washburn 1979, Haeberli & Vonder Mühll 1996).

A long-standing discussion on rockglacier origin, internal structure, rheology and nomenclature has sprung from this diversity, but it is not the subject of the present work. In the given context, only the terms 'talus-derived' rockglaciers and 'moraine-derived' rockglaciers will be used. The term 'talus-derived' is applied to rockglaciers that originated primarily from periglacial talus. The term 'moraine-derived', in contrast, is used for rockglaciers that developed from glacier-transported debris, mostly out of lateral and terminal moraines (see above). It should be clear, however, that permafrost conditions, i.e. negative ground temperatures throughout the year, are considered a crucial pre-requisite for the long-term maintenance of whatever form of ice contained in a rockglacier (see also Haeberli 2000).

2.2 Controls on rockglacier distribution

Although the understanding of rockglacier formation processes is far from complete, it is generally accepted that several conditions must be fulfilled in order for a rockglacier to form. As seen in Figure 2.2 ①, there must exist (a) a headwall composed of weathering-susceptible rock, (b) a relief permitting the accumulation of talus, (c) a climate cold enough to allow the build-up and preservation of ground ice (super-saturation) over the typical time scales (millennia) and dry enough to inhibit the formation of glaciers, (d) hydrological and lithological preconditions that allow the formation of a cohesive debris-ice matrix, and (e) the thickness of accumulated talus and the slope angle must be sufficient to generate the shear stress that causes deformation. To enable the further development of an initiated rockglacier (see Figure 2.2 ②), ground temperatures must remain in a range enabling flow, and talus thickness has to be maintained by (continuous) debris supply (mass conservation). The inactivation and subsequently the relictification of a rockglacier (see Figure 2.2 ③) are caused by either climatic or dynamic inactivation processes:

– Climatic inactivity: melting of the ice due to the upward shift of the lower permafrost limit or melting of the ice due to movement of the rockglacier into non-permafrost areas;
– Dynamic inactivity: slope angle below threshold and/or reduction in debris supply and/or decreasing incorporation of ice into the system.

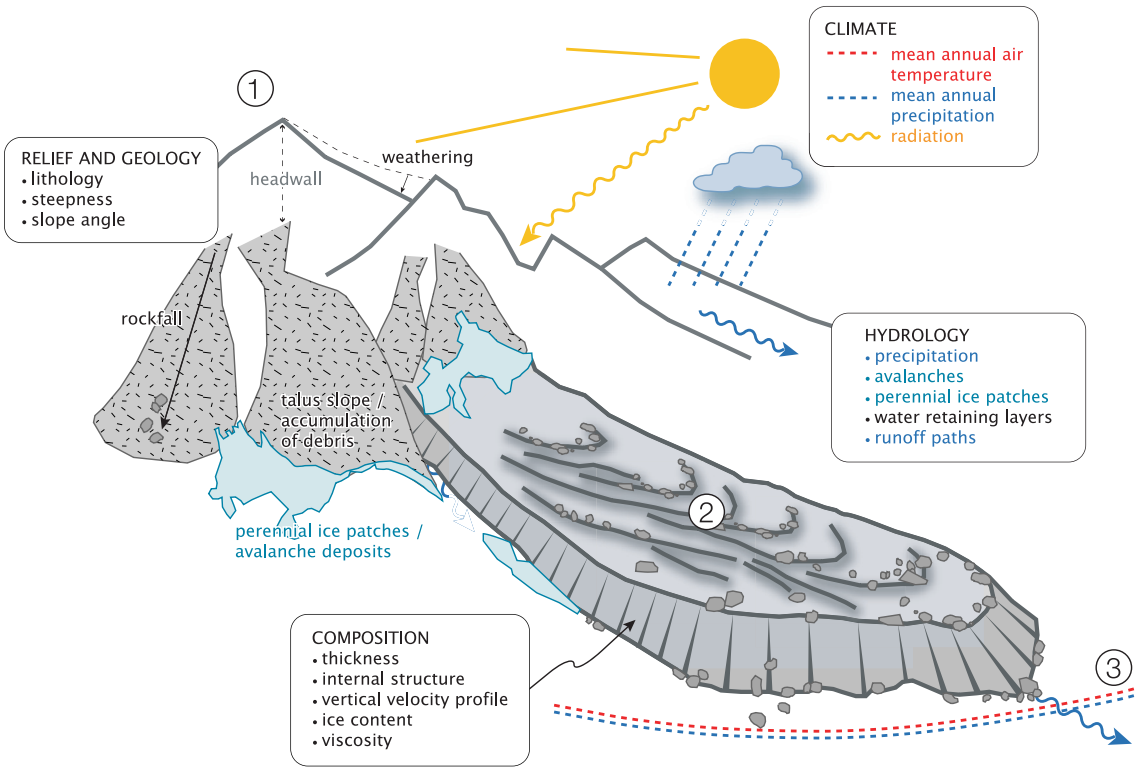

Figure 2.2 *Qualitative sketch of important boundary conditions for: ① the initiation, ② the growth, and ③ the inactivation/relictification of a talus-derived rockglacier. See text for further explanations.*

In both cases, the reaction of the rockglacier is governed by a considerable thermal inertia caused by the rockglacier's own characteristic microclimate. Due to this thermal inertia, the interior of a rockglacier can maintain its low temperature for a considerable period of time even under unfavourable thermal conditions. Thus a rockglacier does not melt immediately when it exceeds the limits of permafrost, and the time lag between this moment and the total melt-out of the ice can be in the order of decades or centuries.

2.2.1 The influence of relief, geology and water

2.2.1.1 Relief and geology

For a rockglacier to form, there must be a supply of rock debris which is sufficient to trigger and maintain its development. This debris has two main sources: (1) talus deposits that owe their existence to the mechanical weathering of rock faces under periglacial conditions, and to periodical rockslides, debris flows and/or debris transport by avalanches (→ talus-derived rockglaciers), and (2) moraine deposits from the Lateglacial and the Holocene (→ moraine-derived rockglaciers).

The geology of the headwall affects the rate and intensity of weathering, which in turn determines the amount of debris available of a size suitable for the formation of rockglaciers. In this sense, one speaks of a geological control on the distribution of rockglaciers (e.g. Wahrhaftig & Cox 1959). Luckman & Crockett (1978) describe how this geological control acts on two levels: "firstly, large-scale structural and lithological controls [...] partially determine the availability of suitable sites for rockglaciers. Secondly, [...] the bedding and structural characteristics of individual lithologies control the size and nature of weathered debris [...]". Generally, areas characterized by crystalline rock types or certain limestones (weathering into coarse blocky fragments) show an abundance of rockglaciers, while areas with a dominance of rock types weathering into fine-grained material (e.g. shale, schist, certain dolomites) have fewer rockglaciers (e.g. Wahrhaftig & Cox 1959, Luckman & Crockett 1978, Chueca 1992). In *Section 5.1.1*, consequences of these findings are discussed together with this author's results on the influence of relief parameters and lithology on the distribution of rockglaciers (see also *Paper II*).

As mentioned above, the rate of debris input is critical for rockglacier formation. Debris input itself is controlled by climate-dependent weathering or episodic events. Frequent (or continuous) weathering results in pebbles or fine debris. Seasonal weathering follows annual freeze-thaw cycles, produces larger blocks and is influenced by snow avalanching and heavy rains. One large seasonal event can equal or by far exceed mean annual rock wall retreat rates. Episodic events (e.g. rockslides) are set off by geological failures due to endogenic parameters or exogenic processes, such as permafrost melting, glacier retreat, earthquakes, etc. (N. Matsuoka, personal communication, 2001).

When modelling rockglaciers over longer time periods (e.g. the Holocene, see *Section 4.2*), the fact that rockglaciers react after individual time lags to changes in climate and/or debris supply rates must be taken into account. The order of the time lag depends on factors such as the initial size of the rockglacier, its temperature, its location, etc. Olyphant (1987) modelled such lag times based on a model of pure deformation (no sliding or basal shearing). His results suggest, for instance, that a 500 m long rockglacier may take over 400

years to react to an increase in debris supply. For a longer rockglacier this time lag would be correspondingly greater.

2.2.1.2 Water

The formation of rockglaciers is linked with the hydrology in debris slopes. In mountainous terrain, the availability of water is spatially and temporally heterogeneous. The assumed influences of water on the formation of rockglaciers are manifold and involve processes such as the dislocation of fine-grained material from the surfaces of talus slopes and rockglaciers into lower-lying layers, the build-up of (interstitial) ice, energy exchanges during freeze-/thaw-cycles, etc.

Studies on rockglacier hydrology have been focused mostly on the importance of rockglaciers as water reservoirs within high-mountain hydrological systems (e.g. Corte 1976, Barsch 1996, Gardaz 1998, Schrott 1998). Little is known, to date, about the role of water itself in the formation of rockglaciers. The variability of the water content in debris slopes, the existence of water retaining layers, etc., would be important parameters for investigation, but have not been analyzed in the present study.

2.2.2 Climate as a limiting factor

On a *global* scale the distribution of glaciers and permafrost is often explained on the basis of the cryosphere model (see Figure 2.3). This simple model shows that the global distribution of glaciers and permafrost – and thus the occurrence of associated phenomena such as, for example, the rockglaciers discussed in this study – depends, for the most part, on the mean annual air temperature (MAAT) and the mean annual precipitation (P).

Haeberli (1985) states that active rockglaciers exist above the lower boundary of permafrost distribution and where the precipitation is too low to allow the formation of glacier ice, i.e. below the equilibrium line of glaciers (ELA). The ELA of glaciers can occur below the lower boundary of permafrost in humid regions with abundant precipitation, and, in extreme cases, is even below the 0°C MAAT-isotherm. The ELA rises with decreasing precipitation and crosses (according to the cryosphere model) the lower boundary of permafrost at approximately 2500 mm precipitation.

The course of the lower boundary of (discontinuous) permafrost distribution in mid-latitude alpine regions is often approximated by the -1° to -2°C mean annual air temperature isotherm (Guodong 1983). Its actual course, however, is strongly dependent on radiation effects and snow cover conditions, because the amount of energy available for transfer into the ground is dependent on the energy balance at the surface. In the Alps, the regional variability of radiation is very strong (due to differences in aspect, slope and horizon) and radiation is, therefore, an important factor for the determination of the permafrost distribution pattern on a *regional* to *local* scale (e.g. Guodong 1983, Hoelzle 1996, Etzelmüller *et al.* 2001b, Hoelzle *et al.* 2001, Marchenko 2001, Stocker-Mittaz 2002).

On a *local* scale, the importance of the seasonality of the snow conditions (thickness, depletion history, etc.) increases greatly: near-surface characteristics (albedo, roughness, etc.) are responsible for the actual heat transfer into the subsurface layers, i.e. into the active layer, and subsequently, into the permafrost body of the rockglacier (e.g. Raymond 2001, Hanson & Hoelzle 2003).

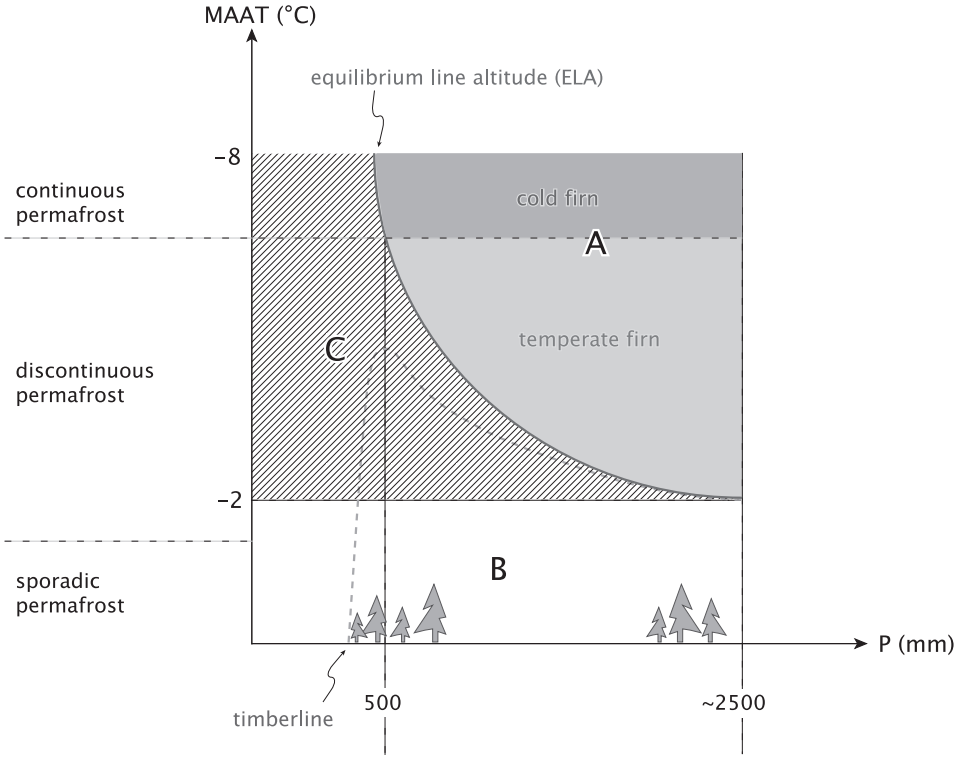

Figure 2.3 *Schematic diagram of the cryosphere by Shumskii (1964), modified after Haeberli (1990) and Haeberli & Burn (2002). MAAT = mean annual air temperature in °C, P = mean annual precipitation in mm, A = accumulation zone of glaciers, where debris cannot accumulate significantly, B = zone without permafrost, where debris can accumulate, but is not perennially frozen, C = potential zone of rockglacier formation, where debris can accumulate and can be perennially frozen.*

Humlum (1998) compared precipitation and temperature ranges of rockglacier sites and continental, periglacial sites without rockglaciers. He showed that the typical rockglacier climate is not a purely continental one (see above), but rather a dry to moderately humid climate with regional annual precipitation not exceeding approximately 1700 mm, and cool summers with a mean summer air temperature below 5° to 6°C. His findings are supported by rockglacier occurrences in Iceland (e.g. Martin *et al.* 1994, Whalley & Martin 1994), Svalbard (e.g. Sollid & Sørbel 1992, André 1994) and Greenland (e.g. Humlum 1982). Upon comparing precipitation values and temperatures given by Haeberli (1985) and Humlum (1998) it becomes clear, however, that the argued difference in the understanding of the term 'maritime' is more a question of nomenclature than of semantics.

2.2.3 Lateglacial and Holocene climate in the study region[2]

During the maximum stage of the Lateglacial (about 20,000 y BP) the entire region of the Upper Engadine was part of a major dome within the accumulation zone of Ice Age

[2] This section is compiled from studies by Maisch (1995), Roberts (2000), Maisch *et al.* (2003), and Labeyrie *et al.* (2003). Ages in y BP refer to conventional ^{14}C, uncalibrated years before present (cf. List of Abbreviations, p. viii).

glaciers. These glaciers received precipitation predominantly from mediterranean sources in the south and flowed in various directions (cf. Florineth 1998). Only ridges above ca. 2600 to 3000 m a.s.l. protruded from the firn surface as nunataks. Deep penetration of subglacial permafrost, especially on valley slopes, and conditions of continuous mountain permafrost on ice-free ridges and summits must be assumed.

During the final stages of the Lateglacial (ca. 17,000–10,000 y BP) temperatures increased and rapid deglaciation began. This general warming was interrupted by climatic oscillations, the first one ending around 13,000 y BP known as the 'Oldest Dryas' cold phase. A partial return to warmer conditions followed until around 11,000 y BP. After that the rapid stepwise onset of the intensely cold Younger Dryas period took place and lasted until shortly before 10,000 y BP. At that time the Younger Dryas ended suddenly over a few decades and the climate shifted back to relative warm and moist conditions.

A general warm period followed, with temperatures peaking during the middle Holocene between 8000 and 5000 y BP. Cooler conditions followed this early-to-mid Holocene warm period and permafrost became more widespread. Between 1550 and 1850 AD, a period known as the 'Little Ice Age' (LIA), temperatures were about 1°C cooler than at present.

Parts of the valley floors and most of the modern periglacial belt in the Engadine were last covered by glaciers during the early Younger Dryas cold event. Since that time, post-glacial activity has been limited to re-advances of valley glaciers within the limits of the LIA moraines and the appearance/disappearance of glacierets. Decrease in glacier size was accompanied by an increase in the relative importance of discontinuous permafrost and periglacial debris, favouring rockglacier development. Periglacial activity is thought to have been one of the predominant landscaping factors in the area during the last several thousand years.

Chapter 3

Methods

This chapter gives a brief summary of the main measurement techniques and numerical modelling methods applied in the study.

3.1 Field measurements with the Schmidt-hammer

The Schmidt-hammer is a portable instrument originally developed in the early 1950s to measure the surface hardness of concrete by recording the rebound of a spring-loaded bolt impacting a surface (Schmidt 1950). In geomorphology, the Schmidt-hammer is used to determine the rock hardness, and thus, the weathering degree of rock surfaces in the field, and has been successfully applied for relative age dating of moraines (e.g. Matthews & Shakesby 1984, Winkler & Shakesby 1995, Rune & Sjåstad 2000), rockfall deposits (e.g. Nesje *et al.* 1994) and debris flow deposits (e.g. Lippert 2001).

Rock hardness, as reflected by hammer rebound values (R), is a function of the inherent intact rock strength. Weathering generally decreases rock strength and this is reflected in the measured surface rebound values (Sumner & Nel 2002).

The principle of the instrument is quite simple: a light-weight steel hammer, free to move in a tubular frame, is drawn against a spring tension by means of a trigger. The base of the frame is firmly pressed against the rock surface, and when the hammer is fully drawn, the trigger is released, allowing the fully-extended spring to drive the hammer against the rock (Schmidt 1951). In modern instruments, the rebound value is then readable from the display of the accompanying storage module.

In this study, the results of the Schmidt-hammer measurements were compared to measurements of weathering rind thicknesses from Laustela *et al.* (2003) and discussed together with the age estimates derived from photogrammetrical streamline interpolations (see *Paper I*).

3.2 Velocity measurements and streamline interpolations

By using digital photogrammetry, multi-temporal digital elevation models (DEMs) are derived from overlapping digital aerial photography using the commercial photogrammetric software SOCET SET (LH Systems, San Diego, California, USA). Multi-temporal orthophotos are computed on the basis of these DEMs and the aerial photographs. The special photogrammetric software CIAS (= Correlation Image Analysis, © by Kääb & Vollmer (2000)) then permits the derivation of horizontal displacements of

individual terrain features from such multi-temporal digital orthophotos. For details on the methodology refer to Kääb *et al.* (1997, 1998), and Kääb & Vollmer (2000).

The age structure of a rockglacier can be assessed from streamlines interpolated from its surface velocity field (e.g. Kääb *et al.* 1997, Kääb *et al.* 1998). Assuming steady-state conditions, these streamlines represent the trajectories of specific particles on the surface. Thus, time or age of the surface can be integrated for the path of particles along such streamlines. This allows for both relative and absolute rockglacier age estimates (see *Paper I*). Since flow velocities rise from zero to current values during the initial stages of rockglacier development, and temporal variations in velocity are likely to exist also during the 'life span' of a fully developed rockglacier, photogrammetrically determined ages are minimum rather than maximum values (Haeberli *et al.* 2003).

3.3 Morphometrical terrain analysis

Geomorphometry, the application of morphometry (i.e. the measurement of shape) to the earth's surface, provides an aid for quantitatively describing the form of the topography. This description of the land surface promotes better understanding of landscape development and landform formation at different temporal and spatial scales (Fredriksen *et al.* 1985). Chorley (1957) defined geomorphometry as the science "which treats the geometry of the landscape". Systematic descriptions of the characteristics of surface forms date back to the co-founders of academic geography, Alexander von Humboldt (Humboldt 1808ff., 1817) and Carl Ritter (Ritter 1852a, 1852b). The field was revolutionized late in the 20th century by the development of computer technology, mass production of grid-based DEMs, and image processing technology, among others (Pike 1995). Recent promotion of the method has occurred mainly through the works of Evans (1972), Mark (1975), and Pike (1995, 2000). Today, morphometric procedures are implemented routinely in commercial geographic information systems (GIS) as well as in specialized software (Pike 2002).

The method of geomorphometry is based on the quantitative analysis of topographic characteristics expressed in topographic parameters, and builds upon the basic assumption that a close relationship between surface processes and particular topographic characteristics exists. The topographic attributes related to this concept are normally estimated on the basis of altitude matrixes. Comprehensive compilations of topographic attributes to be computed from DEMs are given in Moore *et al.* (1990) and Wilson & Gallant (2000). Concepts of the semantics of landform modelling were reviewed, for example, by Dikau (1988), Dehn *et al.* (1999), and Schmidt & Dikau (1999).

Geomorphometry has been applied successfully in the field of glaciology (e.g. Etzelmüller & Sollid 1997, Sulebak *et al.* 1997, Hagen *et al.* 2000, Etzelmüller *et al.* 2001a) but, to the author's knowledge, has not been applied before to quantify rockglacier distribution.

3.4 Permafrost distribution modelling

Permafrost distribution modelling in this study has been carried out using the program code of Hoelzle (1996). The original model for predicting mountain permafrost distribu-

tion was developed in the mid-1970s on the basis of several geophysical methods as well as on the morphological description of creeping permafrost bodies, natural outcrops, surface characteristics (vegetation, surface roughness) and the analysis of active-layer temperatures, temperatures of water in springs and bottom temperatures of the snow cover (BTS) (Haeberli 1975).

Permafrost as well as the BTS are functions of the mean annual surface temperature (MAST) and therefore a result of the entire energy balance at the surface. Hoelzle (1992) found that permafrost can be represented using a statistical relation between BTS measurements, MAAT and potential direct solar radiation. Based on this relation, the model PERMAMAP was implemented in the GIS system Arc/Info (Hoelzle 1994, 1996). In contrast to the original model by Haeberli (1975), PERMAMAP allows the detection of permafrost occurrences at low altitudes (for instance in extremely shaded areas) but does not, on the other hand, take into account slope foot areas. The model distinguishes between two permafrost classes: 'probable permafrost' and 'no permafrost'. The program was developed for estimation of the permafrost distribution on a regional scale and needs a DEM as the main input.

Although the permafrost model itself is a static model without any feedback mechanisms, i.e. it describes a state at a specific instant in time, the program allows the simulation of general past and future permafrost distribution patterns. This is done by introducing a decrease/increase of the MAAT and correspondingly a lowering/rising of the local limit of permafrost distribution through a 'climate factor' (Hoelzle & Haeberli 1995).

3.5 Dynamic modelling

Dynamic modelling builds upon static modelling, such as the permafrost modelling approach described above, by incorporating the time component (e.g. Van Deursen 1995, Wesseling *et al.* 1996, Karssenberg 2002).

A dynamic model describes, thus, how a parameter system can transform from one qualitative state into another. Each qualitative state is described by a static model. The dynamic spatio-temporal behaviour of the system is modelled as an interaction between spatial and temporal processes. The word 'spatial' refers to the geographic domain which the model represents (i.e. the two- or three-dimensional space), while 'temporal' refers to simulated changes through time by using rules of cause and effect (Lundell 1996).

The model that is designed in the present study (*Section 4.2*) is based on the approach of cellular automata (Von Neumann 1966). Cellular automata are dynamical systems in which space and time are discrete. A cellular automaton consists of a regular grid of cells, each of which can be in one of a finite number of k possible states, updated synchronously in discrete time steps according to a local, identical interaction rule. The state of a cell is determined by the previous states of a surrounding neighbourhood of cells (Sipper 1997).
The presented 4D model allows the numerical simulation of the spatial and temporal evolution of rockglacier occurrence and was tested for the region of the Upper Engadine. The time scale considered encompasses the entire Holocene (i.e. the last 10,000 years) but can also be extended into the future or further back into the past (i.e. the Lateglacial).

Chapter 4

Summary of research

4.1 Summary of papers

I **Frauenfelder, R.**, Laustela, M. & Kääb, A. 2005. Relative age dating of Alpine rockglacier surfaces. *Zeitschrift für Geomorphologie N.F.* 49 (2): 145–166.

This paper discusses the application of photogrammetry, and the measurements of Schmidt-hammer rebound values and weathering rind thicknesses for relative age dating on six rockglaciers in the Swiss Alps.

Rockglaciers are formed by the continuous deformation of ice-rich debris material, with the result that the age of the surface becomes greater along the flowlines from the root zone to the rockglacier front. This can be demonstrated by applying both the Schmidt-hammer rebound values (which diminish as weathering, or duration of surface exposure, increases) and the weathering rind thicknesses (which grow as weathering increases). The results of these two methods correlate well with chronologies estimated from photogrammetric streamline interpolations. They indicate that the minimum surface age of the investigated rockglaciers is between 3 and 5 ka, and that the age of the surface does, indeed, increase along flowlines from the top towards the front.

Four of the investigated rockglaciers presumably started to evolve shortly after the fast glacier decay at the end of the YD, i.e. during the early phases of the Holocene, or alternatively, after the early-to-mid Holocene climate optimum (8000 to 5000 y BP). Before this time, the areas where these rockglaciers are located today were glacierized. This suggests, furthermore, that the debris material from which the rockglaciers developed may have been partly reworked and pre-transported by glaciers. In contrast to this, two of the investigated rockglaciers (an inactive and an active one) theoretically could have been active already at the end of the Lateglacial because their locations seem to have been ice-free during that time.

II **Frauenfelder, R.**, Haeberli, W. & Hoelzle, M. 2003. Rockglacier occurrence and related terrain parameters in a study area of the Eastern Swiss Alps. *In* Phillips, M., Springman, S. & Arenson, L. (eds.), *8th International Conference on Permafrost, Proceedings* 1, Zürich. Swets & Zeitlinger, Lisse: 275–280.

In this study, the relationship of terrain parameters (rock wall extent, geology, etc.) and rockglacier parameters (size, slope, velocity, etc.) is analyzed statistically. Two main questions are addressed: (a) is the extent of a rockglacier (used as a proxy for volume) dependent on the size of its source headwall area (used as a proxy of debris supply), and (b) can topographic or climatic controls on rockglacier speed be identified by statistical analyses of terrain derived parameters? To explore these questions two empirical data sets containing information on 84 and 44 rockglaciers, respectively, are used.

The main conclusions can be summarized as follows:
- The relative size of contemporaneous rockglaciers are, to a certain extent, controlled by the area of the source headwall, but the relation is complex and involves factors such as cliff recession rates (as a function of geology, temperature, water content, etc.) and subsequent talus input variations.
- Talus-derived rockglaciers are more closely related to their debris-supplying headwalls than moraine-derived rockglaciers. The former are part of a direct process chain linking frost weathering, rockfall, and debris displacement by permafrost creep. For the latter, an additional, both spatially and temporally complex transport module (including the whole glacier history) is involved in the process chain. A moraine-derived rockglacier is not fed primarily by continuous debris input but evolves out of an already existent debris 'reservoir'. The characteristics of this debris are significantly different from the original, weathered material accumulated before glacial transport.
- Flow velocities appear to exert an important influence on rockglacier length, and seem to depend on temperature conditions. Mean annual air temperature at the rockglacier front (introduced as a rough proxy for the temperature of the permafrost) shows an exponential relationship to maximum surface velocity.
- The insignificant influence of slope on rockglacier length points to the fact that the thickness of the accumulating and deforming ice/rock-mixture might be less dependent of stress controls than generally assumed: with a constant basal shear stress and a given volume of frozen debris, thickness would decrease and length correspondingly increase with increasing slope – a relation which is not found in the analyzed data.

In conclusion, spatial variations in thermo-dynamic conditions and/or in internal structure may predominate over effects from stress-related geometry (slope-dependent thickness), and other variables must significantly influence rockglacier transport rates. Examples are (a) the vertical velocity profile including deformation rates, thickness, internal structure with stiff layers or sliding processes at depth, shearing within the permafrost, etc., and (b) variable ice content.

III **Frauenfelder, R.**, Schneider, B. & Etzelmüller, B. submitted. Morphometric modelling of rockglaciers – A case study from the Alps. *Earth Surface Processes and Landforms*.

The present study seeks to evaluate and advance existing knowledge of regional rockglacier distribution, especially the understanding of their spatio-temporal variability, by the application of numerical modelling. The focus hereby is on the distribution of talus-derived rockglaciers.

The occurrence of talus-derived rockglaciers is governed primarily by climatic and topographic preconditions. Therefore, they are found in areas characterized by specific topographic attributes:

- they occur within a certain altitudinal band (due to the prevailing influence of mean annual air temperature),
- their formation is favoured on certain aspects (due to differences in incoming radiation),
- they are found in locations with particular slope values (flow of the ice-debris mixture must be possible), and
- they need a rock-contributing headwall above them ensuring debris supply.

Morphometry enables these topographic attributes to be extracted from a DEM. The goal of the study is to map potential *rockglacier root zones (RRZs)* and evaluate deviations between modelled and real data. *RRZs* are the zones in which the accumulated debris below a headwall is triggered to creep if all the conditions necessary for the deformation of ice-rich sediments are met (Barsch 1996). The main characteristics of the *RRZs* are similar for all talus-derived rockglaciers and, therefore, they are considered as representative points of such features.

Three strategies are tested to automatically detect *RRZs* at a regional scale: (A) a probabilistic approach based on the distribution of the values of the selected topographic attributes, (B) a deterministic approach using the range of occurring values, and (C) an extension of the deterministic approach (B) by including rockfall accumulation areas.

Comparing the results of the three different modelling approaches reveales a trade-off between a modelling approach with narrow boundary conditions and one with wide boundary conditions. While the former leads to an increased number of objects that are not reproduced by the model, (i.e. that lie outside the mapped *RRZ* areas), the latter produces a large overestimation of the modelled *RRZ* areas. The inclusion of rockfall accumulation areas, even if based on simple modelling schemes, permits a much better estimate of *potential RRZ* areas.

In conclusion, it can be shown that geomorphometry is a valuable tool for delineating *potential RRZs*. *Actual* rockglacier occurrence, however, is also determined by factors that are not influenced primarily by topography (e.g. lithology, hydrology, climate, weathering). Discrepancies between modelling results and reality have, therefore, to be expected.

IV **Frauenfelder, R.** & Kääb, A. 2000. Towards a palaeoclimatic model of rock glacier formation in the Swiss Alps. *Annals of Glaciology* 31: 281–286.

In this paper the focus is on the distribution and morphology of rockglaciers in the Swiss Alps, with the aim of reconstructing their evolution in both historical and morphological terms.

While considering two different time scales (Holocene and Alpine Lateglacial) two approaches are followed: (I) a photogrammetry-based analysis of the morphology and dynamics of selected active rockglaciers, in order to derive their age structure and theoretical concepts of shape-types for active/inactive rockglaciers, (II) an inventory-based investigation of the spatial distribution of relict rockglaciers to estimate past limits of alpine permafrost distribution.

(I) The present-day morphology of active rockglaciers does not primarily reflect their present dynamic state, but rather their dynamic history. Complex and non-coherent shapes, rich in vertically and horizontally distinguishable creep systems, might point to a complex history. Uniform creep streams, in contrast, suggest a history of less dynamic variations. This implies that the potential significance of rockglaciers for paleoclimatic conclusions strongly depends on their age and the expressiveness of their dynamic history.

Two theoretical shape concepts of active rockglacier morphology are derived: a 'monomorphic' type, representing the presumably undisturbed, continuous development over several millennia, in contrast to a 'polymorphic' type, reflecting a system of (possibly climatically affected) individual creep streams several centuries to millennia old. This later shape concept is comparable to the 'multi-unit' rockglacier as introduced by Barsch (1996).

(II) A data set on 741 individual rockglaciers (253 active ones, 203 inactive ones and 285 relict ones) is established by compiling six existing rockglacier inventories from different regions of the Swiss Alps. This data set is used to study the spatio-temporal distribution pattern of rockglaciers, especially of the relict ones. The method applied is based on the key assumption that alpine permafrost is strongly dependent on the interplay of temperature and radiation. If the effect of radiation is parameterized, rockglaciers can be used as inter-comparable indicators of temperature conditions.

Furthermore, the lowest active rockglaciers in a given region can be interpreted as an outline of the lower limit of discontinuous mountain permafrost. This being the case, those rockglaciers which are now relict would have approximated the permafrost limit by the time of their transition from active/inactive to relict rockglaciers, i.e. at the time of their decay.

The topoclimatic-based inventory analysis yields an *average* temperature increase at Alpine relict rockglacier fronts of approximately +2°C since the time of their decay, which is a sign of relict rockglacier ages reaching back to the Alpine Lateglacial. The temperature difference of some tenths of a degree Celsius found for active/inactive rockglaciers is typical for the bandwidth of Holocene climate variations.

V **Frauenfelder, R.**, Haeberli, W., Hoelzle, M. & Maisch, M. 2001. Using relict rock-glaciers in GIS-based modelling to reconstruct Younger Dryas permafrost distribution patterns in the Err-Julier area, Swiss Alps. *Norwegian Journal of Geography* 55 (4): 195–202.

In this paper the results presented in *Paper IV* are used to estimate the depression of the permafrost limit during the Alpine Lateglacial relative to the present-day distribution, and to compare it with previously determined changes in glacier equilibrium line altitudes.

Differences in MAAT between the Younger Dryas period (YD) and today are estimated at the fronts of 32 relict rockglaciers in the Err-Julier area, eastern Swiss Alps. The analyses are based on a case-by-case calculation of the potential direct incoming solar radiation and the MAAT using a DEM and meteo data of recent years. The method is explained in more detail in *Paper IV* (full version in *Part II*).

The results suggest that the MAAT during the YD was lowered by approximately 3 to 4°C. Temperature reconstructions from other disciplines, for example $\delta^{18}O$-measurements and pollen analyses on lake sediments (Eicher 1994) point to temperature depression values for the YD in the same order of magnitude.

The findings imply, furthermore, that the lower limit of permafrost distribution during that time was depressed 500 to 600 m as compared to today. A model simulation of the corresponding spatial permafrost distribution during the YD indicates that glaciers in the study area were mostly surrounded by permafrost at that time and probably had a polythermal structure of englacial temperatures. This implies temperate firn in the accumulation areas but slightly cold near-surface ice in the ablation areas, and margins which were frozen to the bed.

"All models are wrong, but some are useful"
(Chatfield 1995)

4.2 Dynamic modelling of talus-derived rockglacier occurrence

4.2.1 Background and aim

As mentioned earlier (*Section 1.1*) a comprehensive understanding of intra-regional variability of rockglacier occurrence is lacking. In a previous study a static approach to model potential rockglacier root zone areas was analyzed (*Paper III*). The dynamic model goes one step further by incorporating more information about internal and external parameters (see below) and the temporal variability of the climate.

The prototype model allows the numerical simulation of the spatial and temporal distribution of rockglaciers, i.e. it is a 4D model. Its main goal is to help evaluate and increase knowledge about dynamics and distribution patterns of rockglaciers by detailed comparison of the model outcome with the actual occurrence of rockglaciers (cf. Bras *et al.* 2003, for an in-depth discussion of mathematical modelling in geomorphology). The area considered is the Upper Engadine, eastern Swiss Alps; the represented time-scale is the Holocene (i.e. ~10,000 y BP to today).

4.2.2 'Pre-Holocene' DEM

Technically, each DEM with a resolution sufficient to adequately represent rockglacier features (spatial resolution denser or equal to ca. 30 m) can be used as an input for the model. For the testing of the prototype model, a DEM with 25 metres cell size from *swisstopo* (the former Swiss Federal Office of Topography) was used. This so-called DEM25 is generated from the height information of the national 1:25,000 maps through vectorization of contour lines and lake contours, digitizing of the spot heights, and subsequent interpolation of a DEM with 25 m raster width from these data. Comparisons with photogrammetrically determined control points have shown that the average accuracy reaches approximately 3 m in the Alps (Hurni 1995).

This DEM portrays the topographic surface *including* the rockglaciers. Therefore, the rockglaciers had to be extracted from the DEM before modelling. With a few exceptions, the bedrock topography below the rockglaciers in the study area is not known. In order to obtain a 'pre-Holocene' DEM devoid of rockglaciers, the existing DEM was transformed into a point layer, where each original grid cell is represented by one point. For rockglaciers with known bedrock topography the height of the points were set to the bedrock heights reported by Vonder Mühll (1993). For rockglaciers with unknown bedrock topography, the points where set to values equal to the values of the surrounding talus slopes. Finally, a new surface topography was interpolated from this altered point layer. The resulting DEM was then used for the modelling. Possible problems arising from this procedure are discussed in *Section 4.2.5*.

4.2.3 Structure of the dynamic model

The dynamic model considers processes in the spatial and temporal domain and accounts for both external and internal processes, implemented by means of six modules (A to G).

The external processes considered are:

(A) rock-debris accumulation,
(B) hydrology,
(C) climate,
(D) glacier extent.

The internal processes are:

(E) creep initiation ('trigger'),
(F) advance rate,
(G) creep termination.

The model has been implemented as a stand-alone program. Crucial parameters, e.g. flow law parameters, climate parameters, and glacier extent history, are entered in editable spreadsheets before a model run. This allows for easy testing and tuning of the model. The program is written in C++, while the input grids are generated in Arc/Info.

4.2.3.1 External processes

(A) Rock debris accumulation

In this module, the following four questions are resolved:

(i) Where are the contributing rock walls?
(ii) Where are the debris accumulation areas and what is their extent?
(iii) How thick are the debris accumulations?
(iv) Which postglacial debris supply rates can be considered reasonable?

(i) A simple method for identifying rockfall source areas is the defining of thresholds for mean slope gradients (Dorren 2003). In the present test area, values above 37° showed the best agreement with rock walls as mapped in the 1:25,000 Swiss Topographical Maps of the area. For a study area in the Valais Alps, Zemp (2002) found that best results are achieved when modelling rock walls as areas steeper than 34°. Van Dijke & van Westen (1990) defined potential rockfall source cells by a mean slope gradient greater than 60° (this implies that only very steep rock walls are considered). The broad range of values found in the literature shows that the threshold values have to be parameterized in each study area individually. More complex identifications of rockfall source areas on the basis of a GIS could include: aspect, slope curvature, slope gradient, rock type and land cover (Dorren 2003).

(ii) Rockfall is defined as "free falling blocks of different sizes (smaller than 5 m^3) that detach from a cliff or a steep rock wall, show no interactions among each other, and follow an independent propagation mode"[3]. The extent of the debris accumulation areas is

[3] http://rockfor.grenoble.cemagref.fr/texte/A3chutedepierres.htm

calculated using a programme by Brändli (2001) which is based on the so-called 'overall-slope' or 'reach-angle' approach, also known as 'Fahrböschung' (Heim 1932). Rocks are simulated to fall from the contributing headwalls, i.e. the debris sources, and to follow the path of steepest descent. The movement of falling rocks is assumed to stop when the slope of the straight line connecting the current position of the rock with its origin reaches 31°, which is an empirically derived value (Gerber 1994). All cells that a rock passes during its fall are marked as 'rock accumulation areas'. Finally, areas of contributing headwalls are excluded from these 'rock accumulation areas'.

(iii) The thickness of talus accumulation is variable and depends mainly on the debris production of the headwall (i.e. on headwall height, rock characteristics, type of weathering, permafrost presence, etc.) and the original relief of the slope beneath the headwall. Based on the investigation of a small sample of comparably large talus accumulations, some authors give typical thicknesses of alpine talus accumulations as 30 to 50 m. They describe the course of the slope bedrock as 'often quasi parallel to the surface slope until close to the foot of the headwall' (VAW 1992a). Because of the lack of reported information about the parameterization of talus thickness, a rough approximation of the debris thickness is used: for each debris accumulation area the length between its highest and its lowest point is calculated. Then the maximum thickness of the layer is approximated as 10% of this accumulation area length, with the maximum in the middle of the distance and a parabolic decrease in thickness towards the edges of the accumulation area. Compared to the values reported by C. Hauck (personal communication, 2003) and in the VAW report cited above, this estimate seems to be a feasible first-order approximation.

(iv) Rates of rock wall retreat have been evaluated by different methods. For the most part, the computations are based on the volume of sediments at the base of a rock wall, a procedure which yields long-term average rock wall retreat rates (Barsch 1977, Ballantyne & Kirkbride 1987, Hoffmann & Schrott 2002). A few of the values are based on direct observations (e.g. Rapp 1960). For the Alps, estimated values of postglacial denudation rates are in the order of 0.1 to >3 mma^{-1} (Poser 1954, Barsch 1977, Hoffmann & Schrott 2002).

The prototype model presented here operates with a 'debris supply module' that allows debris supply into the cells which already contain debris at the start of a model run, i.e. into the initial debris distribution cells, or in other words, into cells representing talus slopes. Different 'supply' procedures were tested, ranging from the supply of a given amount of debris per year to complete refilling of a cell if its debris content decreases to a value lower than the initial value. Spatial heterogeneity of weathering rates and, hence, debris supply rates (induced, for example, by different lithologies) is neglected in this first prototype version.

(B) Hydrology

As mentioned earlier (*Section 2.2.1.2*), the influence of water on the formation of rockglaciers has been scarcely investigated to date. As a result, the prototype model has been simplified as follows: (1) the lithological preconditions relative to water storage capabilities are assumed to be spatially homogenous; (2) the topographical preconditions for water storage (concavity, convexity, etc.) are approximated with the wetness index of

the terrain (e.g. Beven & Kirkby 1979, Moore *et al.* 1990), which is calculated by means of a drainage routine allowing divergent flow (Skaug 2000); (3) any possibly existing differences in the snow depletion history are neglected.

(C) Climate

Climate (i.e. temperature, precipitation, radiation) has a significant influence on the thermal state of the ground (see also *Section 2.2.2*). Theoretically, this range of influences could be accounted for by the combination of three modules: one for temperature (including isotherms, the regional temperature gradient, a climate factor to cool/warm the climate, etc.), one for radiation (including radiation thresholds for the formation of frozen ground, cloud cover intensities during different phases of the Holocene, etc.), and one for precipitation (including isohyetes, a regional precipitation gradient, information about precipitation changes during the Holocene, etc.). In the present prototype, temperature and radiation influences are approximated by the inclusion of permafrost distributions at different points in time, modelled with the PERMAMAP model (see Section 3.4, Hoelzle 1994, 1996). As mentioned before, this permafrost model incorporates the influences of the MAAT and the potential direct radiation on the thermal state of the ground. The permafrost distribution as modelled with this program is, hence, considered as a proxy of the thermal and radiation-induced influences of climate.

Two main permafrost extents have been modelled for initial tests:

(1) Present conditions: extent under the current temperature realm
(2) LIA conditions: extent with a MAAT = 1°C lower than at present

The period of validity for each stage is inferred from glacier and climate reconstructions for the Holocene, mainly from Maisch *et al.* (2000), Roberts (2000) and Labeyrie (2003). Precipitation is assumed to be spatially and temporally homogenous. The spatial homogeneity seems to be justified by regional precipitation interpolations, as for instance, performed by Schwarb *et al.* (2000). The assumption of a temporal homogeneity, however, is certainly a subject of debate.

(D) Glacier extent

Due to varying climate conditions, glacier extents changed largely during the Holocene, oscillating various times between the maximum extent reached during the LIA and the minimum extent reached probably during the prime of the Holocene temperature optimum (8000–5000 y BP).

Two different glacier extents are integrated into the model:

(1) Glacier extent from 1999 (Paul 2003)
(2) Glacier extent around 1850, the maximum extent of the LIA (Maisch 1992)

As in module (C), periods of validity for the different glacier extents are determined from studies by Maisch *et al.* (2000), Roberts (2000) and Labeyrie (2003), and in addition, from reports about minimum glacier extents during the Holocene, e.g. from Holzhauser (1995) and Haeberli *et al.* (2004).

4.2.3.2 Internal processes

(E) Creep initiation ('trigger')

This module determines whether creep is initiated or not. Creeping is described as a flow process which is affected by parameters such as shear stress and viscosity differences at material boundaries. When sliding at the bed is neglected (as suggested by Haeberli 1985), the largest amount of the movement can be attributed to the plastic deformation of the ice-content of the ice-debris matrix. In rockglacier science, this deformation has been described most often until present by using Glen's glacier flow law for pure ice (Glen 1955, Paterson 1994):

$$\dot{\varepsilon} = A\tau^n \tag{1}$$

where $\dot{\varepsilon}$ is the strain rate, τ the shear stress, A the flow or rate factor and n a dimensionless power law exponent. A depends on the ice temperature (warm ice = 'soft', cold ice = 'stiff'), the unfrozen water content, the size of the ice crystals and the amount of dirt in the ice. n depends upon a variety of conditions, for example, overload. For large, thick glaciers n is usually set at 3, for the considerably smaller, thinner rockglaciers, n is set at 1 (Wagner 1996). Both A and n are empirically determined and various values for glaciers can be found in the literature (e.g. Paterson 1994).

Glen's glacier flow law states that deformation of the ice starts if the thickness of the ice exceeds a critical value, or in other words, when a critical threshold for the basal shear stress τ is surpassed. The basal shear stress τ is described as:

$$\tau = \rho g h \sin\alpha \tag{2}$$

with ρ the density of the rock-ice mixture, g the acceleration due to gravity (9.81 ms^{-2}), h the thickness of the frozen debris layer, and α the surface slope averaged over a length of $5h$ along the path of steepest descent. Values for ρ are taken from borehole measurements as reported, for example, by Barsch *et al.* (1979), Wagner (1992), Vonder Mühll (1993), and Arenson (2002) and are in the order of 1.5–1.8 gcm^{-3}.

A rockglacier matrix has to be supersaturated in ice to allow creep deformation. Therefore, the volumetric increase of the talus accumulation caused by this ice content, has to be considered in a model. Exact values for this volumetric increase are not known. Based on observations from drilling, it can be assumed that the overall ice content in supersaturated frozen rockglacier sediments is higher than the porosity of comparable non-frozen sediments by a factor of two to three (e.g. Barsch *et al.* 1979, Haeberli 1985, Konrad & Humphrey 2000, Arenson 2002).

Creep initiation is tested for by analyzing whether the topographic settings lead to a shear stress within the creeping matrix that is large enough to initiate cumulative deformation. The minimal shear stress is taken as τ = 50 kPa, an empirical value derived from borehole measurements (Wagner 1996). When this value is exceeded, a cell is

considered as starting to creep. It has to be noted that the time lags after which rockglaciers react to changes in climate and/or debris supply rates (cf. Olyphant 1987) are not accounted for in the present version of the model.

(F) Advance rate

If creeping is possible, the movement of the rockglacier is calculated. Two approaches are implemented: (F1) modelling of the 'advance of rockglacier fronts', (F2) modelling of 'mass transport' (*Section 4.2.4*).

For both approaches, (F1) and (F2), the surface velocity v_s is calculated according to Glen's flow law for glaciers:

$$v_s - v(z) = \frac{2A}{n+1}(F\rho g \sin\alpha)^n (h-z)^{n+1} \quad (3)$$

$$v_s - v_b = \frac{2A}{n+1}(F\rho g \sin\alpha)^n h^{n+1} \quad (4)$$

where v_b is the velocity at the base, v is the velocity at depth $(h\text{-}z)$, F is a shape factor, and all other parameters are the same as in Eqs. (1) and (2). F is dependent on the bed topography and considers the friction at the valley flanks (Paterson 1994). In the present model, values for A were taken from borehole measurements at Murtèl rockglacier as determined by Wagner (1996). In addition, a new value for A was determined by reproducing empirically measured flow velocities of three Alpine rockglaciers (*Paper I*) using $n = 1$ and $F = 0.75$. This value for A equals $1.2*10^{-12}$ $s^{-1}kPa^{-n}$, a value in the same order of magnitude as the values given for the ice-rich layer (without the soft-deforming layer) at Murtèl when n equals 1 or 1.1, respectively (Wagner 1996). Both Wagner's values and the value for A determined here are notably higher than the values calculated for glaciers. Wagner (1996) found that with equal shear stress (τ = 40 kPa) and temperature, the strain rate $\dot{\varepsilon}$ of the ice in the rockglacier Murtèl is slightly higher than for glacier ice.

The average velocity $\bar{v}$ at which a rockglacier creeps can be considerably smaller than the maximal velocity which is found at its surface v_s (see Figure 4.1). Integration of Eq. 3 gives $\bar{v}$, the velocity averaged over the total thickness of the rockglacier body:

$$\bar{v} = \frac{1}{h}\int_0^h v(z)dz = \frac{2A}{n+2}(F\rho g \sin\alpha)^n h^{n+1} \quad (5)$$

The advance rate $v_{adv.}$, however, is not only a function of the form of the velocity profile (see below), but also of the melting and re-freezing of ice/water within the advancing material. The ice in the ice-debris matrix, especially in the fine-grained layers at the rockglacier front, is not shielded against temperature and radiation as well as it is within the coarse blocky surface layer. As a result, heat can penetrate more efficiently into the matrix and cause (considerable) ice melting. This leads to a further reduction of the advance rate of the rockglacier. To account for this, a correction factor C_{melt} is included. The advance rate $v_{adv.}$ subsequently used in the model is then calculated as:

$$v_{adv.} = C_{melt}\bar{v} = C_{melt}\left(\frac{2A}{n+2}(F\rho g\sin\alpha)^n h^{n+1}\right) \quad (6)$$

Precise values for C_{melt} are scarce. Kääb (2004) derived empirical values accounting for both the velocity decrease with depth and reduction of the advance rate due to ice melt. These values range from 0.1 to 0.5, depending on the ice content of the rockglacier. With $n = 1$ and $\bar{v} = 2/3\ v_s$ (Paterson 1994) values for C_{melt} result in 0.15–0.75. The advance rate $v_{adv.}$ multiplied by the time step Δt yields the distance the rockglacier front moves forward during Δt.

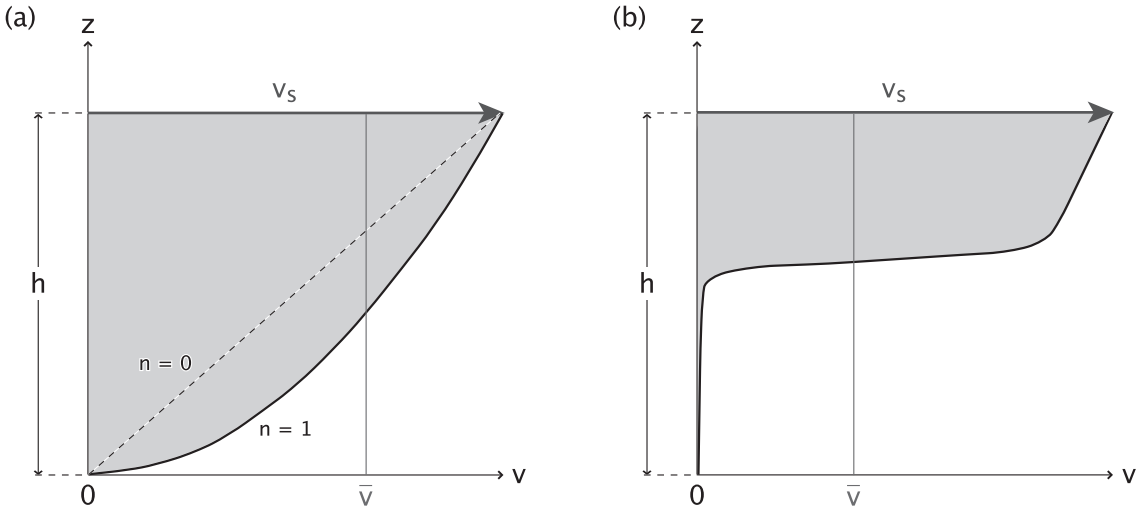

Figure 4.1 *Sketches of selected velocity profiles of a creeping rockglacier mass, with z = depth, h = thickness of creeping mass, v_s = maximal surface velocity, $\bar{v}$ = average velocity. (a) Velocity profiles for $n = 0$ and $n = 1$, respectively, (b) velocity profile as deducible from borehole measurements. The in-situ measurements on four Alpine rockglaciers suggest that they are all characterized by a (comparably thin) shear zone with deformations of 50 to 97% of the total surface deformation (Arenson et al. 2002). As the depth of these shear zones seems to vary for different rockglaciers and modelling of their depths has, thus far, not been performed, this phenomenon is not considered in the model presented here.*

(G) Creep termination

As outlined in *Section 2.2*, several conditions can lead to the halt of a rockglacier, subsequently causing either its climatic or dynamic inactivity:

(a) Climatic inactivity due to movement of the rockglacier into non-permafrost areas, either actively by creeping or, passively due to a rise in the permafrost limit.

(b) Dynamic inactivity caused by:
- topographic blockage (e.g. shallow or increasing slope), and/or
- reduction in debris supply, and/or
- decreasing ice incorporation.

In both cases the rockglacier's inactivation and, subsequently its relictification, is governed by the high thermal inertia of the system. In the model, climatic inactivity (a) is automatically induced when the lowest cell of a rockglacier reaches the permafrost limit. Dynamic activity (b) is accounted for by Equation (2): if the slope and/or the debris depth

fall below a threshold necessary to keep up the required shear stress, the velocity approximates zero. The mentioned thermal inertia related to the decay of rockglaciers (and the melt of ice in general) is, however, not yet considered in the model.

4.2.4 Initial results

4.2.4.1 F1: Advance of rockglacier front

In this approach, the emphasis is on the questions: *"Where does creeping occur?"* and *"Where is the front of a rockglacier at a given point in time?"*. The modelling involves a check for creep initiation and the tracking of the front advance.

Figure 4.2 shows the modelling scheme: (a) the direction of the steepest descent is extracted from a DEM for each cell; (b) flow paths and (c) initial shear stresses are calculated; (d) cells with shear stresses greater than the pre-defined threshold of 50 kPa (0.5 bar in the graph) are marked as 'active rockglacier front'; (e) for each cell, the creep front is defined as the centre of the cell and the initial creep distances are set at 0 m; (f) after twenty time steps (e.g. Δt = 1 year), for example, the rockglacier fronts crept forward several metres, but have not yet reached lower cells; (g) after another 20 time steps, the fastest rockglacier front (at the lower right of the Figure) moved into the next cell, which is now also marked as 'active rockglacier front'. As long as the front has not yet reached the centre of this cell, creep distances are recorded in the cell the rockglacier front has just left; (h) as soon as the front moves across the centre of this downslope cell, the upper cell, now devoid of a front, is marked as 'active rockglacier cell', its creep distance set back at 0 m, and flow is assigned to the 'active rockglacier front' cell; (i) after sufficient time steps, all upslope cells 'drained' their front into downslope cells, and the upslope cells are set back to 'active rockglacier cells'.

After a complete model run, cells are either labelled as 'active rockglacier cell', 'active rockglacier front, 'relict rockglacier cell', or 'relict rockglacier front', depending on their position in relation to the permafrost distribution found at the end of the model run.

Figure 4.3 shows the result of a model run for 10,000 years for the Corvatsch-Furtschellas test region, Upper Engadine, Switzerland. When compared with the inventory data, the results of the modelling show two main peculiarities: ① the 'active rockglacier fronts' in the model correspond to existing active talus-derived rockglaciers, but in most cases the modelled fronts do not reach the fronts of the real rockglaciers (for explanations see below). ② The model calculates 'rockglacier fronts' in areas where the inventory does not show such geomorphological features (Hoelzle 1989, 1998).

The advantage of approach F1 is the possibility to track the actual positions of the 'rockglacier fronts'. In addition, reduction of the advance rate by frontal ice melt (see above) can be accounted for. The approach neglects, however, that mass transport occurs throughout the rockglacier body which strongly affects physical properties such as thickness and velocity. Moreover, creep is only possible where debris is present in the first place. Therefore, this approach is highly sensitive to the initial debris distribution (see above, no. ①) and rockglaciers with thin initial talus and/or small initial debris supply areas (see Figure 4.3, ③) cannot be modelled accurately. In addition, the possibility of convergent/divergent flow (thinning/thickening of the creeping debris layers) is not

considered, and the use of non-stochastic flow paths leads to erroneous results caused by the raster data model structure.

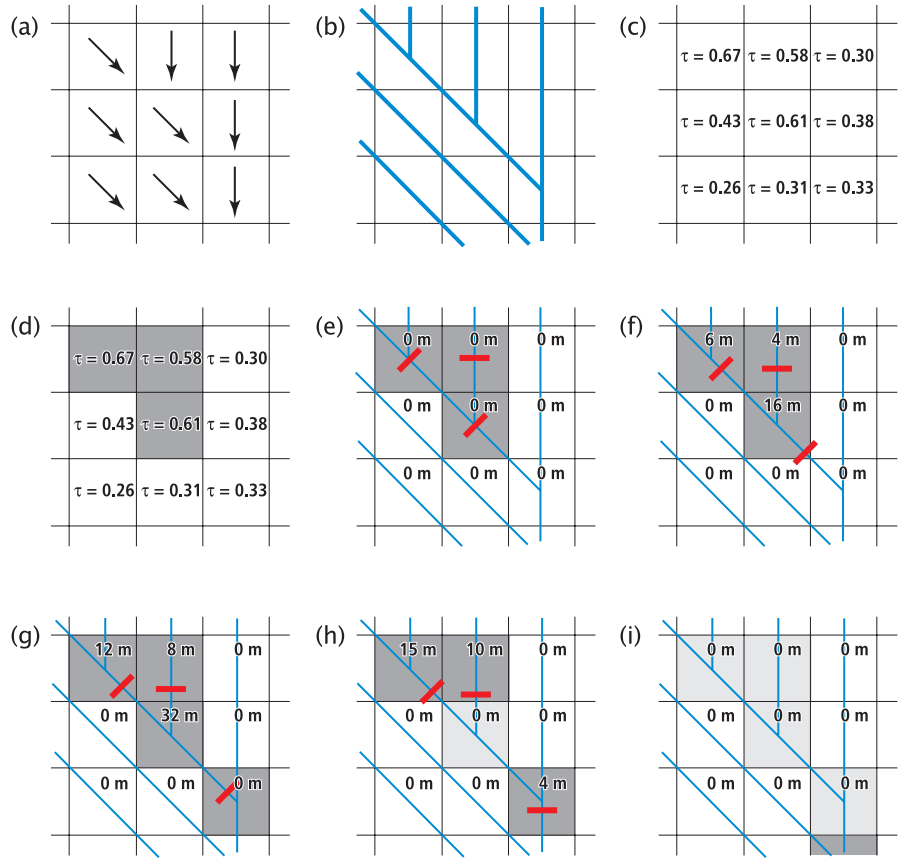

Figure 4.2 *Schematic plot of approach F1 'advance of rockglacier front'. See text for further explanations.*

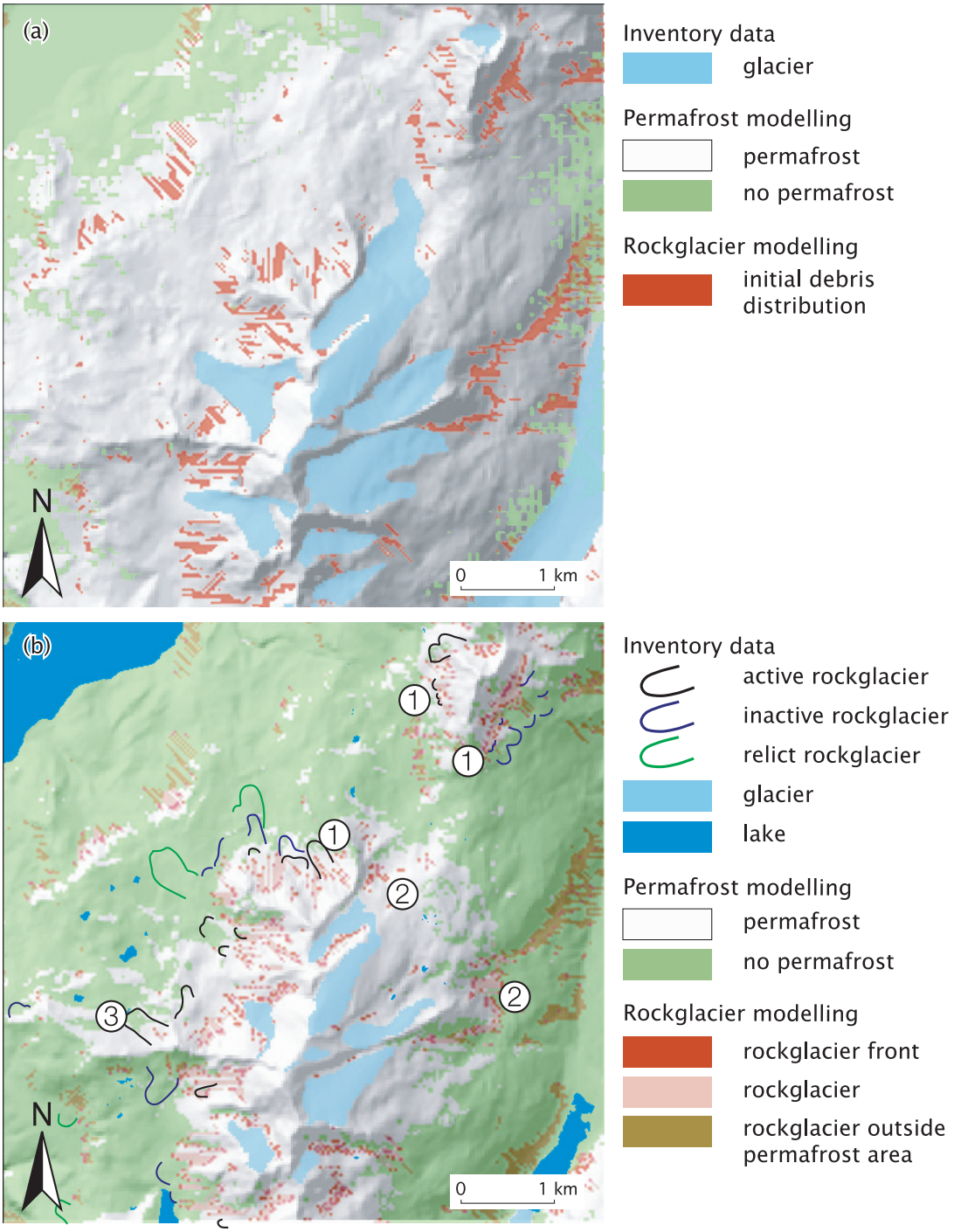

Figure 4.3 *Modelling of rockglacier distribution using approach F1 'advance of rockglacier front' for a test area in the Corvatsch-Furtschellas region, Upper Engadine, Switzerland. (a) Initial stage 10,000 y BP (beginning of Holocene). (b) Situation after 10,000 time steps of 1 year (present situation). Glacier extent in (a) as reconstructed by Maisch (1992), glacier extent in (b) corresponds to the extent in 1999 and was extracted from satellite imagery by Paul (2003), rockglacier distribution as inventoried by Hoelzle (1989, 1998). Background: DEM25 © 2004 swisstopo (BA045979). Model parameters:* $n = 1$, $A = 1.2*10^{-12}$ $s^{-1}kPa^{-n}$, $C_{melt} = 0.37$.

4.2.4.2 F2: Mass transport

In F2, an attempt is made to overcome some of the restrictions inherent in F1. First, the creeping mass strictly follows the rule of mass conservation and mass flux is considered at each cell within the rockglacier. Second, a 'debris supply module' is included that allows a controlled debris supply during the model run (see *Section 4.2.3.1* for details). Third, this approach allows the use of stochastic flow paths, which strongly reduces the occurrence of erroneous results. Fourth, and most important, debris transport is possible beyond the initial debris accumulation areas. A minor drawback of this approach is that the real advance of the rockglacier fronts is not modelled. The decrease of the advance rate due to frontal ice melt can, therefore, not be accounted for.

Emphasis in F2 is on *the creep of the debris-ice mass, i.e. the transport of volume from one cell to the next*. The modelling includes control of creep initiation and tracking of changes in thickness of the debris-ice mass. Figure 4.4 shows the modelling scheme: situation (a) shows two cells, an upper one, holding a volume of debris-ice mass, and a lower one, devoid of mass. The mass is creeping with $\bar{v}$, the velocity averaged over the total thickness of the rockglacier body, i.e. the accumulated thickness h (Eq. 5); (b) during a time step Δt, the mass is transported forward over the distance d; (c) the advanced mass is interpreted as an overflow from cell to cell: the upper cell loses a corresponding amount of its thickness, while the lower cell is filled evenly with the analogous amount. In the initial debris cells (but exclusively in those) the 'debris supply module' allows a refilling of the discharged mass volume if the thickness in these cells becomes less than their initial thickness (i.e. if they discharge more mass than they receive from their upslope cells). This enables the inclusion of (continuous) debris supply during a model run.

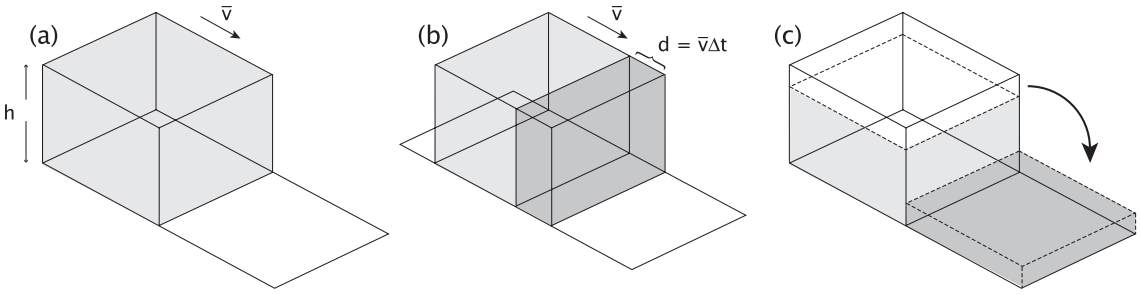

Figure 4.4 Schematic plot of approach F2 'mass transport'. See text for further explanations.

After a complete model run, three output grids are written: a 'cell status grid', the 'thickness distribution' and the 'velocity distribution'. Figure 4.5 shows the result of a model run for 10,000 years for the same test region as presented in Figure 4.3.

For a model run with $n = 1$, $A = 1.2{*}10^{-12}$ $s^{-1}kPa^{-n}$, modelled debris depth thicknesses range in the order of a few centimetres to over 100 m. Modelled velocities are in the order of centimetres to metres per year. Compared to field evidence, debris depths thicknesses of up to ca. 100 m and velocities below 1.5 ma^{-1} are seen as reasonable values for the area concerned (cf. Vonder Mühll (1993) for debris depths of active rockglaciers, and Kääb (2000) and *Paper I* for velocity measurements). Higher debris depths (exceeding 100 m thickness) and higher velocities (over 2 ma^{-1}) are reached at the edge of the model

perimeter (e.g. right border of the test area) and in some local small-scale depressions. These are undesired side-effects of the modelling caused by the fact that debris cannot flow out of the model perimeter or further onto a flat plane and is, therefore, dammed up, which subsequently leads to increasing debris depth and rising flow velocities.

The amount of debris supplied to the initial cells during the aforementioned model run corresponds to roughly 3–4 mma^{-1} vertical accumulation. These values are in the same order as rock wall retreat rates estimated by Barsch (1977), but considerably higher than those found, for example, by Hofmann & Schrott (2002). There are two main explanations possible for these comparably high values attained during the modelling: (a) The areal extent of talus slopes beneath a headwall is often less than that of the potentially debris-supplying headwall areas (projection normal to the surface), which leads to concentrated accumulation of the supplied debris in the receiving areas. (b) In active talus-derived rockglaciers, ice content by volume averages between 50 and 90%. Taking such values into account reduces actual debris supply rates in the modelling to 0.3–2 mma^{-1}.

The modelling results are regarded as representations of rockglaciers where both debris depth and velocity lie over user-defined thresholds. Characteristic mean active layer depths in the study area are around 3 to 3.5 m in coarse blocky material and 4 to 5 m in rock faces (M. Hoelzle, personal communication, 2003). Velocities above 0.05 ma^{-1} are considered as indicators of 'creep at a significant rate' (cf. *Paper I*). Hence, thicknesses greater than 5 m and velocities greater than 0.05 ma^{-1} were defined as thresholds for the identification of creeping debris and, consequently, cells above this threshold mapped as rockglaciers. Figure 4.6 shows the rockglaciers that result when these thresholds are applied to the values visualized in Figure 4.5.

Comparison between field evidence and modelling results yields the following (numbers refer to numerals in Figure 4.6):

① Most active and inactive talus-derived rockglaciers are reproduced accurately by the model, and the extents they exhibit in nature are also shown, approximately, in the model, although deviations of course exist.

② Certain active rockglaciers are not reproduced by the modelling. Careful consultation of the inventory data reveals that (at least) some of these rockglaciers are moraine-derived forms, and thus cannot be reproduced by a model that is based entirely on the processes involved in the development of talus-derived rockglaciers.

③ In a model run for 10,000 years, the modelled rockglacier fronts do not advance into regions where relict rockglaciers are found in the inventory. Based on temperature reconstructions (see *Papers IV, V*) and relative age dating on selected rockglaciers (see *Paper I*), it can be assumed that relict rockglaciers in the area evolved as early as the Alpine Lateglacial. These findings seem to be supported by the model results with 'virtual rockglaciers' not exceeding the extents of active (and some inactive) rockglaciers.

The areas modelled as being affected by creeping are considerably larger than the areas in which creep features have actually been observed in field investigations. Such 'overestimations' occur both in areas outside the present permafrost distribution ④, and within the current permafrost zone. Possible explanations for these deviations involve time, relations between debris supply rates and creep rates, thermal dependence of creep rates, hydrological preconditions, composition of the talus slopes (fine-grained, coarse-

grained), etc. and are discussed in detail in *Chapter 5*. In certain cases (cf. ⑤), the overestimations are localized in glacier forefields that became deglaciated after the LIA. Here, the errors are based on the fact that the permafrost distribution used as an input variable for the model does not take into account the absence/discontinuity of permafrost in recently deglaciated areas (cf. *Section 3.4*).

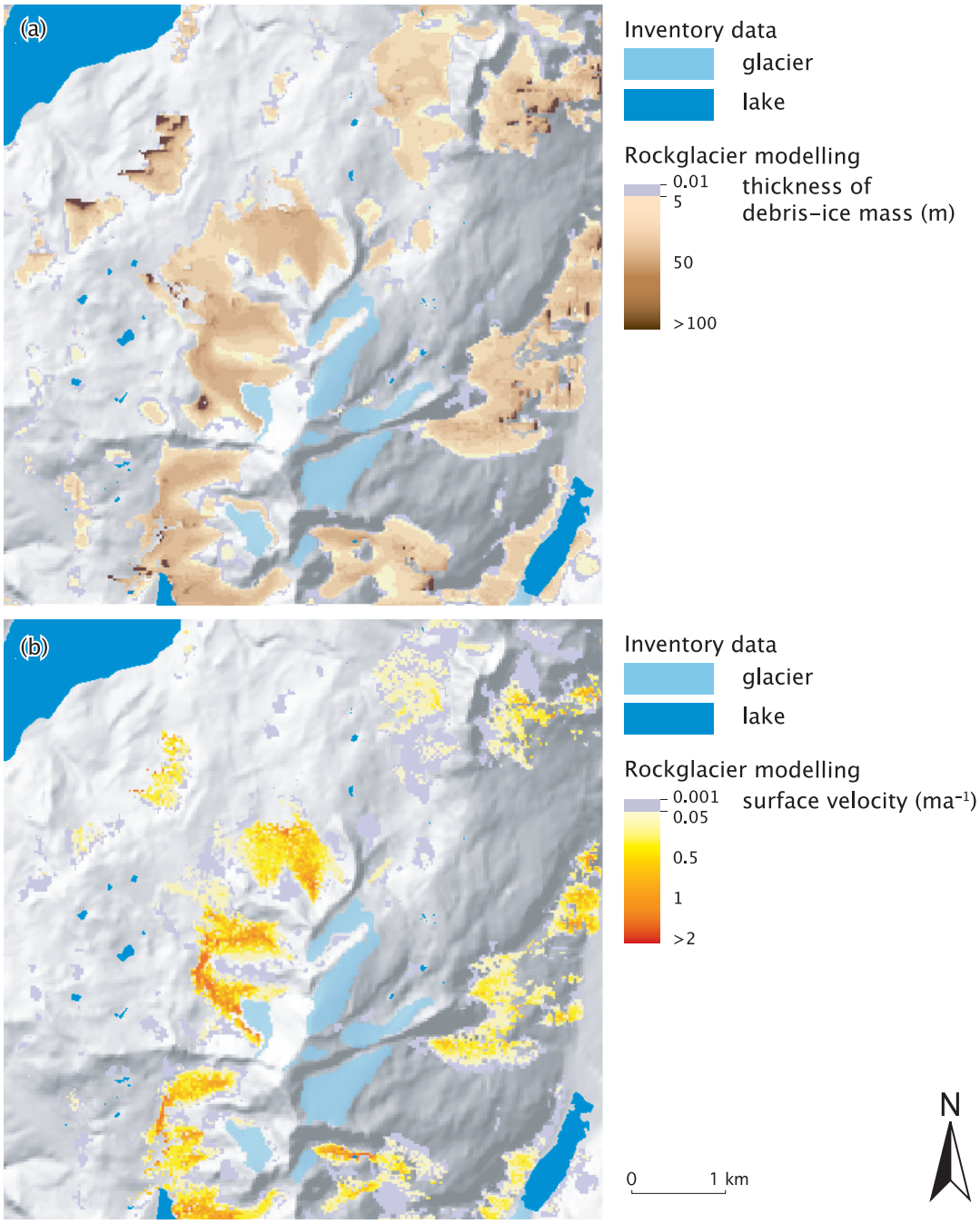

Figure 4.5 *Modelling of rockglacier distribution using approach F2 'mass transport' for a test area in the Corvatsch-Furtschellas region, Upper Engadine, Switzerland. Situation after 10,000 years: (a) thickness distribution, (b) velocity distribution. Sources for glacier extents and rockglacier distribution as in Figure 4.3. Background: DEM25 © 2004 swisstopo (BA045979). Model parameters: $n = 1$, $A = 1.2*10^{-12}$ $s^{-1}kPa^{-n}$.*

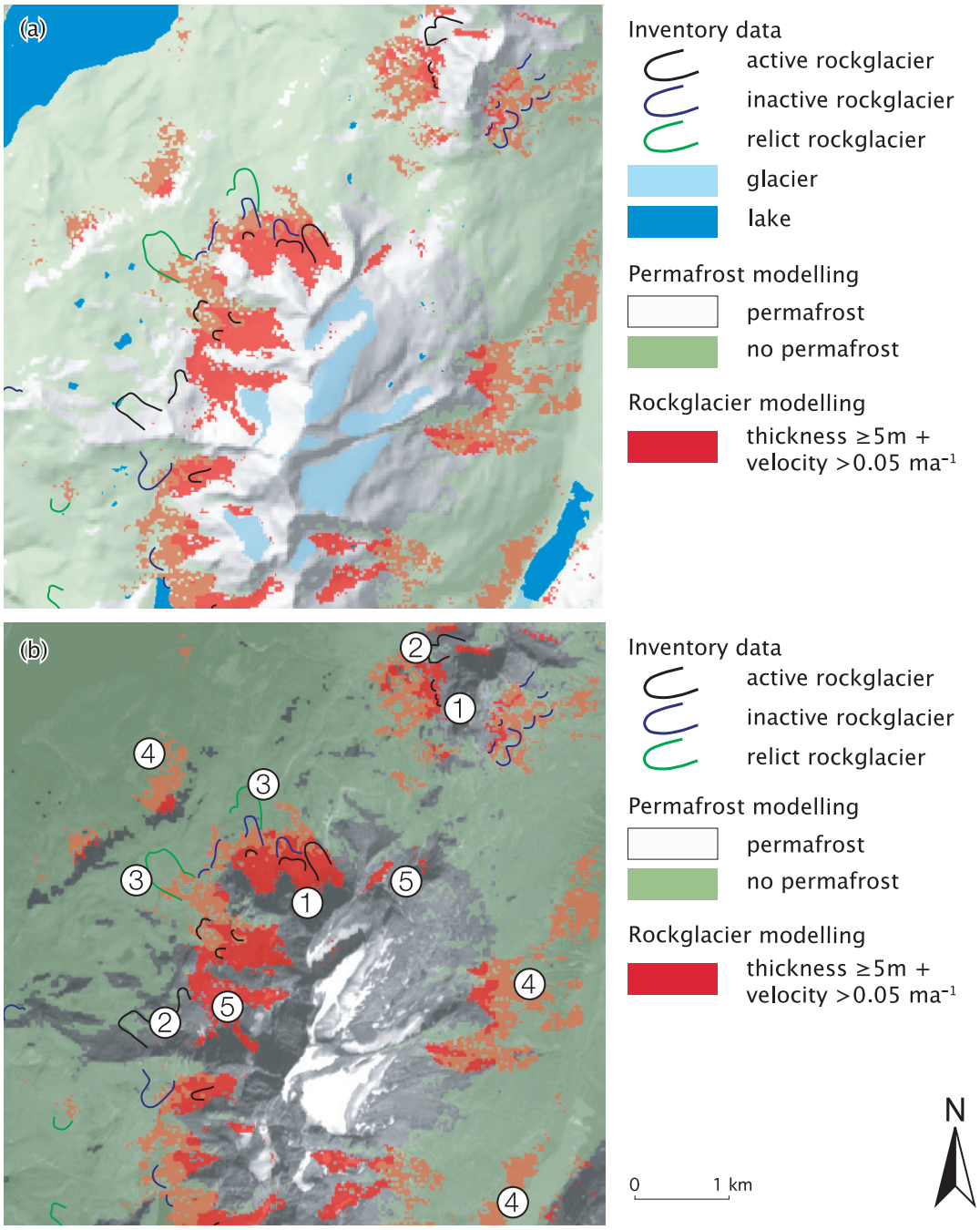

Figure 4.6 *Rockglaciers as modelled according to approach F2. Zones in red represent areas where thickness of the debris-ice mass is greater or equal to 5 m and velocities are greater than 0.05 ma^{-1}(see Figure 4.5). (a) Background: DEM25 © 2004 swisstopo (BA045979). (b) Background: satellite image of the panchromatic channel of the Indian Remote Sensing Satellite (IRS-1C), 25.09.1997, © Eurimage/NPOC.*

4.2.5 Main challenges and outlook

In general, the simulation of regional rockglacier distribution with the 4D prototype model shows promising results. Nonetheless, these preliminary findings reveal some major problems involved with the modelling approach applied. They have been recognized and

analyzed and are summarized below. Future research activities should address these problems.

– *Availability of rock debris:* the availability of rock debris has been identified as a very important parameter. It is, however, very difficult to model. In the prototype model, uncertainty about the debris availability arises from three main sources: (a) the simplified identification of debris-producing headwalls, (b) the difficulty in estimating the thickness of rockfall accumulations, and (c) the uncertainty relating to postglacial debris supply rates. (a) In the present version of the model, all slopes steeper than 37° are considered as debris-producing headwalls. Although feasible as a crude approximation, this simple approach is a source of large errors. For instance, differences in production rates due to different lithologies cannot be accounted for. A future version of the model should allow a better parameterization of debris-producing headwalls, including regional calibration. This would allow a better estimation of the debris input into the system. (b) A number of approaches are available to estimate the *extent* of debris accumulations, for example, from air- or space-borne remote sensing (e.g. Bishop *et al.* 1999, Kieffer & others 2000, Taschner & Ranzi 2002, Paul 2003). Literature on the estimation of debris accumulation *thickness*, in contrast, is generally sparse. Some data is available from geophysical measurements on individual scree slopes (e.g. VAW 1992b, Kneisel *et al.* 2000, Delaloye *et al.* 2001, Gude *et al.* 2003, Hoffmann & Schrott 2003). The talus thicknesses reported there generally agree with the values modelled as an input for the prototype model. Still, the applied estimation of the talus thickness is certainly a critical one (see *Section 4.2.3*). (c) As mentioned before, great uncertainty exists about the amount of postglacial denudation in periglacial areas and, thus, the spatio-temporal characteristics of debris input into the model. On the other hand, the model presented here allows sensitivity studies to be performed in such a way that theoretical concepts of the spatio-temporal behaviour of debris supply can be tested with reference to their effect on modelled rockglacier distribution.

– *Climatic limitation of rockglacier movement*: in the present version of the model, the movement of a rockglacier stops as soon as the rockglacier's front reaches the edge of the permafrost occurrence. This approach has two weaknesses: firstly, the calculation of the extent of the permafrost distribution is, to some extent, uncertain (e.g. Hoelzle 1996, Imhof 1996, Frauenfelder *et al.* 1998). Secondly, the occurrence of rockglaciers is not purely limited by the extent of permafrost. On the one hand, the initiation of creeping depends on the continuous presence of ground ice which is only possible where permafrost occurs. On the other hand, creeping alters the physical properties of the rock-ice-composite through compression, expansion, and translation. And, as mentioned before, the thermal inertia of ice and the rockglacier's own microclimate prevent its immediate melt when coming into unfavourable climate conditions (see *Section 2.2*).

– *Digital elevation models depict present topographies*: DEMs generated from maps or aerial photography portray the topographic surface including existing geomorphological forms such as, for example, rockglaciers. The creeping occurs in layers below the visible surface. In most cases, neither the topography of these layers nor of the

underlying bedrock is known. In the study area, the depth of both the shearing layers and the bedrock are known for a few rockglaciers only: for three rockglaciers from borehole inclinometer measurements (Vonder Mühll & Holub 1992, Arenson *et al.* 2002), for one rockglacier from geoelectrical and seismic soundings (Vonder Mühll 1993). The knowledge base for the extraction of rockglaciers from the DEM is, therefore, rather thin. Still, the rockglaciers had to be extracted in order to get a 'Pre-Holocene' topography. Interpolation of the topography before rockglacier initiation from the values of the surrounding neigbourhood, as effectuated in the present study (see *Section 4.2.2* for details), is a possible but problematic solution to this problem: for the areas where rockglaciers are located in the 'present-day' DEM, interpolation produces height values comparable to the adjacent talus slopes where no creeping is observed today. In addition, presumably pre-existing concavities in the bedrock underneath the rockglaciers found today cannot be reproduced.

– *Influence of the rate factor A*: Various tests of the model yielded a high sensitivity of the velocity v and, consequently, of the maximum debris thickness reached, to relatively small variations (in the range of several $1.0*10^{-12}$) of the rate factor A. This, in turn, greatly influences the rockglacier distribution present at the end of a model run. In the present model, all rockglaciers are modelled with one value for A, a simplification not given in nature. The inclusion of a spatio-temporally varying A would presumably lead to significantly improved modelling results, with several disagreements between modelling results and field evidence becoming explainable. Results from 2D numerical modelling (Kääb 2004), laboratory testing (Arenson 2002) and field evidence (*Paper II*) have shown a clear temperature dependence of A. Therefore, the inclusion of a temperature-dependent spatial variation of A as an input parameter seems highly recommendable for a future version of the model.

Chapter 5

General discussion

In this chapter, three topics are discussed, linking together the research presented in *Papers I–V* and *Section 4.2*: (1) climatic and topographic constraints on rockglacier distribution, (2) importance of rockglaciers for paleoclimatic reconstructions, and (3) enhancements in rockglacier research by static and dynamic modelling of rockglacier occurrence.

In an early stage of this study, the combination of debris-covered areas and permafrost areas as a potential proxy for Alpine rockglacier occurrence was evaluated (see Figure 5.1).

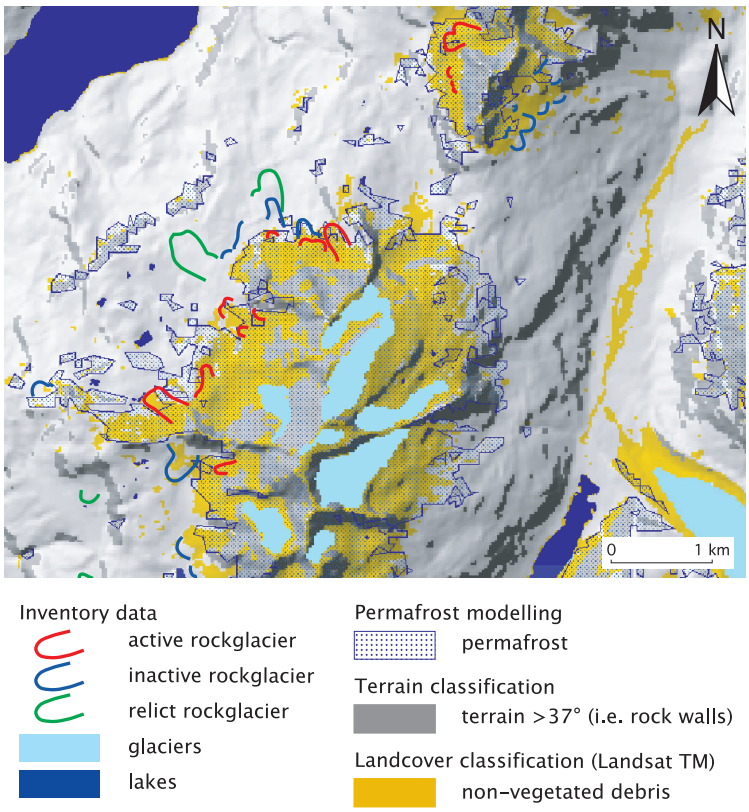

Figure 5.1
Rockglacier occurrence as compared to the permafrost distribution and debris accumulations in the Corvatsch-Furtschellas region, Upper Engadine, Switzerland. Permafrost distribution is modelled with the model PERMAMAP by Hoelzle (1994), see Section 3.4. Debris accumulations are extracted from a LANDSAT TM scene; for methodology, refer to Paul et al. (2002). Background: DEM25 © 2004 swisstopo (BA04 5979).

Non-vegetated debris areas actually turned out to be a reasonable representative for permafrost areas, a fact already applied by Haeberli (1975) for compiling his 'rules of thumb' for the detection of Alpine permafrost. However, for the detection of rockglaciers, the approach proved to be too crude. Although all rockglaciers are located in, or at least

evolve from, non-vegetated debris-covered areas, much larger areas are covered by non-vegetated debris without being characterized by rockglaciers.

One of the crucial questions is, therefore, why certain scree slopes exhibit a rockglacier, while other comparable scree slopes do not. Besides other aspects discussed in the following, light is also shed on this specific question.

5.1 Topographic and climatic constraints

5.1.1 Geological and relief-induced constraints

As shown before (*Section 2.2.1*), debris supply is an important parameter for the development of talus-derived rockglaciers and is a function of climatically and geologically induced weathering of the rock wall, rockslide and debris flow activity, avalanche intensity (particularly in springtime), and topography.

Rockglacier occurrence seems to dominate in bedrock geology, producing coarse-blocky material rather than fine debris (see *Section 2.2.1*). In addition, Matsuoka & Ikeda (2001) found that rockglaciers located below rock walls composed of, for example, shale or schist (rock types bound to weather into pebbles and finer material) are generally limited in size (Figure 5.2a). They introduce the term 'pebbly rockglaciers' for such instances, in contrast to 'bouldery rockglaciers', which are composed of coarse-blocky material and originate mainly from resistant rock types (e.g. gneiss, granites, certain limestones; Figure 5.2b)

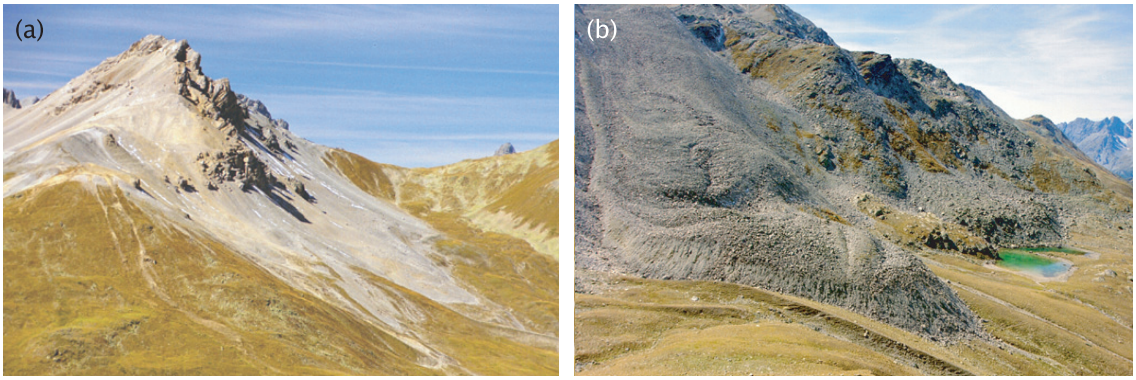

Figure 5.2 *Two examples for the influence of geology on rockglacier type (as defined by Matsuoka & Ikeda 2001): (a) pebbly rockglacier developing from a headwall composed of dolomites and limestone, Piz Mezdi, Val S-Charl, Swiss Alps. (b) bouldery rockglacier developing from a gneissic and verrucano headwall, Piz Plazèr, Val Sesvenna, Swiss Alps. Geology after Spitz & Dyhrenfurth (1907–1912).*

In *Paper II*, relations between rockglacier size and size and character of headwall areas were investigated for a sample of 84 rockglaciers. The results depicted in Figure 5.3 substantiate the findings of Matsuoka & Ikeda (2001): all of the investigated pebbly rockglaciers originate from headwalls $<10^5$ m^2 and their surface areas are smaller than $1.1*10^5$ m^2. In contrast, bouldery rockglaciers originate from headwalls of 10^4 to $2.3*10^5$ m^2 in size, with extents of up to $1.8*10^5$ m^2. Although small bouldery rockglaciers also occur, of course, the pebbly rockglaciers are clearly limited in their extents when compared to the bouldery rockglaciers.

These findings seem to contradict the conventional understanding of the susceptibility of different rock types to weathering but can, according to Matsuoka & Ikeda (2001), be explained when two main conditions are taken into account: (a) weak rocks can only support low rock walls. The source area and the total debris input is thus smaller than for high rock walls composed of 'hard' rock types. (b) Pebbly rockglaciers are more prone to solifluction than bouldery rockglaciers, due to the high content of fine material in the former. Solifluction tends to remove surficial debris which prevents the accumulation of thick debris layers. Argument (a) is reinforced by the results visualized in Figure 5.3. As mentioned earlier, the maximal headwall extent of the investigated pebbly rockglaciers is considerably smaller than that of bouldery rockglaciers. Argument (b) might be counterbalanced by the fact that the material dislocated by solifluction processes is likely to become reincorporated into the creeping debris-ice mass of a newly developing rockglacier.

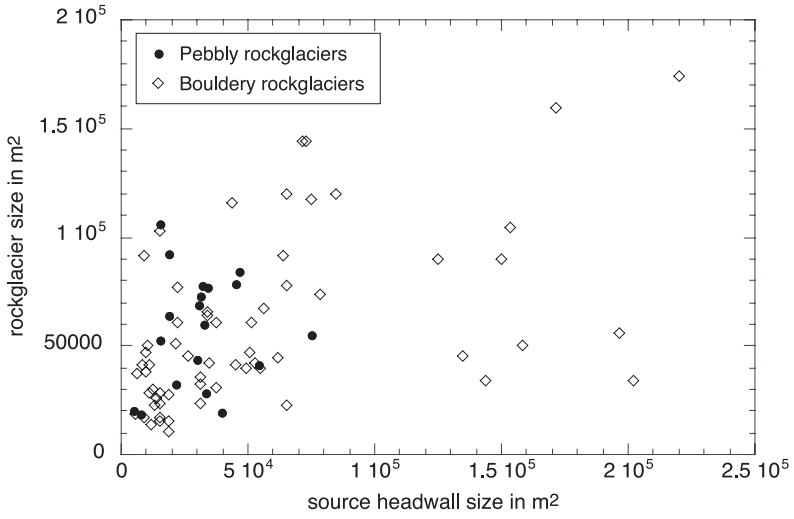

Figure 5.3 Relation between rockglacier size and source headwall size for pebbly and bouldery rockglaciers in the Upper Engadine. Sample size = 84.

Talus delivery has to come from both regular weathering processes and episodic events. Regular (daily) weathering provides the fine material necessary for the build-up of a cohesive debris-ice matrix. Seasonal to episodic events deliver the coarse blocky material which is important in two ways: (1) accumulation of a debris layer thick enough to induce the needed weight (or shear stress) for creeping, and (2) formation of the characteristic coarse blocky surface layer enabling air penetration, surface cooling, etc. If either one of the two weathering processes is absent, or dominant to an unfavourable degree, rockglacier development is inhibited, even though favourable lithological preconditions might be present.

Another possible answer to the question formulated at the beginning can be found in the fact that rockglacier creeping is in competition with other dislocation processes (e.g. solifluction, rockfall) which might in some cases be superimposed on the permafrost creep. Large rockfall deposits might, for instance, repeatedly cover newly developing creep features. In other cases, creeping might not be visible because the typical rockglacier forms do not develop (e.g. due to very small creep rates or due to extending flow on steep

slopes). Presumably, a considerably larger amount of scree slopes is actually in a creeping state than is visibly observable. Indeed, very small movements (at rates of cma^{-1}) could recently be measured with radar interferometry in scree slopes formerly considered as motionless (e.g. Rott *et al.* 1999, e.g. Strozzi *et al.* 2003) and in very slow-moving rockglaciers (Rignot *et al.* 2002, Strozzi *et al.* 2004).

Furthermore, a rockglacier is a cumulative form spanning the entire history since its origin. Thus, there is a chance that we are examining the landscape 'too early', i.e. at a point in time when permafrost creep did not (yet) manifest itself as rockglaciers. In this regard, a frozen scree slope without creep features could also be seen as the first link in a process chain from such slopes, via protalus ramparts to fully developed rockglaciers. The prototype model presented in *Section 4.2* could give indications, where such processes could be ongoing.

5.1.2 The influence of climate, in particular temperature

Long-term creep deformation of rockglaciers requires permafrost conditions, regardless of the exact origin of the subsurface ice (Haeberli & Vonder Mühll 1996). Climate with its long-term variability governs ground thermal conditions and, for this reason, represents one of the important factors controlling the temporal and spatial distribution of Alpine rockglaciers (*Section 2.2.2*). In turn, some rockglaciers may provide a complete record of major Holocene climatic changes, as short-term climatic changes become filtered by internal self-adjustment of the rockglacier debris transport system (Olyphant 1987).

When trying to infer paleoinformation from rockglaciers one has to consider that rockglaciers may react in a non-uniform way to climatic changes, depending on their initial size, their location and other factors. This can be illustrated by comparing monomorphic and polymorphic rockglaciers as given in *Paper I* and *Paper IV*: monomorphic rockglaciers show a continuous increase in age from their root zones to their fronts and presumably represent widely undisturbed conditions, for instance by external climate forcing, throughout their entire existence. No distinct inactivation/reactivation cycles can be detected. Polymorphic rockglaciers, by contrast, consist of individual lobes which often mark different generations and may have undergone strong variations in their degree of activity. Temporary altitudinal shifts in the permafrost limit around the location of a specific rockglacier are considered as one of the key causes for these changes in activity. Indeed, borehole temperatures of different rockglaciers seem to strengthen such a thermally-dependent definition of form, with polymorphic rockglaciers tending to be located in warmer permafrost, and monomorphic ones in colder permafrost (Table 5.1).

The analyzed sample is, of course, very small and the above assumption, therefore, tentative. Further confirmation or weakening of the hypothesis can only be made on the basis of future borehole temperature measurements or modelling.

The statistical analysis of data from 34 rockglaciers revealed a strong dependence of flow velocities on thermal conditions. Maximum surface velocity shows a highly significant exponential relationship with the MAAT at the rockglacier front, which was introduced as a proxy for the temperature of the permafrost (see *Paper II*). This confirms that flow velocity is a function of ice temperature with warmer ice deforming faster than cold ice. As

found for glacier ice, the rate factor *A* (see *Section 4.2.3.2*) increases significantly and in a non-linear way for temperatures approaching the melting point of ice (Paterson 1994). Similar findings are reported from borehole measurements and laboratory experiments, e.g. by Azizi & Whalley (1996), and Arenson *et al.* (2002).

Table 5.1 Possible thermally-dependent definition of rockglacier form

Rockglacier	Shape type	10 m-temperature (°C)	Source of temperature data
Gruben	monomorphic	-1.1	(Haeberli 1985)
Murtèl	monomorphic	-1.8	(Vonder Mühll *et al.* 1998)
Muragl	polymorphic	-0.2	(Arenson *et al.* 2002)
Schafberg I	polymorphic	-0.8	(Vonder Mühll *et al.* 1998)
Schafberg II	polymorphic	-0.3	(Vonder Mühll *et al.* 1998)

This thermal dependence provides another possible answer to the initial question, that is, why certain scree slopes exhibit a rockglacier, while other comparable scree slopes do not. Results by Isaksen (2001), Kääb *et al.* (2002) and Ødegård *et al.* (2003), for example, show that rockglaciers move at very small rates below a MAAT of approximately -5°C. Reported maximum velocities are in the order of ≤ 0.11 m per year. Hence, permafrost temperatures might in some specific cases (e.g. northerly expositions at very high altitudes, areas in high latitudes) be too low to allow creep rates considerable enough to enable rockglacier formation over the course of a few thousand years. Isaksen (2001) for instance, reports ages of over 10 ka for rockglaciers in the continuous permafrost of Svalbard of only 190 m to 370 m in length, which would result in a form of 19 to a maximum of 37 m in length in 1 ka.

In the Upper Engadine, this thermal influence is of minor importance, as the MAAT in the periglacial belt is in the order of -2°C at 2700 m a.s.l. (Stocker-Mittaz 2002), nevertheless, it is certainly an important factor in higher mountains and, as shown above, in high-latitude areas.

5.2 The paleoclimatic significance of rockglaciers

Rockglaciers are landforms of a few to several millennia of age. Based on the studies presented in *Papers I, IV,* and *V* it can be concluded that the majority of the active rockglaciers in the study area started to evolve during the early phases of the Holocene. Relict rockglaciers are attributed in most cases a Lateglacial origin, or in individual cases during the second half of the Holocene.

Rockglaciers may be used for climate reconstructions in areas where other archives (e.g. glacier ice, moraines, lake sediments, trees) are lacking or complementary to data derived from such archives. Corresponding information can be gained (a) from measurements of rockglacier surface characteristics, (b) from analyses of information contained within the ice-debris matrix of the rockglacier body and/or (c) from numerical modelling:

(a) On the surface, age estimates can be drawn from streamline calculations computed from surface flow fields by using modern photogrammetric methods (e.g. Kääb *et al.* 1997, Kääb & Vollmer 2000), or from indicators of substrate age such as mechanical weathering degrees (e.g. Ballantyne 1986), weathering rind thickness (e.g. Kirkbride & Brazier 1995, Laustela *et al.* 2003), or the growth of crustose lichens, as for example *Rhizocarpon geographicum* (e.g. Haeberli *et al.* 1979, Dyke 1990, Whalley & Martin 1994).

(b) The ice within rockglaciers may contain organic matter allowing for direct and absolute dating by the radiocarbon method (Haeberli *et al.* 1999b). The fines of samples from the frontal debris can be dated by the luminescence method (e.g. Lehmkuhl & Lang 2001), yielding the time of the last exposure to daylight, and thus, providing true travel times of buried near-surface particles which have participated in the long-term creep process of the perennially frozen talus. The cosmogenic exposure dating (e.g. Cerling & Craig 1994, Ivy-Ochs *et al.* 1996) of coarse blocks, for example, in the talus apron at relict rockglacier fronts, indicates the time since rockglacier movement came to a stop. For comprehensive overviews on classic and new dating methods in geomorphology see, for example, Lang *et al.* (1999) and Haeberli *et al.* (2003).

(c) The lowest active rockglaciers in a given region can be interpreted as a rough delineation of the lower limit of discontinuous mountain permafrost. Consequently, relict rockglaciers can be interpreted as an approximation of the permafrost limit at the time of their transition from active/inactive to relict rockglaciers, i.e. the time of their decay (Barsch 1996). Calculation of the temperature increase between the time of the presumed decay of presently relict rockglaciers and the present day allows for the estimation of the depression of the permafrost limit in the past (see *Papers IV, V*). The potential of this third approach lies in its ability to draw conclusions about both the fluctuations of the permafrost limit during the Holocene – by studying active/inactive rockglaciers – and the course of the Alpine Lateglacial permafrost limit – by analyzing relict rockglaciers (see *Papers IV, V*). Comparison of the calculated temperature difference at individual relict rockglacier fronts combined with the application of the above-mentioned dating methods, especially with absolute-age dating methods as listed in (b), will allow for reconstruction of isotherms and thus for temperature reconstruction in space and time.

5.3 Enhancements from static and dynamic modelling

Static morphometric modelling of rockglacier occurrence (see *Paper III*) allows the derivation of topographic attributes with a close relationship to gravity-driven slope processes and, therefore, a major significance for rockglacier occurrence. Moreover, the study showed that geomorphometry is a suitable tool to delineate *potential* rockglacier root zones. However, morphometry is not an approach for exactly reproducing reality, as the latter is also determined by factors that are not topographically influenced (as e.g. lithological preconditions, climatic control of weathering rates). Hence, they cannot be considered on the basis of a purely morphometric approach.

Based on the conclusions drawn from the morphometric modelling, a dynamic process-based modelling approach is designed as a next step towards a comprehensive understanding of intra-regional variability of rockglacier distribution. As for every model,

the dynamic model presented here (*Section 4.2*) is inherently based upon a number of assumptions. Despite these simplifications, the model provides a tool for further identification and evaluation of important parameters related to rockglacier initiation and growth, and also helps to illustrate the complexity of the 'rockglacier' phenomenon. In this respect, the modelling process promotes an increase in the knowledge of rockglacier distribution and also permits gaps in this knowledge to be highlighted and directions for crucial future research to be pointed out (*Section 6.2*).

Chapter 6

Conclusions and outlook

6.1 Main results

The overall aim of this thesis was the investigation of the intra-regional variability of rockglacier distribution in order to better understand rockglacier evolution in general, and to assess the potential of rockglaciers for paleoclimatic reconstructions.

The main achievements and results of this research can be summarized as follows:

Constraints on rockglacier formation

- Assuming that year-round negative ground temperatures, i.e. permafrost, are a prerequisite for rockglacier development and existence, rockglacier formation is primarily controlled by the availability of debris and the temperature of the permafrost: the talus accumulation has to be sufficiently thick to induce creep and composed in a manner enabling stress-transfer (cohesive debris-ice matrix). The warmer the temperature of the permafrost, the faster a once-formed rockglacier will most likely creep. Therefore, a scree slope might not develop into a talus-derived rockglacier if it is too thin, consists of coarse blocks or of fine materials only, or if the scree slope is very cold (< -15°C MAAT, Payne 1998). Below a MAAT of -5°C, rockglaciers creep at such low rates (cma^{-1}) that creeping might not be detectable by conventional methods (e.g. photogrammetry) before a considerable amount of time (several decades) has passed. In such a case, new methods such as radar interferometry can give further insights into the dynamic state of a scree slope.
- Although hydrological constraints for rockglacier formation were not investigated in the present study, they are believed to set important boundary conditions. In high-relief regions like the Alps, water is heterogeneously available, both spatially and temporally. Its assumed influences are manifold and involve processes such as the dislocation of fine-grained material from the surface of a talus slope or rockglacier down to lower layers, the build-up of (interstitial) ice, energy exchanges during freeze/thaw cycles, etc.
- In view of the results obtained in *Paper II*, the widely applied shear-stress approach to model rockglacier creep merits reconsideration. Non-linear thermal influences on strain rates probably predominate over effects from stress-related geometry (slope-dependent thickness). Other variables must significantly influence rockglacier transport rates; examples are (a) the vertical velocity profile including deformation rates, thickness, internal structure with stiff layers or sliding processes at depth, shearing within the

permafrost, etc., and (b) variable ice content. These qualitative considerations are supported by findings of Arenson (2002). Based on laboratory testing on samples recovered from rockglacier coring and on artificial samples, he found a modified creep equation where the influence of temperature is strongly enhanced as compared to the original creep law by Glen (1955). In a qualitative way, these findings are confirmed by the results of the dynamic model presented in *Section 4.2*, where it is shown that the application of the shear-stress approach alone cannot entirely explain the rockglacier distribution pattern found in nature (see *Section 4.2.4* for more detailed explanations).

Alpine rockglacier ages

– All rockglaciers investigated in the study area are at least a few to several thousand years old. Age estimates from photogrammetrically derived streamline interpolation and relative age dating techniques suggests (minimum) rockglacier surface ages between 3 to 5 ka for the six under investigation. This implies that these rockglaciers started to evolve either after the early-to-mid Holocene temperature optimum (8000 to 5000 y BP) or, alternatively, already during the early periods of the Holocene after the fast glacier decay at the end of the YD. Before that time, most areas where active rockglaciers are located today were glacierized.

Modelling approaches

– Numerical modelling of rockglacier distribution shows that geomorphometry is a useful tool for delineating potential rockglacier root zone areas. However, a precise modelling of rockglacier occurrences demands a *dynamic* rather than a static modelling approach.

– Dynamic modelling enables the simulation of spatio-temporal creep processes but proves to be highly dependent on the accurate modelling of the relevant input parameters. The quantification of the extent and thickness of rockfall accumulation and of postglacial debris supply rates, which are important input parameters for the model, is difficult. In addition, the inclusion of hydrological constraints is not easy because research on this subject is scant.

Paleopermafrost reconstruction

– The lower limit of permafrost distribution in the eastern Swiss Alps was depressed 500 to 600 m during the early Younger Dryas as compared to today. Glacier equilibrium line depression between the early Younger Dryas and today is estimated to be around 300 m. This relative difference in altitude change indicates strongly reduced precipitation (30 to 40% reduction) and much larger abundance of mountain permafrost at that time. The glaciers in the study area must have been mostly surrounded by permafrost and probably had a polythermal structure of englacial temperatures.

6.2 Future work

Based on the results mentioned above, it can be concluded that future progress in rockglacier research must come from the combination of physical research (such as borehole measurements, core testing, kinematic analyses) and dynamic numerical modelling.

Physical research

Field studies and laboratory experiments should focus on:

- the study of weathering rates and their dependence of geological and climatic parameters (e.g. Matsuoka 1990, Sass 1998, André 2002, Hall *et al.* 2002, Prick 2003), in order to realistically account for decadal to millennial rockfall in source headwalls,
- the question whether rockglacier development is driven by low-magnitude high-frequency rockfall events or rather by high-magnitude low-frequency events,
- the influence of water on the formation of rockglaciers,
- the study of the characteristic micro-climate of rockglaciers, thereby focusing on energy fluxes in both the coarse blocky top layer and in the layers of fine substrate underneath,
- and the measuring of creep and seasonal, inter-annual, and decadal creep variations by photogrammetry, terrestrial survey, borehole measurements, etc.

Dynamic numerical modelling

In modelling operations, the following questions should be addressed:

- *What does the pre-Holocene topography look like?*
  Based on geophysical data about the course of the bedrock topography, knowledge about talus thickness and postglacial denudation rates, a DEM of the bedrock surface (i.e. surface without periglacial talus accumulations) could be generated and serve as an input into the dynamic model presented here, for example.
- *What are the constraints on rockglacier creep?*
  As an alternative to the shear-stress approach, a 'fixed thickness approach' is suggested. The thickness of the creeping layer would be fixed by the creep process itself: the talus starts creeping at an accelerated rate once a certain thickness of ice-rich fine material is reached. As soon as creep velocity is high, frontal discharge and overriding of boulders from the surface starts and forms a stiff (saturated) basal layer. The thickness of the creeping supersaturated layer thus remains limited.
- *How does a rockglacier decay?*
  Based on the initial study by Olyphant (1987) the reaction time of rockglaciers should be investigated further. This would lead to the study of the thermal inertia of rockglaciers in general.

References

André, M.-F. 1994. Rock glaciers in Svalbard. Tentative dating and inferred long-term velocities. *Geografiska Annaler, Series A* 76: 235–245.

—. 2002. Do periglacial landscapes evolve under periglacial conditions? *Geomorphology* 52 (1/2): 149–164.

Anisimov, O.A. & Nelson, F.E. 1996. Permafrost distribution in the Northern Hemisphere under scenarios of climatic change. *Global and Planetary Change* 14: 59–72.

Arenson, L. 2002. Unstable alpine permafrost: a potentially important natural hazard. Variations of Geotechnical behaviour with time and temperature. PhD-thesis No. 14801, Swiss Federal Institute of Technology, Zurich: 271 pp.

Arenson, L., Hoelzle, M. & Springman, S. 2002. Borehole deformation measurements and internal structure of some rock glaciers in Switzerland. *Permafrost and Periglacial Processes* 13 (2): 117–135.

Azizi, F. & Whalley, W.B. 1996. Numerical modelling of creep behaviour of ice-debris mixtures under variable thermal conditions. *International Offshore and Polar Engineering Conference, Proceedings,* Los Angeles: 362–366.

Ballantyne, C.K. 1986. Protalus rampart development and limits of former glaciers in the vicinity of Baosbhein, Western Ross-Shire. *Scottish Journal of Geology* 22: 13–25.

Ballantyne, C.K. & Kirkbride, M.P. 1987. Rockfall activity in upland Britain during the Loch Lomond Stadial. *Geographical Journal* 153: 86–92.

Barsch, D. 1977. Eine Abschätzung von Schuttproduktion und Schutttransport im Bereich aktiver Blockgletscher der Schweizer Alpen. *Zeitschrift für Geomorphologie* 28: 148–160.

—. 1996. *Rockglaciers. Indicators for the present and former geoecology in high mountain environments.* Springer, Berlin: 331 pp.

Barsch, D., Fierz, H. & Haeberli, W. 1979. Shallow core drilling and borehole measurements in permafrost of an active rock glacier near the Grubengletscher, Wallis, Swiss Alps. *Arctic and Alpine Research* 11 (2): 215–228.

Berthling, I., Etzelmüller, B., Eiken, T. & Sollid, J.L. 1998. Rock glaciers on Prins Karls Forland, Svalbard. I: Internal structure, flow velocity and morphology. *Permafrost and Periglacial Processes* 9 (2): 135–145.

Beven, K.J. & Kirkby, M.J. 1979. A physically based, variable contribution area model of basin hydrology. *Hydrological sciences* 24: 43–69.

Bishop, M.P., Shroder, J.F.J. & Hickman, B.L. 1999. SPOT Panchromatic imagery and neural networks for information extraction in a complex mountain environment. *Geocarto International* 14: 19–28.

Brändli, M. 2001. Steinschlagmodellierung. HTML-page: http://www.geo.unizh.ch/~gis2/pro/steinschlag/helps/pg/c-prog-new.html, edition: 26.6.2001.

Bras, R.L., Tucker, G.E. & Teles, V. 2003. Six myths about mathematical modeling in geomorphology. *In* Wilcock P. & Iverson R. (eds.), *Prediction in Geomorphology*. American Geophysical Union: 63–79.

Brown, W.H. 1925. A probable fossil glacier. *Journal of Glaciology* 33 (4): 464–466.

Burn, C.R. 1998. Field investigations of permafrost and climatic change in Northwest North America. *In* Lewkowicz A.G. & Allard M. (eds.), *7th International Conference on Permafrost, Proceedings,* 57, Yellowknife, Canada. Centre d'Etudes Nordiques, Université Laval: 107–120.

Capps, S.R. 1910. Rock glaciers in Alaska. *Journal of Geology* 18: 359–375.

Cerling, T.E. & Craig, H. 1994. Geomorphology and in-situ cosmogenic isotopes. *Annual Review of Earth and Planetary Sciences* 22: 273–317.

Chaix, A. 1919. Coulées de blocs dans le Parc National Suisse de la Basse-Engadine. *Compte rendu des séances de la Société Physique et d'Histoire Naturelle de Genève* 36: 12–15.

Chatfield, C. 1995. Model uncertainty, data mining and statistical inference. *Journal of the Royal Statistical Society. Series A (Statistics in Society)* 158 (3): 419–466.

Chorley, R.J., Malm, D.E. & Pogorzelski, H.A. 1957. A new standard for estimating drainage basin shape. *American Journal of Science* 255 (2): 138–141.

Chueca, J. 1992. A statistical analysis of the spatial distribution of rock glaciers, Spanish Central Pyrenees. *Permafrost and Periglacial Processes* 3 (3): 261–265.

Corte, A.E. 1976. The hydrological significance of rock glaciers. *Journal of Glaciology* 17: 157–158.

Dehn, M., Gärtner, H. & Dikau, R. 1999. Principles of semantic modeling of landform structures. *4th International Conference on GeoComputation, Proceedings,* Fredericksburg VA, Mary Washington College, 25-28 July: http://www.geovista.psu.edu/geocomp/geocomp99/Gc99/067/gc_067.htm.

Delaloye, R., Reynard, E. & Lambiel, C. 2001. Pergélisol et construction de remontées mécaniques: l'exemple des Lapires (Mont-Gelé, Valais). Publication de la Société suisse de Mécanique des Sols et des Roches, *Frost in der Geotechnik – Le gel en géotechnique* 141: 103–113.

Dikau, R. 1988. Entwurf einer geomorphologisch-analytischen Systematik von Reliefeinheiten. *Heidelberger Geographische Bausteine (Heidelberg geogr Contrib.)* 5: 45 pp.

Dorren, L.K.A. 2003. A review of rockfall mechanics and modelling approaches. *Progress in Physical Geography* 27 (1): 69–87.

Dyke, A.S. 1990. A lichenometry study of Holocene rock glaciers and neoglacial moraines, Frances Lake Map Area, southeastern Yukon Territory and Northwest Territories. *Geological Survey of Canada Bulletin* 394: 1–33.

Eicher, U. 1994. Sauerstoffisotopenanalysen durchgeführt an spät- sowie frühpostglazialen Seekreiden. *In* Lotter A.F. et al. (eds.), *Festschrift Gerhard Lang*: 277–286.

Etzelmüller, B. & Sollid, J.L. 1997. Glacier geomorphometry – an approach for analysing glacier surface changes using grid-based digital elevation models (DEM). *Annals of Glaciology* 24: 135–141.

Etzelmüller, B., Ødegård, R.S., Berthling, I. & Sollid, J.L. 2001a. Terrain parameters and remote sensing data in the analysis of permafrost distribution and periglacial processes: principles and examples from Southern Norway. *Permafrost and Periglacial Processes* 12 (1): 79–92.

Etzelmüller, B., Hoelzle, M., Heggem, E.S.F., Isaksen, K., Mittaz, C., Vonder Mühll, D., Ødegård, R.S., Haeberli, W. & Sollid, J.L. 2001b. Mapping and modelling the occurrence and distribution of mountain permafrost. *Norwegian Journal of Geography* 55 (4): 186 –194.

Evans, I.S. 1972. General geomorphometry, derivatives of altitude, and descriptive statistics. *In* Chorley R.J. (ed.), *Spatial Analysis in Geomorphology*. Mathuen & Co Ltd.: 17–92.

Fisch sen., W., Fisch jun., W. & Haeberli, W. 1977. Electrical D.C. resistivity soundings with long profiles on rock glaciers and moraines in the Alps of Switzerland. *Zeitschrift für Gletscherkunde und Glazialgeologie* 13 (1/2): 239–260.

Florineth, D. 1998. Surface geometry of the Last Glacial Maximum (LGM) in the southeastern Swiss Alps (Graubünden) and its paleoclimatolological significance. *Eiszeitalter und Gegenwart* 48: 23–37.

Frauenfelder, R., Allgöwer, B., Haeberli, W. & Hoelzle, M. 1998. Permafrost investigations with GIS – a case study in the Fletschhorn area, Wallis, Swiss Alps. *In* Lewkowicz A.G. & Allard M. (eds.), *7th International Conference on Permafrost, Proceedings,* 57, Yellowknife, Canada. Centre d'Etudes Nordiques, Université Laval: 291–295.

Fredriksen, P., Jacobi, O. & Kubik, K. 1985. A review of current trends in terrain modelling. *ITC Journal* 1985 (2): 101–106.

Gardaz, J.-M. 1998. Permafrost prospecting, periglacial and rock glacier hydrology in mountain areas. Case studies in the Valais Alps, Switzerland. PhD-thesis No. 1222, Institute of Geography, University of Fribourg: 184 pp.

Gerber, W. 1994. Beurteilung des Prozesses Steinschlag. Schweiz. Forstl. Arbeitsgruppe Naturgefahren (FAN), Herbstkurs, 20.-22. Oktober 1994, Poschiavo. Kursunterlagen.

Glen, J.W. 1955. The creep of polycrystalline ice. *Proceedings of the Royal Society, Series A* 228: 513–538.

Gude, M., Hauck, C., Kneisel, C., Krause, S., Molenda, R., Ruzicka, V. & Zacharda, M. 2003. Evaluation of permafrost conditions in non-alpine scree slopes in Central Europe by geophysical methods. *EGS, 28th General Assembly,* Nice, Geophysical Research Abstracts 5: 08966 (CD–ROM).

Guodong, C. 1983. Vertical and horizontal zonation of high-altitude permafrost. *In* Péwé T.L. (ed.), *4th International Conference on Permafrost, Proceedings*, Fairbanks, Alaska. National Academy Press, Washington D.C.: 136–141.

Haeberli, W. 1975. Untersuchungen zur Verbreitung von Permafrost zwischen Flüelapass und Piz Grialetsch (Graubünden). *Mitteilungen der VAW-ETH Zürich* 17: 221 pp.

—. 1985. Creep of mountain permafrost. Internal structure and flow of alpine rock glaciers. *Mitteilungen der VAW-ETH Zürich* 77: 142 pp.

—. 1990. Scientific, environmental and climatic significance of rockglaciers. *Mem. Soc. Geol. italiana* 45: 823–831.

—. 2000. Modern research perspectives relating to permafrost creep and rock glaciers: a discussion. *Permafrost and Periglacial Processes* 11: 290–293.

Haeberli, W. & Vonder Mühll, D. 1996. On the characteristics and possible origins of ice in rock glacier permafrost. *Zeitschrift für Geomorphologie* 104: 43–57.

Haeberli, W. & Burn, C.R. 2002. Natural hazards in forests: glacier and permafrost effects as related to climate change. *In* Sidle R.C. (ed.), *Environmental Change and Geomorphic Hazards in Forests*. CABI Publishing, Wallingford/New York: 167–202.

Haeberli, W., King, L. & Flotron, A. 1979. Surface movement and lichen-cover studies at the active rockglacier near the Grubengletscher, Wallis, Swiss alps. *Arctic and Alpine Research* 11 (4): 421–441.

Haeberli, W., Frauenfelder, R., Hoelzle, M. & Maisch, M. 1999a. On rates and acceleration trends of global glacier mass changes. *Geografiska Annaler* 81 A (4): 585–591.

Haeberli, W., Kääb, A., Wagner, S., Vonder Mühll, D., Geissler, P., Haas, J.N., Glatzel-Mattheier, H. & Wagenbach, D. 1999b. Pollen analysis and ^{14}C-age of moss remains recovered from a permafrost core of the active rock glacier Murtèl/Corvatsch (Swiss Alps): geomorphological and glaciological implications. *Journal of Glaciology* 45 (149): 1–8.

Haeberli, W., Brandova, D., Burga, C., Egli, M., Frauenfelder, R., Kääb, A., Maisch, M., Mauz, B. & Dikau, R. 2003. Methods for absolute and relative age dating of rock-glacier surfaces in alpine permafrost. *In* Phillips M., Springman S. & Arenson L. (eds.), *8th International Conference on Permafrost, Proceedings,* 1, Zürich. Swets & Zeitlinger, Lisse: 343–348.

Haeberli, W., Frauenfelder, R., Kääb, A. & Wagner, S. 2004. Characteristics and potential climatic significance of "miniature ice caps" (crest- and cornice-type low-altitude ice archives). *Journal of Glaciology* 50 (168): 129–136.

Hagen, J.O., Etzelmüller, B. & Nutall, A.-M. 2000. Runoff and drainage pattern derived from digital elevation models, Finsterwalderbreen, Svalbard. *Annals of Glaciology* 31: 147–152.

Hall, K., Thorn, C., Matsuoka, N. & Prick, A. 2002. Weathering in cold regions: some thoughts and perspectives. *Progress in Physical Geography* 26 (4): 577–603.

Hanson, S. & Hoelzle, M. 2003. The thermal regime of the coarse blocky active layer at the Murtèl rock glacier in the Swiss Alps. *In* Haeberli W. & Brandova D. (eds.), *8th International Conference on Permafrost, Extended Abstracts,* Zürich. University of Zurich: 51–52.

Heim, A. 1932. Bergsturz und Menschenleben. *Beiblatt zur Vierteljahresschrift der Naturforschenden Gesellschaft in Zürich* 20: 217.

Hoelzle, M. 1989. Untersuchungen zur Permafrostverbreitung im Oberengadin. Unpublished MSc-thesis, Swiss Federal Institute of Technology, Zurich: 79 pp.

—. 1992. Permafrost occurrence from BTS measurements and climatic parameters in the eastern Swiss Alps. *Permafrost and Periglacial Processes* 3 (2): 143–147.

—. 1994. Permafrost und Gletscher im Oberengadin. Grundlagen und Anwendungsbeispiele für automatisierte Schätzverfahren. *Mitteilungen der VAW-ETH Zürich* 132: 119 pp.

—. 1996. Mapping and modelling of mountain permafrost distribution in the Alps. *Norwegian Journal of Geography* 50: 11–15.

—. 1998. Rock Glaciers, Upper Engadin, Switzerland. Circumpolar active-layer permafrost system (CAPS), version 1.0. International Permafrost Association, Data and Information Working Group, National Snow and Ice Data Center/World Data Center for Glaciology, Boulder, CO. (CD ROM).

Hoelzle, M. & Haeberli, W. 1995. Simulating the effects of mean annual air temperature changes on permafrost distribution and glacier size. An example from the Upper Engadin, Swiss Alps. *Annals of Glaciology* 21: 400–405.

Hoelzle, M., Mittaz, C., Etzelmüller, B. & Haeberli, W. 2001. Surface energy fluxes and distribution models of permafrost in European mountain areas: an overview of current developments. *Permafrost and Periglacial Processes* 12 (1): 53–68.

Hoffmann, T. & Schrott, L. 2002. Modelling sediment thickness and rockwall retreat in an Alpine valley using 2D-seismic refraction (Reintal, Bavarian Alps). *Zeitschrift für Geomorphologie* 127: 153–173.

—. 2003. Determining sediment thickness of talus slopes and valley fill deposits using seismic refraction – a comparison of 2D interpretation tools. *Zeitschrift für Geomorphologie* 132: 71–87.

Holzhauser, H. 1995. Gletscherschwankungen innerhalb der letzten 3200 Jahre am Beispiel des Grossen Aletsch- und des Gornergletschers. Neue Ergebnisse. *In* Salm B. (ed.), *Gletscher im ständigen Wandel*, vdf-Hochschulverlag AG, Zürich: 101–122.

Humboldt, A.v. 1808ff. Nivellement barométrique fait dans les régions équinoxiales du Nouveau Continent 1799–1804. Rapport 4,2: 21/22. (in French; barometric surveying in equatorial regions of the Americas).

—. 1817. *De distributione geographica plantarum secundum coeli temperiem et altitudinem montium, Prolegomena*. Lutetiae Parisiorum, Paris/Lübeck: 250 pp. (in Latin; on the geogr. distr. of plants in the new world, temperatures, and heights of mountains).

Humlum, O. 1982. Rock glacier types on Disko, central West Greenland. *Geografisk Tidskrift* 82: 59–66.

—. 1997. Active layer thermal regime at three rock glaciers in Greenland. *Permafrost and Periglacial Processes* 8 (4): 383–408.

—. 1998. The climatic significance of rock glaciers. *Permafrost and Periglacial Processes* 9 (4): 375–395.

—. 2000a. The climatic and palaeoclimatic significance of rock glaciers. HTML-page: http://www.unis.no/RESEARCH/GEOLOGY/Geo_research/Ole/RockGlacierClimatic Significance.htm, edition: 2.2.2000.

—. 2000b. The geomorphic significance of rock glaciers: estimates of rock glacier debris volumes and headwall recession rates in West Greenland. *Geomorphology* 35: 41–67.

Hurni, L. 1995. Digital cartographic and topographic products from the Swiss Federal Office of Topography. *LIBER Quarterly. The Journal of European Research Libraries* 5: 255–261.

Imhof, M. 1994. Die Verbreitung von Permafrost in den Berner Alpen. Unpublished MSc-thesis, Department of Geography, University of Berne: 212 pp.

—. 1996. Modelling and verification of the permafrost distribution in the Bernese Alps (Western Switzerland). *Permafrost and Periglacial Processes* 7 (3): 267–280.

IPA. 1998. Circumpolar active-layer permafrost system (CAPS), version 1.0. International Permafrost Association, Data and Information Working Group, National Snow and Ice Data Center/World Data Center for Glaciology, Boulder, CO. (CD ROM).

Isaksen, K. 2001. Past and present ground thermal regime, distribution and creep of permafrost – case studies in Svalbard, Sweden and Norway. PhD-thesis No. 144, Faculty of Mathematics and Natural Sciences, University of Oslo: 48 pp. + Annex (5 Papers).

Ivy-Ochs, S., Schlüchter, C., Kubik, P.W., Synal, H.-A., Beer, J. & Kerschner, H. 1996. The exposure age of an Egesen moraine at Julier Pass, Switzerland, measured with the cosmogenic radionuclides ^{10}Be, ^{26}Al and ^{36}Cl. *Eclogae geol. Helv.* 89 (3): 1049–1063.

Jäckli, H. 1957. Gegenwartsgeologie des bündnerischen Rheingebietes: ein Beitrag zur exogenen Dynamik alpiner Gebirgslandschaften. *Beiträge zur Geologie der Schweiz. Geotechnische Serie; Lfg. 36*. Kümmerly & Frey, Bern: 136 pp. + 6 p. + 5 maps.

Johnson, J.P. & Nickling, W.G. 1979. Englacial temperature and deformation of a rock glacier in the Kluane Range, Yukon Territory, Canada. *Canadian Journal of Earth Sciences* 16 (12): 2275–2283.

Kääb, A. 2004. Mountain glaciers and permafrost creep. Research perspectives from remote sensing technologies and geoinformatics. Habilitation, Department of Geography, University of Zurich: 205 pp.

Kääb, A. & Vollmer, M. 2000. Surface geometry, thickness changes and flow fields on permafrost streams: automatic extraction by digital image analysis. *Permafrost and Periglacial Processes* 11 (4): 315–326.

Kääb, A., Haeberli, W. & Gudmundsson, G.H. 1997. Analysing the creep of mountain permafrost using high precision aerial photogrammetry: 25 years of monitoring Gruben rock glacier, Swiss Alps. *Permafrost and Periglacial Processes* 8 (4): 409–426.

Kääb, A., Gudmundsson, G.H. & Hoelzle, M. 1998. Surface deformation of creeping mountain permafrost. Photogrammetric investigations on Murtèl rock glacier, Swiss Alps. *In* Lewkowicz A.G. & Allard M. (eds.), *7th International Conference on Permafrost, Proceedings,* 57, Yellowknife, Canada. Centre d'Etudes Nordiques, Université Laval: 531–537.

Kääb, A., Isaksen, K., Eiken, T. & Farbrot, H. 2002. Geometry and dynamics of two lobe-shaped rock glaciers in the permafrost of Svalbard. *Norwegian Journal of Geography* 56 (2): 152–160.

Karssenberg, D. 2002. Building dynamic spatial environmental models. *Netherlands Geographical Studies* 305: 222 pp.

Keller, F., Frauenfelder, R., Gardaz, J.-M., Hoelzle, M., Kneisel, C., Lugon, R., Phillips, M., Reynard, E. & Wenker, L. 1998. Permafrost map of Switzerland. *In* Lewkowicz A.G. & Allard M. (eds.), *7th International Conference on Permafrost, Proceedings,* 57, Yellowknife, Canada. Centre d'Etudes Nordiques, Université Laval: 557–562.

Kieffer, H.H. & 41 others. 2000. New eyes in the sky measure glaciers and ice sheets. *EOS, Transactions American Geophysical Union* 81 (24): 265, 270–271.

Kirkbride, M. & Brazier, V. 1995. On the sensitivity of Holocene talus-derived rock glaciers to climate change in the Ben Ohau Range, New Zealand. *Journal of Quaternary Science* 10 (4): 353–365.

Kneisel, C., Hauck, C. & Vonder Mühll, D. 2000. Permafrost below the timberline confirmed and characterized by geoelectrical resistivity measurements, Bever Valley, Eastern Swiss Alps. *Permafrost and Periglacial Processes* 11 (4): 295–304.

Konrad, S.K., Humphrey, N.F., Steig, E.J., Clark, D.H., Potter, N.J. & Pfeffer, W.T. 1999. Rock glacier dynamics and paleoclimatic implications. *Geology* 27 (12): 1131–1134.

Konrad, S.K. & Humphrey, N.F. 2000. Steady-state flow model of debris-covered glaciers (rock glaciers). *Proceedings of the workshop on 'Debris-covered Glaciers',* Seattle, Washington, USA. *IAHS Publ.* 264: 255–263.

Labeyrie, L., Cole, J., Alverson, K.D. & Stocker, T. 2003. The history of climate dynamics in the Late Quaternary. *In* Alverson K.D., Bradley R.S. & Pedersen T.F. (eds.), *Paleoclimate, global change and the future*. Springer, Berlin/Heidelberg: 33–61.

Lang, A., Moya, J., Corominas, J., Schrott, L. & Dikau, R. 1999. Classic and new dating methods for assessing the temporal occurrence of mass movements. *Geomorphology* 30: 33–52.

Laustela, M., Egli, M., Frauenfelder, R., Kääb, A., Maisch, M. & Haeberli, W. 2003. Weathering rind measurements and relative age dating of rockglacier surfaces in crystalline regions of the Eastern Swiss Alps. *In* Phillips M., Springman S. & Arenson L. (eds.), *8th International Conference on Permafrost, Proceedings,* 1, Zürich. Swets & Zeitlinger, Lisse: 627–632.

Lehmkuhl, F. & Lang, A. 2001. Geomorphological investigations and luminescence dating in the southern part of the Khangay and the Valley of the Gobi Lakes (Central Mongolia). *Journal of Quaternary Science* 16: 69–87.

Lehmkuhl, F., Stauch, G. & Batkhishig, O. 2003. Rock glacier and periglacial processes in the Mongolian Altai. *In* Phillips M., Springman S. & Arenson L. (eds.), *8th International Conference on Permafrost, Proceedings,* 1, Zürich. Swets & Zeitlinger, Lisse: 639–644.

Lippert, A. 2001. Das Alter der Muren im Larstigtal/Tirol - Anwendung von Lichenometrie und Schmidt-Hammer zur Altersbestimmung von kleinräumigen Murablagerungen. Unpublished MSc-thesis: 118 pp.

Luckman, B.H. & Crockett, K.J. 1978. Distribution and characteristics of rock glaciers in the southern part of Jasper National Park, Alberta. *Canadian Journal of Earth Sciences* 15: 540–550.

Lundell, M. 1996. Qualitative modelling and simulation of spatially distributed parameter systems. PhD-thesis, Swiss Federal Institute of Technology, Lausanne: 264 pp.

Maisch, M. 1992. Die Gletscher Graubündens: Rekonstruktionen und Auswertung der Gletscher und deren Veränderungen seit dem Hochstand von 1850 im Gebiet der östlichen Schweizer Alpen (Bündnerland und angrenzende Regionen). *Physische Geographie* 33A/B: 324 pp./128 pp.

Maisch, M., Wipf, A., Denneler, B., Battaglia, J. & Benz, C. 2000. *Die Gletscher der Schweizer Alpen. Gletscherhochstand 1850, Aktuelle Vergletscherung, Gletscherschwund-Szenarien.* vdf-Hochschulverlag, Zürich: 373 pp.

Maisch, M., Haeberli, W., Frauenfelder, R., Kääb, A. & Rothenbühler, C. 2003. Lateglacial and Holocene evolution of glaciers and permafrost in the Val Muragl, Upper Engadin, Swiss Alps. *In* Phillips M., Springman S. & Arenson L. (eds.), *8th International Conference on Permafrost, Proceedings,* 2, Zürich. Swets & Zeitlinger, Lisse: 717–722.

Marchenko, S.S. 2001. A model of permafrost formation and occurrences in the intracontinental mountains. *Norwegian Journal of Geography* 55 (4): 230–234.

Mark, D.M. 1975. Geomorphometric parameters: a review and evaluation. *Geografiska Annaler, Series A* 57: 165–177.

Martin, H.E., Whalley, W.B., Orr, J. & Caseldine, C. 1994. Dating and interpretation of rock glaciers using lichenometry, South Tröllaskagi, North Iceland. *In* Stötter J. & Wilhelm F. (eds.), *Environmental Change in Iceland* 12: 205–224.

Matsuoka, N. 1990. The rate of rock weathering by frost action: field measurements and predective model. *Earth Surface Processes and Landforms* 15: 73–90.

Matsuoka, N. & Ikeda, A. 2001. Geological control on the distribution and characteristics of talus-derived rock glaciers. *Annual Report of the Institute of Geosciences, University of Tsukuba, Japan* 27: 11–16.

Matthews, J.A. & Shakesby, R.A. 1984. The status of the 'Little Ice Age' in southern Norway: relative-age dating of Neoglacial moraines with Schmidt hammer and lichenometry. *Boreas* 13: 333–346.

McCarthy, J.J., Canziani, O.F., Leary, N.A., Dokken, D.J. & White, K.S. 2001. Contribution of Working Group II to the Third Assessment Report of the Intergovernmental Panel on Climate Change (IPCC). Cambridge University Press, UK: 1000 pp.

Moore, I.D., Grayson, R.B. & Ladson, A.R. 1990. Digital terrain modelling: a review of hydrological, geomorphological and biological applications. *Hydrological processes* 5: 3–30.

Nesje, A., Blikra, L.H. & Anda, E. 1994. Dating rockfall-avalanche deposits from degree of rock-surface weathering by Schmidt-Hammer tests – a study from Norangsdalen, Sunnmøre, Norway. *Norwegian Journal of Geography* 74 (2): 108–113.

Ødegård, R.S., Isaksen, K., Eiken, T. & Sollid, J.L. 2003. Terrain analyses and surface velocity measurements of the Hiorthfjellet rock glacier, Svalbard. *Permafrost and Periglacial Processes* 14: 359–365.

Olyphant, G.A. 1987. Rock glacier response to abrupt changes in talus production. *In* Giardino J.R., Shroder J.F. & Vitek J.D. (eds.), *Rock Glaciers*. Allen & Unwin, London: 55–64.

Osborn, G.D. 1975. Advancing rock glaciers in the Lake Louise area, Banff National Park, Alberta. *Canadian Journal of Earth Sciences* 12: 1060–1062.

Osterkamp, T.E. & Gosink, J.P. 1991. Variations in permafrost thickness in response to changes in paleoclimate. *Journal of Geophysical Research* 96 (B3): 4423–4434.

Outcalt, S.A. & Benedict, J.B. 1965. Photo-interpretation of two types of rock glaciers in the Colorado Front Range, USA. *Journal of Glaciology* 5 (42): 849–856.

Paterson, W.S.B. 1994. *The Physics of Glaciers*. Pergamon Press Ltd.: 380 pp.

Paul, F. 2003. The new Swiss Glacier Inventory 2000. Application of Remote Sensing and GIS. PhD-thesis, Department of Geography, University of Zurich: 192 pp.

Paul, F., Kääb, A., Maisch, M., Kellenberger, T. & Haeberli, W. 2002. The new remote sensing derived Swiss glacier inventory: I. Methods. *Annals of Glaciology* 34: 355–361.

Payne, D. 1998. Climatic implications of rock glaciers in the arid Western Cordillera of the Central Andes. *Glacial Geology and Geomorphology* rp03/1998: HTML-page: http://ggg.qub.ac.uk/ggg/papers/full/1998/rp031998/rp03.htm.

Pike, R.J. 1995. Geomorphometry – process, practice and prospect. *Zeitschrift für Geomorphologie* 101: 221–238.

—. 2000. Geomorphometry – diversity in quantitative surface analysis. *Progress in Physical Geography* 24 (1): 1–20.

—. 2002. A bibliography of terrain modeling (geomorphometry), the quantitative representation of topography – Supplement 4.0. U.S. Department of the Interior, U.S. Geological Survey, Open-file report 02-465.

Poser, H. 1954. Die Periglazial-Erscheinungen in der Umgebung der Gletscher des Zemmgrundes (Zillertaler Alpen). *Göttinger Geographische Abhandlungen* 15: 125–180.

Prick, A. 2003. Frost weathering and rock fall in an arctic environment, Longyearbyen, Svalbard. *In* Phillips M., Springman S. & Arenson L. (eds.), *8th International Conference on Permafrost, Proceedings,* 2, Zürich. Swets & Zeitlinger, Lisse: 907–912.

Rapp, A. 1960. Recent development of mountain slopes in Kärkevagge and surroundings, northern Scandinavia. *Geografiska Annaler* 42: 71–200.

Raymond, M.J. 2001. Analysis of near-surface temperatures in high mountain permafrost environment, Study at Murtèl-Corvatsch, Swiss Alps. Unpublished MSc-thesis, Swiss Federal Institute of Technology, Zurich: 65 pp.

Rignot, E., Hallet, B. & Fountain, A. 2002. Rock glacier surface motion in Beacon Valley, Antarctica, from synthetic-aperture radar interferometry. *Geophysical Review Letters* 10.1029/2001GL013494 29 June 2002.

Ritter, C. 1852a. Bemerkungen über Veranschaulichungsmittel räumlicher Verhältnisse bei graphischen Darstellungen durch Form und Zahl. *Sammlung der Abhandlungen Ritters*: 129–150.

—. 1852b. Über geographische Stellung und horizontale Ausbreitung der Erdteile. *Sammlung der Abhandlungen Ritters*: 103–128.

Roberts, N. 2000. *The Holocene. An environmental history.* Blackwell Publishers Ltd., Oxford: 316 pp.

Rott, H., Scheuchl, B., Siegel, A. & Grasemann, B. 1999. Monitoring very slow slope movements by means of SAR interferometry; a case study from a mass waste above a reservoir in the Oetztal Alps, Austria. *Geophysical Research Letters* 26 (11): 1629–1632.

Rune, A. & Sjåstad, J.A. 2000. Schmidt hammer age evaluation of the moraine sequence in front of Bøyabreen, western Norway. *Norwegian Journal of Geology* 80 (1): 27–32.

Sass, O. 1998. Die Steuerung von Steinschlagmenge und -verteilung durch Mikroklima, Gesteinsfeuchte und Gesteinseigenschaften im westlichen Karwendelgebirge (Bayerische Alpen). *Münchener Geographische Abhandlungen B* 29: 175 pp.

Schmidt, E. 1950. Der Beton-Prüfhammer – Ein Gerät zur Bestimmung der Qualität des Betons im Bauwerk. *Schweizerische Bauzeitung* 68 (28): 378–379.

—. 1951. A non-destructive concrete tester. *Concrete* 59 (8): 34–55.

Schmidt, J. & Dikau, R. 1999. Extracting geomorphometric attributes and objects from digital elevation models – semantics, methods, future needs. *In* Dikau R. & Saurer H. (eds.), *GIS for Earth Surface Systems. Analysis and modelling of the natural enviroment*. Gebrüder Bornträger, Stuttgart: 153–174.

Schrott, L. 1998. The hydrological significance of high mountain permafrost and its relation to solar radiation. A case study in the high Andes of San Juan, Argentina. *Bamberger Geographische Schriften* 15: 71–84.

Schwarb, M., Frei, C., Schär, C. & Daly, C. 2000. Mean annual precipitation throughout the European Alps 1971–1990. Hydrological Atlas of Switzerland, Zurich: Plate 2.6.

Shumskii, P.A. 1964. *Principles of structural glaciology*. Dover Publications, Inc., New York: 497 pp.

Sipper, M. 1997. *Evolution of parallel cellular machines: the cellular programming approach*. Springer, Heidelberg: 198 pp.

Skaug, Ø. 2000. Påvirkning fra skala, datastruktur og representasjon på kvalitet av terrengparametre brukt i digital relieffanalyse. Unpublished MSc-thesis, Department of Physical Geography, University of Oslo: 88 pp.

Sollid, J.L. & Sørbel, L. 1992. Rock glaciers in Svalbard and Norway. *Permafrost and Periglacial Processes* 3: 215–220.

Spitz, A. & Dyhrenfurth, G. 1907–1912. Geologische Karte der Engadiner Dolomiten zwischen Schuls, Scanfs und dem Stilfserjoch. 1:500'000. Beiträge zur geologischen Karte der Schweiz, Neue Folge, Lief. XLIV: Spezialkarte No. 72.

Stocker-Mittaz, C. 2002. Permafrost distribution modeling based on energy balance data. PhD-thesis, Department of Geography, University of Zurich: 122 pp.

Strozzi, T., Wegmüller, U., Kääb, A. & Frauenfelder, R. 2003. Satellite radar interferometry for detecting and quantifying mountain permafrost creep. *In* Haeberli W. & Brandova D. (eds.), *8th International Conference on Permafrost, Extended Abstracts,* Zürich. University of Zurich: 155–156.

Strozzi, T., Kääb, A. & Frauenfelder, R. 2004. Detecting and quantifying mountain permafrost creep from in situ inventory, space-borne radar interferometry and airborne digital photogrammetry. *International Journal of Remote Sensing* 25 (15): 2919–2931.

Sulebak, J.R., Etzelmüller, B. & Sollid, J.L. 1997. Landscape regionalisation by automatic classification of terrain elements. *Norwegian Journal of Geography* 51: 35–45.

Sumner, P. & Nel, W. 2002. The effect of rock moisture on Schmidt Hammer rebound: tests on rock samples from Marion Island and South Africa. *Earth Surface Processes and Landforms* 27: 1137–1142.

Taschner, S. & Ranzi, R. 2002. Landsat-TM and ASTER data for monitoring a debris covered glacier in the Italian Alps within the GLIMS project. *IGARSS 2002, Proceedings,* 4, Toronto, Canada: 1044–1046.

Van Deursen, W.P.A. 1995. Geographical Information Systems and Dynamic Models – Development and application of a prototype spatial modelling language. PhD-thesis, Faculty of Spatial Sciences, University of Utrecht: 126 pp.

van Dijke, J.J. & van Westen, C.J. 1990. Rockfall hazard, a geomorphological application of neighbourhood analysis with ILWIS. *ITC Journal* 1: 40–44.

VAW. 1992a. Murgänge 1987: Dokumentation und Analyse. Teil 1. Bericht im Auftrag des Bundesamtes für Wasserwirtschaft. Versuchsanstalt für Wasserbau, Hydrologie und Glaziologie, ETH Zürich, Unpublished report 97.6.: 264 pp.

—. 1992b. Murgänge 1987: Dokumentation und Analyse. Teil 2. Bericht im Auftrag des Bundesamtes für Wasserwirtschaft. Versuchsanstalt für Wasserbau, Hydrologie und Glaziologie, ETH Zürich, Unpublished report 97.6: p. 175 pp. + Annex.

Vikhamar, D. 2003. Snow-cover mapping in forests by optical remote sensing. PhD-thesis No. 259, Faculty of Mathematics and Natural Sciences, University of Oslo: 127 pp.

Von Neumann, J. 1966. *Theory of self-reproducing automata.* Urbana/University of Illinois Press, Illinois: 388 pp.

Vonder Mühll, D. 1993. Geophysikalische Untersuchungen im Permafrost des Oberengadins. *Mitteilungen der VAW-ETH Zürich* 122: 222 pp.

Vonder Mühll, D. & Holub, P. 1992. Borehole logging in Alpine permafrost, Upper Engadin, Swiss Alps. *Permafrost and Periglacial Processes* 3 (2): 125–132.

Vonder Mühll, D., Stucki, T. & Haeberli, W. 1998. Borehole-temperatures in alpine permafrost: a ten year series. *In* Lewkowicz A.G. & Allard M. (eds.), *7th International Conference on Permafrost, Proceedings,* 57, Yellowknife, Canada. Centre d'Etudes Nordiques, Université Laval: 1089–1095.

Wagner, S. 1992. Creep of Alpine permafrost, investigated on the Murtèl-rock glacier. *Permafrost and Periglacial Processes* 3 (2): 157–162.

—. 1996. Dreidimensionale Modellierung zweier Gletscher und Deformationsanalyse von eisreichem Permafrost. *Mitteilungen der VAW-ETH Zürich* 146: 104 pp.

Wahrhaftig, C. & Cox, A. 1959. Rock glaciers in the Alaska Range. *Bulletin of the Geological Society of America* 70: 383–436.

Washburn, A.L. 1979. *Geocryology – A survey of periglacial processes and environments.* Edward Arnold Ltd., London: 406 pp.

Wesseling, C.G., Karssenberg, D., Van Deursen, W.P.A. & Burrough, P.A. 1996. Integrating dynamic environmental models in GIS: the development of a dynamic modelling language. *Transactions in GIS* 1: 40–48.

Whalley, W.B. & Martin, H.E. 1992. Rock glaciers. Part II: Models and mechanisms. *Progress in Physical Geography* 16 (2): 127–186.

—. 1994. Rock glaciers in Tröllaskagi: their origin and climatic significance. *In* Stötter J. & Wilhelm F. (eds.), *Environmental Change in Iceland* 12: 289–308.

White, P.G. 1979. Rock glacier morphometry, San Juan Mountains, Colorado. *Bulletin of the Geological Society of America* 90: 515–518.

Wilson, J.P. & Gallant, J.C. 2000. *Terrain analysis – principles and applications*. John Wiley & Sons, New York: 479 pp.

Winkler, S. & Shakesby, R.A. 1995. Anwendung von Lichenometrie und Schmidt-Hammer zur relativen Altersdatierung prä-frührezenter Moränen am Beispiel der Vorfelder von Guslar-, Mitterkar-, Rofenkar- und Vernagtferner (Ötztaler Alpen/Österreich). *Petermanns Geographische Mitteilungen* 139 (5/6): 283–304.

Zemp, M. 2002. GIS-basierte Modellierung der glazialen Sedimentbilanz. Unpublished MSc-thesis, Department of Geography, University of Zurich: 99 pp.

Personal bibliography

The papers which this thesis is based on are marked with an asterisk *), see *List of Papers*, p. v and *Part II: Full papers*.

Reviewed journals

Burga, C., Frauenfelder, R., Ruffet, J., Hoelzle, M. & Kääb, A. 2004. Vegetation on Alpine rock glacier surfaces: a contribution to abundance and dynamics on extreme plant habitats. *Flora* 199: 505–515.

*) Frauenfelder, R. & Kääb, A. 2000. Towards a palaeoclimatic model of rock glacier formation in the Swiss Alps. *Annals of Glaciology* 31: 281–286.

*) Frauenfelder, R., Haeberli, W., Hoelzle, M. & Maisch, M. 2001. Using relict rock-glaciers in GIS-based modelling to reconstruct Younger Dryas permafrost distribution patterns in the Err-Julier area, Swiss Alps. *Norwegian Journal of Geography* 55 (4): 195–202.

Frauenfelder, R., Kääb, A. & Haeberli, W. in prep. Perennial ice patches in mountain areas: origin, processes, distribution and age.

*) Frauenfelder, R., Schneider, B. & Etzelmüller, B. submitted. Morphometric modelling of rockglaciers – A case study from the Alps. *Earth Surface Processes and Landforms*.

*) Frauenfelder, R., Laustela, M. & Kääb, A. 2005. Relative age dating of Alpine rockglacier surfaces. *Zeitschrift für Geomorphologie N.F.* 49 (2): 145–166.

Haeberli, W., Frauenfelder, R., Hoelzle, M. & Maisch, M. 1999a. On rates and acceleration trends of global glacier mass changes. *Geografiska Annaler* 81A (4): 585–591.

Haeberli, W., Frauenfelder, R., Kääb, A. & Wagner, S. 2004. Characteristics and potential climatic significance of "miniature ice caps" (crest- and cornice-type low-altitude ice archives). *Journal of Glaciology* 50 (168): 129–136.

Strozzi, T., Kääb, A. & Frauenfelder, R. 2004. Detecting and quantifying mountain permafrost creep from in situ inventory, space-borne radar interferometry and airborne digital photogrammetry. *International Journal of Remote Sensing* 25 (15): 2919–2931.

Conference proceedings and contributions to books

Frauenfelder, R. 1998. Permafrostuntersuchungen mit GIS. Eine Studie im Fletschhorn-gebiet. *In* Vonder Mühll, D. (ed.), Beiträge aus der Gebirgs-Geomorphologie, Samedan, Schweiz. *Mitteilungen der VAW-ETH Zürich* 158: 55–68.

Frauenfelder, R., Allgöwer, B., Haeberli, W. & Hoelzle, M. 1998. Permafrost investigations with GIS - a case study in the Fletschhorn area, Wallis, Swiss Alps. *In* Lewkowicz A.G. & Allard M. (eds.), *7th International Conference on Permafrost, Proceedings,* 57, Yellowknife, Canada. Centre d'Etudes Nordiques, Université Laval: 291–295.

*) Frauenfelder, R., Haeberli, W. & Hoelzle, M. 2003. Rockglacier occurrence and related terrain parameters in a study area of the Eastern Swiss Alps. *In* Phillips, M., Springman, S. & Arenson, L. (eds.), *8th International Conference on Permafrost, Proceedings,* 1, Zürich. Swets & Zeitlinger, Lisse: 253–258.

Frauenfelder, R., Laustela, M. & Kääb, A. 2004. Velocities and relative surface ages of selected Alpine rockglaciers. *In* Minor, H.-E., Bezzola, G.R. & Semadeni, N. (eds.), Turbulenzen in der Geomorphologie. Jahrestagung der Schweizerischen Geomorphologischen Gesellschaft (SGmG) der SANW. *Mitteilungen der VAW/ETH Zürich*, 184: 103–118

Haeberli, W., Brandova, D., Burga, C., Egli, M., Frauenfelder, R., Kääb, A., Maisch, M., Mauz, B. & Dikau, R. 2003. Methods for absolute and relative age dating of rockglacier surfaces in alpine permafrost. *In* Phillips, M., Springman, S. & Arenson, L. (eds.), *8th International Conference on Permafrost, Proceedings,* 1, Zürich. Swets & Zeitlinger, Lisse: 343–348.

Keller, F., Frauenfelder, R., Gardaz, J.-M., Hoelzle, M., Kneisel, C., Lugon, R., Phillips, M., Reynard, E. & Wenker, L. 1998. Permafrost map of Switzerland. *In* Lewkowicz A.G. & Allard M. (eds.), *7th International Conference on Permafrost, Proceedings,* 57, Yellowknife, Canada. Centre d'Etudes Nordiques, Université Laval: 557–562.

Laustela, M., Egli, M., Frauenfelder, R., Kääb, A., Maisch, M. & Haeberli, W. 2003. Weathering rind measurements and relative age dating of rockglacier surfaces in crystalline regions of the Eastern Swiss Alps. *In* Phillips, M., Springman, S. & Arenson, L. (eds.), *8th International Conference on Permafrost, Proceedings,* 1, Zürich. Swets & Zeitlinger, Lisse: 627–632.

Maisch, M., Haeberli, W., Frauenfelder, R., Kääb, A. & Rothenbühler, C. 2003. Late-glacial and Holocene evolution of glaciers and permafrost in the Val Muragl, Upper Engadin, Swiss Alps. *In* Phillips, M., Springman, S. & Arenson, L. (eds.), *8th International Conference on Permafrost, Proceedings,* 2, Zürich. Swets & Zeitlinger, Lisse: 717–722.

Non-reviewed

Etzelmüller, B., Heggem, E.S.F., Frauenfelder, R., Sharkhuu, N., Jambaljav, Y., Tumentsetseg, S., Romanovsky, V. & Kääb, A. 2002. Permafrost mapping and distribution modelling at the eastern shore of Lake Hövsgöl, northern Mongolia. Report from the field campaign in summer 2002. Report to the GEF/World Bank, Project MSP-R080601.

Frauenfelder, R. 1998. Rock Glaciers, Fletschhorn Area, Valais, Switzerland. Circumpolar active-layer permafrost system (CAPS), version 1.0. International Permafrost Association, Data and Information Working Group, National Snow and Ice Data Center/World Data Center for Glaciology, Boulder, CO. (CD ROM).

Frauenfelder, R., Etzelmüller, B. & Schneider, B. 2002. Geomorphometric modeling of rockglaciers. *ESRI International User Conference 2002, 8–12 July, Proceedings*, San Diego, U.S: http://gis.esri.com/library/userconf/proc02/pap1190/p1190.htm.

Frauenfelder, R., Haeberli, W., Kääb, A., Busarello, C., Hager, P. & Wagner, S. 2001. Low altitude ice archives. Scientific report from partner 7 (GIUZ), WP3(C). *In* Wagenbach, D. (ed.), *Environmental and Climatic Records from High Elevation Alpine Glaciers (ALPCLIM)*, Final Report, Third year activity report of individual partners: Appendix.

Frauenfelder, R. & Schneider, B. 2003. Dynamic modelling of rockglaciers with GIS. *In* Wood, J. (ed.), *GIS Research UK, 11th Annual Conference 2003, 7–9 April, Proceedings,* 1, London: 58–61.

Goulden, C., Sharkhuu, N., Jambaljav, Ya., Etzelmüller, B., Heggem, E.S.F., Romanovsky, V., Frauenfelder, R., Kääb, A., Ariuntsetseg, L. & Saruul, N., Tumentsetseg S. 2003. New permafrost studies at Lake Hövsgöl, North-central Mongolia. *In* Haeberli, W. & Brandova, D. (eds.), *8th International Conference on Permafrost, Extended Abstracts,* Zürich: 45–46.

Hoelzle, M., Dischl, M. & Frauenfelder, R. 2000. Weltweite Gletscherbeobachtung als Indikator der globalen Klimaänderung. *Vierteljahresschrift der Naturforschenden Gesellschaft Zürich* 145 (1): 5–12.

IAHS(ICSI)/UNEP/UNESCO. 1999. Glacier Mass Balance Bulletin no. 5. Haeberli, W., Hoelzle, M. & Frauenfelder, R. (eds.), World Glacier Monitoring Service, University of Zurich and ETH Zurich: 96 pp.

IAHS(ICSI)/UNEP/UNESCO. 1998. Fluctuations of Glaciers 1990-1995, Vol. VII. Haeberli, W., Hoelzle, M., Suter, S. & Frauenfelder, R. (eds.), International Association of Hydrological Sciences, Paris: 296 pp.

IAHS(ICSI)/UNEP/UNESCO/WMO. 2001. Glacier mass balance bulletin no. 6. Haeberli, W., Frauenfelder, R. & Hoelzle, M. (eds.), World Glacier Monitoring Service, University of Zurich and ETH Zurich: 93 pp.

—. 2003. Glacier mass balance bulletin no. 7. Haeberli, W., Frauenfelder, R., Hoelzle, M. & Zemp, M. (eds.), World Glacier Monitoring Service, University of Zurich: 87 pp.

Strozzi, T., Wegmüller, U., Kääb, A. & Frauenfelder, R. 2003a. Satellite radar interferometry for detecting and quantifying mountain permafrost creep. *In* Haeberli, W. & Brandova, D. (eds.), *8th International Conference on Permafrost, Extended Abstracts,* Zürich: 155–156.

Strozzi, T., Kääb, A., Frauenfelder, R. & Wegmüller, U. 2003b. Detection and monitoring of unstable high-mountain slopes with L-band SAR Interferometry. *Learning from Earth's shapes and colors. International Geoscience and Remote Sensing Symposium (IGARSS), 21-25 July 2003, Proceedings*, Toulouse, France. 0-7803-7930-6, FR09_1040 (CD-ROM).

Strozzi, T., Wegmüller, U., Wiesmann, A., Kääb, A., Frauenfelder, R., Werner, C., Graf, K., Rätzo, H. & Lateltin, O. 2003. Differential interferometric applications in Alpine regions. *Third ESA International Workshop on ERS SAR Interferometry and first Workshop on ASAR interferometry: ADVANCES in SAR interferometry from ERS and ENVISAT missions, 2–5 December 2003, Proceedings,* ESA ESRIN, Frascati, Italy. (CD-ROM).

Suter, S., Haeberli, W., Hoelzle, M., Frauenfelder, R., Rossi, G. & Wagner, S. 2001. Glacio-Climatology of Alpine ice archives. *In* Wagenbach, D. (ed.), *Environmental and Climatic Records from High Elevation Alpine Glaciers (ALPCLIM)*, Final Report, Scientific reports: II-131 – II-162.

Acknowledgements

"To write a doctoral thesis is a research education, but also a life experience"
(Vikhamar 2003)

Although it looked like an easy trip at the beginning, my journey to Mt. PhD turned out to be a strenuous, lengthy expedition with, at times, a rather unsure outcome. Fortunately, I was accompanied by a great and helpful team which, in the end, made the climb a both successful and rewarding experience.

My sincerest thanks go, therefore, to:

- Wilfried Haeberli, who inspired me to venture this climb, gave me the necessary post to do so and trusted me to find my own route to the summit, although I know I sometimes strained his trust quite a bit,
- Martin Hoelzle and Bernhard Schneider, who had the difficult task of being both friend and tour guide, but handled the job brilliantly. Their enthusiasm, encouragement and most helpful contributions were critical for my journey,
- Bernd Etzelmüller, who invited me to a training camp in Norway where I had the opportunity to learn new skills which proved to be helpful during my climb,
- Max Maisch, for making unpublished maps and data available to me, but especially for many good discussions and for his belief in my ability to reach the summit, and his constant encouragement to go on,
- Stefan Imfeld, Phillipe Meuret, Peter Schmid, Bruno Weber, Thomas Werschlein, Othmar Wigger, and Daniel Wirz, who tended the expedition equipment 365 days a year and 24 hours a day, and solved (almost) all the hard- and software problems I managed to run into,
- Frank Paul who provided, whenever needed, satellite imagery of the area concerned, helped by offering a thousand (sometimes life-saving) tips and tricks, and by reading the first version of this expedition report with incredible attention to detail,
- Ivan Woodhatch who solved many fiddly technical problems and improved my knowledge of the English language,
- Susan Braun-Clarke, for polishing the English of the present expedition report,

– Perscheng Assef, Michaela Honegger, and Waldemar A. Keller, for clearing away bureaucratic obstacles, keeping the material depot always filled, organizing summit permits and much, much more,

– Sven Girsperger, for loaning me his large archive of literature and giving me access to a considerable amount of unpublished data on the Val Sassa rockglacier,

– all the colleagues at the Department of Geography for a most enjoyable time. In particular to those colleagues at expedition headquarters on the H- and K-floors, for being the best bunch of people one could ever wish to share such an expedition with! Thank you all: Perscheng Assef, Christof Benz, Dagmar Brandova, Sabina Dürrenberger, Eileen Eckmeier, Markus Egli, Stephan Gruber, Samuel Guex, Patrick Hager, Karen Hammes, Susanne Hanson, Alexander Heim, Christian Hitz, Martin Hoelzle, Christian Huggel, Anna Jablonkay, Andreas Kääb, Bruno Kägi, Stefan Kappeler, Matias Laustela, Guido Lüniger, Stephan Margreth, Jeannette Nötzli, Frank Paul, Nadine Salzmann, Catherine Stocker-Mittaz, Andreas Wipf, Ivan Woodhatch, Remo Zanelli, Michael Zemp, and Sonja Zgraggen-Oswald,

– Mirjam Friedli, Susanne Hanson, Barbara Klinger, Michael Kollmair, Sabine Mühlinghaus, and Heidi Preisig who helped me train my "brain, body and soul" in the lush forests at Zürichberg, in the Gaswerk or in some scary rock wall,

– Eva Heggem, Anne Ines, Ketil Isaksen, G. Nína Petersen, Ranghild Riise, Rolf Sethre, and Vigdis Solhaug for helping me to make the most of the training camp in Norway,

– Brigitte Birk-Hölzle, Milena Conzetti, Charis and Felix Keller-Lengen, Christine Rothenbühler, and Barbara Schellenberg, with daughters, for letting me use their base camps,

– the 'Stiftung zur Förderung der wissenschaftlichen Forschung an der Universität Zürich' and the Research Council of Norway, Oslo, for financially supporting the expedition.

And last, but certainly not least, my thanks go to:

– my parents for unfailing moral support, and, perhaps even more important, for letting me follow my own path, even though it clearly did not lead to a career in banking,

– all my friends, for not tiring, over the years, of my frosty business and for being part of many most rewarding base camp activities,

– Andi, for immense support in various fields (photogrammetry, modelling, etc.), but even more important, for being my rock in the sea of life.

Zurich, 1st of April 2004

Part II: Papers

I

Z. Geomorph. N.F.	**49**	2	145–166	Berlin · Stuttgart	Juni 2005

Relative age dating of Alpine rockglacier surfaces

by

R. FRAUENFELDER, M. LAUSTELA and A. KÄÄB

with 10 figures and 1 table

Summary. The present work discusses the application of photogrammetry, and the measurements of Schmidt-hammer rebound values and weathering rind thicknesses, for the relative age dating of Alpine rockglaciers, based on data from six rockglaciers in the Swiss Alps. Rockglaciers are formed by the continuous deformation of ice-rich debris material, with the result that the age of the surface becomes greater along the flowlines from the root zone to the rockglacier front. This can be demonstrated by applying both the Schmidt-hammer rebound values (which diminish as weathering, or duration of surface exposure, increases) and the weathering rind thicknesses (which grow as weathering increases). The results of these two methods correlate well with chronologies estimated from photogrammetric streamline interpolations. They also indicate that the minimum surface age of the investigated rockglaciers is between 3 and 5 ka. This implies that most of these rockglaciers began to evolve during the early Holocene or, at the latest, after the end of the Holocene temperature optimum (approx. 5000 y BP).

Zusammenfassung. *Relative Altersdatierung alpiner Blockgletscheroberflächen.* – In der vorliegenden Studie wird anhand von sechs Fallbeispielen aus den Schweizer Alpen über die Anwendung von Photogrammetrie und die Messung von Schmidt-Hammer Rückprallwerten und Verwitterungsrindendicken zur Relativdatierung von alpinen Blockgletschern berichtet. Blockgletscher resultieren aus der kontinuierlichen Deformation von eisreichem Schuttmaterial, daher nimmt das Alter der Blöcke entlang einer Fliesslinie gegen die Blockgletscherfront hin zu. Dies kann sowohl anhand der Schmidt-Hammer Rückprallwerte (die mit steigendem Verwitterungsgrad einer Oberfläche abnehmen) als auch anhand der Verwitterungsrindendicken (die mit steigendem Verwitterungsgrad zunehmen) gezeigt werden. Die Resultate beider Methoden korrelieren gut mit Chronologien photogrammetrisch erstellter Fliesslinien. Die Messungen deuten auf ein minimales Oberflächenalter der untersuchten Blockgletscher von 3 bis 5 ka hin. Dies impliziert, dass die Entwicklung der Mehrzahl dieser Blockgletscher im frühen Holozän eingesetzt hat, oder spätestens nach dem Ende des Holozänen Temperaturoptimums (ca. 5000 Jahre vor heute).

Résumé. *Datation relative de surfaces de glaciers rocheux alpins.* – Ce travail traite de l'application de la photogrammétrie, des mesures de rebondissement Schmidt-hammer et des épaisseurs de croûte d'altération pour la datation relative de glaciers rocheux alpins, basé sur des données obtenues sur six glaciers rocheux dans les Alpes suisses. Les glaciers rocheux sont formés par la déformation continue de matériaux sédimentaires riches en glace, ce qui résulte en une augmentation de l'âge de la surface le long des lignes de fluage entre les racines du glacier rocheux et sont front. Ceci peut être mis en évidence par l'application des valeurs de la méthode Schmidt-hammer (qui diminuent lorsque la durée d'exposition de la surface augmente) et des épaisseurs de croûte d'altération (qui augmentent lorsque la durée de l'altération augmente). Les résultats de ces deux méthodes corrèlent

bien avec des chronologies estimées à partir d'interpolations photogrammétriques. Ils indiquent également que l'âge minimum de la surface des glaciers rocheux investigués est d'entre 3 et 5 ka, et que la plupart de ces glaciers rocheux ont commencé à évoluer au début de l'Holocène, ou au plus tard, après la fin de l'optimum climatique de l'Holocène (environ 5000 a BP).

1 *Research questions and geographical setting*

Rockglaciers are characteristic creep features of frozen material in high mountains. Their shape is the cumulative expression of their entire history, and they store information, in a complex way, about both their past and present environments. Permafrost conditions are a prerequisite for the formation and development of rockglaciers, hence climate is clearly one of the main determining factors in their evolution. As most rockglaciers evolved during historical and Holocene time periods (e.g. BARSCH 1996, HAEBERLI et al. 1999), they can potentially be used as paleoclimatic geo-indicators (e.g. BARSCH 1978, KERSCHNER 1983, HUMLUM 1998, FRAUENFELDER et al. 2001). The quantitative reconstruction of paleoclimatic data from rockglaciers still relies heavily on the dating of their age. This task has not yet been adequately fulfilled, however, as age estimates cannot be made properly on the basis of a sole indicator. For this reason, HAEBERLI et al. (2003) have proposed a dating strategy using a combination of absolute and relative age-determination methods, such as photogrammetric streamline interpolations, Schmidt-hammer rebound, weathering rind thickness, lichenometry, luminescence dating, cosmogenic (exposure) dating, and radiocarbon dating. Similar integrated approaches were suggested previously in other geomorphological fields, e.g. for the assessment of the temporal occurrence of landsliding (LANG et al. 1999).

The main aim of this study is to apply a subset of the techniques proposed above – namely photogrammetric velocity measurements and subsequent derivation of streamlines, measurements of weathering rind thicknesses and Schmidt-hammer rebound values – in order to estimate the relative age pattern on six selected rockglaciers in the Swiss Alps. Subsequently, the results will promote the better understanding of the surface evolution and surface age structure of Alpine rockglaciers in general. An overview of the measurements carried out on each rockglacier is given in Table 1. The locations of the investigated rockglaciers are indicated in Fig. 1.

Table 1 Measurements conducted on each rockglacier

Velocity measurements	Streamline interpolations	Schmidt-hammer measurements	Weathering rind thickness
Gianda Grischa	Gianda Grischa	Gianda Grischa	Gianda Grischa
Suvretta	Suvretta	Suvretta	Suvretta
Munteratsch	–	Munteratsch	Munteratsch
Albana	–	Albana	Albana
–	–	Bleis Marscha	Bleis Marscha
Findletälli	Findletälli	–	–

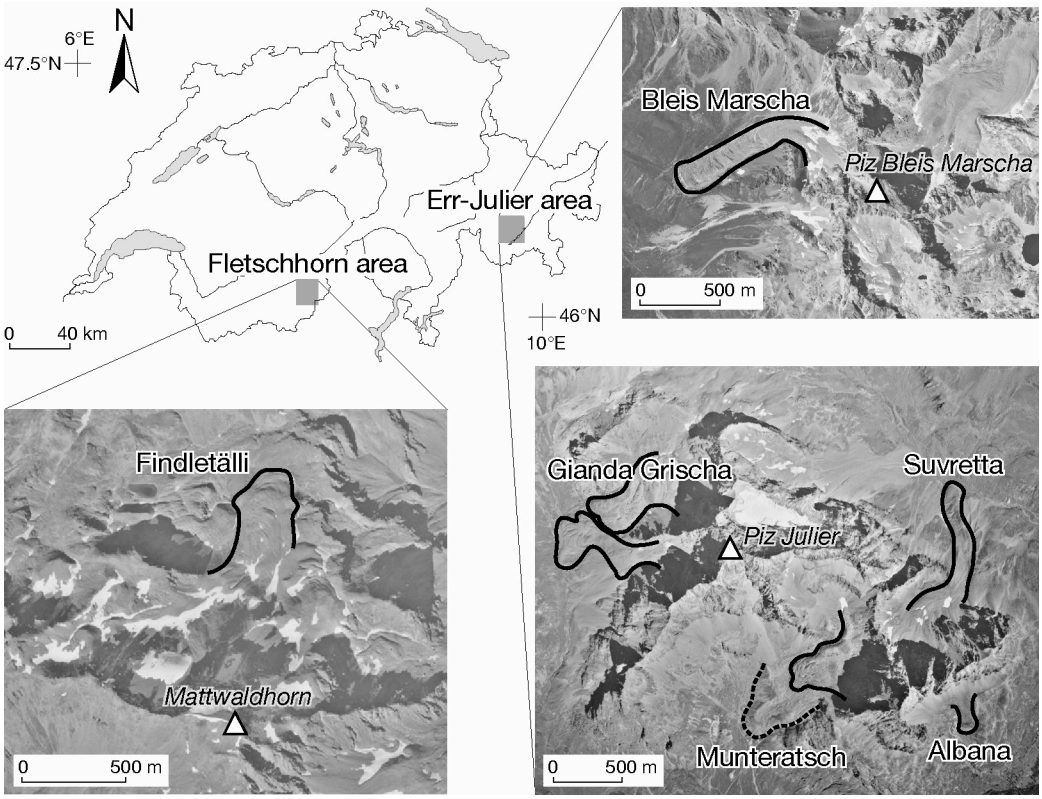

Fig. 1 Sketch map of Switzerland showing the locations of the rockglaciers studied and sections of aerial photographs with outlined rockglacier contours (continuous lines = active/ inactive rockglaciers, dashed line = relict rockglacier). Black-and-white aerial photographs from swisstopo (former Swiss Federal Office of Topography), upper right: 7.08.1991, Flight-line 54, Image-No. 7807, lower left: 1.9.1999, Flight-line 116, Image-No. 2641, lower right: 11.8.1998, Flight-line 152, Image-No. 4646.

2 *Methods and data*

2.1 *Velocity measurements and streamline calculations*

Multi-temporal digital elevation models with 10 m resolution were acquired automatically from overlapping digital aerial images using the commercial photogrammetric software SOCET SET© (LH Systems, San Diego, California, USA). Ortho-images with 0.2 m resolution were computed digitally using the scanned aerial photography and the respective digital elevation models. Horizontal surface displacements were then derived from these digital ortho-images using an image correlation technique developed by VOLLMER (1999) and described in detail in KÄÄB & VOLLMER (2000). Subsequently, entire surface flow fields can be measured either automatically (measurement points are then distributed on an evenly-spaced grid), or by selecting the measurement points manually.

The age structure of a rockglacier surface can be assessed from streamlines interpolated from such surface velocity fields (e.g. KÄÄB et al. 1998). Assuming steady-state conditions, these streamlines represent the trajectories of specific particles on the surface and can thus be used for both relative and absolute rockglacier age estimates.

In the present study, velocity measurements were conducted on five rockglaciers, while streamline interpolations were carried out for three rockglaciers only. On two rockglaciers (Munteratsch and Albana, see below), streamlines were not calculated, for two main reasons: firstly, the present-day movement of these rockglaciers is within the noise level of the measurements. Streamline interpolations would produce random and, therefore, valueless results. Secondly, the insignificant movement obtained during measuring indicates that these rockglaciers are inactive. Hence, their current velocity fields are not regarded as representative of past flow conditions.

2.2 *Schmidt-hammer measurements*

The Schmidt-hammer is a portable instrument originally developed in the early 1950s to measure the surface hardness of concrete by recording the rebound of a spring-loaded bolt impacting a surface (SCHMIDT 1950). Rock hardness, as reflected by hammer rebound values (R), is a function of the inherent intact rock strength. Weathering generally reduces rock strength and this is reflected in the rebound values measured (SUMNER & NEL 2002).

In this study, the Schmidt-hammer was used on five selected rockglaciers. On each rockglacier several transects were measured between its root zone and its front. The transects were measured on ridges, or in areas without ridges, perpendicular to the central flowline of the rockglacier. On each transect a random sample of fifty measurements was recorded, selecting clean surfaces of comparable lithology which were dry, flat, and free of lichens, visual fissures and cracks (cf. suggestions by WILLIAMS & ROBINSON 1983, SUMNER & NEL 2002). The mean of the values is taken as representative of the effective hardness of the rocks in the analyzed transect. To get a statistically significant and interpretable age difference between individual Schmidt-hammer transects, the standard error is given according to suggestions by WINKLER (2000), who calculated the standard error based on the standard deviation in a 95% confidence interval as:

$$x \pm 1.96 \times \sqrt{\frac{\sigma}{\sqrt{n}}}$$

where x is the statistical mean, σ the standard deviation and n the number of measurements.

2.3 *Weathering rind thickness measurements*

The weathering rind thickness, a reddish outer crust around the rock, corresponds to the extent to which oxidation of the minerals has penetrated below the surface of a boulder. In general, the thickness of the weathering rind increases with time and offers an indication of relative ages. Along the flow paths of a rockglacier surface, rock particles are increasingly subject to weathering processes. Consequently, the thickness of the weathering rind should increase along the central flowline(s) of a rockglacier.

At suitable sites with surface-exposed boulders, around 50 to 100 rind samples were chipped from boulders and cobbles with a hammer. Rind thicknesses were measured normal to the surface using a 0.1 mm scale graduated magnifying glass. Where possible, samples were measured on the same transects as the Schmidt-hammer measurements. The

measured values >0.5 mm were classified, following suggestions by McSAVENEY (1992), to the nearest of 0.2 mm; the data ≤0.5 mm were taken as measured. The data were then plotted in a frequency histogram which displays distribution patterns and modal values. The mode and additionally the median value are taken as relative age indicators (LAUSTELA 2003).

3 *Results*

The rockglaciers discussed in the following are named after the location names found on the 1:25,000 maps of *swisstopo* (former Swiss Federal Office of Topography). These location names go back many centuries and often illustrate how the landscape was perceived by the local residents.

3.1 *Gianda Grischa*

3.1.1 *Characteristics*

The name is derived from the pre-Roman words *gianda* standing for 'debris slope', 'stone pile' and *grischa* meaning 'grey' (SCHORTA 1991).

The large Gianda Grischa rockglacier is located on the western slopes of the Piz Julier and consists of two individual parts: a W-exposed active one of polymorphic (cf. FRAUENFELDER & KÄÄB 2000), or multi-lobe, multi-unit (cf. BARSCH 1996) and spatulate shape, and a W- to SW-oriented inactive rockglacier just north of the active one. This inactive rockglacier occupies a flat niche and is characterized by ridge-and-furrow surface topography. The active rockglacier considered here exhibits a flat root zone separated from the moderately flat tongue by a steep slope, and shows less pronounced ridges and furrows. In the steep slope, which is close to the maximum angle of repose, such structures are absent. This rockglacier is over 1000 m long, and the width of its transfer zone is ca. 170 m while its tongue is approximately 390 m wide. The rocks within the contributing headwalls belong to the Err-Bernina nappe, which is composed primarily of different types of granites, diorites and para-gneiss (SPICHER 1980).

According to SUTER (1981) and OHLENDORF (1998) the area in which the rockglacier is located was covered by a small mountain glacier during the Egesen stage of the Younger Dryas (YD) cold phase. In the subsequent warming periods, this glacier gradually decayed. During the 'Little Ice Age' (LIA) the catchment area of the currently active rockglacier was already free of surface ice, while the root zone of the northern, presently inactive rockglacier was still covered by a small cirque glacier (COAZ 1850). Today, both cirques are free of surface ice except for some very small (probably perennial) ice patches.

3.1.2 *Surface velocities and streamlines*

Horizontal average annual surface velocities between 1971 and 1998 were determined photogrammetrically. During the 27 years under observation, the active rockglacier crept downslope with an average velocity of approximately 0.4 to 0.5 ma^{-1}, reaching maximum velocities of up to 0.8 ma^{-1} in the steep slope between the root zone and the frontal parts (Fig. 2, above). The inactive rockglacier shows movements in the order of 0 to 0.16 ma^{-1}

(see area close to the upper edge of Fig. 2, above). These values are within or close to the range of error of the method for the aerial photography used and the time period considered (RMS ≈ 0.05 ma^{-1}, cf. KÄÄB & VOLLMER 2000).

Streamlines interpolated from the surface velocity field of the active rockglacier (Fig. 2 below) indicate a minimum surface age of 4 to 5 ka. Both frontal lobes of the spatulate tongue seem to be of comparable age and lie on an overridden, older tongue which shows no movement.

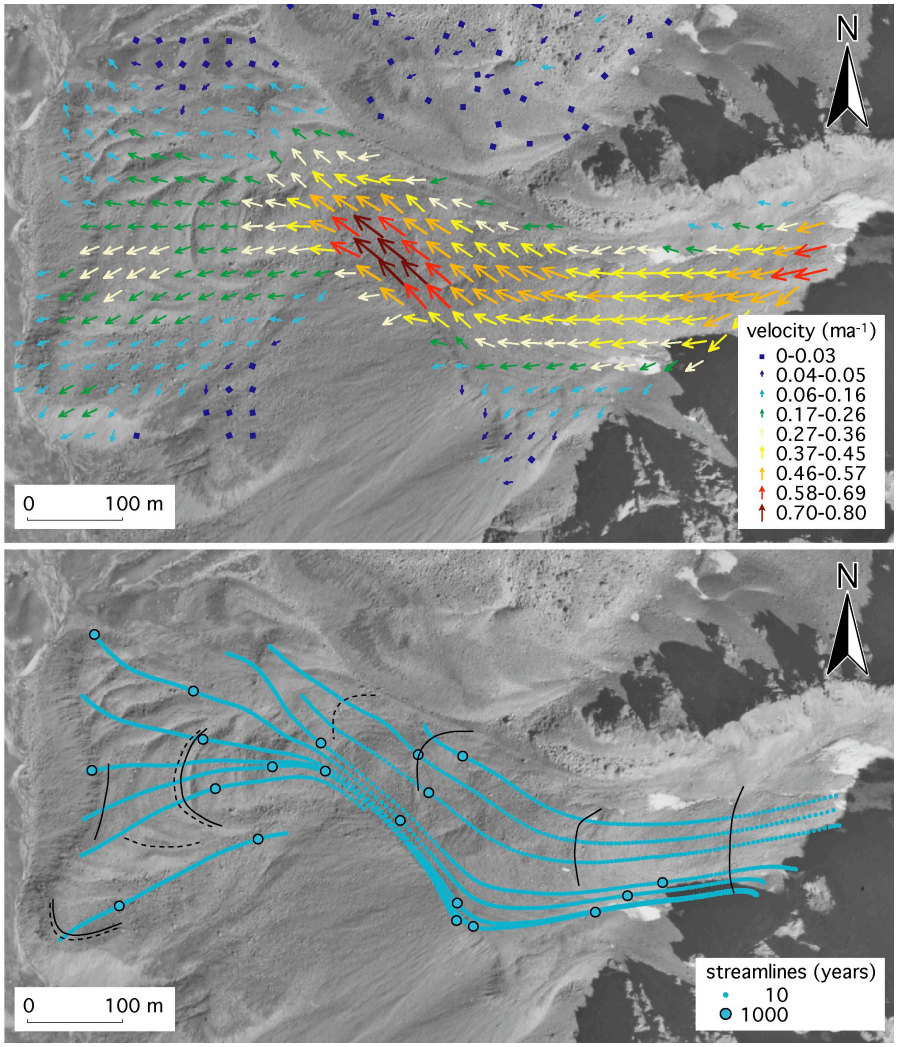

Fig. 2 Photogrammetrical measurements on the Gianda Grischa rockglacier, which is located at about 46°29'30"N/9°45'E. Upper image: horizontal average annual surface velocities between 1971 and 1998; lower image: streamline calculations. Black solid lines indicate Schmidt-hammer measurement transects; black dashed lines represent weathering rind measurement transects (see Fig. 3). Black-and-white aerial photograph from swisstopo, 11.08.1998, Flight-line 152, Image-No. 4647.

3.1.3 *Weathering*

Schmidt-hammer measurements on six transects present a complicated picture, although a trend to decreasing rebound values between the uppermost transect in the root zone and the lowermost transect at the front can be discerned (Fig. 3, left). The upper three transects (between the root zone and the steep slope) show similar rebound values, the values of the second three transects (closer to the front) decline from one transect to the next. However, in the steep slope between these two groups of transects, rocks are increasingly subject to gravity. This causes some boulders to tumble down and thus be turned around. The 'weathering clock' is restarted, resulting in higher values in the fourth transect (130 m from the front) than in the preceding ones (>370 m from the front).

Despite the rather complex picture presented by the Schmidt-hammer values, the general trend of the data seems to be confirmed by the results of the weathering rind measurements (Fig. 3, right). In a series of four transects on the orographic left side of the active rockglacier, steadily increasing degrees of weathering are indicated by both the modal and the median values of the weathering rind thicknesses. Maximum recorded weathering thickness is 1.6 mm (modal value) and 2.1 mm (median value), respectively (LAUSTELA 2003). On the orographic right side (not shown here) this trend cannot be discerned as clearly. Still, the measured weathering rind thicknesses are in the same range of values as on the left side of the rockglacier, indicating a similar age structure on both sides of the spatulate tongue.

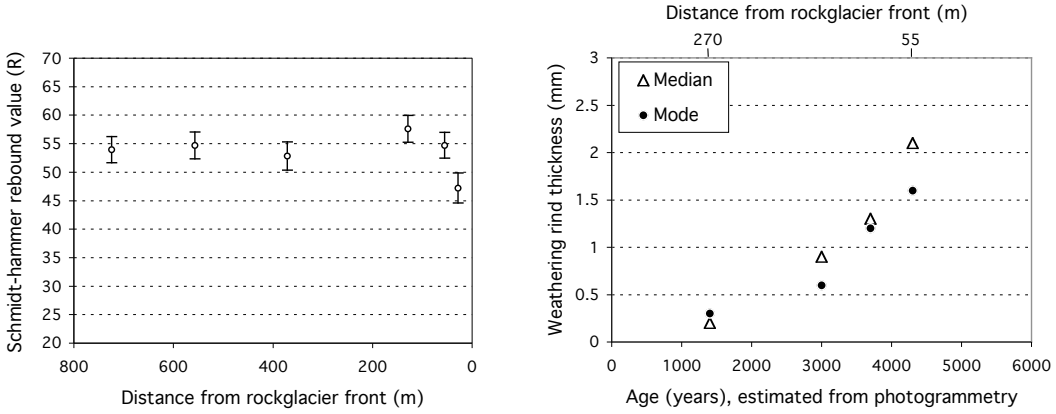

Fig. 3 Results of field measurements on the Gianda Grischa rockglacier. Left: Schmidt-hammer rebound values (R) showing the arithmetic mean on each transect with the corresponding standard error after WINKLER (2000); right: estimated age of weathering rind thickness transects, as derived from streamline interpolations (modified after LAUSTELA 2003). Creep direction in both graphs is from left to right.

As explained above, the weathering degree can be viewed as a proxy of the relative age. The results found here represent the anticipated increase in age of the surface material, and consequently of the whole creeping part of the rockglacier body from the root zone to its front (cf. HAEBERLI et al. 1998, HAEBERLI et al. 2003). In Fig. 3 (right) the measured rind thicknesses are shown in relation to the age as estimated from the photogrammetically derived streamlines. This comparison yields a growth rate of roughly 0.5 mm in 1 ka, a

value in the same range as values reported, for example, from measurements on sandstone (e.g. CHINN 1981, WHITEHOUSE et al. 1986).

3.2 *Suvretta*

3.2.1 *Characteristics*

The Suvretta rockglacier was named by its first investigators for the valley into which it creeps. Its exact location, however, is called *padriöl* which is a Rhaetoromanic word meaning 'funnel' (G.C. FEUERSTEIN, personal communication, 2004).

This name aptly describes the shape and the setting of the rockglacier (see Fig. 4) which is characterized by a large root zone surrounded by high contributing headwalls and a comparably thin monomorphic body (cf. FRAUENFELDER & KÄÄB 2000). This monomorphic body creeps ENE-ward out of the root zone, and turns N-ward over a steep slope before fronting on the alpine meadows 400 m below. The rockglacier has a total length of approximately 1270 m, and is between 150 and 170 m wide. Its tongue crept over a little brook (now flowing underneath it) and onto an alpine hiking trail which is re-located in sections according to the rockglacier's position. The surface topography is characterized by structures of compressive flow (ridge-and-furrow topography) in the lower, flatter part and by structures of extending flow (longitudinal ridges) in the steep slope. The rockglacier consists mainly of granitic boulders of the Err-Bernina nappe (SPICHER 1980).

Both Suter (1981) and Ohlendorf (1998) conclude that the area around the rockglacier was free of extensive surface ice during the end of the Lateglacial and the Holocene. In the oldest maps available of the area, the tongue of the rockglacier is marked very clearly and the rockglacier front is drawn close to the brook that the rockglacier has, in the meantime, overcrept (e.g. COAZ 1850, SCHWEIZ. EIDG. STABSBUREAU 1875). Similar to the Gianda Grischa rockglacier, the root zone area of the Suvretta rockglacier is free of surface ice today, except for some small ice patches.

3.2.2 *Surface velocities and streamlines*

Horizontal surface displacement rates for the period from 1971 to 1998 are in the range of 0.06 to 1.6 ma^{-1}, with maximum velocities in the steeply sloping middle part of the rockglacier (Fig. 4, left).

KÄÄB & FRAUENFELDER (2001) found slightly higher maximum velocities (up to 2 ma^{-1}) for the period from 1992 to 1997, with speed variations within several years reaching ±15%.

The mimimum surface age at the rockglacier front as calculated from streamlines derived from the current velocity field amounts to approximately 3 ka (Fig. 4, right).

3.2.3 *Weathering*

Schmidt-hammer measurements were carried out by CASTELLI (2000) and are shown in Fig. 5 (left). A clear decrease in rebound values can be discerned between the uppermost transect, just below the steep slope, and the second-lowermost one, at 95 m from the

rockglacier front. The transect at the very front shows a slightly higher mean than the second-last transect.

These findings are supported by the results of weathering rind measurements (LAUSTELA 2003, LAUSTELA et al. 2003): the thickness of the rinds shows a clear increase between the uppermost transect (modal value = 0.1 mm, median value = 0.2 mm) and the lowermost transect at the front (modal value = 3 mm, median value = 2.6 mm). Comparison with the photogrammetrically derived streamlines (Fig. 5, right) yields a weathering rind growth rate of approximately 1 mm in 1 ka. This result is in the same order of magnitude as values reported by CHINN (1981), for example, but considerably higher than values found by OGUCHI (2001). Furthermore, the value is twice as high as the one obtained on Gianda Grischa rockglacier (see Fig. 3, right), although both rockglaciers are composed of the same rock types.

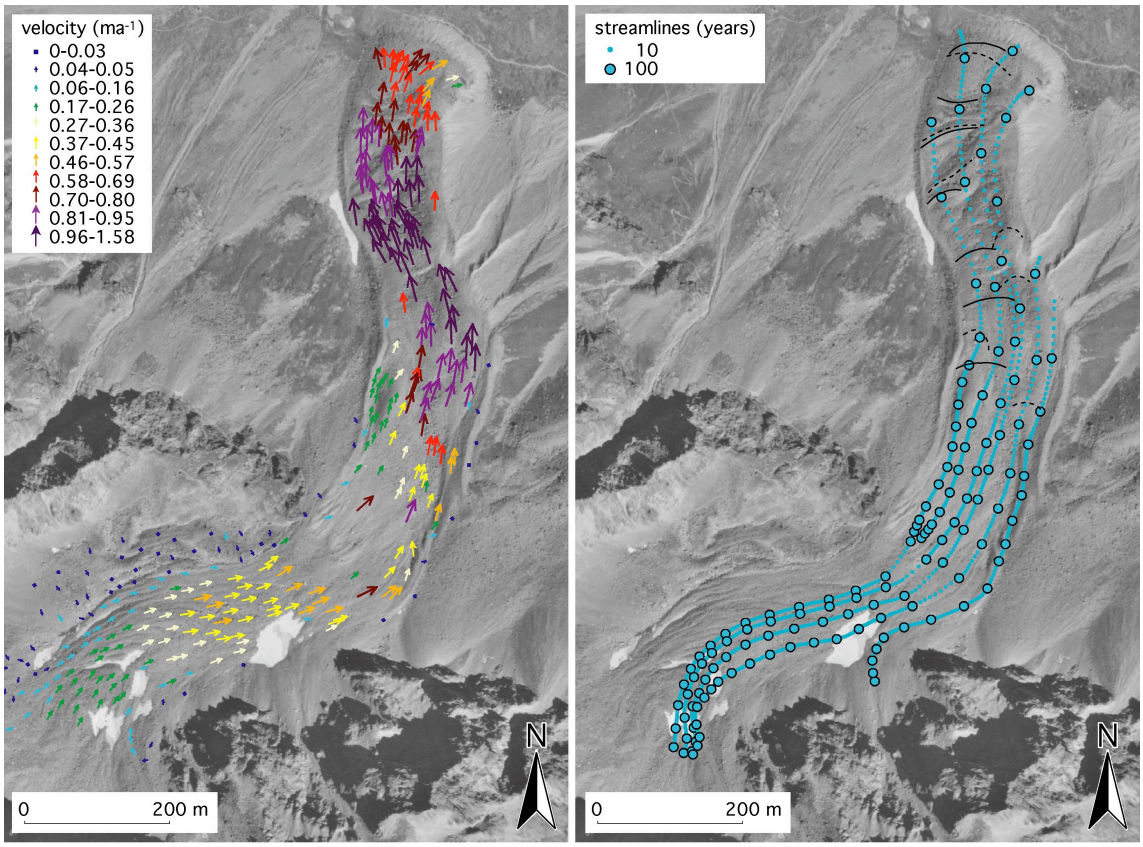

Fig. 4 Photogrammetrical measurements on the Suvretta rockglacier, which is located at about 46°29'30"N/9°47'15"E. Left: horizontal average annual surface velocities between 1971 and 1998; right: streamline calculations. Black solid lines indicate Schmidt-hammer measurement transects, black dashed lines represent weathering rind measurement transects (see Fig. 5). Black-and-white aerial photograph from swisstopo, 11.08.1998, Flight-line 152, Image-No. 4644.

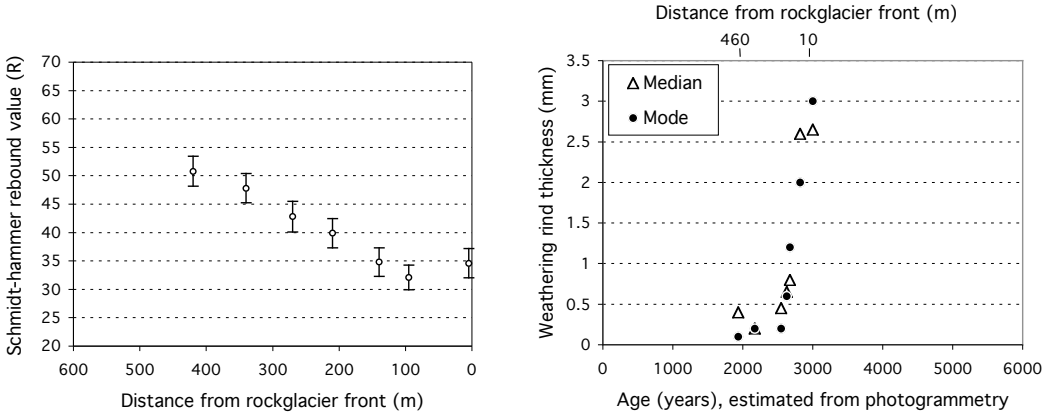

Fig. 5 Results of field measurements on the Suvretta rockglacier. Left: Schmidt-hammer rebound values (R) showing the arithmetic mean on each transect with the corresponding standard error after Winkler (2000), (source data from Castelli 2000); right: estimated age of weathering rind thickness transects as derived from streamline interpolations (modified after Laustela 2003). Creep direction in both graphs is from left to right.

3.3 *Munteratsch*

3.3.1 *Characteristics*

The name originates from the words *munter/murter* derived from the Latin word *mortarium* for 'mortar', probably as a landform specification for 'trough' or 'hollow' (SCHORTA 1991).

This rockglacier is situated on the south-western slopes of the Piz Julier. The rockglacier comprises two individual generations: the lower, older part is about 1000 m long and 400 m wide, its sides are densely vegetation-covered, and its furrow-ridge topography looks collapsed. The younger generation above it has an extent of approximately 550 m x 230 m and is free of vegetation except for large lichen thalli. Both generations are composed mainly of granitic boulders, intermingled with some schistose rock types (SPICHER 1980). These latter rocks were not included in the investigations due to the fact that they produce unreliable rates of weathering rind growth (cf. GELLATLY 1984). While velocity measurements were carried out on both generations, measurements of weathering rinds and Schmidt-hammer rebound values were concentrated on the younger, upper generation.

During the Egesen stage of the YD, the cirque of Munteratsch rockglacier was covered by a small glacier (SUTER 1981, OHLENDORF 1998). During the LIA the cirque seems to have been free of surface ice except for a (probably perennial) ice patch in the uppermost zone of the cirque (COAZ 1850, SUTER 1981).

3.3.2 *Surface velocities*

According to creep velocity measurements for the period between 1971 and 1998, the younger generation, ending about 400 m from the frontal talus of the older one, seems to be in a state of inactivity. Measured surface movement for the period considered lies between 0 and 0.1 ma^{-1} (Fig. 7, left). Yet, flow vectors still indicate a uniform creep direction which might point to very low movement rates. It must be kept in mind,

however, that these results are a mean over 27 years. To check whether (very slow) movement was still ongoing in the 1990s, it would be necessary to analyze aerial photography from this period only. In any case, the rockglacier could not have acquired its present shape and size with the movement rates observed at present. This indicates that the velocity field measured today does not represent conditions valid for the evolution during the entire Holocene. Therefore, streamline calculations were not carried out (cf. also *Section* 2.1).

The lower, older generation shows no movement, except in the steep tongue where movement can be attributed to gravitational sliding of individual rocks. This older generation is regarded as relict.

3.3.3 *Weathering*

Schmidt-hammer rebound values were measured for eight transects on the upper, younger generation of the rockglacier (Fig. 6, left). The overall trend of the measurements shows decreasing rebound values (R) towards the front, however, the detailed picture is inconsistent, especially closer to the front. There, rebound values of the three transects at 200, 120, and 85 m from the front show an increasing trend, followed by a much lower value at the transect at 35 m and finally, a higher value once again at the transect at the very front.

Compared to the Schmidt-hammer measurements, the weathering rind results (Fig. 6, right) show a more homogenous picture with slightly increasing thicknesses between the upper transects and the transects closer to the front. Maximum recorded weathering rind thickness on the inactive, younger generation are 1.2 mm (modal value) and 1.25 mm (median value), respectively (LAUSTELA 2003).

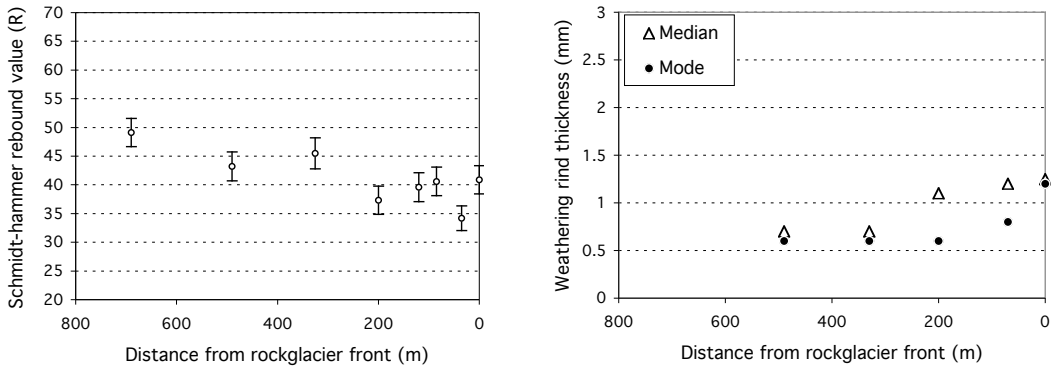

Fig. 6 Results of field measurements on the upper (inactive) part of the Munteratsch rockglacier. Left: Schmidt-hammer rebound values (R) showing the arithmetic mean on each transect with the corresponding standard error after Winkler (2000); right: modal and median values of the measured weathering rind thickness transects. (Left graph modified after Laustela 2003, right graph modified after Laustela et al. 2003). Creep direction in both graphs is from left to right.

3.4 *Albana*

3.4.1 *Characteristics*

The name of the rockglacier's location is derived from the pre-Roman stem *alb-* meaning 'rise, hill' (SCHORTA 1991).

The rockglacier is located on the southern slopes of the Piz Julier. It is oriented towards SSE, is 420 m long and 115 m wide and has a monomorphic tongue-shaped form. The notably high front (about 70 m, cf. BARSCH 1996) is covered with vegetation. The Albana rockglacier originates in the granite of the Err-Bernina nappe (SPICHER 1980), similar to the rockglaciers described previously.

Glacier reconstructions suggest that the area of the rockglacier's location was free of glaciers during the entire Holocene and probably even before, during the YD (SUTER 1981). The rockglacier body was mapped as early as the 1850s by the cartographer COAZ with an extent comparable to the current one (COAZ 1850).

3.4.2 *Surface velocities*

BARSCH (1996) reports decreasing velocities between 1955 and 1971 and regards the rockglacier as inactive since about the 1970s. Photogrammetrically derived horizontal surface displacement rates for the period from 1971 to 1998 show, indeed, only very slow movement of the tongue in the order of 0.05 to 0.19 ma^{-1} (Fig. 7, right), values close to the error range of the method (see above). As for the Munteratsch rockglacier, these values are the mean over 27 years and movement in the 1990s is supposedly (close to) zero. It is admissible to assume that the present velocity field is not representative of past flow conditions. Therefore, streamline calculations were not carried out for this rockglacier either.

3.4.3 *Weathering*

Schmidt-hammer measurements were carried out on five transects (Fig. 8, left). Weathering rind thicknesses were measured on four of the five Schmidt-hammer measurement transects (Fig. 8, right).

In general, the Schmidt-hammer rebound values show a decreasing trend between the root zone of the rockglacier (at 280 m from the front) and the front (0 m), with the exception of the (inverse) difference between the transects at 20 m and 0 m from the front. The significance of the trend is greatest in the upper part of the rockglacier and diminishes towards its front.

Despite the relatively simple morphology of the rockglacier, the modal values of the weathering rind thicknesses indicate no clear trend. In contrast to this, the median values show a clear increase of weathering thickness from the youngest zones near the headwall to the oldest ones at the front of the rockglacier. Maximum recorded weathering thickness is 1.2 mm (modal value) and 1.3 mm (median value), respectively (LAUSTELA 2003).

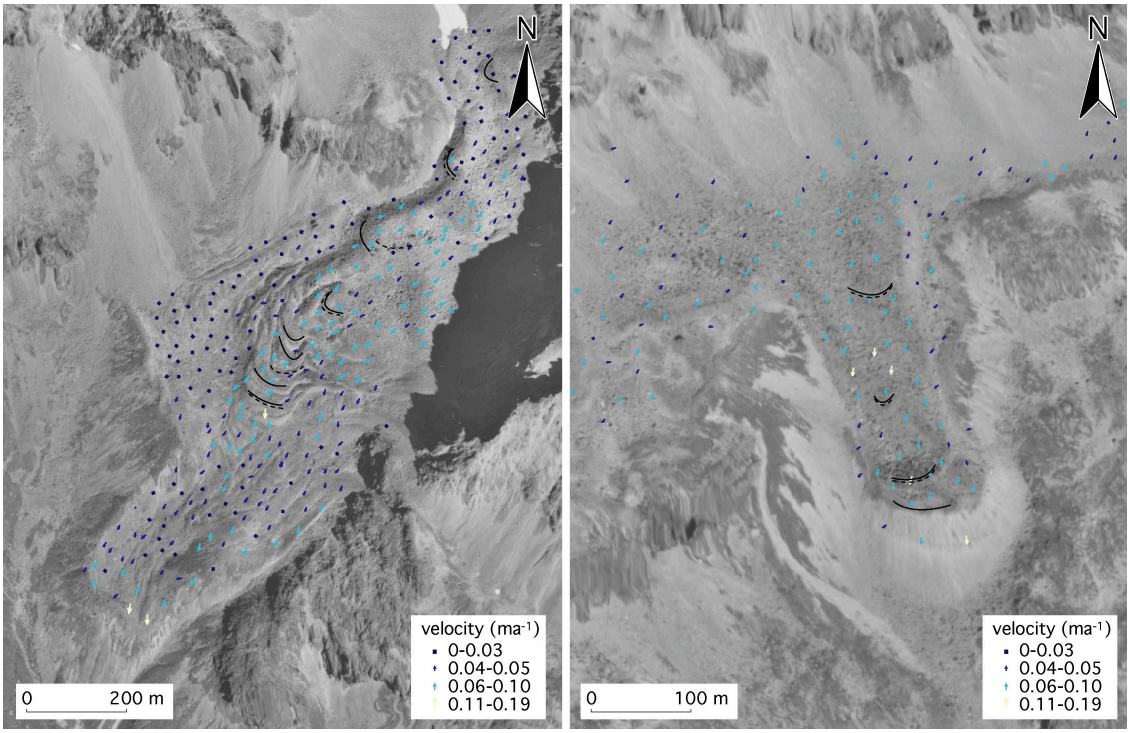

Fig. 7 Horizontal average annual surface velocities between 1971 and 1998, with the Munteratsch rockglacier (46°29'N/9°46'20"E) on the left and the Albana rockglacier (46°28'45"N/9°47'10"E) on the right. Black solid lines indicate Schmidt-hammer measurement transects, black dashed lines represent weathering rind measurement transects (see Fig. 6 for corresponding measurements on Munteratsch, and Fig. 8 for Albana). Black-and-white aerial photographs from *swisstopo*: (left) 11.08.1998, Flight-line 152, Image-No. 4645, (right) 11.08.1998, Flight-line 152, Image-No. 4644.

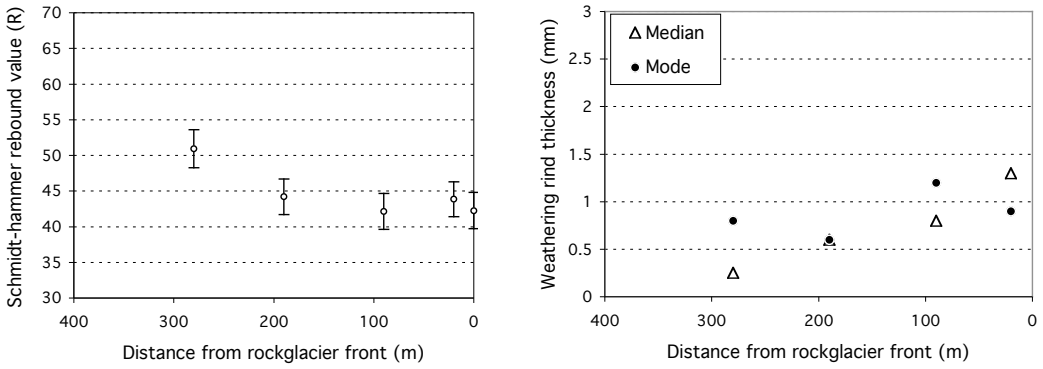

Fig. 8 Results of field measurements on the Albana rockglacier. Left: Schmidt-hammer rebound values (R) showing the arithmetic mean on each transect with the corresponding standard error after Winkler (2000); right: modal and median values of the measured weathering rind thickness transects. (Left graph modified after Laustela 2003, right graph modified after Laustela et al. 2003). Creep direction in both graphs is from left to right.

3.5 *Bleis Marscha*

3.5.1 *Characteristics*

Onomatologically the name is derived from the following two words: *bleis* from the Rhaetoromanic word *blais* meaning 'steep grass-overgrown slope' and *marsch* from the Latin word *marcidus* meaning 'rotting, decaying' (SCHORTA 1991).

The Bleis Marscha rockglacier is located in the Val d'Err, a valley in the north-western part of the study area. It developed out of a NW-exposed cirque on Piz Bleis Marscha and is composed of a single stream creeping NW-ward out of the cirque gradually turning towards SW. The stream can be seen as a continuum from active to relict stages with an active zone in the upper part and a densely vegetation-covered possibly relict frontal zone, a fact which might have contributed to its name (see above). The rockglacier is approximately 1200 m long and 210 m wide. Its debris-supplying headwalls are mostly composed of granite, slate and limestone, while the tongue of the rockglacier rests primarily on limestone (CORNELIUS 1929).

The lower part of the rockglacier lies within the lateral moraines of a now-vanished cirque glacier. Based on relative dating and comparison with other moraines in this valley, SCHLOSSER (1990) concluded that these moraines originated from a late YD advance (Egesen). During the LIA, the root zone was covered, at the most, by a small glacier or perennial ice-patch (SCHWEIZ. EIDG. STABSBUREAU 1887). Today, the only visible surface ice consists of a small ice patch.

3.5.2 *Weathering*

Schmidt-hammer measurements were performed on nine transects starting at the root zone of the rockglacier and following the central flowline down to the front (Fig. 9, left).

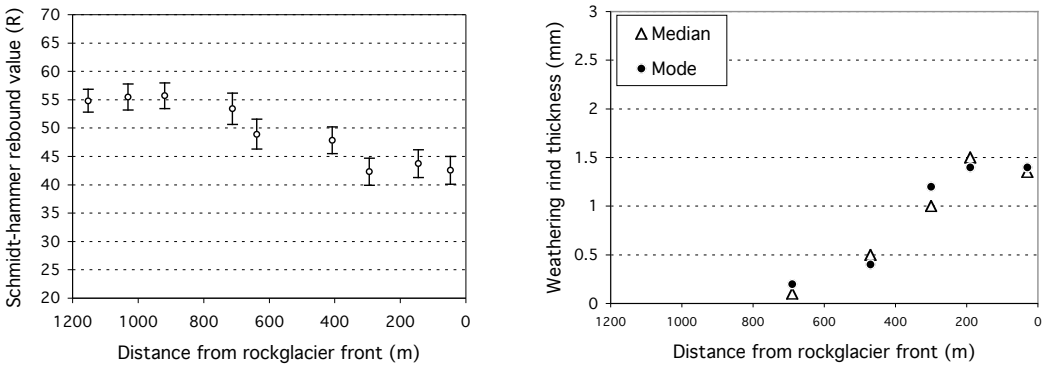

Fig. 9 Results of field measurements on the Bleis Marscha rockglacier. Left: Schmidt-hammer rebound values (R) showing the arithmetic mean on each transect with the corresponding standard error after WINKLER (2000); right: modal and median values of the measured weathering rind thickness transects (modified after LAUSTELA et al. 2003). Creep direction in both graphs is from left to right.

The analysis of the mean values of each transect shows similar values for the uppermost three transects followed by a decreasing trend towards the rockglacier front for the

following transects (Fig. 9, left). These results agree well with weathering rind measurements (Fig. 9, right) and chemical analysis (not shown here) performed by LAUSTELA et al. (2003). The weathering rind measurements show a clear trend with weathering rind thicknesses increasing steadily from the root zone towards the front. Maximum recorded weathering thickness is 1.4 mm (modal value) or 1.35 mm (median value), respectively. Chemical analysis of the free iron content – the content of Fe increases with time of exposure to weathering – shows also a clear increase between the upper and the lower transects.

3.6 *Findletälli*

3.6.1 *Characteristics*

The name of this rockglacier refers to the topographical depression in which it is situated. The high-alpine meadows of the *Findletälli* belong to the hamlet *Finilu*, located on the other side of the mountain ridge at the old Roman pathway towards the south. *Finilu* is derived from the Latin word *fenile*, meaning 'barn, shed' (ANDEREGG & ZIMMERMANN 1995). *Tälli* is Swiss German and means 'small valley'. As the name refers to a place outside the rockglacier's location, it has less onomatological force of expression than the names of the other rockglaciers described.

This rockglacier is the largest of a group of six rockglaciers located at the northern foot of the Mattwaldhorn, the mountain confining the Nanztal, Valais, towards the south. In contrast to the other (much) smaller rockglaciers of this group which are of the talus-derived type, this tongue-shaped rockglacier crept out of morainic material of a former, now-vanished cirque glacier (see also glacial history below). This explains its large extent (length = 750 m, width = 220 to 340 m) which seems to contradict the comparably small debris-supplying headwall area. With a slope angle of 14°, this rockglacier is the flattest of those investigated here. Geologically speaking, the rockglacier belongs to the crystalline of the Fletschhorn group and is composed mainly of garnet-muscovite slate and amphibolithic gneiss and quarzite (BEARTH 1973).

While the area was certainly glaciated during the latter part of the Lateglacial and the early Holocene, the glacial history during the LIA is controversial. On the 'Dufour map' published in 1854 (SCHWEIZ. EIDG. TOPOGR. BUREAU 1854) the cirque which is nowadays occupied by the rockglacier is mapped as fully glacier-covered. A debris apron is indicated at the front of the mapped glacier. MAISCH et al. (1999) have mapped the area as glacier-free during that time, except for a small cirque glacier at the foot of the headwall. The pronounced ridge-and-furrow topography of the rockglacier tongue indicates that a complete glacier coverage during the LIA is questionable. It seems more likely that Dufour (the cartographer) mistakenly interpreted the rockglacier in front of the cirque glacier as its debris-covered continuation and, therefore, mapped both landforms as one glacier. Such mapping errors are also known from other locations (M. MAISCH, personal communication, 2004). Today, the cirque is free of surface ice except for some small perennial ice patches.

3.6.2 *Surface velocities and streamlines*

Horizontal surface displacement rates for the period from 1975 to 1999 amount to 1.2 ma^{-1}, with an average velocity of 0.3 to 0.6 ma^{-1}. The fastest creep rates are observed in a longitudinal furrow on the orographic right side of the rockglacier (Fig. 10, left).

The minimum surface age at the rockglacier front as calculated from streamlines derived from the current velocity field amounts to 3 ka (Fig. 10, right). Due to a large snow patch on the rockglacier in the 1975 orthophoto, velocity measurements were not possible in the upper part of the transport zone, just below the root zone. Therefore the streamlines could not be calculated for the entire rockglacier, and the age of 3 ka is clearly a minimum estimate for the rockglacier's surface age.

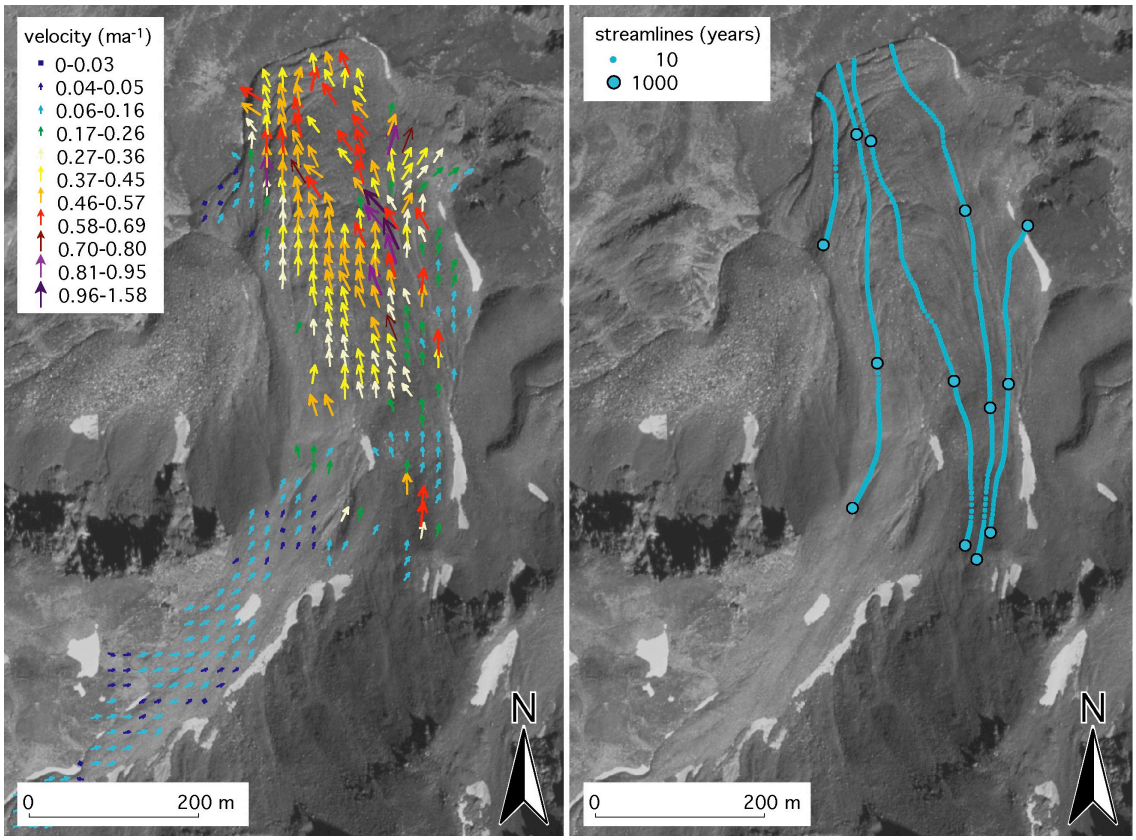

Fig. 10 Photogrammetrical measurements on the Findletälli rockglacier, which is located at about 46°12'30"N/7°57'10"E. Left: Horizontal average annual surface velocities between 1975 and 1999; right: streamline calculations. Black-and-white aerial photograph from *swisstopo*, 1.09.1999, Flight-line 116, Image-No. 2640.

4 *Discussion and implications*

As mentioned above, rockglaciers can be used for quantitative paleoclimatic reconstructions if (approximate) dating of the frozen bodies is possible. In this study, three different kind of relative age dating methods were applied: photogrammetrically derived

streamline interpolations, Schmidt-hammer rebound value measurements, and weathering rind thickness measurements. A synthesis of the obtained findings leads to the following results:

– The investigated rockglaciers are at least 3 to 5 ka old, and the age of the surface increases along flowlines from the top towards the front. These findings correspond well with the results reported for the active rockglacier Murtèl: the surface age at the rockglacier front of Murtèl as calculated from the present-day velocity field amounts to approximately 5 to 6 ka (HAEBERLI et al. 2003). Dating of moss remains contained in a core recovered by drilling through the permafrost of this rockglacier (at 5.94 m depth and ca. 300 m from the foot of the headwall) yielded a mean conventional ^{14}C age of 2250 ± 100 years (HAEBERLI et al. 1999). Assuming that 6 m of ice and debris had accumulated above the moss remains and that the rate of ice and debris accumulation remained constant through time, the age of the layers within a shear horizon, found at 30 m depth, are estimated at some 10^4 years (HAEBERLI et al. 1999).
  For the Gianda Grischa and Suvretta rockglaciers age estimates were obtained by comparing streamline calculations and weathering data. For the Findletälli rockglacier, the age estimate is based on streamline calculations. Comparison of the Schmidt-hammer rebound values and the weathering rind thicknesses measured on the rockglaciers Munteratsch, Albana and Bleis Marscha, with the values obtained on the other rockglaciers suggests ages of several thousand years also for these latter three. For the Bleis Marscha rockglacier this age estimate is supported by geomorphological evidence (see *Section* 3.5.1).
– The surface velocity of a creeping mass is the cumulative horizontal deformation over depth and thus, is the maximum horizontal velocity found over the vertical velocity profile. The overall advance rate of the entire creeping body is mainly determined by the average horizontal velocity with depth and mass loss due to ice melt at the front. As a consequence, the actual advance rate can be considerably smaller than the surface velocity and, therefore, surface ages obtained on the base of surface velocity streamline interpolations constitute a minimum age. KÄÄB (2004) derived empirical values of rockglacier advance rates and found that the total age of the considered rockglaciers is 2–5 times higher than the minimum age obtained for the surface.
  This implies that the rockglaciers Gianda Grischa, Munteratsch, Bleis Marscha and Findletälli presumably started to evolve shortly after the fast glacier decay at the end of the YD or, at the latest, after the early-to-mid Holocene temperature optimum (ending around 5000 y BP conventional ^{14}C, uncalibrated, e.g. ROBERTS 2000). Before the Holocene period, the areas where these rockglaciers are located today were glaciated. This suggests, furthermore, that the debris material out of which the rockglaciers developed was in many cases partly reworked and pre-transported by glaciers. In contrast to this, the rockglaciers Suvretta and Albana could theoretically have been active by the end of the Lateglacial already because their locations seemed to have been ice-free during that time. A lateglacial origin seems, however, more likely for the currently inactive rockglacier Albana than for the active and very fast-moving rockglacier Suvretta.
– The covering of some of these rockglaciers by glaciers during the LIA does not necessarily contradict the above interpretations: many smaller cirque glaciers in the

Alps were probably polythermal during the advances of 1850, with a temperate accumulation area and a slightly cold ablation area (HAEBERLI 1976, HOOKE et al. 1983). Thus, permafrost and pre-existing rockglaciers may well have outlasted beneath such glaciers during the LIA, or been re-activated thereafter. Evidence of outlasting or reforming permafrost in recently deglaciated glacier forefields are reported by KNEISEL (1999, 2003), and interactions between LIA glaciers and rockglaciers are reported by, for example, MÉTRAILLER et al. (2003), REYNARD et al. (2003), and DELALOYE et al. (in press).

– Decadal maximum velocities for the observed rockglaciers lie in the range of several decimetres up to over a metre per year. Mean annual velocities range between 0.2 m and 0.7 ma^{-1}. The variability in velocity from year to year has not been analyzed, but is reported by several authors (e.g. KÄÄB & FRAUENFELDER 2001, IKEDA et al. 2003, ROER et al. submitted) and is assumed to exist for (at least) some of the rockglaciers described here as well. Both the measured mean as well as the maximum velocities are of the same order of magnitude as velocities measured on other rockglaciers in the Alps (e.g. BARSCH & ZICK 1991, KAUFMANN 1996, KÄÄB 1998) and in other mid-latitude mountain regions (e.g. BRYANT 1971, KONRAD et al. 1999).
– In general, decreasing Schmidt-hammer rebound values and increasing weathering rind thicknesses correlate well with increasing photogrammetrically determined age, or decreasing distance from the rockglacier front. This relation is clearer for the weathering rinds than for the Schmidt-hammer values. The rather strong variability of the Schmidt-hammer measurements makes an interpretation more difficult and often leaves the measured trends statistically rather weak. It seems that weathering rinds (as a product of chemical weathering) are more useful for the detection of fine age differences within comparably short time periods than are the (mechanically induced) rebound values. On the other hand, Schmidt-hammer results measured on different landforms (e.g. moraines, rockglaciers) lend themselves well to comparison (see e.g. WINKLER & SHAKESBY 1995). This seems difficult in the case of weathering rind measurements, due to observed differences in weathering rind growth rates on comparable lithologies.

5 *Concluding remarks*

Digital photogrammetry allows for detailed determination and analysis of horizontal surface displacements on rockglaciers, and for the derivation of streamline calculations. The measurement of weathering rind thicknesses and Schmidt-hammer rebound values enables the relative dating of rockglacier bodies. These results can be tied to the photogrammetrically derived streamline interpolations. The present findings define the age of the Alpine rockglacier surfaces under investigation as several thousand years old, and the start of rockglacier evolution as the early-to-mid Holocene.

Future work should focus on the combination of the described relative dating methods with results from absolute dating techniques, such as exposure dating and luminescence dating as proposed by LANG et al. (1999) and HAEBERLI et al. (2003). This will open up interesting perspectives for chronological work on both rockglaciers and other

high-alpine landforms (moraines, debris cones, talus slopes, etc.) and enable the decoding of late-glacial and Holocene landscape evolution.

Acknowledgements

The work by R. Frauenfelder was supported by a research grant of the 'Stiftung zur Förderung der wissenschaftlichen Forschung' at the University of Zurich. Phillipe Meuret and Bruno Weber installed and managed the photogrammetry station. Max Maisch made as-yet unpublished data available to us and shared his knowledge of glacier reconstructions. Gian Cla Feuerstein and Reinhard Furrer supported us in the translation of geographical place names. Mr. Dosch, municipal secretary of the community of Tinizong-Rona, helped with obtaining the necessary driving permits. Martin Hoelzle and Markus Egli provided field assistance. Barbara Schellenberg and Brigitte Birk-Hoelzle opened their homes to tired field-workers. Emmanuel Reynard provided helpful suggestions and comments on an earlier version of the manuscript, an anonymous reviewer revised the final version of the paper. Susan Braun-Clarke improved the English. We are greatly indebted to all these persons.

References

ANDEREGG, K. & ZIMMERMANN, R. (1995): Gspon und die St. Anna-Kapelle. – NBV, Visp: 116 pp.

BARSCH, D. (1978): Rockglaciers as indicators of discontinuous alpine permafrost. An example from the Swiss Alps. – In: BROWN, R. J. E. (ed.): 3rd International Conference on Permafrost, Proceedings, Edmonton, **1**. National Research Council of Canada, Ottawa: 4–9.

– (1996): Rockglaciers. Indicators for the present and former geoecology in high mountain environments. – Springer, Berlin: 331 pp.

BARSCH, D. & ZICK, W. (1991): Die Bewegung des Blockgletschers Macun I von 1965–1988, Unterengadin, Graubünden. – Schweizerische Zeitschrift für Geomorphologie **35**: 1–14.

BEARTH, P. (1973): Geologischer Atlas der Schweiz, 1:25'000. Erläuterungen zum Kartenblatt Simplon. – Schweizerische Geologische Kommission, Basel.

BRYANT, B. (1971): Movement measurement on two rock glaciers in the eastern Elk Mountains, Colorado. – US Geological Survey, Professional Paper **750-B**: B108–116.

CASTELLI, S. (2000): Geomorphologische Kartierung im Gebiet Julierpass, Val Suvretta und Corvatsch (Oberengadin, GR), sowie Versuche zur Relativdatierung der morphologischen Formen mit der Schmidt-Hammer Methode. – Dept. of Geography, University of Zurich, Unpublished Diploma-thesis: 82 pp.

CHINN, T. J. H. (1981): Use of rock weathering-rind thickness for Holocene absolute age-dating in New Zealand. – Arctic and Alpine Research **13**: 33–45.

COAZ, J. W. F. (1850): Blatt XX, Unterabthlg. 2, 1:50'000 (Original Messtischblatt). Archiv-Nr. L+T 468. Schweiz. Eidg. Stabsbureau, Bern.

CORNELIUS, H. P. (1929): Geologische Karte der Err-Julier Gruppe, 1:25'000. Bern.

DELALOYE, R., LUGON, R., LAMBIEL, C. & REYNARD, E. (in press): Réponse du pergélisol à l'avancée glaciaire du Petit Age Glaciaire: quelques exemples alpins et pyrénéens. – Environnements périglaciaires, Bulletin de l'Association Française du Périglaciaire **10**.

FRAUENFELDER, R. & KÄÄB, A. (2000): Towards a palaeoclimatic model of rock glacier formation in the Swiss Alps. – Annals of Glaciology **31**: 281–286.

FRAUENFELDER, R., HAEBERLI, W., HOELZLE, M. & MAISCH, M. (2001): Using relict rockglaciers in GIS-based modelling to reconstruct Younger Dryas permafrost distribution patterns in the Err-Julier area, Swiss Alps. – Norwegian Journal of Geography **55**: 195–202.

GELLATLY, A. F. (1984): The use of rock weathering-rind thickness to redate moraines in Mount Cook National Park, New Zealand. – Arctic and Alpine Research **16**: 225–232.

HAEBERLI, W. (1976): Eistemperaturen in den Alpen. – Zeitschrift für Gletscherkunde und Glazialgeologie **11**: 203–220.

HAEBERLI, W., HOELZLE, M., KÄÄB, A., KELLER, F., VONDER MÜHLL, D. & WAGNER, S. (1998): Ten years after drilling through the permafrost of the active rock glacier Murtèl, Eastern Swiss Alps: answered questions and new perspectives. – In: LEWKOWICZ, A.G. & ALLARD, M. (eds.): 7th International Conference on Permafrost, Proceedings, Yellowknife. Centre d'Etudes Nordiques, Université Laval **57**: 403–410.

HAEBERLI, W., KÄÄB, A., WAGNER, S., VONDER MÜHLL, D., GEISSLER, P., HAAS, J. N., GLATZEL-MATTHEIER, H. & WAGENBACH, D. (1999): Pollen analysis and ^{14}C-age of moss remains recovered from a permafrost core of the active rock glacier Murtèl/Corvatsch (Swiss Alps): geomorphological and glaciological implications. – Journal of Glaciology **45**: 1–8.

HAEBERLI, W., BRANDOVA, D., BURGA, C., EGLI, M., FRAUENFELDER, R., KÄÄB, A., MAISCH, M., MAUZ, B. & DIKAU, R. (2003): Methods for absolute and relative age dating of rock-glacier surfaces in alpine permafrost. – In: PHILLIPS, M., SPRINGMAN, S., ARENSON, L. (eds.): 8th International Conference on Permafrost, Proceedings, Zürich, **1**. Swets & Zeitlinger, Lisse: 343–348.

HOOKE, R. L., GOULD, J. E. & BRZOZOWSKI, L. L. (1983): Near-surface temperatures near and below the equilibrium line on polar and subpolar glaciers. – Zeitschrift für Gletscherkunde und Glazialgeologie **19**: 1–25.

HUMLUM, O. (1998): The climatic significance of rock glaciers. – Permafrost and Periglacial Processes **9**: 375–395.

IKEDA, A., MATSUOKA, N. & KÄÄB, A. (2003): A rapidly moving small rock glacier at the lower limit of the mountain permafrost belt in the Swiss Alps. – In: PHILLIPS, M., SPRINGMAN, S. & ARENSON, L. (eds.): 8th International Conference on Permafrost, Proceedings, Zürich, **1**. Swets & Zeitlinger, Lisse: 455–460.

KÄÄB, A. (1998): Oberflächenkinematik ausgewählter Blockgletscher des Oberengadins. – In: VONDER MÜHLL, D. (ed.): Beiträge aus der Gebirgs-Geomorphologie, Samedan. Mitteilungen der VAW/ETH Zürich **158**: 121–140.

– (2004). *Mountain glaciers and permafrost creep. Research perspectives from remote sensing technologies and geoinformatics.* – Habilitation, Department of Geography University of Zürich, 205 pp.

KÄÄB, A. & VOLLMER, M. (2000): Surface geometry, thickness changes and flow fields on permafrost streams: automatic extraction by digital image analysis. – Permafrost and Periglacial Processes **11**: 315–326.

KÄÄB, A. & FRAUENFELDER, R. (2001): Temporal variations of mountain permafrost creep. – In: HARRIS, C. (ed.): 1st European Permafrost Conference, Abstracts, Rome: 56.

KÄÄB, A., GUDMUNDSSON, G. H. & HOELZLE, M. (1998): Surface deformation of creeping mountain permafrost. Photogrammetric investigations on Murtèl rock glacier, Swiss Alps. – In: LEWKOWICZ, A.G. & ALLARD, M. (eds.): 7th International Conference on Permafrost, Proceedings, Yellowknife. Centre d'Etudes Nordiques, Université Laval **57**: 531–537.

KAUFMANN, V. (1996): Geomorphometric monitoring of active rock glaciers in the Austrian Alps. – 4th International Symposium on High Mountain Remote Sensing Cartography, Karlstad-Kiruna-Tromsø: 97–113.

KERSCHNER, H. (1983): Lateglacial paleotemperatures and paleoprecipitation as derived from permafrost-glacier relationships in the Tyrolean Alps, Austria. – In: PÉWÉ, T. L. (ed.): 4th

International Permafrost Conference, Proceedings, Fairbanks. National Academy Press, Washington D.C.: 589–594.

KNEISEL, C. (1999): Permafrost in Gletschervorfeldern – Eine vergleichende Untersuchung in den Ostschweizer Alpen und Nordschweden. – Trierer Geographische Studien **22**: 156.

– (2003): New insights of mountain permafrost occurrence and characteristics in recently deglaciated glacier forefields through the application of electrical resistivity tomography. – In: HAEBERLI, W. & BRANDOVA, D. (eds.): 8th International Conference on Permafrost, Extended Abstracts, Zürich: 81–82.

KONRAD, S., HUMPHREY, N. F., STEIG, E. J., CLARK, D. H., POTTER, N. J. & PFEFFER, W. T. (1999): Rock glacier dynamics and paleoclimatic implications. – Geology **27**: 1131–1134.

LANG, A., MOYA, J., COROMINAS, J., SCHROTT, L. & DIKAU, R. (1999): Classic and new dating methods for assessing the temporal occurrence of mass movements. – Geomorphology **30**: 33–52.

LAUSTELA, M. C. (2003): Messung und Analyse von Verwitterungsrinden zur relativen Altersdatierung ausgewählter Blockgletscher in den Bündner Alpen. – Dept. of Geography, University of Zurich, Unpublished Diploma-thesis: 86 pp.

LAUSTELA, M., EGLI, M., FRAUENFELDER, R., KÄÄB, A., MAISCH, M. & HAEBERLI, W. (2003): Weathering rind measurements and relative age dating of rockglacier surfaces in crystalline regions of the Eastern Swiss Alps. – In: PHILLIPS, M., SPRINGMAN, S. & ARENSON, L. (eds.): 8th International Conference on Permafrost, Proceedings, Zürich, **1**. Swets & Zeitlinger, Lisse: 627–632.

MAISCH, M., HAEBERLI, W., HOELZLE, M. & WENZEL, J. (1999): Occurrence of rocky and sedimentary glacier beds in the Swiss Alps as estimated from glacier-inventory data. – Annals of Glaciology **28**: 231–235.

MCSAVENEY, M. J. (1992): A manual for weathering-rind dating of grey sandstones of the Torlesse Supergroup, New Zealand. – Institute of Geological & Nuclear Sciences Limited, Lower Hutt.

MÉTRAILLER, S., DELALOYE, R. & LUGON, R. (2003): Recent evolution of permafrost in both Becs-de-Bosson and Lona glacier/rock glacier complexes (western Swiss Alps). – In: HAEBERLI, W. & BRANDOVA, D. (eds.): 8th International Conference on Permafrost, Extended Abstracts, Zürich: 107–108.

OGUCHI, C. T. (2001): Formation of weathering rinds on Andesite. – Earth Surface Processes and Landforms **26**: 847–858.

OHLENDORF, C. (1998): High Alpine lake sediments as chronicles for regional glacier and climate history in the Upper Engadine, southeastern Switzerland. – PhD-thesis no. 12705, ETH Zürich: 203 pp.

REYNARD, E., LAMBIEL, C., DELALOYE, R., DEVAUD, G., BARON, L., CHAPELLIER, D., MARESCOT, L. & MONNET, R. (2003): Glacier/permafrost relationships in forefields of small glaciers (Swiss Alps). – In: PHILLIPS, M., SPRINGMAN, S. & ARENSON, L. (eds.): 8th International Conference on Permafrost, Proceedings, Zürich, **1**. Swets & Zeitlinger, Lisse: 947–952.

ROBERTS, N. (2000): The Holocene. An environmental history. – Blackwell Publishers Ltd, Oxford: 316 pp.

ROER, I., KÄÄB, A. & DIKAU, R. (submitted): Rockglacier kinematics derived from small-scale aerial photography and digital airborne pushbroom imagery. – Z. Geomorph. N.F.

SCHLOSSER, O. (1990): Geomorphologische Kartierung und glazialmorphologische Untersuchungen in der Err-Gruppe (Oberhalbstein, Kt. Graubünden). – Dept. of Geography, University of Zurich, Unpublished Diploma-thesis: 90 pp.

SCHMIDT, E. (1950): Der Beton-Prüfhammer – Ein Gerät zur Bestimmung der Qualität des Betons im Bauwerk. – Schweizerische Bauzeitung **68**: 378–379.

SCHORTA, A. (1991): Wie der Berg zu seinem Namen kam. Kleines Rätisches Namenbuch mit zweieinhalbtausend geographischen Namen Graubündens. – Terra Grischuna Verlag, Chur: 159 pp.

SCHWEIZ. EIDG. TOPOGR. BUREAU. (1854): Topographische Karte der Schweiz, Blatt XVIII (Brieg–Airolo), 1:100'000. – Erstausgabe, Dufour, G.H. direxit, Genf.

SCHWEIZ. EIDG. STABSBUREAU (1875): Topographischer Atlas der Schweiz, St. Moritz, Blatt 518 (Section 2, Bl. XX), 1:50'000. – Bern.

– (1887): Topographischer Atlas der Schweiz, Savognin, Blatt 426 (Section XV, 13), 1:50'000. – Bern.

SPICHER, A. (1980): Geologische Karte der Schweiz 1:500'000. – Schweizerische Geologische Kommission, Basel.

SUMNER, P. & NEL, W. (2002): The effect of rock moisture on Schmidt Hammer rebound: tests on rock samples from Marion Island and South Africa. – Earth Surface Processes and Landforms **27**: 1137–1142.

SUTER, J. (1981): Gletschergeschichte des Oberengadins: Untersuchungen von Gletscherschwankungen in der Err-Juliergruppe. – Physische Geographie **2**: 170 pp. – Geographisches Institut, Universität Zürich.

VOLLMER, M. (1999): Kriechen alpinen Permafrostes: Grundlagen zur digitalen photogrammetrischen Bewegungsmessung. – Dept. of Geography, University of Zurich, Unpublished Diploma-thesis: 46 pp.

WHITEHOUSE, I. E., MCSAVENEY, M. J., KNUEPFER, P. L. K. & CHINN, T. J. H. (1986): Growth of weathering rinds on Torlesse Sandstone, Southern Alps, New Zealand. – In: COLMAN, S. M. & DETHIER, D. P. (eds.): Rates of chemical weathering of rocks and minerals: 419–435.

WILLIAMS, R. B. G. & ROBINSON, D. A. (1983): The effect of surface texture on the determination of the surface hardness of rock using the Schmidt Hammer. – Earth Surface Processes and Landforms **8**: 289–292.

WINKLER, S. (2000): The little ice age maximum in the Southern Alps, New Zealand: preliminary results at Mueller Glacier. – The Holocene **10**: 643–647.

WINKLER, S. & SHAKESBY, R. A. (1995): Anwendung von Lichenometrie und Schmidt-Hammer zur relativen Altersdatierung prä-frührezenter Moränen am Beispiel der Vorfelder von Guslar-, Mitterkar-, Rofenkar- und Vernagtferner (Ötztaler Alpen/Österreich). – Petermanns Geographische Mitteilungen **139**: 283–304.

Addresses of the authors: R. Frauenfelder and A. Kääb, Glaciology and Geomorphodynamics Group, Department of Geography, University of Zurich, Winterthurerstr. 190, CH-8057 Zurich, Switzerland. – M. Laustela, Frohbergstrasse 5, CH-8342 Wernetshausen, Switzerland.

II

Permafrost, Phillips, Springman & Arenson (eds)
© 2003 Swets & Zeitlinger, Lisse, ISBN 90 5809 582 7

Rockglacier occurrence and related terrain parameters in a study area of the Eastern Swiss Alps

R. Frauenfelder, W. Haeberli & M. Hoelzle
Glaciology and Geomorphodynamics Group, Department of Geography, University of Zurich, Switzerland

ABSTRACT: Rockglaciers act as a transport mechanism of frozen debris in the periglacial alpine environment, and represent a link in a process chain, combining frost weathering, rock fall, and debris transport by permafrost creep. In this study, the relationship of terrain parameters (rock wall extent, geology, etc.) and rockglacier parameters (rockglacier size, slope, velocity, etc.) are statistically analysed. Two empirical data sets containing information on 84 and 44 rockglaciers, respectively, were used. The results show that a relation between rock-wall extent and rockglacier size indeed exists but is complex and involves factors such as cliff recession rates (as a function of geology, temperature, water content, etc.) and subsequent talus input variations. Concerning flow velocities, the findings indicate that non-linear thermal influences on strain rates probably predominate over effects from stress-related geometry (slope-dependent thickness).

1 INTRODUCTION

Rockglaciers are transport systems of frozen rock debris in the periglacial alpine environment. They are part of a process chain linking frost weathering, rock fall, and debris displacement by permafrost creep. Their development is dependent upon the supply of debris from the source headwall(s) and the long-term preservation of an ice matrix or ice core inducing flow (Morris 1981). According to Barsch (1996) there exists a close relationship between the size of a rockglacier, the size of the source area for its material, and the intensity of talus production in the source area. Olyphant (1983) modelled the rockglacier debris transport system by mathematically linking it to its bedrock-cliff source area and by combining expressions for debris input and rockglacier flow with a continuity approach.

It is often assumed that the transport of debris, i.e. the movement of the rockglacier, follows a viscous deformation law similar to the one of glacier ice (e.g. Wahrhaftig & Cox 1959, Haeberli 1985, Barsch 1996, Konrad et al. 1999). The deformation or creep of rockglaciers can then be described by Glen's flow law (Paterson 1994).

The purpose of this study is to investigate if any topographical and/or rheological relationships can be identified from statistical analyses of regional inventory data. Two main questions are addressed: (a) is there a dependence between rockglacier size and the extent of the debris-supplying source headwall (also known as "rock free face above a rockglacier", e.g. Humlum 2000), and (b) can topographic or climatic controls on transport rates of rockglaciers be identified?

In the presented study, first results from statistical analysis of terrain parameters (rock wall extents, geology, etc.) and their relationship to rockglacier parameters (rockglacier size, slope, velocity, etc.) are discussed.

2 DATA BASE AND METHODS

Two main data sources are used: *Data set no. 1 (DS#1)* comprises a rockglacier inventory of the Engadin and its adjacent regions as compiled by Hoelzle (1998). The inventory contains spatial data on 84 active rockglaciers. *Data set no. 2 (DS#2)* contains selected measurements on 44 rockglaciers in eleven different regions of the European Alps and the Rocky Mountains sensu lato as compiled from publications of various authors.

In *DS#1*, information on length (l_{RG}) and width (b_{RG}) for each rockglacier was extracted from the inventory. Additional data such as height (l_F) and width (b_F) of the source headwall, average slope of the rockglacier body (α_{RG}), and dominant rock types were compiled using a digital elevation model, and both digital and analogue maps of the region (Fig. 1). This data was then used to explore the relation between parameters of the debris source area, i.e. the source headwall, and the spatial extents of the rockglacier bodies.

In *DS#2*, information relating to rockglacier rheology was compiled from published literature and map evaluation. The following parameters were derived (cf. also Fig. 1): rockglacier length (l_{RG}), elevation of rockglacier front (H_{min}), average slope of the creeping body (α_{RG}), mean and maximum surface velocity (v_{mean}, v_{max}), altitude of regional 0°C-isotherm and regional temperature lapse rate. Using regional temperature lapse rates and altitude of the 0°C-isotherm, the mean annual air temperature at the front of each presently active rockglacier was estimated ($MAAT_{RGF}$). For several rockglaciers in the Swiss Alps, where digital

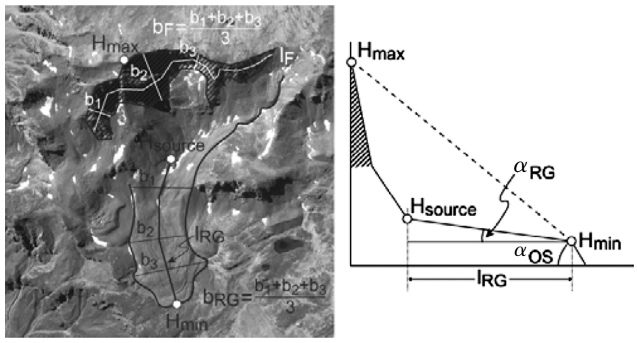

Figure 1. Schematic sketch displaying the parameters measured and discussed in the text. Black-and-white aerial photograph of the Swiss Federal Office of Topography, 1.9.1999, Flight-line 116, Image-No. 2641.

terrain models are available, potential direct solar radiation at the rockglacier front was computed.

3 RESULTS

3.1 *Debris supplyand rockglacier size*

Concerning the source of debris, 64 of the rockglaciers in *DS#1* presumably originated from periglacial talus. The other 20 rockglaciers developed from glacier-transported debris (mostly lateral and terminal moraines); the first group of rockglaciers will be referred to as talus-derived rockglaciers, the latter as moraine-derived rockglaciers. Different interactions of the various parameters analysed might apply for these two groups of rockglaciers, a fact which is accounted for in the interpretations.

Mean length (l_{RG}) of the talus-derived rockglaciers amounts to 410 m ± 209 m (min = 125, max = 1274), mean width (b_{RG}) to 136 m ± 64 m. The mean source headwall above such a rockglacier is 117 m ± 77 m high (l_F) and 405 m ± 255 m wide (b_F). Average values for a moraine-derived rockglacier are slightly higher, with l_{RG} = 487 m ± 207 m, b_{RG} = 154 m ± 61 m, l_F = 110 m ± 88 m, and b_F = 499 m ± 273 m. In general, the talus-derived rockglaciers in the Engadin are somewhat smaller in size (mean area = ca. 57,700 m^2 ± 45,500 m^2) than moraine-derived rockglaciers (mean area = ca. 79,000 m^2 ± 40,100 m^2). The mean source headwall area, approximated by mean height multiplied by mean width, is similar for both types of rockglaciers with a mean area of 50,000 to 53,000 m^2.

To investigate the possible dependence of rockglacier size on source headwall area, we performed three analysing steps: Firstly, the relationship between rockglacier length (l_{RG}) and source headwall area (A_F) was analysed. Rockglacier length (l_{RG}) is the simplest parameter describing rockglacier extent. However, it is only one proxy of the three dimensions

Table 1. Correlation values for different parameters of talus-derived rockglaciers and moraine-derived rockglaciers when compared versus source headwall area.

Analysis type	Talus-derived r-value	Moraine-derived r-value	All r-value
l_{RG} vs. A_F	0.56	0.32	0.49
A_{RG} vs. A_F	0.58	0.66	0.55
A_{RG} vs. $A_{F,\ weighted}$	0.62	0.33	0.55

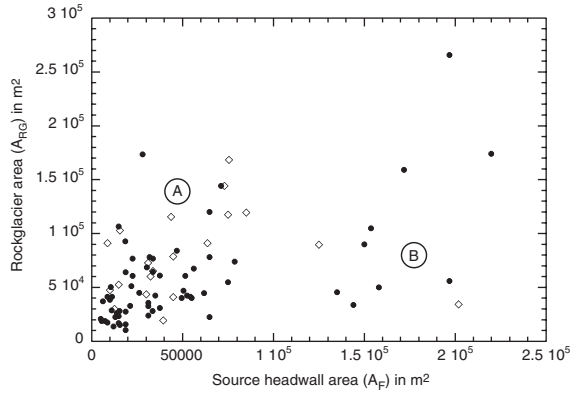

Figure 2. Relation between rockglacier area (A_{RG}) and source headwall area (A_F). Black dots represent talus-derived rockglaciers, outlined rhombi mark moraine-derived rockglaciers. Total sample size n = 84.

of a rockglacier, and, as we will see later, it might correlate with other factors such as, for example, the velocity of the rockglacier. Therefore, we compared rockglacier area (A_{RG}) and source headwall area (A_F) in a second step. Rockglacier area (A_{RG}) is that parameter of rockglacier volume (V_{RG}) which can be most easily and directly determined. Thirdly, to account for different rock weathering rates and, thus, for different debris supply rates, a weighting factor for different rock types was introduced.

The analyses yielded the following results:

- The overall statistical relationship between rockglacier length (l_{RG}) and source headwall area (A_F) is moderate, with r = 0.49 (no graph shown). A separate treatment of talus- and moraine-derived rockglaciers shows that the correlation is more significant for the talus-derived rockglaciers than for the moraine-derived rockglaciers (Table 1).
- The comparison between rockglacier area (A_{RG}) and source headwall area (A_F) seems, as in the first analysis, to indicate two more or less distinct clusters (Fig. 2).

One cluster of values (A) incorporates rockglaciers with source headwall areas below 100,000 m^2, the area of these rockglaciers varies between 10^4 m^2 and $1.7 * 10^5$ m^2. Rockglaciers in the second cluster (B) are characterised by source headwall areas exceeding

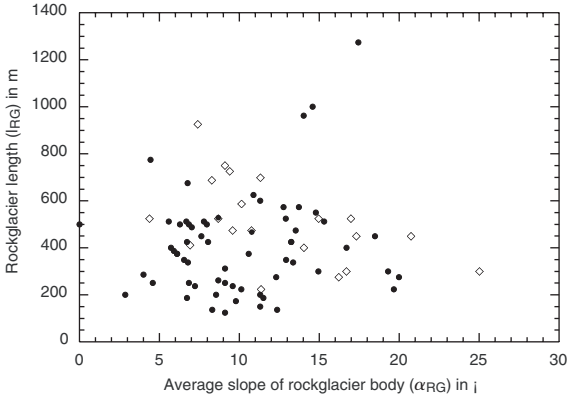

Figure 3. Relation between rockglacier length (l_{RG}) and average slope of the rockglacier body (α_{RG}). Markers as in Figure 2, total sample size n = 82.

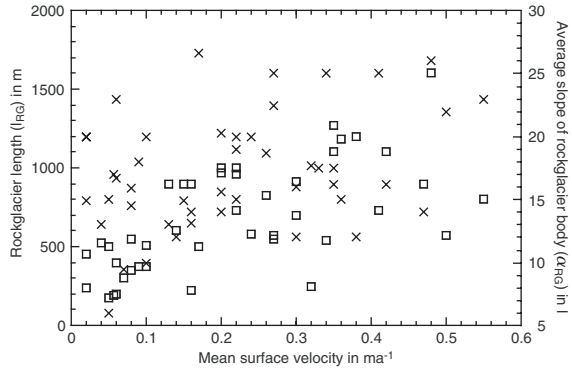

Figure 4. Boxes: relation between mean surface velocity (v_{mean}) and rockglacier length (l_{RG}); crosses: relation between mean surface velocity (v_{mean}) and average slope of the rockglacier body (α_{RG}). Total sample size n =45. Data are from Barsch & Zick (1991), Berthling (2001), Chaix (1942), Von Elverfeldt (2002), Evin & Assier (1983), Evin, Assier & Fabre (1990), Isaksen et al. (2000), Kääb et al. (1997), Kääb (1998), Kääb et al. (2002), Kaufmann (1996), Kaufmann & Ladstädter (2000), Sloan & Dike (1998), and own unpublished data.

100,000 m^2, while the area of these rockglaciers varies between $3.4 * 10^4$ m^2 and $2.6 * 10^5$ m^2. Both clusters show a positive relation between rockglacier length and the size of the debris source area, but with only medium statistical significance (cluster A: r = 0.52, cluster B: r = 0.43, both clusters together r = 0.49). Compared to the first analysis, the correlation value is slightly higher for talus-derived rockglaciers and considerably higher for the moraine-derived rockglaciers (Table 1).

The analysis of the source headwall lithology showed that granite, diorite, and gneiss are the predominant rock types, followed by dolomite, limestone, and marble. Approximately two thirds of the source headwalls are composed of two or more different rock types. In the weighting, headwalls mostly composed of granite or diorite got a weighting factor of 1, headwalls composed of faster weathering rock types, such as gneiss, limestone and dolomites, got larger weightings, and headwalls composed of rocks prone to slow weathering, such as gabbros or syenites, got smaller weighting factors. The weathering rates were derived from works by Rapp (1960), Ballantyne & Harris (1994), French (1996), André (1997), and Matsuoka et al. (1997). This procedure resulted in a moderation of the clustering effect, an increase in the correlation for talus-derived rockglaciers, and a considerable decrease in correlation for moraine-derived rockglaciers (Table 1).

Testing for a dependence between length (l_{RG}) and average slope of the rockglacier body (α_{RG}) shows a large scatter rather than distinct trends (Fig. 3). Interestingly, the moraine-derived rockglaciers seem to show an inverse relationship. Indeed, if three outliers are excluded from the analysis of the talus-derived rockglaciers (Fig. 3, three points in the upper middle) also this group shows a weak inverse correlation.

A multiple regression with rockglacier length (l_{RG}) as the dependent variable, and, both source headwall height (l_F) and average rockglacier slope (α_{RG}) as independent variables does not substantially change the picture for either of the two groups. The same applies for a multiple regression analysis with rockglacier length (l_{RG}), source headwall area (A_F), and average rockglacier slope (α_{RG}).

3.2 *Control on surface velocities*

To identify possible topographic or climatic controls on surface velocities of rockglaciers, we investigated data in *DS#2*.

Figure 4 shows that rockglacier length (l_{RG}) is rather correlated to mean surface velocity (v_{mean}) than to average slope of the rockglacier body (α_{RG}): the analysis of rockglacier length against mean surface velocity yields a clearly positive relation with an r-value of 0.63 (marked with boxes), whereas the relation between mean surface velocity and average slope is hardly statistically significant (marked with crosses).

Using mean annual air temperature at the rockglacier front ($MAAT_{RGF}$) as a rough proxy for the temperature of the permafrost allows for comparison between mean surface velocity and ice temperature (Haeberli 1985). Figure 5a shows, as expected from field measurements and laboratory experiments by different authors (e.g. Paterson 1994, Arenson et al. 2002), a positive relationship between v_{mean} and $MAAT_{RGF}$, with an r-value of 0.56 for a linear relationship, and r = 0.65 for an exponential relationship.

Maximal surface velocity (v_{max}) versus $MAAT_{RGF}$ seems to indicate an even better exponential relation (r = 0.82) between the two parameters (Fig. 5b).

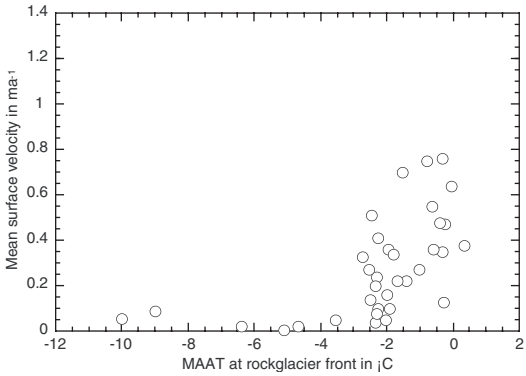

Figure 5a. Relation between *mean* surface velocity (v_{mean}) and MAAT at the present rockglacier front ($MAAT_{RGF}$). Total sample size n = 35. Note: the front of Val Sassa rockglacier in the Eastern Swiss Alps, reaches into non-permafrost areas ($MAAT_{RGF}$ above 0°C). Permafrost modelling results confirm this observation.

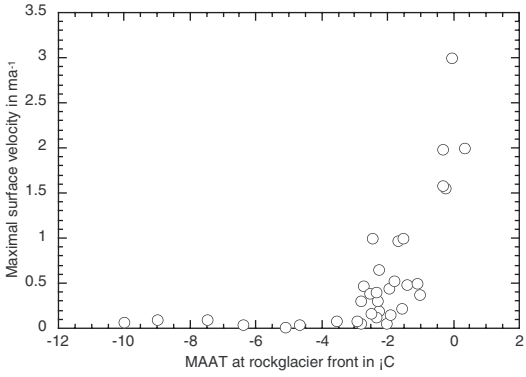

Figure 5b. Relation between *maximal* surface velocity (v_{max}) and MAAT at the present rockglacier front ($MAAT_{RGF}$). Total sample size n = 34.
Data in 5a and 5b: from Barsch & Zick (1991), Berthling (2001), Chaix (1942), Von Elverfeldt (2002), Humlum (1997), Isaksen et al. (2000), Kääb et al. (1997), Kääb (1998), Kääb et al. (2002), Kaufmann (1996), Kaufmann & Ladstädter (2000), Koning & Smith (1999), Krainer & Mostler (2000), Krummenacher (1998), Sloan & Dike (1998), and own unpublished data.

4 DISCUSSION

4.1 *Rockglacier size and debris-supply area*

The size of the talus-derived rockglaciers in the Engadin is comparable to rockglacier size in other mountain regions (e.g. North America: White 1979, Central Asia: Gorbunov 1983). The moraine-derived rockglaciers, however, are considerably smaller than, for instance, occurrences in Central Asia (Gorbunov 1983) or on Greenland (Humlum 1982).

Sloan & Dike (1998) attribute the aspect of the rockglaciers a high importance, based on a study in the Selwyn Mts. (Yukon) where they found that rockglaciers facing NE were significantly longer and moved faster than rockglaciers facing other directions. A similar relationship is not apparent in either dataset *DS#1* or *DS#2*. Mean rockglacier length in *DS#1* is greatest with aspects from SW through W to NW. Investigation of fourteen rockglaciers in *DS#2* showed no relation between mean surface velocity and potential direct solar radiation (of which aspect can be viewed as a proxy).

Figure 2 indicates that the relative size of contemporaneous rockglaciers are, to a certain extent, controlled by the area of the source headwall. This confirms that debris supply – together with flow velocity – is an important factor determining rockglacier size. Additionally, although we could not consider this factor in our study, the availability of water/snow is of fundamental importance: in the source headwall, water availability influences the rate of rock weathering, while at the foot of the talus cone, where creeping will be initiated, it is a prerequisites for the build-up of (interstitial) ice and, thus, of a cohesive matrix allowing creep.

The correlation between the size of talus-derived rockglaciers and source headwall area increases when rockglacier length is replaced by rockglacier area, and weathering rates are considered (Table 1). With moraine-derived rockglaciers, in the contrary, a sharp decrease in correlation occurs when weathering rates are introduced (Table 1). This suggests that talus-derived rockglaciers are more closely related to their debris supplying headwalls than moraine-derived rockglaciers. For the latter group, an additional, both spatially and temporally complex transport module (including e.g. the whole glacier history) is involved in the process chain. A moraine-derived rockglacier is not primarily fed by continuous debris input but evolves out of an already (fully) existent debris "reservoir". There, debris characteristics are significantly different from the original, weathered material accumulated before glacial transport.

The source headwall area is only a proxy for debris supply rates and, in itself, a function of geology, temperature, water content, jointing, etc.). Morris (1981) investigated nineteen rockglaciers in the Sangre de Cristo Mts. (Colorado) concerning their relation with altitude, radiation and rock wall jointing and found that interaction among these factors, rather than additive independent effects, determines the development of rockglaciers in different locations. The same is certainly true for the factors investigated in our study. Other authors, e.g. André (1996), Humlum (2000), Matsuoka et al. (1997), and Matsuoka & Ikeda (2001) found indications for a geological control (rock jointing, headwall retreat rates) on the distribution and characteristics of rockglaciers.

The insignificant influence of slope on rockglacier length points to the fact that the thickness of the

accumulating and deforming ice/rock-mixture is rather independent of stress controls: with a constant basal shear stress and a given volume of frozen debris, thickness would decrease and length correspondingly increase with increasing slope – a relation which is obviously not found in the analysed data.

4.2 *Velocities*

The good correlation between rockglacier length and both, mean and maximal surface velocity (Figs 5) seems to confirm that all rockglaciers had a similar time span for their development (e.g. time since the onset of the Holocene, i.e. approximately 10,000 years) and a similar initial thickness (possibly zero – no pre-deposited debris): rockglaciers that crept far would therefore have had to move faster than short rockglaciers. Obviously, this assumption would be a black-box approach and does neither enlighten the processes involved nor account for special topographic features such as obstacles, etc. However, it seems that such an idea works just well for the given sample of rockglaciers.

The rather weak relation between average surface slope and mean surface velocity (Fig. 4) again indicates that stress control on geometry and flow are less important than other influences. Such an other influence may be the temperature effect on strain rates in ice-supersaturated frozen materials.

In fact, Figure 5 confirms that flow velocity is a function of ice temperature with warmer ice deforming faster than cold one. As found for glacier ice, the rate factor A increases significantly and in a non-linear way for temperatures approaching the melting point of ice (Paterson 1994). Similar findings are confirmed for rockglacier deformation from borehole measurements and laboratory experiments e.g. by Arenson et al. (2002), and Azizi & Whalley (1996). Furthermore, it can be observed that rockglaciers at high latitudes (i.e. in colder environments) tend to deform significantly slower than rockglaciers in mid-latitude environments such as they were considered here (e.g. Humlum 1997, Bertling 2001, Kääb et al. 2002). Our results support this influence of temperature. The effect of warmer and faster deforming ice, however, could be compensated for by greater thickness and, thus, higher stresses at the base of cold permafrost. The formation of a coarse blocky layer with damped creep at a depth controlled by the original talus geometry (Haeberli et al. 1998) could explain the predominance of effects from the rate factor.

5 CONCLUSIONS

The results of our study on a selected sample of parameters document that a relation between source headwall area, surface velocity and rockglacier size exists but is complex. The analyses show that obviously neither individual parameters nor their combinations are able to fully explain rockglacier evolution.

Flow velocities appear to exert an important influence on rockglacier length and appear to depend on temperature conditions. Even though MAAT is certainly a very rough proxy for permafrost temperature, the latter is indeed likely to act as an important boundary condition for creep in the frontal part of rockglaciers, especially near local permafrost limits. In contrast to that stress conditions might be critical for triggering creep in the talus cone but seem to have limited effects on further rockglacier evolution.

Other variables must significantly influence rockglacier transport rates. Examples are (a) the vertical velocity profile including deformation rates, thickness, internal structure with stiff layers or sliding processes at depth, shearing within the permafrost, etc., and (b) variable ice content.

A better understanding of the involved parameters and processes may be reached by further analyses of the collected inventory data. The main progress, however, will come from more complete borehole and geophysical data collected on active rockglaciers.

ACKNOWLEDGEMENTS

The presented study was supported by a research grant of the "Stiftung zur Förderung der wissenschaftlichen Forschung" at the University of Zurich. Our thanks go to Dr. L. Arenson for stimulating scientific discussions. Furthermore, we would like to thank Dr. A. Kääb, Dr. B.R. Rea (University of Leicester), and an anonymous reviewer for their most constructive comments on the manuscript, which significantly improved the paper.

REFERENCES

André, M.F. 1996. Geological control of slope processes in northwest Spitsbergen. *Norsk Geografisk Tidsskrift* 50: 37–40.

André, M.F. 1997. Holocene rockwall retreat rates in Svalbard: a triple-rate evolution. *Earth Surface Processes and Landforms* 22: 423–440.

Arenson, L., Hoelzle, M. & Springman, S. 2002. Borehole deformation measurements and internal structure of some rock glaciers in Switzerland. *Permafrost and Periglacial Processes* 13(2): 117–135.

Azizi, F. & Whalley, W.B. 1996. Numerical modelling of creep behaviour of ice-debris mixtures under variable thermal conditions. *Proceedings, International Offshore and Polar Engineering Conference*, Los Angeles: 362–366.

Ballantyne, C.K. & Harris, C. 1994. *The Periglaciation of Great Britain*. Cambridge: Cambridge University Press.

Barsch, D. 1996. *Rockglaciers*. Berlin: Springer.

Barsch, D. & Zick, W. 1991. Die Bewegung des Blockgletschers Macun I von 1965–1988, Unterengadin, Graubünden. *Schweizerische Zeitschrift für Geomorphologie* 35: 1–14.

Berthling, I. 2001. Slow periglacial mass wasting – processes and geomorphological impact. Case studies form Finse, southern Norway and Prins Karls Forland, Svalbard. Series of dissertations submitted to the Faculty of Mathematics and Natural Sciences. Oslo, University of Oslo.

Chaix, A. 1943. Les coulées de blocs du Parc National Suisse: Nouvelle mesures et comparaison avec les "rock streams" de la Sierra Nevada de Californie. *Le Globe* 82: 121–128.

Evin, M. & Assier, A. 1983. Glacier et glaciers rocheux dans le Haut-Vallon du Loup, (Haute-Ubaye, Alpes du Sud, France). *Zeitschrift für Gletscherkunde und Glazialgeologie* 19: 27–41.

Evin, M., Assier, A. & Fabre, D. 1990. Les glaciers rocheux du Marinet (Haute-Ubaye, France). *Rev Geomorphol Dyn* 39: 139–155.

French, H.M. 1996. *The Periglacial Environment*. Essex: Longman.

Gorbunov, A.P. 1983. Rock glaciers of the mountains of middle Asia. In Péwé, T.L. (ed.), *Proceedings, 4th International Permafrost Conference*, Fairbanks: 359–362. Washington: National Academy Press.

Haeberli, W. 1985. Creep of mountain permafrost. Internal structure and flow of alpine rock glaciers. *Mitteilungen der VAW-ETH Zürich* 77: 142 p.

Haeberli, W., Hoelzle, M., Kääb, A., Keller, F., Vonder Mühll, D. & Wagner, S. 1998. Ten years after drilling through the permafrost of the active rock glacier Murtèl, Eastern Swiss Alps: answered questions and new perspectives. *Seventh International Conference on Permafrost, Proceedings*, Collection Nordicana 57: 403–410.

Hoelzle, M. 1998. Rock Glaciers, Upper Engadin, Switzerland, International Permafrost Association, Data and Information Working Group, NSIDC, University of Colorado at Boulder. CD-ROM.

Humlum, O. 1982. Rock glacier types on Disko, Central West Greenland. *Geografisk Tidskrift* 84: 35–39.

Humlum, O. 1997. Active layer thermal regime at three rock glaciers in Greenland. *Permafrost and Periglacial Processes* 8: 383–408.

Humlum, O. 2000. The geomorphic significance of rock glaciers: estimates of rock glacier debris volumes and headwall recession rates in West Greenland. *Geomorphology* 35: 41–67.

Isaksen, K., Ødegård, R.S., Eiken, T. & Sollid, J.L. 2000. Composition, flow and development of two tongue-shaped rock glaciers in the permafrost of Svalbard. *Permafrost and Periglacial Processes* 11: 241–257.

Kääb, A. 1998. Oberflächenkinematik ausgewählter Blockgletscher des Oberengadins. In Vonder Mühll, D. (ed.), Beiträge aus der Gebirgs-Geomorphologie, *Mitteilungen der VAW-ETH Zürich* 158: 121–140.

Kääb, A., Haeberli, W. & Gudmundsson, G.H. 1997. Analysing the creep of mountain permafrost using high precision aerial photogrammetry: 25 years of monitoring Gruben rock glacier, Swiss Alps. *Permafrost and Periglacial Processes* 8: 409–426.

Kääb, A., Isaksen, K., Eiken, T. & Farbrot, H. 2002. Geometry and dynamics of two lobe-shaped rock glaciers in the permafrost of Svalbard. *Norwegian Journal of Geography* 56(2): 152–160.

Kaufmann, V. 1996. Geomorphometric monitoring of active rock glaciers in the Austrian Alps. *Proceedings, 4th International Symposium on High Mountain Remote Sensing Cartography*, Karlstad-Kiruna-Tromsø: 97–113.

Kaufmann, V. & Ladstädter, R. 2000. Spatio-temporal analysis of the dynamic behaviour of the Hochebenkar rock glaciers (Oetztal Alps, Austria) by means of digital photogrammetric methods. *Proceedings, 6th International Symposium on High Mountain Remote Sensing Cartography*: Ethiopia, Kenya, Tanzania.

Koning, D.M. & Smith, D.J. 1999. Movement of King's Throne rock glacier, Mount Rae area, Canadian Rocky Mountains. *Permafrost and Periglacial Processes* 10(2): 151–162.

Konrad, S., Humphrey, N.F., Steig, E.J., Clark, D.H., Potter, N. Jr. & Pfeffer, W.T. 1999. Rock glacier dynamics and paleoclimatic implications. *Geology* 27(12): 1131–1134.

Krainer, K. & Mostler, W. 2000. Reichenkar rock glacier: a glacier derived debris-ice system in the Western Stubai Alps, Austria. *Permafrost and Periglacial Processes* 11: 267–275.

Krummenacher, B., Budmiger, K., Mihajlovic, D. & Blank, B. 1998. *Periglaziale Prozesse und Formen im Furggentälti, Gemmipass*. Davos: Eidg. Institut für Schnee- und Lawinenforschung (SLF).

Matsuoka, N., Hirakawa, K., Watanabe, T. & Moiwaki, K. 1997. Monitoring of periglacial slope processes in the Swiss Alps: the first two years of frost shattering, heave and creep. *Permafrost and Periglacial Processes* 8: 155–177.

Matsuoka, N. & Ikeda, A. 2001. Geological control on the distribution and characteristics of talus-derived rock glaciers. *Ann. Rep. Inst. Geosci., Univ. Tsukuba* 27: 11–16.

Morris, S.E. 1981. Topoclimatic factors and the development of rock glacier facies, Sangre de Cristo Mountains, Southern Colorado. *Arctic and Alpine Research* 13: 329–338.

Olyphant, G.A. 1983. Computer simulation of rock-glacier development under viscous and pseudoplastic flow *Geol. Soc. Am. Bull.* 94: 499–505.

Paterson, W.S.B. 1994. *The Physics of Glaciers*. Pergamon Press Ltd.

Rapp, A. 1960. Talus slopes and mountain walls at Tempelfjorden, Spitsbergen. *Norsk Polarinstitutt Skrifter* 119: 1–96.

Sloan, V.F. & Dike, L.D. 1998. Decadal and millennial velocities of rock glaciers, Selwyn Mountains, Canada. *Geografiska Annaler* 80A: 237–249.

Von Elverfeldt, K. 2002. Analyse der Blockgletscherkinematik im Turtmanntal, Wallis, mittels digitaler Photogrammetrie. Unpublished MSc-thesis, Geographisches Institut. Bonn, Rheinische Friedrich-Wilhelms-Universität: 114 p.

Wahrhaftig, C. & Cox, A. 1959. Rock glaciers in the Alaska Range. *Geol. Soc. Am. Bull.* 70: 383–436.

White, P.G. 1979. Rock glacier morphometry, San Juan Mountains, Colorado. *Geol. Soc. Am. Bull.* 90: 515–518.

MORPHOMETRIC MODELLING OF ROCKGLACIERS – A CASE STUDY FROM THE ALPS

R. FRAUENFELDER[1], B. SCHNEIDER[2] AND B. ETZELMÜLLER[3]

[1] *Department of Geography, University of Zurich, 8057 Zürich, Switzerland*
[2] *Department of Earth Sciences, University of Basel, 4056 Basel, Switzerland*
[3] *Department of Geography, University of Oslo, Blindern, 0316 Oslo, Norway*

ABSTRACT

Rockglaciers – permafrost creep features on mountain slopes – are common landforms in high mountain areas. Despite their frequency, knowledge and understanding with respect to temporal and spatial variability of regional rockglacier occurrence is still limited. The present study seeks to evaluate and advance existing knowledge by means of geomorphometrical modelling of rockglacier distribution. In this study, terrain analysis and classification were applied, based on digital elevation models (DEMs), to model rockglacier occurrence in a study area in the Swiss Alps. The results show (a) that geomorphometry is a suitable tool for reproducing *potential* rockglacier root zones, and (b) that deviations of the modelling results from the empirical findings are mainly caused by the fact that rockglacier occurrence is not purely topographically defined.

INTRODUCTION

Rockglaciers are debris accumulations produced, deposited, and deformed during historical and Holocene time periods. They originate from periglacial talus ('talus-derived' rockglaciers, Figure 1) and/or glacier-transported debris, mostly from lateral and terminal moraines ('moraine-derived' rockglaciers).

Rockglaciers are efficient transport systems of rock debris in the periglacial alpine environment. They can be classified as active, inactive or relict depending on their ice content and their movement, i.e. depending on their activity as debris transport systems. When active, they typically take the form of 20–100 m thick tongue- or lobe-shaped bodies with cascading frontal slopes standing at the angle of repose (Humlum, 2000a). Their length may be as many as several kilometres, but the typical length is 200–800 m (Barsch, 1996). The surfaces of the creeping frozen bodies are covered with coarse rock fragments and have curving transverse furrows and ridges up to several metres in height (Humlum, 2000a). Average surface velocities of active rockglaciers vary between less than a few centimetres per year and several metres per year. Hence, rockglacier velocity is one order of magnitude slower than the velocity of glaciers. The flow regimes of rockglaciers change slowly with time. Consequently, and considering the low average surface velocities, rockglacier bodies of several hundred metres' length are at least some centuries, often several millennia, old (e.g. Barsch, 1996; Frauenfelder *et al.*, submitted; Haeberli *et al.*, 1999; Humlum, 2000b).

Talus-derived rockglaciers are located at the foot of headwalls with a high supply of debris and represent a process chain linking frost weathering and rockfall from headwalls with debris displacement by permafrost creep (Figure 2). In general, the occurrence of these landforms is influenced primarily by climatic and topographic preconditions. Therefore, talus-derived rockglaciers are found in areas characterized by specific topographic attributes: they occur within a certain altitudinal band – due to the prevailing mean annual air temperature; and they favour certain slope aspects – due to differences in incoming radiation. Furthermore,

they require a particular slope – flow of the ice-debris mixture must be possible, and they need a rock-contributing headwall above them – in order to ensure debris supply. These characteristics give rise to the theoretical possibility of modelling regional rockglacier distribution by means of digital terrain analyses or geomorphometry. Geomorphometry, the quantitative treatment of the morphology of landforms, builds upon the basic assumption that there exists a close relationship between surface processes and particular topographic characteristics, represented by topographic attributes (e.g. Evans, 1972; Mark, 1975; Pike, 1995).

Figure 1. Oblique photograph of an active talus-derived rockglacier in the eastern Swiss Alps. The rockglacier root zone (= *RRZ*, see explanations in the text below) is partly visible in the snow-covered upper right of the picture.

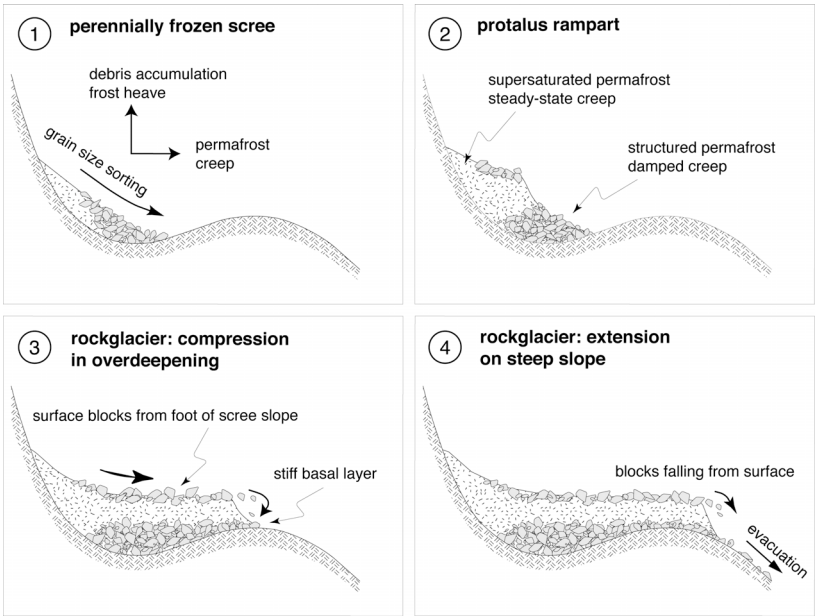

Figure 2. Schematic diagrams of the evolution of a periglacial talus-derived rockglacier from a perennially frozen scree slope, to a protalus rampart, to a 'fully grown' rockglacier (reprinted with permission of the Centre d'Etudes nordiques, Université Laval, Canada from Haeberli *et al.*, 1998, p. 407, Figure 4).

Detailed knowledge and understanding of the temporal and spatial variability of regional rockglacier occurrence is still limited. The objective of this study is to evaluate

morphometrical techniques for modelling the regional distribution of talus-derived rockglaciers. As mentioned above, they tend to occur in locations characterized by certain topographic conditions. The basic hypotheses for this study is, hence, that the distribution of talus-derived rockglaciers can be described by relief parameters, in a way that the statistical likelihood of their occurrence in a certain topographical situation may be predicted. By analyzing digital elevation models and derivation of topographic attributes typical for these locations, empirical relationships between talus-derived rockglacier distribution and certain combinations of topographic attributes are established.

Geomorphometric modelling of the entire rockglacier bodies is difficult as these landforms vary considerably in form and size. There are, however, areas within each talus-derived rockglacier that possess specific characteristics similar to all these forms: in the so-called *rockglacier root zone (RRZ)* the accumulated debris is triggered to creep (cf. Barsch, 1996). This zone is located within or at the end of a concave landform where debris can accumulate (see Figure 1, area in the upper right corner). In order to allow accumulation, the *RRZ* must not exceed a specific slope angle. On the other hand, the *RRZ* needs to be steep enough to enable the triggering of debris creep. Hence, *RRZs* are considered as representative points of rockglaciers, and the more specific goal of this study is, therefore, to map potential *RRZs*.

This paper presents empirical modelling of *RRZ* distribution, and evaluates discrepancies between modelled and real data. The focus hereby is on the distribution of talus-derived rockglaciers, and the explanations in the following text refer, by implication, to these forms.

STUDY AREA AND DATASETS

Geographical setting and field data

The study is carried out in the Upper Engadine, eastern Swiss Alps. The area covers approximately 530 km^2, stretching from 46°22'N to 46°35'N, and 9°39'E to 9°59'E. The study area is characterized by a high-situated valley floor with an average altitude of 1700 m a.s.l. It is surrounded by mountain peaks reaching up to 4000 m a.s.l (or slightly higher). Mean annual precipitation for the years 1971–1990, measured at two stations on the valley floor (Bever at 1712 m a.s.l. and St. Moritz at 1832 m a.s.l.) was 840 mm and 902 mm, respectively (data from *MeteoSwiss*, former Swiss Meteorological Service). Due to the high elevation of the area, annual temperatures are low. Mean annual air temperature was +1.8°C at Samedan for the period 1991–2000 (station with temperature measurements located at 1705 m a.s.l. and 2.5 km from the Bever station), and +2.1°C at St. Moritz for the period 1970–1980 (data from *MeteoSwiss*). Together with a regional lapse rate of 0.55°C/100 m (Maisch, 1992), this yields a mean annual 0°C-isotherm at about 2200 m a.s.l.

Hoelzle (1998) identified 84 active rockglaciers in the study area by means of field investigation and analyses of aerial photography; 64 of these rockglaciers were identified as (periglacial) talus-derived forms.

An overview on the study area, including the locations of the rockglaciers, some additional land-cover information and the most important place names mentioned in the text is given in Figure 3.

Digital elevation model (DEM)

To map the potential *RRZs*, topographic attributes need to be identified that correlate with their occurrence. The surface parameterization must be carried out at an appropriate scale, determined by the considered process. Potential *RRZs* are influenced by landforms in the

range of decametres to hectometres. Therefore, the reference scale for the modelling is several tens of metres to hundreds of metres. For this purpose, the use of a raster-based digital elevation model (DEM) with a resolution in the range of decametres seemed adequate. A DEM with 50 metres or 100 metres cell size would be too coarse to allow *RRZ* detection, as they do not capture all topographic features relevant for the development and occurrence of rockglaciers. Hence, primary and secondary topographic attributes are extracted from a DEM with a 25 m cell size from *swisstopo* (the former Swiss Federal Office of Topography). This so-called DEM25 is generated from the height information of the national 1:25,000 maps through vectorization of contour lines and lake contours, digitizing of the spot heights (the number of height values for each map sheet, which are also valid for the DHM25, varies between 7500 and 333,000 or an average of 35 to 1600 points per km^2) and subsequent interpolation of a DEM with 25 m raster width from these data using the programme CONGRID (written at *swisstopo*). Comparisons with photogrammetrically determined control points have shown that the average accuracy of this DEM reaches approximately 3 m in the Alps (www.swisstopo.ch, Hurni, 1995).

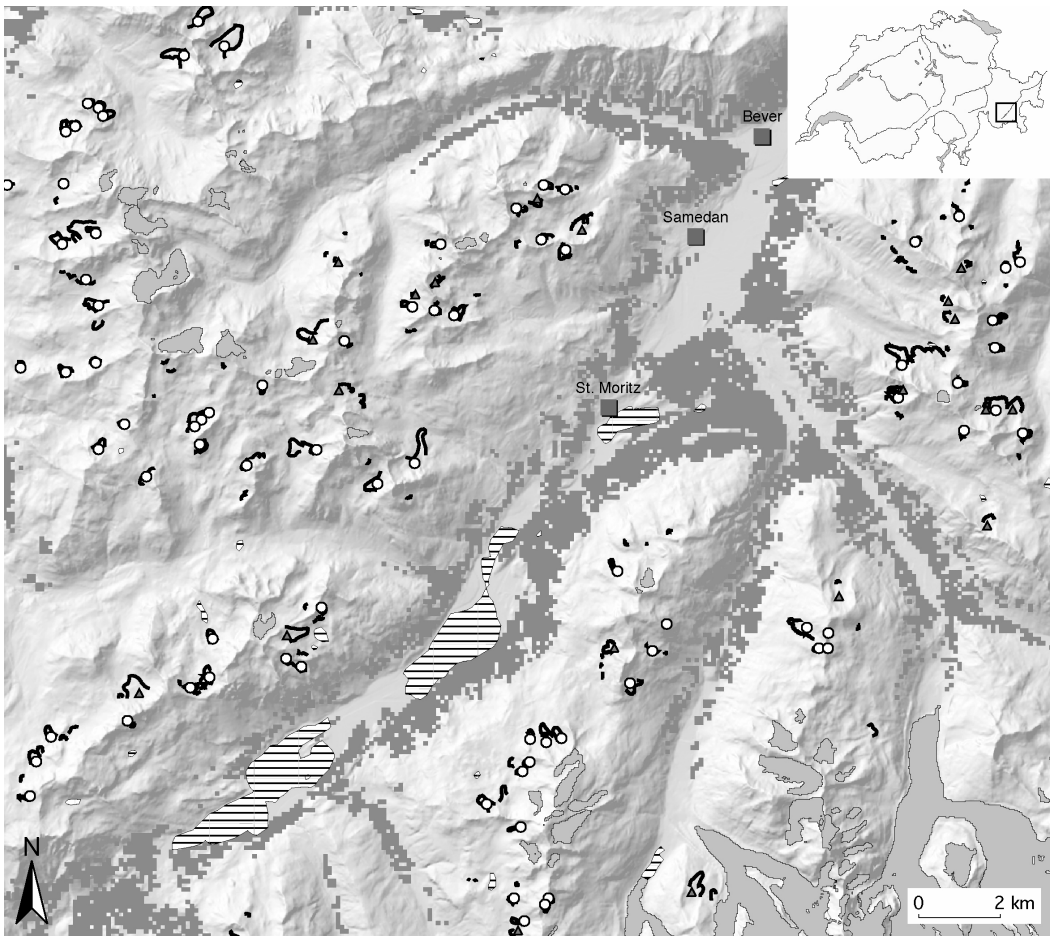

Figure 3. Shaded DEM25 of the study region in the Upper Engadine, eastern Swiss Alps (25 m resolution). Size of original DEM: 2201 x 1781 Pixels (ca. 55 x 44.5 km). Rockglacier outlines are represented by black lines, circles mark empirically derived talus-derived *RRZs*, triangles stand for root zones of moraine-derived rockglaciers (not considered in this modelling). The locations of the climatic stations mentioned in the text are marked with black squares. Glaciers are depicted with light grey, lakes are striped, dark grey pixelated zones represent forested areas. Data sources: glacier extent as derived from satellite imagery by Paul (2003), rockglacier distribution as inventoried by Hoelzle (1989; 1998), forest areas extracted from the data base of the Swiss Land Use Statistics (BFS, 1992), DEM25 © 2004 *swisstopo* (BA046054).

METHODS AND PROCEDURES

Derivation of topographic attributes

The modelling applied in this study follows the approach of Weibel and DeLotto (1988) which consists of three steps: the choice of the variable, the determination of the geometric signature of this variable, and the terrain classification as such.

Comprehensive compilations of topographic attributes to be computed from DEM data are given, for example, in Moore et al. (1990) and Wilson and Gallant (2000). An overview on the significance of terrain parameters in periglacial research can be found in Etzelmüller et al. (2001) and Etzelmüller & Sulebak (2003). Based on the suggestions of the above-mentioned authors, we selected attributes with close relationships to gravity-driven slope processes, such as:

- *primary* topographic attributes:
  altitude, aspect, slope (for scale levels equivalent to 25 m and 50 m resolution), total curvature, plan curvature and profile curvature (see Figure 4),

- *secondary* topographic attributes (i.e. statistical, mathematical or logical combinations of primary attributes):
  local relief, elevation-relief ratio, skewness of altitude, distance to nearest ridge (slope length), topographic wetness index, roughness index, radiation balance.

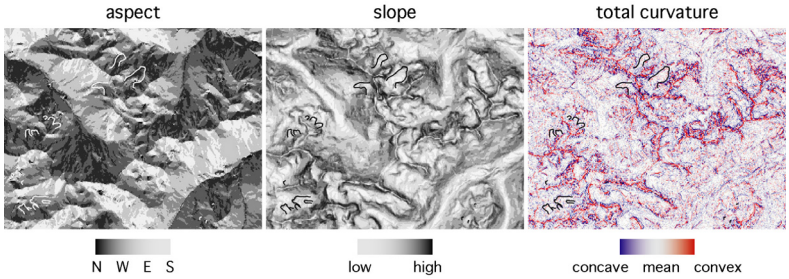

Figure 4. Computations of aspect (left), slope (middle) and total curvature(right) visualized for a subregion of the study area. White lines (left) and black lines (middle, right) outline tongues of active talus-derived rockglaciers. Data sources as in Figure 3.

These topographic attributes are calculated for all *RRZs* using standard routines within the GIS software package ArcInfo (® ESRI) and stored as individual grids. Accordingly, co-ordinates are obtained for each topographic attribute. Together with the DEM these new grids represent a multidimensional geometric description of the *RRZs*. A thoughtful choice of selected topographic attributes from this geometric description should result in a set of measures that describe the *RRZs* well enough to distinguish them from other different landforms. To prevent the choice of auto-correlated topographic attributes, their correlation matrices have to be analyzed prior to the selection of attributes to be used in the modelling (see Tables I, II).

The distributions of the *RRZ*s are derived with respect to the selected topographic attributes. Firstly, the statistical values (min, max, mean, and standard deviation) of each of the topographic attributes are derived. The values obtained are then used to classify each topographic attribute into six classes of equal size with class borders at μ, $\mu \pm 0.5\sigma$, and $\mu \pm \sigma$, where μ is the mean of the attribute values and σ the relevant standard deviation. These results are plotted as histograms, which allows for the qualitative distinction between

attributes for which the *RRZs* are evenly distributed, i.e. attributes that are ineffective for modelling, and attributes showing clear accumulations of *RRZs* in distinct classes, in other words, attributes suitable for the modelling (Table II). Based on the results of the histogram analyses and the check for auto-correlation, those topographic attributes which seem to be representative of the sought *RRZs* and which show no auto-correlations are chosen for the modelling procedure.

Table I. Correlation matrix for derived primary and secondary topographic attributes

Attribute	altitude	aspect	slope	curv. total	curv. plan	curv. profile	local relief	elev.-relief ratio	skewn.	slope length	wetness index	roughn. index	rad.
altitude	1	0.003	0.340	0.078	-0.055	-0.089	0.321	0.662	0.507	-0.005	-0.067	0.355	-0.072
aspect	0.003	1	0.064	0.005	-0.004	-0.004	0.063	0.048	0.026	0.001	-0.043	0.075	0.625
slope	0.340	0.064	1	0.055	-0.079	-0.033	0.861	0.281	0.146	-0.011	-0.106	0.731	-0.404
curvature, total	0.078	0.005	0.055	1	-0.793	-0.857	0.053	0.008	0.002	-0.021	-0.107	0.030	0.050
curvature, plan	-0.055	-0.004	-0.079	-0.793	1	0.465	-0.092	-0.001	-0.004	0.015	0.132	-0.026	-0.009
curvature, profile	-0.089	-0.004	-0.033	-0.857	0.465	1	-0.025	-0.018	-0.007	0.020	0.058	-0.029	-0.064
local relief	0.321	0.063	0.861	0.053	-0.092	-0.025	1	0.231	0.138	-0.018	-0.124	0.623	-0.443
elevation relief ratio	0.662	0.048	0.281	0.008	-0.001	-0.018	0.231	1	0.413	-0.003	-0.001	0.349	-0.025
skewness of altitude	0.507	0.026	0.146	0.002	-0.004	-0.007	0.138	0.413	1	0.001	-0.021	0.145	-0.002
slope length	-0.005	0.001	-0.011	-0.021	0.015	0.020	-0.018	-0.003	0.001	1	0.005	0.003	0.002
wetness	-0.067	-0.043	-0.106	-0.107	0.132	0.058	-0.124	-0.001	-0.021	0.005	1	-0.025	0.019
roughness	0.355	0.075	0.731	0.030	-0.026	-0.029	0.623	0.349	0.145	0.003	-0.025	1	-0.278
radiation	-0.072	0.625	-0.404	0.050	-0.009	-0.064	-0.443	-0.025	-0.002	0.002	0.019	-0.278	1

Table II. Qualitative interpretation of frequency distribution histograms, and analysis of correlation matrices for the analyzed topographic primary and secondary attributes.

Attribute	Frequency distribution		Correlation with: (see Table II)
	RRZs homogeneously distributed between classes	*RRZs* clustered in one or more classes	
altitude		x	elevation-relief r., skewness
aspect	x		radiation
slope		x	local relief, roughness index
curvature, total		x	curvature, profile, plan
curvature, plan		x	total curvature
curvature, profile		x	total curvature
local relief		x	slope, roughness index
elevation-relief ratio		x	altitude
skewness of altitude		x	altitude
slope length	x		
wetness index		x	
roughness index		x	slope, local relief
radiation		x	aspect

Classification procedures

Three different methods are applied for terrain classification:

(A) a probabilistic approach based on the distribution of the values of the selected topographic attributes,

(B) a deterministic approach using the range of occurring values,
(C) an extension of the deterministic approach (B) by including rockfall accumulation areas.

(A) Probabilistic approach

The quantitative information of the frequency distribution histograms is interpreted as an indication of probability where higher occurrence of *RRZs* in individual attribute value classes indicates higher probability, and vice versa, i.e. lower occurrence of *RRZs* in individual attribute value classes indicates lower probability. An example of this procedure is given in Table III for the topographic attribute 'slope'. The same procedure was applied for all topographic attributes which are found suitable for the modelling, i.e. which are inhomogeneously distributed between the classes (see above).

The probabilities for the different topographic attributes are then multiplied in order to obtain combined probabilities of rockglacier occurrence for all locations in the test area. This was done for different combinations of topographic attributes without auto-correlations (see Table II).

Table III. Absolute and percent distribution of the *RRZs* relative to the topographic attribute slope.

Class	Relative boundaries	Absolute boundaries	Number of *RRZs*	Percent	Probability
1	$< \mu-\sigma$	< 12.1°	9	8.3	0.083
2	$\mu-\sigma$ to $\mu-0.5\sigma$	12.1°–18.9°	16	14.7	0.147
3	$\mu-0.5\sigma$ to μ	18.9°–25.7°	34	31.2	0.312
4	μ to $\mu+0.5\sigma$	25.7°–32.5°	23	21.1	0.211
5	$\mu+0.5\sigma$ to $\mu+\sigma$	32.5°–39.3°	14	12.8	0.128
6	$> \mu+\sigma$	> 39.3	13	11.9	0.119

(B) Deterministic approach

In this approach, the range of occurring values (see Table IV) for each significant topographic attribute is used and values outside these ranges ruled out. For example, active rockglaciers in the study area are found at elevations between 2230 m a.s.l. and 3500 m a.s.l., in areas with medium wetness index, and on slopes with a steepness between 7° and 52°. In a boolean procedure, values outside these defined ranges (between the minimum and maximum values) are marked as 'no *RRZs* possible'.

Table IV. Range of occurring values of each significant topographic attribute. For those attributes used in approach (B), the values listed below correspond to the boundary conditions applied.

Attribute	Minimum value	Maximum value
altitude	2172	3105
aspect	0	360
slope	6.58	52.45
curvature, total	-2.66	4.22
curvature, profile	-1.72	1.46
curvature, plan	-2.50	1.19
local relief	6	92
elevation-relief ratio	0.37	0.57

Table IV. Continued.

Attribute	Minimum value	Maximum value
skewness of altitude	-0.18	1.83
slope length	0.00	1744.98
wetness index	0.00	7.52
roughness index	34.85	66.67
radiation	7.47	32.11

(C) Inclusion of rockfall accumulation areas

The third approach broadens the *deterministic approach (B)* to include rockfall accumulation areas, which can be modelled using a (semi-)geomorphometrical approach. The expansion is based on the (banal) observation that rockglaciers can only develop where rock debris is available. As mentioned before, the rock debris incorporated in talus-derived rockglaciers originates from contributing headwalls. Hence, if it is possible to locate these debris-supplying headwalls geomorphometrically and to estimate the extent of the relevant rockfall, the potential *RRZs* may be significantly reduced.

The so-called 'overall-slope' or 'reach-angle' approach (also known as 'Fahrböschung', Heim, 1932) is used to compute rockfall and rockfall accumulation (Brändli, 2001). In a first approximation, areas with a slope angle equal to or greater than 37° (an empirical value found to adequately represent real rock walls in the study area) are identified as debris supplying rock walls. Rocks are then simulated to fall from these debris sources along the path of steepest descent. The movement of falling rocks is assumed to stop when the slope of the straight line connecting the current position of the rock with its origin reaches 31°, which is an empirically derived value (Gerber, 1994). All of the cells which a falling rock passes during its fall are marked as rock accumulation areas. This procedure is repeated up to 1000 times, simulating decadal rockfall events. Finally, areas of contributing headwalls are excluded from the resulting areas (Figure 5). Assuming that a rockglacier can only emerge where rock accumulation takes place, the potential *RRZ* occurrence areas resulting from approach (B) are intersected with the rock accumulation areas (see below, Figure 9).

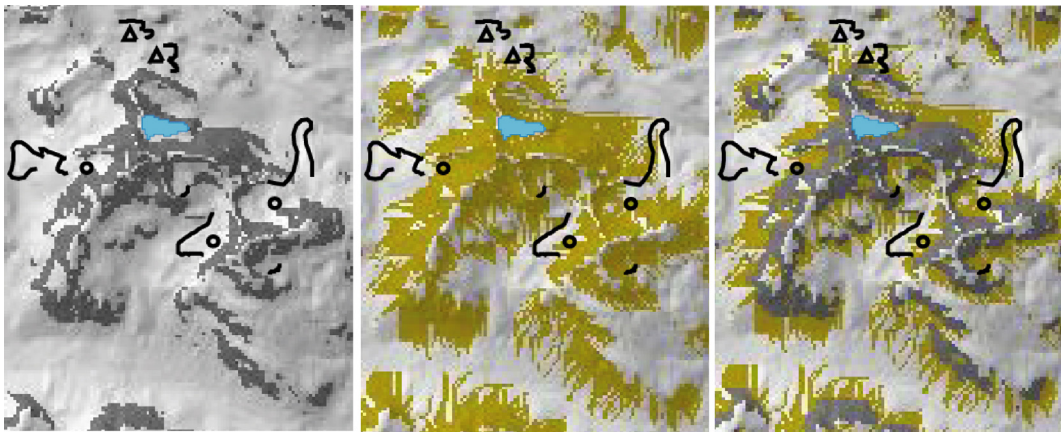

Figure 5. (left) modelled rock faces (areas steeper than 37°) in dark grey, (middle) modelled rockfall accumulation areas derived using the 'overall slope' approach (Brändli, 2001; Heim, 1932) in ochre, (right) combination of (a) and (b). Data sources as in Figure 3.

RESULTS

(A) Probabilistic approach

With a probabilistic approach the regions classified as potential *RRZs* (a) are too large, and (b) have a significant number of *RRZs* located in areas that were assigned low probabilities of rockglacier occurrence (see Figure 6 for spatial visualization and Figure 7 for statistical distribution).

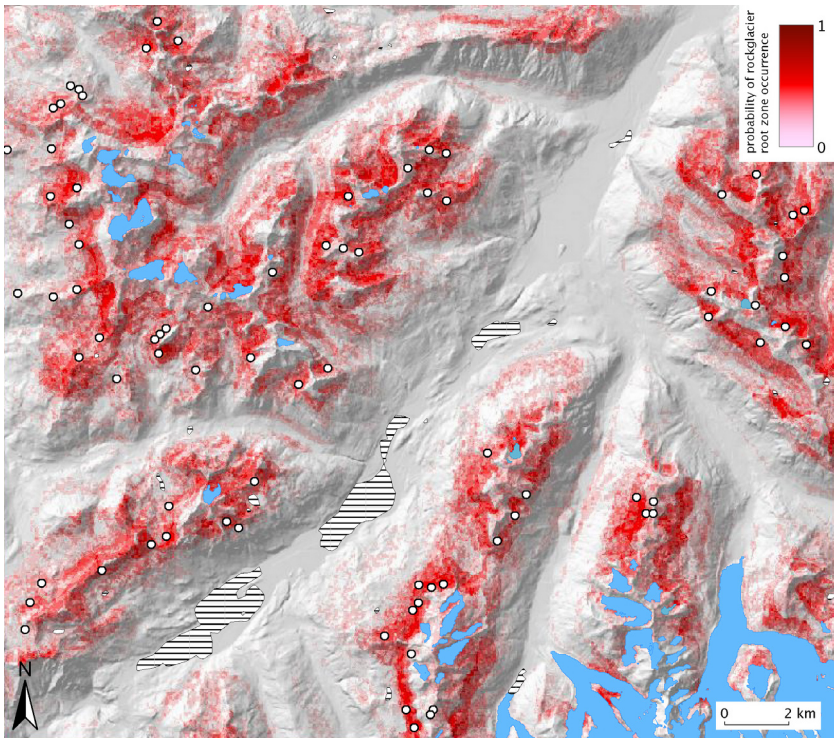

Figure 6. Approach (A): combination of the most significant topographic attributes for the modelling of talus-derived rockglacier occurrence using a probability approach. Attributes used are altitude, aspect, slope, curvature, local relief, elevation-relief ratio, skewness of altitude, and roughness index. *RRZs* of active talus-derived rockglaciers are depicted with circles, glaciers are coloured light-blue and lakes are striped. Data sources as in Figure 3.

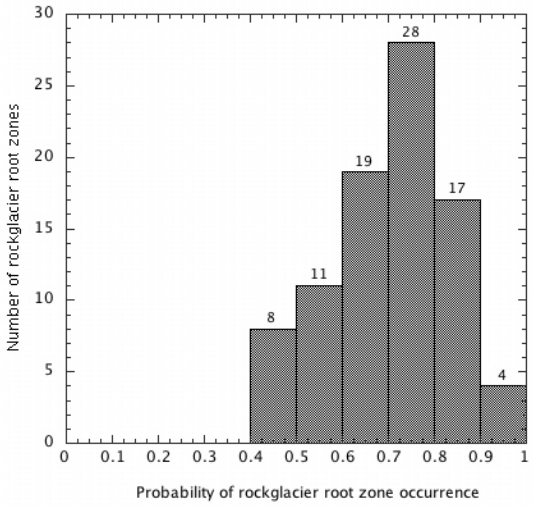

Figure 7. Probability distribution of *RRZ* modelling with approach (A)

The modelling result cannot be improved by removing a topographic attribute from the criteria list, nor by adding a new one. Removing would enlarge the area with high probability, while adding would result in even more rockglaciers being located in areas with low probability for rockglacier occurrence.

(B) Deterministic approach

Compared to the results of approach (A), two main differences are obvious when modelling the *RRZs* with a deterministic approach (Figure 8): (a) the problem of rockglaciers occurring outside the modelled zones could be solved, i.e. all *RRZs* lie within the modelled potential *RRZ* areas, and (b) the zones modelled as potential *RRZs* (depicted in red) are, however, much too large. This results from the very conservative procedure that is applied. Additionally, there is no weighting of the modelled zones included. A specification of the probability of occurrence within the modelled zones as in approach (A) is, therefore, not possible.

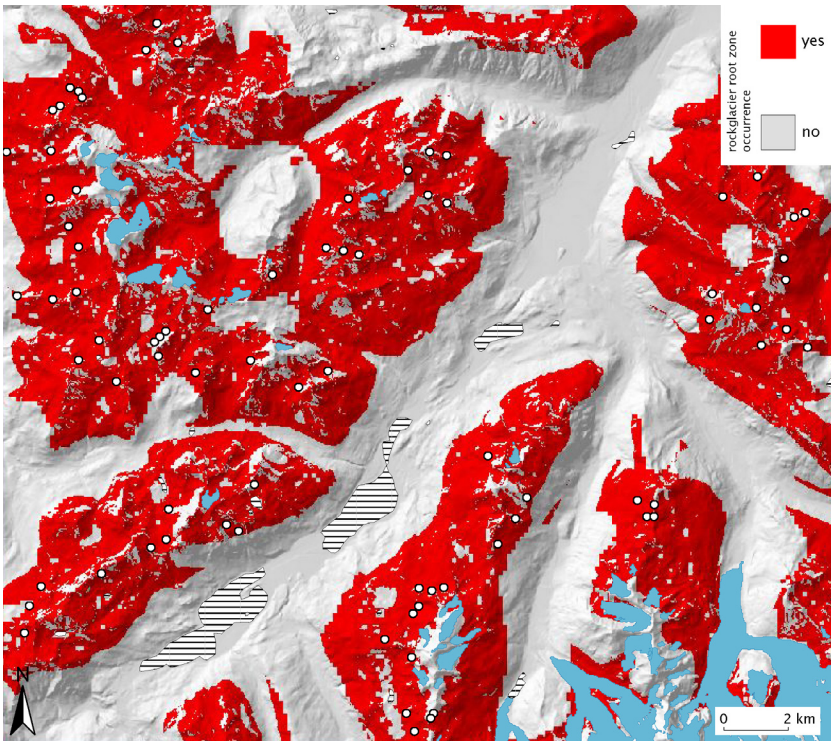

Figure 8. Approach (B): combination of the most significant topographic attributes for the modelling of talus-derived rockglacier occurrence using a procedure that takes the range of occurring values into account. Attributes used are altitude, aspect, slope, plan curvature, profile curvature, local relief, elevation-relief ratio, skewness of altitude, wetness index, and roughness index. Cartographic representation of *RRZs*, glaciers and lakes as in Figure 6, data sources as in Figure 3.

(C) Inclusion of rockfall accumulation areas

With the inclusion of rockfall accumulation areas in the modelling, the number of falsely modelled potential *RRZs* is significantly decreased compared to the results from Approach (A) and (B); however, overestimations still occur (see Figure 9). As explained above, rockfall accumulations are modelled by calculating a random number of rockfall trajectories. Due to undesired side-effects caused by the raster data model of the DEM, rockfall accumulation

patterns tend to exhibit 'holes' between the individual trajectories. *RRZs* that are located in such 'holes', which presumably do not exist as frequently in nature as implied by the model results, are considered as 'falsely' modelled (see Table V). Upon analyzing the individual cases it can be argued with reasonable certainty, however, that *RRZ*s modelled ≤ 25 m away (which corresponds to 1 grid-cell), can be considered as 'correctly' modelled as well.

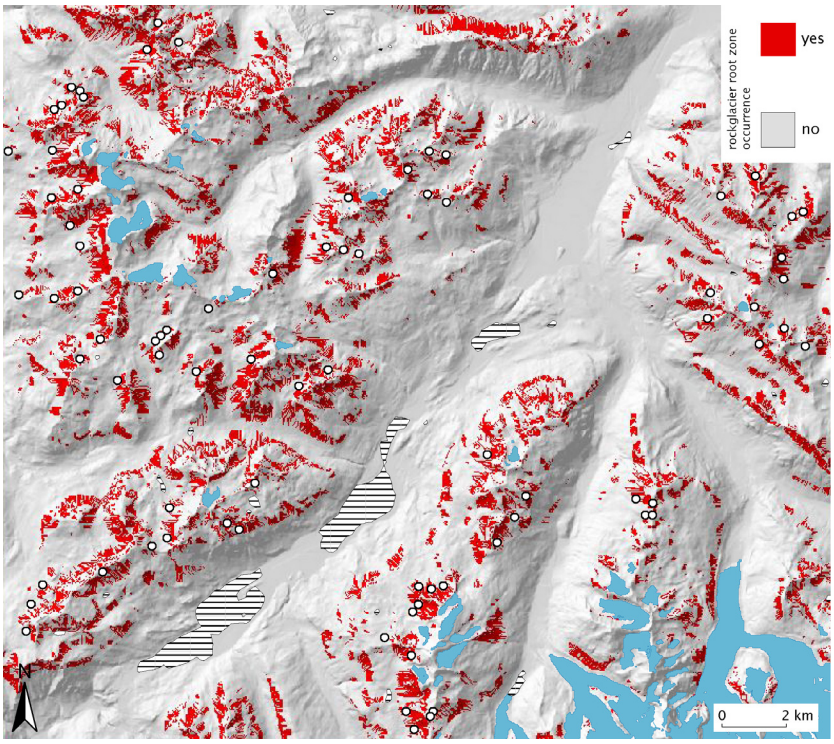

Figure 9. Approach (C): approach (B) with inclusion of the modelled rockfall accumulation areas (see Figure 5), representing zones where debris is available. Cartographic representation of *RRZs*, glaciers and lakes as in Figure 6, data sources as in Figure 3.

Table V. Amount of correctly and falsely modelled *RRZs* with approach (C)

modelled correctly	modelled max. 25 m apart	modelled max. 50 m apart	modelled max. 75 m apart	modelled max. 125 m apart	modelled > 150 apart
67	7	5	5	2	0

DISCUSSION

In approach (A), the size of the areas classified as potential *RRZs* without actually having any rockglaciers in reality is considerably large. At the same time, some rockglaciers that actually exist lie in areas with low probabilities (of ≤ 0.6) for the occurrence of *RRZs* (see Figures 6, 7). As the results of this approach indicate, a modelling based only on a univariate consideration of topographic attributes seems unfeasible. Hence, simply multiplying the probabilities of the individual attributes is not a suitable approach for the detection of rockglaciers *RRZs*. A continued study of this approach would need to specify in detail the potential correlations between the individual topographic attributes. This might reveal that individual attribute values only occur in specific combinations, which would improve the

criteria for rockglacier modelling. Such multivariate classification schemes have been used for different geomorphological applications (e.g. Sulebak *et al.*, 1997; Wood-Smith and Buffington, 1996) but were not carried out in this study.

Modelling with the deterministic approach (B) enables the inclusion of the *RRZs* of all talus-derived rockglaciers which occur. However, due to the very conservative procedure, the number of areas that are falsely modelled as potential *RRZ* areas increases significantly (see Figure 8) compared to approach (A).

In contrast to this, the inclusion of rockfall accumulation areas in approach (C) leads to a distinct decrease in falsely modelled areas (Figure 9, Table V). A certain number of problematic cases remain even with this approach, however. They are basically of three kinds: (a) for very small (and often steep) rockglaciers the contributing headwall is not represented in a DEM with 25 m resolution. Therefore, rockfall is not modelled in these areas, and consequently, the root zones lie outside the modelled potential *RRZ* areas. (b) Some rockglaciers do not (any longer) have a contributing headwall in nature. It is likely that their activity will decrease in the near future, due to a lack of debris supply. (c) The main difficulty, however, is the modelling of rockfall accumulation areas itself. Both the localization of contributing headwalls and the estimation of the rockfall extent are calculated with very simple models, partly because topographic information alone is employed (see also above).

Several authors (e.g. Blaszczynski, 1997; Etzelmüller *et al.*, 1998; Sulebak *et al.*, 1997) successfully applied geomorphometry for large-scale modelling, such as regional terrain classification or landscape regionalization on meso- to macro-scales. A large difference between these studies and our application is, however, that the objects/points we model (i.e. the *RRZs*) are inherently discrete objects. We can only model them either correctly or not correctly. In landscape regionalization such unerring proofs are often absent, and the delineation of a landform class remains, to some degree, subjective.

CONCLUSIONS

Comparing the results of the three different modelling approaches reveals that there is generally a trade-off between a modelling approach with narrow boundary conditions, leading to an increased number of objects that are not reproduced by the model, i.e. that lie outside the mapped *RRZ* areas (A), and a modelling approach with wide boundary conditions, leading to large overestimation of the modelled *RRZ* areas (B). The inclusion of rockfall accumulation areas, even if based on simple modelling schemes, allows a much better estimate of *potential RRZ* areas. The modelled *RRZ* areas remain *potential* areas, as the presented modelling approach does not enable a distinction to be made between *RRZs* and other periglacial slope foot areas. However, exactly these periglacial slope foot areas are potential areas for rockglacier formation, and therefore, their recognition by a morphometric model is most desirable. The question of why many of these potential *RRZ* areas are devoid of rockglaciers involves various factors (e.g. time, climate, hydrology, composition of the talus slopes) that are not reproducible by a purely morphometric approach.

ACKNOWLEDGEMENTS

This study was supported by an international scholarship of the Research Council of Norway, Oslo and a research grant of the ‘Stiftung zur Förderung der wissenschaftlichen Forschung’ at the University of Zurich, Switzerland. We are indebted to Martin Hoelzle for compiling the

rockglacier inventory on which this study is based on. Thanks are also extended to Susan Braun-Clarke who improved the English.

REFERENCES

Barsch D. 1996. *Rockglaciers. Indicators for the present and former geoecology in high mountain environments*. Springer: Berlin.

BFS. 1992. Die Bodennutzung der Schweiz – Arealstatistik 1979/85, Kategorienkatalog. Bundesamt für Statistik: Bern.

Blaszczynski JS. 1997. Landform characterization with Geographic Information Systems. *Photogrammetric Engineering and Remote Sensing* **63** (2): 183–191.

Brändli M. 2001. Steinschlagmodellierung. HTML-page: http://www.geo.unizh.ch/~gis2/pro/steinschlag/helps/pg/ c-prog-new.html. Edition: 26.6.2001.

Etzelmüller B, Sulebak JR. 2003. Developments in the use of digital elevation models in periglacial geomorphology and glaciology. In *Entwicklungstendenzen und Zukunftsperspektiven in der Geomorphologie. Publikation zur Jahrestagung der Schweizerischen Geomorphologischen Gesellschaft (SGmG) anlässlich des 180. Jahreskongress der Schweizerischen Akademie der Naturwissenschaften (SANW) in Winterthur (11.-13. Oktober 2000)*, Maisch M, Vonder Mühll D, Monbaron M (eds.). Department of Geography, University of Zurich: 35–58.

Etzelmüller B, Berthling I, Sollid JL. 1998. The distribution of permafrost in southern Norway – a GIS approach. *Proceedings of the 7th International Conference on Permafrost, Yellowknife, Canada*: 251–257.

Etzelmüller B, Ødegård RS, Berthling I, Sollid JL. 2001. Terrain parameters and remote sensing data in the analysis of permafrost distribution and periglacial processes: principles and examples from Southern Norway. *Permafrost and Periglacial Processes* **12** (1): 79–92.

Evans IS. 1972. General geomorphometry, derivatives of altitude, and descriptive statistics. In *Spatial analysis in geomorphology*, Chorley RJ (ed.). Mathuen & Co Ltd, 17–92.

Frauenfelder R, Laustela M, Kääb A. submitted. Relative age dating of Alpine rockglacier surfaces. *Zeitschrift für Geomorphologie N.F.*

Gerber W. 1994. Beurteilung des Prozesses Steinschlag. Schweiz. Forstl. Arbeitsgruppe Naturgefahren (FAN), Herbstkurs, 20.-22. Oktober 1994, Poschiavo. Unpublised scriptum.

Haeberli W, Hoelzle M, Kääb A, Keller F, Vonder Mühll D, Wagner S. 1998. Ten years after drilling through the permafrost of the active rock glacier Murtèl, Eastern Swiss Alps: answered questions and new perspectives. *Proceedings of the 7th International Conference on Permafrost, Yellowknife, Canada*: 403–410.

Haeberli W, Kääb A, Wagner S, Vonder Mühll D, Geissler P, Haas JN, Glatzel-Mattheier H, Wagenbach D. 1999. Pollen analysis and 14C-age of moss remains recovered from a permafrost core of the active rock glacier Murtèl/Corvatsch (Swiss Alps): geomorphological and glaciological implications. *Journal of Glaciology* **45** (149): 1–8.

Heim A. 1932. Bergsturz und Menschenleben. *Beiblatt zur Vierteljahresschrift der Naturforschenden Gesellschaft in Zürich* **20**: 217.

Hoelzle M. 1989. Untersuchungen zur Permafrostverbreitung im Oberengadin. Abteilung für Naturwissenschaften, ETH Zürich, Unpublished MSc-thesis.

Hoelzle M. 1998. Rock Glaciers, Upper Engadin, Switzerland. International Permafrost Association, Data and Information Working Group, NSIDC, University of Colorado at Boulder. CD-ROM: version 1.0.

Humlum O. 2000a. The geomorphic significance of rock glaciers: estimates of rock glacier debris volumes and headwall recession rates in West Greenland. *Geomorphology* **35**: 41–67.

Humlum O. 2000b. The climatic and palaeoclimatic significance of rock glaciers. HTML-page: http://www.unis.no/RESEARCH/GEOLOGY/Geo_research/Ole/RockGlacierClimaticSignificance.htm. Edition: 2.2.2000.

Hurni L. 1995. Digital cartographic and topographic products from the Swiss Federal Office of Topography. *LIBER Quarterly. The Journal of European Research Libraries* **5**: 255–261.

Maisch M. 1992. Die Gletscher Graubündens: Rekonstruktionen und Auswertung der Gletscher und deren Veränderungen seit dem Hochstand von 1850 im Gebiet der östlichen Schweizer Alpen (Bündnerland und angrenzende Regionen). *Physische Geographie*, **33**A/B, Department of Geography, University of Zurich.

Mark DM. 1975. Geomorphometric parameters: a review and evaluation. *Geografiska Annaler, Series A* **57**: 165–177.

Moore ID, Grayson RB, Ladson AR. 1990. Digital terrain modelling: a review of hydrological, geomorphological and biological applications. *Hydrological processes* **5**: 3–30.

Paul F. 2003. The new Swiss Glacier Inventory 2000. Application of Remote Sensing and GIS. Department of Geography, University of Zurich, PhD-thesis.
Pike RJ. 1995. Geomorphometry – process, practice and prospect. *Zeitschrift für Geomorphologie* **101**: 221–238.
Sulebak JR, Etzelmüller B, Sollid JL. 1997. Landscape regionalisation by automatic classification of terrain elements. *Norwegian Journal of Geography* **51**: 35–45.
Weibel R, DeLotto JL. 1988. Automated terrain classification for GIS modelling. *GIS/LIS 88, Proceedings*. Virginia, **2**: 618–627.
Wilson JP, Gallant JC. 2000. *Terrain analysis – principles and applications*. John Wiley & Sons: New York.
Wood-Smith RD, Buffington JM. 1996. Multivariate geomorphic analysis of forest streams: implications for assessment of land use impacts on channel condition. *Earth Surface Processes and Landforms* **21** (4): 377–393.

IV

Annals of Glaciology 31 2000
© International Glaciological Society

Towards a palaeoclimatic model of rock-glacier formation in the Swiss Alps

Regula Frauenfelder, Andreas Kääb
Department of Geography, University of Zürich–Irchel, Winterthurerstrasse 190, CH-8057 Zürich, Switzerland

ABSTRACT. Climate and its long-term variability govern ground thermal conditions, and for this reason represent one of the most important impacts on creeping mountain permafrost. The decoding and better understanding of the present-day morphology and distribution of rock glaciers opens up a variety of insights into past and present environmental, especially climatic, conditions on a local to regional scale. The present study was carried out in the Swiss Alps using two different approaches: (1) kinematic analysis of specific active rock glaciers, and (2) description of the altitudinal distribution of relict rock glaciers. Two theoretical shape concepts of active rock-glacier morphology were derived: a "monomorphic" type, representing presumably undisturbed, continuous development over several millennia, and a "polymorphic" type, reflecting a system of (possibly climatically affected) individual creep streams several centuries old. The topoclimatic-based inventory analysis indicated an average temperature increase at relict rock-glacier fronts of approximately +2°C since the time of their decay, which is a sign of rock-glacier ages reaching back to the Alpine Late Glacial. The temperature difference of some tenths of a degree Celsius found for active/inactive rock glaciers is typical for the bandwidth of Holocene climate variations. These results confirm the importance of Alpine rock glaciers as highly sensitive indicators of past temperature evolution.

INTRODUCTION

Rock glaciers are a common landform in high Alpine areas. In recent years there has been a renewal of interest in the climatic and geomorphic significance of these features. Rock glaciers are the cumulative expression of their entire history and, thus, in a complex way, of their present and past environment. Comparisons of their actual thermal and dynamic behaviour, on the one hand, and their shape, on the other hand, enable conclusions to be drawn about past environmental conditions. Since rock glaciers are a phenomenon of creeping mountain permafrost, climate is — in addition to other factors such as geology, ice/water availability, etc. — one of the main controlling factors of their existence. The decoding of the present-day morphology and distribution of rock glaciers, and a better knowledge of the climatic controls on rock glaciers provide important information on past and present climatic conditions.

In this paper the focus is on the distribution and morphology of rock glaciers in the Swiss Alps, with the aim of reconstructing their evolution in both historical and morphological terms. A number of investigations (geophysical soundings, borehole measurements, BTS (bottom temperature of snow cover) mapping, spring water temperatures, etc.) have shown that the rock glaciers dealt with in this study represent creeping mountain permafrost (Barsch, 1978; Haeberli, 1985; Haeberli and others, 1998; Vonder Mühll and others, 1998). For our study the mere existence of the rock glaciers and the creep of the frozen debris is considered, regardless of the origins of the rock glaciers.

While considering two different time-scales, the Holocene and the Alpine Late Glacial, we follow two approaches:

(1) a photogrammetry-based analysis of the morphology and dynamics of selected active rock glaciers, in order to derive their age structure and two theoretical concepts of shape types for active/inactive rock glaciers;

(2) an inventory-based investigation of the spatial distribution of relict rock glaciers in order to estimate past limits of Alpine permafrost distribution.

From the synthesis of these two approaches we then assess the potential of single rock glaciers or groups of rock glaciers for estimating variations of palaeoclimate on a time-scale of millennia.

APPROACH 1: KINEMATICS

The present-day morphology of active rock glaciers reflects, not primarily their present dynamic state, but rather their dynamic history. Hence, complex and non-coherent shapes, rich in vertically and horizontally distinguishable creep systems, might point to a complex history, whereas uniform creep streams could represent a history of less dynamic variations. Furthermore, inactive and relict rock glaciers were obviously more active in the past than they are at present. Therefore, the potential significance of rock glaciers for palaeoclimatic conclusions strongly depends on their age and the expressiveness of their dynamic history. Many independent dating methods point to a general rock-glacier age in the range of millennia (e.g. relative age dating: Birkeland, 1973; surface weathering: Kirkbride and Brazier, 1995; Humlum, 1998; fossil soils: Johnson, 1998; geochemical data: Steig and others, 1998; radiocarbon age: Haeberli and others, 1999). At the same time, such studies give concise evi-

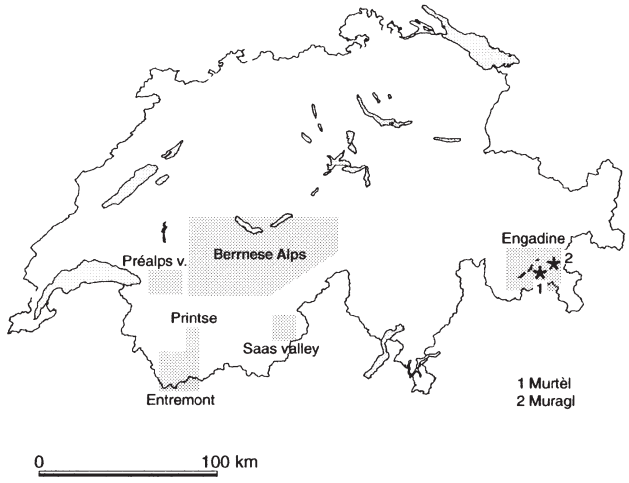

Fig. 1. Sketch map of Switzerland, showing the locations of the two active rock glaciers and the extent of the six rock-glacier inventories discussed in this paper.

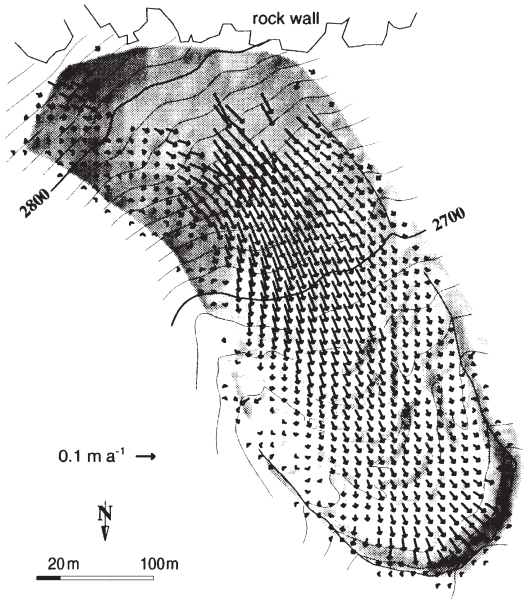

Fig. 2. Horizontal surface velocities of Murtèl rock glacier over the period 1986–96, measured by computer-aided photogrammetry.

dence that rock glaciers can display a complex, multi-system temporal behaviour.

Uniform morphology

In this study a photogrammetric approach was used to assess the age and the spatio-temporal age structure of selected active rock glaciers in the Swiss Alps. Using analytical photogrammetry, multitemporal digital terrain models (DTMs) were determined in order to obtain the spatial pattern of surface elevation changes. Entire surface flow fields were derived from the comparison of repeated imagery and subsequently used for streamline calculations. For details on methodology refer to Kääb and others (1997, 1998). By working out some general conclusions rather than giving a specific analysis of these two objects, the related results are demonstrated using Murtèl and Muragl rock glaciers (Upper Engadine, Swiss Alps; see Fig. 1).

The changes in elevation on the lower part of Murtèl rock glacier between 1987 and 1996 show a conspicuous pattern, with surface lowering of up to 0.1 m a^{-1} on the back of the transverse ridges, and almost unchanged elevation on the front of the ridges with respect to flow direction (cf. Kääb and others, 1998). This pattern results from two overlying processes: (a) a general loss of permafrost thickness by some 10^{-2} m a^{-1}, and (b) the advance of surface topography relative to the spatially fixed photogrammetric coordinate system. Separating the low-frequency effect (a) and the high-frequency effect (b), and considering the slopes of the surface relief enables the calculation of an advance rate of the ridges which approximates 0.05 m a^{-1}. This rate fits very well with the photogrammetrically derived surface velocity field of 1987–96 which shows surface velocities of a similar magnitude (Fig. 2). The transverse surface ridges on Murtèl rock glacier propagate downstream with a velocity that approximately equals that of the surface rocks. This has been shown also for other rock glaciers (White, 1987; Kääb, 1998), so it does not seem to be a random result just for this specific rock glacier and the given observation period. Therefore, we conclude that the surface topography reflects the creep of the permafrost body and can be used as an indicator of the creep field. In that way, the central stream of Murtèl rock glacier seems to represent one single creep system of cumulative and continuous deformation from the rock wall to the front. In our study this morphology type is called "monomorphic". However, bearing in mind the immense variety of rock-glacier shapes in nature, such a definition can only be theoretical. As a consequence, our idea of a "monomorphic" rock glacier refers to the central part of Murtèl rock glacier rather than to the entire rock glacier. In fact, interpretation of the very slow or even no-creeping lateral parts is difficult. These zones could have a dynamic origin (e.g. marginal shearing) and therefore be parts of the main stream, or they could be relicts of an older stage of the rock glacier and indicate some temporal variation in activity.

The age structure of Murtèl rock glacier was assessed from streamlines interpolated from the velocity field (Fig. 3, left). Under steady-state conditions these streamlines would represent the trajectories of specific particles on the surface and could thus be used for rock-glacier age estimates. It is clearly hypothetical and certainly critical to assume that the current velocities of Murtèl rock glacier approximately average the velocity fields of a lengthy time period in the rock-glacier evolution. However, this assumption seems justified by the fact that at Murtèl rock glacier (Fig. 3, left) the curvature of the isochrones (represented by dots of the same age) is similar to that of the transverse ridges. Since the surface topography presumably represents the cumulative surface deformation, as shown above, the average surface velocities over a long period of the rock glacier's existence must have been similar to the current velocities that underlie the calculated streamlines. In principle, the temporal average of velocities but not the temporal variability is considered. Nevertheless, in view of the coherent evolution of the ridge-and-furrow sequence (cf. Kääb and others, 1998), strong temporal variations in the kinetic history of Murtèl rock glacier seem unlikely.

The streamline isochrones indicate that the surface development of the central stream on Murtèl rock glacier took approximately 6 kyr. This age estimate for the central part is independent of the implications for the less active lateral parts (see above). Even introducing an error of some 10% for the above assumption of average velocities does not substan-

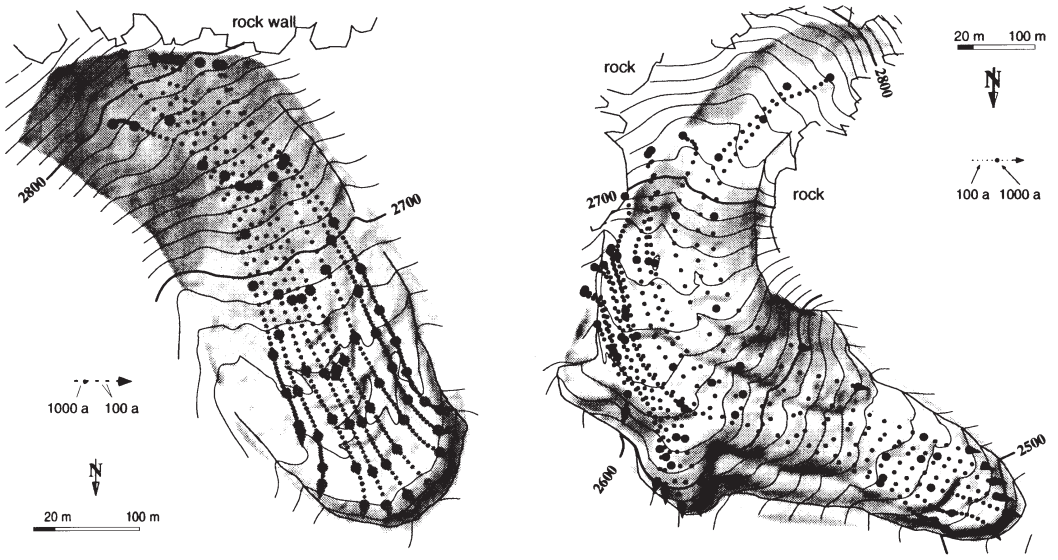

Fig. 3. Streamlines interpolated from the velocity fields of Murtèl rock glacier (left) and Muragl rock glacier (right). Bold dots represent a time-span of 1000 years.

tially affect the basic conclusion that the surface age of Murtèl rock glacier amounts to several (i.e. at least 4 or 5) kyr (cf. Haeberli and others, 1999). Relating this surface age to the present advance rate of the creeping body (about 0.01 m a^{-1}), derived in the same manner as for the ridges, results in a significantly higher total age of the whole rock glacier.

Complex morphology

The velocity field and the surface topography of Muragl rock glacier have a starkly contrasting appearance. The flow field of Muragl rock glacier between 1981 and 1994 reveals the rock glacier to be a complex system of several creep streams (even inactive ones, e.g. close to the northern margin) characterized by different velocities and creep directions (Fig. 4). Muragl rock glacier can be viewed as a system of several creep lobes having different behaviour with respect to time and space, partially overriding each other and/or laterally interacting. Internal processes (flow instabilities, mass-deposition feedbacks) or external forcing (climate variations, variations in mass supply) can be hypothesized as the cause of such complex structures. In contrast to the "monomorphic" type described above, this type of rock glacier is called "polymorphic" in our study.

These two theoretical types differ not only in their velocity field and morphology, but also in their age structure, as estimated from streamlines interpolated from the velocity fields (Fig. 3, right). The assumption that the current velocities approximately equal a temporal average leads to the qualitative conclusion that the surface age of the individual lobes is younger (2–3 kyr) than on Murtèl (at least 4–5 kyr). The fact that Muragl rock glacier consists of several vertically overthrusting streams, and has a clearly less active lower part, suggests a much older age of the entire rock glacier than only a few kyr. Taking into account the variety of transverse surface structures on Muragl rock glacier, there is no clear sign of a creep continuum from the rock wall towards the individual lobe fronts. Thus, in contrast to Murtèl rock glacier, the lobes might originate from somewhere intermediately downstream of the rock walls, leaving the above age assessment for the lobes as a maximum estimate. Introducing a large error for the estimation of the average velocities results in an uncertainty of about 0.1–1 kyr, but does not change the general age contrast between the central Murtèl stream and the Muragl lobes. Furthermore, independently of the age estimates for the individual lobes, Muragl rock glacier consists of active streams overriding those of low or even no kinetic activity. This clearly indicates an age structure different from that of the uniform central stream of Murtèl rock glacier.

APPROACH 2: SPATIO-TEMPORAL DISTRIBUTION

The compilation of six rock-glacier inventories (Delaloye and Morand, 1998; Frauenfelder, 1998; Hoelzle, 1998; Imhof, 1998; Reynard and others, 1998; Schoeneich, 1998b) of the Swiss Alps (Fig. 1) made it possible to put together a dataset

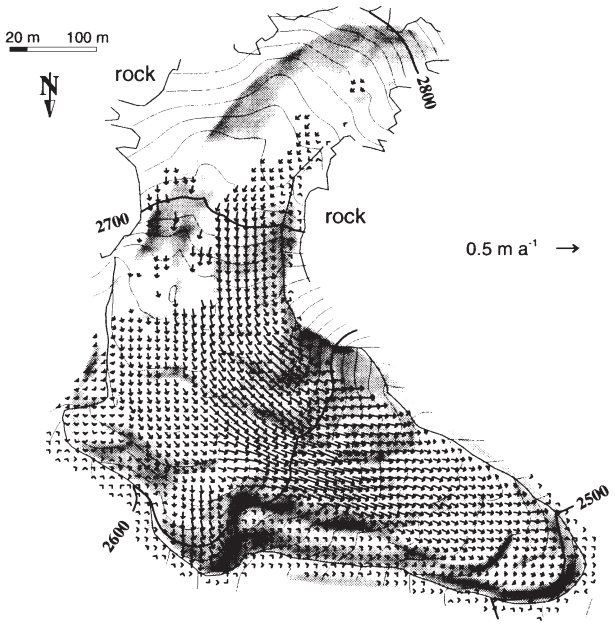

Fig. 4. Horizontal surface velocities of Muragl rock glacier for the period 1981–94, determined by computer-aided photogrammetry.

containing 741 individual rock glaciers, 253 of them active, 203 inactive and 285 relict. This dataset was used to study the spatial distribution pattern of relict rock glaciers. The area covered by the six inventories extends from the eastern main Alpine ridge (Engadine) over the Saas region (close to the central main Alpine ridge) to the southwestern Alps of the Valais (Entremont and Printse) and the western northern slope of the Alps (Préalps). Each inventory contains various data about the individual rock glaciers, including the altitude of each rock-glacier front (H_p).

A new model will now be presented which enables estimation of the permafrost limit since the Alpine Late Glacial by calculating the related lowering of the mean annual air temperature (MAAT) using data on relict rock glaciers.

Our method is based on the following key assumptions: Alpine permafrost reflects, initially, an interplay of temperature and radiation. Thus, creeping mountain permafrost (i.e. rock glaciers) becomes an intercomparable indicator of MAAT if the effect of radiation can be adjusted. Furthermore, the lowest active rock glaciers in a given region can be interpreted as an outline of the lower limit of discontinuous mountain permafrost. Likewise, presently relict rock glaciers have delineated the permafrost limit by the time of their transition from active/inactive to relict rock glaciers, i.e., at the time of their decay.

Our approach follows five calculation steps:

(1) The current MAAT at each rock-glacier front (T_p) is calculated (cf. Equation (2)) using present 0°C isotherm altitudes and temperature gradients for each region (source: annals of the Swiss Meteorological Institute).

(2) The potential direct solar radiation ($I_p(x, y, z)$) is determined for the specific three-dimensional location of each individual rock-glacier front, using Funk and Hoelzle's (1992) model.

(3) The hypothetical altitude is sought for each relict rock glacier considered to be still active. As the potential solar radiation at the rock-glacier fronts is now known, we can use a relation between potential direct solar radiation and MAAT at the limit of permafrost existence (see Equation (1)) as ascertained by Hoelzle and Haeberli (1995) to obtain this hypothetical altitude (H_{lim}).

$$H_{lim} = aI_p(x, y, z) + b\,, \tag{1}$$

where a and b are constants determined empirically from BTS measurements by Hoelzle and Haeberli (1995), and I_p is the potential direct solar radiation at the front of presently relict rock glaciers. Hoelzle and Haeberli's relation is established in a regionally independent way. Therefore, altitude is not replaced by MAAT in their formula because of the regional variability of the 0°C isotherm. The accuracy of H_{lim} depends on the resolution of the DTM which underlies the calculation. In our study, based on a DTM with a 50 m resolution, the accuracy lies in the range of some meters.

(4) The hypothetical MAAT (T_{lim}) is now obtained by converting the altitude H_{lim} into temperature (as in the first step for H_p) using Equation (2).

$$T = (C - H)\frac{\partial T}{\partial h}\,, \tag{2}$$

where C stands for the elevation of the regional 0°C isotherm, and $\partial T/\partial h$ for the regional temperature gradient.

(5) The resulting temperature difference, defined as

$$\Delta T = T_p - T_{lim}\,, \tag{3}$$

corresponds to the temperature increase between the time of the rock glacier's decay and the present day.

There are two factors which may influence the accuracy of our model calculation:

(a) For an exact estimate of the temperature difference ΔT, presently relict rock glaciers would have to have reached the lower limit of discontinuous permafrost, a precondition which certainly does not apply for every relict rock glacier.

(b) A rock glacier creeps down-valley and might, due to its own microclimate (coarse blocky material, advective heat flow, increased turbulent fluxes), move into non-permafrost areas even in a constant climate.

In fact, these two effects might partially cancel each other out. Still, the temperature difference calculated by our model probably underestimates the real temperature differences, because effect (a) presumably occurs more frequently than effect (b).

RESULTS AND DISCUSSION

Approach 1

Morphologic typology and its possible implications for rock-glacier interpretation can be synthesized as follows: The continuous development of a "monomorphic" rock glacier seems to have been widely undisturbed (e.g. by external climate forcing) throughout its existence. No distinct inactivation/reactivation cycles can be detected. Thus, such rock glaciers may have been permanently subject to permafrost conditions. In contrast, "polymorphic" rock glaciers may have undergone some strong variations in their degree of activity. One of the key causes for these changes in activity is considered to be temporary altitudinal variations of the permafrost limit around the location of the specific rock glacier. In fact, borehole temperatures of different Swiss rock glaciers support this hypothesis: 10 m temperatures in 1997 at Murtèl ("monomorphic") were −1.82°C, at Schafberg 1 ("polymorphic") −0.8°C, and at Schafberg 2 ("polymorphic") −0.3°C (Vonder Mühll and others, 1998).

The age of "monomorphic" rock-glacier streams is estimated in the range of several kyr. Their flow fields show the result of continuous, cumulative deformation. In contrast, the movement of individual, at most a few kyr old, lobes of "polymorphic" rock glaciers represents intermittent deactivation or overriding. The relict rock glaciers most likely decayed at the end of the Alpine Late Glacial or the beginning of the Holocene (cf. results of approach 2). Since that time they have been subject to non-permafrost conditions. In contrast, active "monomorphic" rock glaciers must have been predominantly under permafrost conditions since their origin. Active and inactive rock glaciers of the "polymorphic" type have experienced several inactivation/reactivation periods and may possibly be viewed as representatives of Holocene climate oscillations. Although effects inside the debris-ice system may be responsible also for a "polymorphic" structure (Olyphant, 1987; Kirkbride and Brazier,

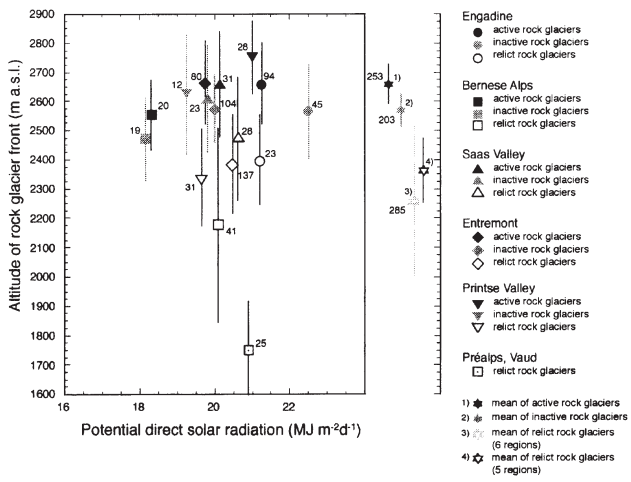

Fig. 5. Mean altitude of active, inactive and relict rock glaciers in six regions of the Swiss Alps, plotted against potential direct solar radiation. Numbers indicate the random sample sizes. Data are from Delaloye and Morand (1998a), Frauenfelder (1998), Hoelzle (1998), Imhof (1998), Reynard and others (1998) and Schoeneich (1998b).

1995), the following results of the inventory analysis clearly show the climate sensitivity of Alpine rock glaciers.

Approach 2

The analysis of the spatial distribution of rock glaciers in the Swiss Alps (Fig. 5) shows, not surprisingly, a pronounced altitudinal zonation: active rock glaciers occupy altitudinal bands between 2439 and 2878 m a.s.l., whereas the occurrence of relict rock glaciers is generally limited to heights below 2556 m a.s.l., except for the Saas valley, where the mean altitude of the relict rock-glacier fronts is 2480 m a.s.l., with a standard deviation of ±211 m. The group of inactive rock glaciers, including both dynamically and climatically inactive ones, varies between these figures without exceeding the limit given by either the active or the relict objects. The mean elevation difference between currently active and inactive rock glaciers, of about 100 m or about 0.5°C, equals a temperature difference typical for Holocene climate variations. While the mean standard deviation of the altitudinal zonation for active and inactive rock glaciers is in the order of ±76 m, the distribution of the relict rock glaciers varies considerably, with a standard deviation of ±263 m. This indicates quite stable climatic conditions for the active rock glaciers, in contrast to large climate variations and a long time-span for the relict rock glaciers. The present mean annual air temperature (T_p), the hypothetical temperature T_{lim} and the resulting temperature difference (ΔT) for each region are plotted in Figure 6. The general pattern shows a wide range for ΔT from 0.7° to 5.3°C in the various regions. Even taking into account regional factors, such as topographic preconditions, this indicates that some relict rock glaciers likely decayed at the end of the Alpine Late Glacial (e.g. Préalps; Schoeneich, 1998a), while others disintegrated during the Holocene.

Looking at the distribution pattern in Figure 5, the relict rock glaciers in the Préalps seem to have a different distribution pattern than those in other regions. Therefore, different values for the variables are given as follows. The mean present temperature (T_p) at all relict rock glaciers included in the inventories (six datasets) is −0.2°C. Excluding the Préalps, the T_p of the other five datasets is −0.7°C. The average of the calculated T_{lim} is −2.3°C for all relict rock glaciers, −3.3°C for the Préalps and −2.1°C for the other five datasets (Préalps excluded), meaning that the relict rock glaciers would need this MAAT to be still active. These results are confirmed by the present average MAAT at active rock-glacier fronts which approximates −2.4°C (five regions). The values for the individual rock glaciers vary considerably, from −5.7°C (maximum) to +0.8°C (minimum).

The difference ΔT is −5.3°C ± 0.7 for the Préalps and −1.4°C ± 0.7 for the other five datasets. Compared to data on Holocene temperature variations as derived from glacier fluctuations in the Swiss Alps (Maisch, 1992), these values for ΔT clearly exceed the range of the Holocene bandwidth of temperature variations which is estimated to be within 0.5° and 1.0°C by different authors (e.g. Patzelt and Bortenschlager, 1973; Maisch, 1992). Referring to glacier reconstruction chronologies (Maisch, 1992), ΔT for the Préalps corresponds to the temperature increase since the end of the Alpine Late Glacial, more precisely since the Oldest Dryas. This value corresponds well with the results obtained by Schoeneich (1998a). The value of ΔT for the other regions corresponds to a temperature increase since the Younger Dryas, or Egesen.

The range of ΔT at individual rock glaciers, varying from −8.2°C (relict rock glacier in the Préalps) to +2.7°C (relict rock glacier in the Saas valley), shows that it is problematic to calculate averages for whole datasets. Nevertheless, the results show the possibility of obtaining initial insights into regional patterns of past permafrost distribution by applying this approach. They also indicate that thorough analyses at individual relict rock glaciers would be a good way to gain more concise information about the depression and the local variation of the past permafrost limit in the Alps.

CONCLUSIONS

The results confirm the importance of rock glaciers as

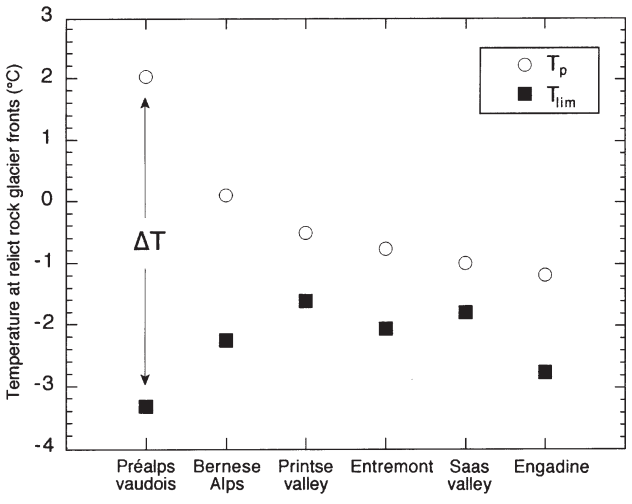

Fig. 6. Comparison of present mean annual air temperature (T_p) at relict rock-glacier fronts vs hypothetical mean annual air temperature (T_{lim}) if these relict rock glaciers were still at or close to the limit of discontinuous mountain permafrost. ΔT corresponds to the temperature increase between the present day and the time of the rock glacier's decay.

highly sensitive indicators of past temperature evolution. Some of the conclusions reached have a definite regional character and cannot be applied directly to other high mountain areas (cf. Brazier and others, 1998). Yet, the potential of the presented approach for inventory analyses lies in its ability to draw conclusions about both the fluctuations of the permafrost limit during the Holocene (by studying active/inactive rock glaciers) and the course of the Alpine Late Glacial permafrost limit (by analyzing relict rock glaciers). Comparison of the calculated temperature differences at individual relict rock-glacier fronts combined with the application of new dating methods will allow for reconstruction of isotherms and thus for temperature reconstruction in space and time. Future needs are for more detailed analysis of rock-glacier inventories in order to eliminate local effects, for more detailed investigations of rock-glacier morphology and response to climate and environment variables, and for the establishment of longer time series with higher temporal resolution. The use of new dating methods (thermoluminescence, exposure dating, etc.) to improve knowledge of rock-glacier age must also be a priority. Quantification of the thermomechanical effects of internal variability (e.g. melting/refreezing mechanisms, flow instabilities) is needed in order to assess the amount of external forcing in observed past and present dynamic changes in permafrost creep.

ACKNOWLEDGEMENTS

Special thanks are due to W. Haeberli for encouraging the authors to conduct the presented analyses. We are also greatly indebted to R. Delaloye, M. Hoelzle, M. Imhof, C. Lambiel, S. Morand, E. Reynard, P. Schoeneich and L. Wenker for compiling rock-glacier inventories in different regions of the Swiss Alps. Without their spadework, the present study would not have been possible. In addition, we would like to thank an anonymous referee for his constructive discussion of the manuscript. Further thanks are directed to S. Braun-Clarke who polished the English. The photogrammetric investigations are based on aerial photographs taken by the Swiss Federal Office of Cadastral Surveys.

REFERENCES

Barsch, D. 1978. Active rock glaciers as indicators for discontinuous Alpine permafrost: an example from the Swiss Alps. *In Proceedings, 3rd International Conference on Permafrost, Edmonton, Alberta. Vol. 1.* Ottawa, Ont., National Research Council of Canada, 349–352.

Birkeland, P.W. 1973. Use of relative age-dating methods in a stratigraphic study of rock glacier deposits, Mt. Sopris, Colorado. *Arct. Alp. Res.*, **5**(4), 401–416.

Brazier, V., M. P. Kirkbride and I. F. Owens. 1998. The relationship between climate and rock glacier distribution in the Ben Ohau Range, New Zealand. *Geogr. Ann.*, **80A**(3–4), 193–207.

Delaloye, R. and S. Morand. 1998. Rock glaciers, Entremont, Valais, Switzerland. *In* IPA Data and Information Working Group, *comp. Circumpolar Active-layer Permafrost System (CAPS), version 1.0.* Boulder, CO, National Snow and Ice Data Center (NSIDC). International Permafrost Association, CD-ROM.

Frauenfelder, R. 1998. Rock glaciers, Fletschhorn area, Valais, Switzerland. *In* IPA Data and Information Working Group, *comp. Circumpolar Active-layer Permafrost System (CAPS), version 1.0.* Boulder, CO, National Snow and Ice Data Center (NSIDC). International Permafrost Association, CD-ROM.

Funk, M. and M. Hoelzle. 1992. Application of a potential direct solar radiation model for investigating occurrences of mountain permafrost. *Permafrost and Periglacial Processes*, **3**(2), 139–142.

Haeberli, W. 1985. Creep of mountain permafrost: internal structure and flow of Alpine rock glaciers. *Eidg. Tech. Hochschule, Zürich. Versuchsanst. Wasserbau, Hydrol. Glaziol. Mitt.* 77.

Haeberli, W., M. Hoelzle, A. Kääb, F. Keller and D. Vonder Mühll. 1998. Ten years after drilling through the permafrost of the active rock glacier Murtèl, eastern Swiss Alps: answered questions and new perspectives. *Université Laval. Centre d'Études Nordiques. Collection Nordicana* 57, 403–410.

Haeberli, W. *and 7 others*. 1999. Pollen analysis and ^{14}C age of moss remains in a permafrost core recovered from the active rock glacier Murtèl–Corvatsch, Swiss Alps: geomorphological and glaciological implications. *J. Glaciol.*, **45**(149), 1–8.

Hoelzle, M. 1998. Rock glaciers, Upper Engadin, Switzerland. *In* IPA Data and Information Working Group, *comp. Circumpolar Active-layer Permafrost System (CAPS), version 1.0.* Boulder, CO, National Snow and Ice Data Center (NSIDC). International Permafrost Association, CD-ROM.

Hoelzle, M. and W. Haeberli. 1995. Simulating the effects of mean annual air-temperature changes on permafrost distribution and glacier size: an example from the Upper Engadin, Swiss Alps. *Ann. Glaciol.*, **21**, 399–405.

Humlum, O. 1998. The climatic significance of rock glaciers. *Permafrost and Periglacial Processes*, **9**(4), 375–395.

Imhof, M. 1998. Rock glaciers, Bernese Alps, western Switzerland. *In* IPA Data and Information Working Group, *comp. Circumpolar Active-layer Permafrost System (CAPS), version 1.0.* Boulder, CO, National Snow and Ice Data Center (NSIDC). International Permafrost Association, CD-ROM.

Johnson, P. G. 1998. Morphology and surface structures of Maxwell Creek rock glaciers, St Elias Mountains, Yukon: rheological implications. *Permafrost and Periglacial Processes*, **9**(1), 57–70.

Kääb, A. 1998. Oberflächenkinematik ausgewählter Blochgletscher des Oberengadins. *Eidg. Tech. Hochschule, Zürich. Versuchsanst. Wasserbau, Hydrol. Glaziol. Mitt.* 158, 121–140.

Kääb, A., W. Haeberli and G. H. Gudmundsson. 1997. Analysing the creep of mountain permafrost using high precision aerial photogrammetry: 25 years of monitoring Gruben rock glacier, Swiss Alps. *Permafrost and Periglacial Processes*, **8**(4), 409–426.

Kääb, A., G. H. Gudmundsson and M. Hoelzle. 1998. Surface deformation of creeping mountain permafrost. Photogrammetric investigations on rock glacier Murtèl, Swiss Alps. *Université Laval. Centre d'Études Nordiques. Collection Nordicana* 57, 531–537.

Kirkbride, M. and V. Brazier. 1995. On the sensitivity of Holocene talus-derived rock glaciers to climate change in the Ben Ohau Range, New Zealand. *J. Quat. Sci.*, **10**(4), 353–365.

Maisch, M. 1992. *Die Gletscher Graubündens: Rekonstruktionen und Auswertung der Gletscher und deren Veränderungen seit dem Hochstand von 1850 im Gebiet der östlichen Schweizer Alpen (Bündnerland und angrenzende Regionen).* Zürich, Universität Zürich. Geographisches Institut. (Physische Geographie 33.)

Olyphant, G. A. 1987. Rock glacier response to abrupt changes in talus production. *In* Giardino, J. R., J. F. Shroder, Jr and J. D. Vitek, *eds. Rock glaciers.* London, Allen and Unwin, 55–64.

Patzelt, G. and S. Bortenschlager. 1973. Die postglazialen Gletscher- und Klimaschwankungen in der Venedigergruppe (Hohe Tauern, Ostalpen). *Z. Geomorphol.*, Supplementband 16, 25–72.

Reynard, E., C. Lambiel and L. Wenker. 1998. Rock glaciers, Printse valley, Valais, Switzerland. *In* IPA Data and Information Working Group, *comp. Circumpolar Active-layer Permafrost System (CAPS), version 1.0.* Boulder, CO, National Snow and Ice Data Center (NSIDC). International Permafrost Association, CD-ROM.

Schoeneich, P. 1998a. *Le retrait glaciaire dans les vallées des Ormonts, de l'Hongrin et de l'Etivaz (Préalpes vaudoises).* Lausanne, Université de Lausanne. Institut de Géographie. (Travaux et Recherches 14.)

Schoeneich, P. 1998b. Rock glaciers of the Préalps, Vaud, Switzerland. *In* IPA Data and Information Working Group, *comp. Circumpolar Active-layer Permafrost System (CAPS), version 1.0.* Boulder, CO, National Snow and Ice Data Center (NSIDC). International Permafrost Association, CD-ROM.

Steig, E. J., J. J. Fitzpatrick, N. Potter, Jr and D. H. Clark. 1998. The geochemical record in rock glaciers. *Geogr. Ann.*, **80A**(3–4), 277–286.

Vonder Mühll, D., Th. Stucki and W. Haeberli. 1998. Borehole temperatures in Alpine permafrost: a ten-year series. *Université Laval. Centre d'Études Nordiques. Collection Nordicana* 57, 1089–1095.

White, S. E. 1987. Differential movement across transverse ridges on Arapaho Rock Glacier, Colorado Front Range, U.S.A. *In* Giardino, J. R., J. F. Shroder, Jr and J. D. Vitek, *eds. Rock glaciers.* London, Allen and Unwin, 145–149.

V

Norsk geogr. Tidsskr. Vol. 55, 195–202. Oslo. ISSN 0029-1951

Using relict rockglaciers in GIS-based modelling to reconstruct Younger Dryas permafrost distribution patterns in the Err-Julier area, Swiss Alps

REGULA FRAUENFELDER, WILFRIED HAEBERLI, MARTIN HOELZLE & MAX MAISCH

Frauenfelder, R., Haeberli, W., Hoelzle, M. & Maisch, M. 2001. Using relict rockglaciers in GIS-based modelling to reconstruct Younger Dryas permafrost distribution patterns in the Err-Julier area, Swiss Alps. *Norsk Geografisk Tidsskrift–Norwegian Journal of Geography* Vol. 55, 195–202. Oslo. ISSN 0029-1951.

Differences in mean annual air temperature between the Younger Dryas period and today were estimated at the fronts of 32 relict rockglaciers in the Err-Julier area, eastern Swiss Alps. The analyses were based on a case-by-case calculation of direct incoming solar radiation and mean annual air temperature using a digital elevation model (DEM) and meteo data of recent years. Our results suggest that mean annual air temperature during the Younger Dryas was lowered by *c.* 3°C to 4°C, and that the lower limit of permafrost occurrence was depressed considerably more than glacier equilibrium lines. This indicates strongly reduced precipitation (30% to 40% reduction) and much larger abundance of mountain permafrost at that time. A model simulation of the corresponding spatial permafrost distribution during the Younger Dryas indicates that glaciers in the study area were mostly surrounded by permafrost at that time and probably had a polythermal structure of englacial temperatures.

Keywords: *GIS, rockglaciers, Swiss Alps, Younger Dryas permafrost distribution*

Regula Frauenfelder, Wilfried Haeberli, Martin Hoelzle & Max Maisch, Department of Geography, University of Zurich, Winterthurerstrasse 190, CH-8057 Zurich, Switzerland. E-mail: regula.frauenfelder@geo.unizh.ch

Introduction

In contrast to the comparatively well-known extent of glaciation during the Alpine Lateglacial time period (e.g. NFP31 1998 for the study region), much less information is available about the spatial distribution of permafrost at that time. Our study aims at filling in this gap, based on an approach originally developed by Haeberli (1982, 1983) and Kerschner (1983, 1985) and redesigned for spatial extrapolation by Frauenfelder & Kääb (2000) using relict rockglacier data as a proxy for reconstructing past permafrost distribution. The main results of the latter publication indicated an average temperature increase at relict rockglacier fronts in six study regions throughout the Swiss Alps of *c.* +2°C since the time of their decay, which is a clear sign of rockglacier ages reaching back to the Alpine Lateglacial. The temperature difference of some tenths of a degree Celsius found for active/inactive rockglaciers is typical for the bandwidth of Holocene climate variations. While the study by Frauenfelder & Kääb (2000) concentrated on the investigation of 285 relict rockglaciers in different areas, the present study is focused on the spatial extrapolation of these findings in one area, i.e. the spatial modelling of the permafrost distribution in the Err-Julier area, eastern Swiss Alps during the Younger Dryas. First results are now presented in this article.

Rockglaciers are effective ice-debris transport systems within high mountain areas. Their thermal inertia, together with low rates of freezing and thawing, both at the permafrost table and at the permafrost base, stabilise boundary conditions. Therefore, the flow regimes of rockglaciers change slowly with time. Consequently, and considering the fact that average surface velocities of alpine rockglaciers vary between less than a few centimetres and several metres (e.g. White 1971, Gorbunov 1983, Barsch 1996, Kaufmann 1998, Konrad et al. 1999, Kääb 2000), rockglacier bodies of several hundred metres length are at least some centuries, more presumably several millennia old (Haeberli 1985, Barsch 1996, Frauenfelder & Kääb 2000). Recent radiocarbon datings (Haeberli et al. 1999, Konrad et al. 1999) and flow-line calculations (Kääb et al. 1997, 1998) on different active rockglaciers strengthen this view.

Long-term creep deformation of such ice-containing debris, i.e. rockglaciers, requires permafrost conditions irrespective of the exact origin of the subsurface ice (Haeberli & Vonder Mühll 1996). Climate, with its long-term variability, governs ground thermal conditions and, for this reason, represents one of the most important factors controlling the temporal and spatial distribution of alpine rockglaciers. Therefore, relict rockglaciers below and outside the present-day Alpine permafrost belt can be used to reconstruct past permafrost conditions. These past permafrost conditions, in turn, reflect past climatic conditions, especially solar radiation and air temperature determining radiative and sensible heat fluxes as primary drivers of the energy balance at the earth/atmosphere interface, with the snow cover representing the main interface modulating these fluxes through albedo, insulation and latent-heat effects (e.g. Keller & Gubler 1993, Mittaz et al. 2000).

Already Haeberli (1982, 1983), Kerschner (1983, 1985), and Sailer & Kerschner (1998) have shown that it is possible to estimate past annual temperature and precipitation on the basis of relative displacements of permafrost boundaries and glacier equilibrium lines. The present study follows the approach to estimate the depression of the permafrost limit during the Alpine Lateglacial relative to the present-day distribution and to compare it with previously determined changes in glacier equilibrium lines (e.g. by Maisch 1992, 1995). Lowering of the mean annual air temperature (MAAT) is calculated using front altitudes of relict rockglaciers together with the program PERMAMAP which estimates spatial permafrost distribution patterns in complex

mountain topography on the basis of potential direct solar radiation and mean annual air temperature (Hoelzle et al. 1993, 2001, Hoelzle & Haeberli 1995). Solar radiation and mean annual air temperature can be calculated for present-day conditions using data from meteorological stations in combination with corresponding algorithms and digital elevation models. If solar radiation and local lapse rates are assumed to have remained roughly constant in time, depressions of palaeo-temperatures can then be calculated for reconstructing the palaeo-permafrost distribution.

Setting

The study area lies in the Err-Julier region, situated in the eastern part of the Swiss Alps, and covers an area of *c.* 530 km^2, stretching from 46°22′ N to 46°35′ N, and 9°39′ E to 9°59′ E (Fig. 1). The area is characterised by a high-situated valley floor with an average altitude of 1700 m a.s.l. and surrounded by mountain peaks reaching up to *c.* 4000 m a.s.l. These high peaks prevent the supply of wet advective air masses from penetrating and, therefore, mean annual precipitation shows a distinct decline from the outer mountain chains to the inner ridges. Mean annual precipitation for the years 1971–1990, at two stations in the valley floor (Bever at 1712 m a.s.l. and St. Moritz at 1832 m a.s.l.) was 839.6 mm and 901.5 mm, respectively (data from MeteoSwiss). Calculation of precipitation in the glacial and periglacial regions of the study area yield somewhat higher values, reaching c. 1100 mm in the mountain ridges to the north and up to 1600 mm in the southern ones (Schwarb et al. 2000). The comparably high elevation of the area leads to low annual air temperatures. Mean annual air temperature in the area was +1.8°C at Samedan for the period 1991–2000 (station with temperature measurements, located at 1705 m a.s.l., 2.5 km from Bever station), and +2.1°C at St. Moritz for the period 1970–1980 (temperature measurements at this station were stopped in 1980; data from MeteoSwiss). Together with a regional lapse rate calculated at 0.55°C/100 m (Gensler 1978, Maisch 1992), this gives a mean annual 0°C-isotherm at *c.* 2180 m a.s.l. The deviation of the regional lapse rate from the standard value of 0.65/100 m results from pronounced cold air effects and subsequently developing air temperature inversions (cf. comparably low MAAT at Samedan station), situations that arise very frequently in this wide mountain valley (Gensler 1978).

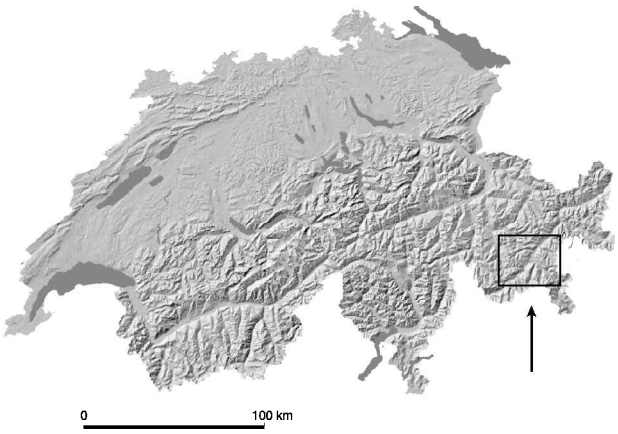

Fig. 1. Shaded digital elevation model of Switzerland showing the location of the Err-Julier area (black rectangle). DEM source: Tydac AG.

Parts of the valley floors and most of the modern periglacial belt were last covered by glaciers during the early Younger Dryas; since then, post-glacial activity has been limited to minor readvances of valley glaciers within the limits of the Little Ice Age moraines, and the appearance/disappearance of glacierets (Suter 1981, Maisch 1992). Periglacial activity (such as intensive weathering, freeze/thaw processes, rockglacier development, etc.) is thought to have been one of the predominant landscaping factors in the area during the last several thousand years.

In 1989, Hoelzle (M. Hoelzle, unpublished data) inventoried the rockglaciers in the area, mapping three categories: (a) active rockglaciers, (b) inactive rockglaciers and (c) relict rockglaciers. The mapping was based on field visits and analyses of infrared aerial photography taken by the Swiss Federal Office of Cadastral Surveys. The methodology applied bears a certain error as it is not always possible to precisely distinguish between relict and inactive forms on aerial photographs. However, quantitative field evidence (e.g. measurements of the bottom temperature of the snow cover, geophysical investigations, etc.) gained in the course of the last decade helped refining the picture and proved that – with the exception of a few landforms not included in the following analyses – the relict rockglaciers had been addressed correctly in the original inventory.

Method

Our model is based on the conception that active rockglaciers creep as long as they remain within areas with permafrost conditions (Haeberli 1985, Barsch 1996) and that, therefore, today's relict rockglaciers (Fig. 2) document the local lower limit of permafrost at the time of their decay where flow is not restricted by topography. The modelling approach (cf. also Frauenfelder & Kääb 2000) follows four main calculation steps which are briefly explained in the following: in a first step, solar radiation and mean annual air temperature (MAAT = T_p) at each relict rockglacier front were calculated for present-day conditions. For the MAAT, this was done using meteorological data (present 0°-isotherm altitude of 2180 m and local lapse rate of 0.55°C/100 m) in combination with a digital elevation model (DEM). Potential direct solar radiation at the relict rockglacier fronts was calculated using model algorithms developed by Funk & Hoelzle (1992), again using a DEM as main input. Then, a former 'hypothetical' MAAT (T_f) was computed which would have had to exist at the sites for permafrost conditions to occur with the given solar radiation, using a relation between potential direct solar radiation and MAAT at the limit of permafrost existence as established by Hoelzle et al. (1993). The resulting difference $\Delta T = T_p - T_f$ was assumed to correspond to the temperature increase between the time of the rockglaciers' presumed decay and today.

For the interpretation of the results, solar radiation and

local lapse rates were assumed to have remained constant in time. This assumption certainly does not fully portray past conditions as variations in cloud thickness, cloud coverage, snow cover thickness and duration, insulation changes, or alterations of lapse rates may have occurred but are not considered by this simplification. In addition, uncertainties given by the natural variability of other variables involved are not accounted for by this approach: for instance, the inactivity of a rockglacier due to dynamic reasons rather than as a consequence of climatic causes, or the movement of a rockglacier into non-permafrost areas even in a constant climate, due to its own microclimate (coarse blocky material, advective heat flow, turbulent fluxes). Also, individual relict rockglaciers certainly did not reach the local lower limit of discontinuous permafrost at the same time but may have become inactive while permafrost boundaries were shifting upwards as a consequence of atmospheric warming, or some presently relict rockglaciers might not have reached the lower limit of discontinuous permafrost at all. However, all these effects might partially cancel each other out in an extended sample of rockglaciers considered, and the reliability of spatial permafrost modelling under modern conditions justifies such simplifications for a first order assessment.

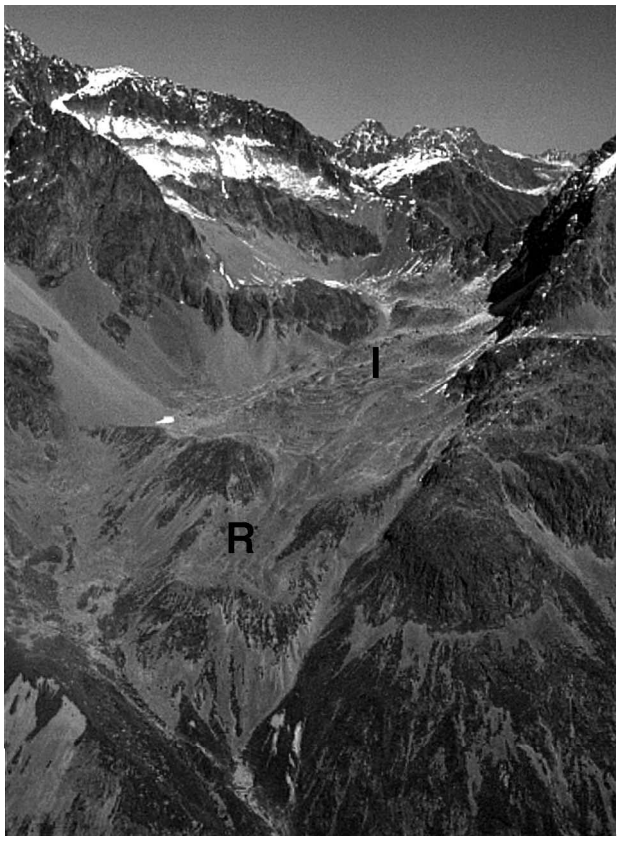

Fig. 2. Example of a relict rockglacier in the Err-Julier study area: rockglacier 'Munteratsch' is situated in a south-west orientated cirque between Piz Julier and Piz Albana, and stretches between *c.* 2850 m a.s.l. and 2500 m a.s.l. The vegetation-covered relict part of the rockglacier (R) is partially overridden by inactive lobes on its upper part (I). Photograph taken in October 1999.

Results

Calculated palaeo-temperatures and age consideration

Calculations were performed for the entire Err-Julier area, using the rockglacier inventory data originally compiled by Hoelzle (M. Hoelzle, unpublished data), additional geomorphological mapping by Schlosser (O. Schlosser, unpublished data), and data (such as complementary rockglacier mapping, etc.) digitised by the authors. As a result, a set of temperature calculations at 32 relict rockglaciers could be compiled (Fig. 3). Values for ΔT vary between 0°C (for relict rockglaciers that could, according to our model, still be active under present-day conditions) and somewhat more than 3°C. Based on previously reconstructed glacier chronologies by Maisch (1992) and Kerschner (1983), a lateglacial rather than a Holocene age was assumed for relict rockglacier fronts with temperature shifts of more than *c.* 1°C, a value which confines the estimated bandwidth of Holocene glacier fluctuations. Accordingly, the Younger Dryas (Egesen stadials) is seen as the most likely candidate for ΔT-values of *c.* −3°C.

Two independent types of data seem to strengthen this latter assumption: on Julierpass, a sequence of several very distinct moraines is located in the valley floor. One of them, an early Younger Dryas (Egesen I) moraine (Suter 1981) shows conspicuous creeping features at its easterly-exposed front (M. Hoelzle, unpublished data); this part is addressed as a transitional form between a push moraine and a rockglacier. In 1995, Ivy-Ochs carried out surface exposure datings on the western part of this moraine. The surface exposure age obtained is 11,300 ± 1500 ^{14}C yr BP (Ivy-Ochs et al. 1996). Our calculated ΔT for the formerly creeping part (orographic right part of the moraine) is −3.4°C, which would, compared to temperature depression values obtained by Kerschner (1983) for the Tyrolian Alps, indeed imply an early Younger Dryas (Egesen I) age. Fig. 4a shows the locality of the moraine, the present-day permafrost distribution, and the presumed permafrost distributions during the Little Ice Age and during the Younger Dryas.

In the Val d'Err, a valley in the north-western part of the study area, geomorphological mapping had been carried out by Schlosser in 1990 (O. Schlosser, unpublished data). At one particular site, a relict rockglacier tongue lies within the lateral moraines of a now vanished cirque glacier (cf. Fig. 4b). Based on relative dating and comparison with other moraines in this valley, Schlosser concluded that these moraines originated from a late Younger Dryas advance (most presumably Egesen III). The ΔT for the relict rockglacier front at this site is −2.1°C, a value which also suggests a late Younger Dryas age.

Modelling of spatial palaeo-permafrost distribution

The average of the five largest, i.e. most negative, values of ΔT (= −3.1°C) was used to calculate the spatial permafrost distribution during the Younger Dryas, thereby simulating a climate of ΔT cooling with respect to the present-day conditions but neglecting possible spatially variable gradi-

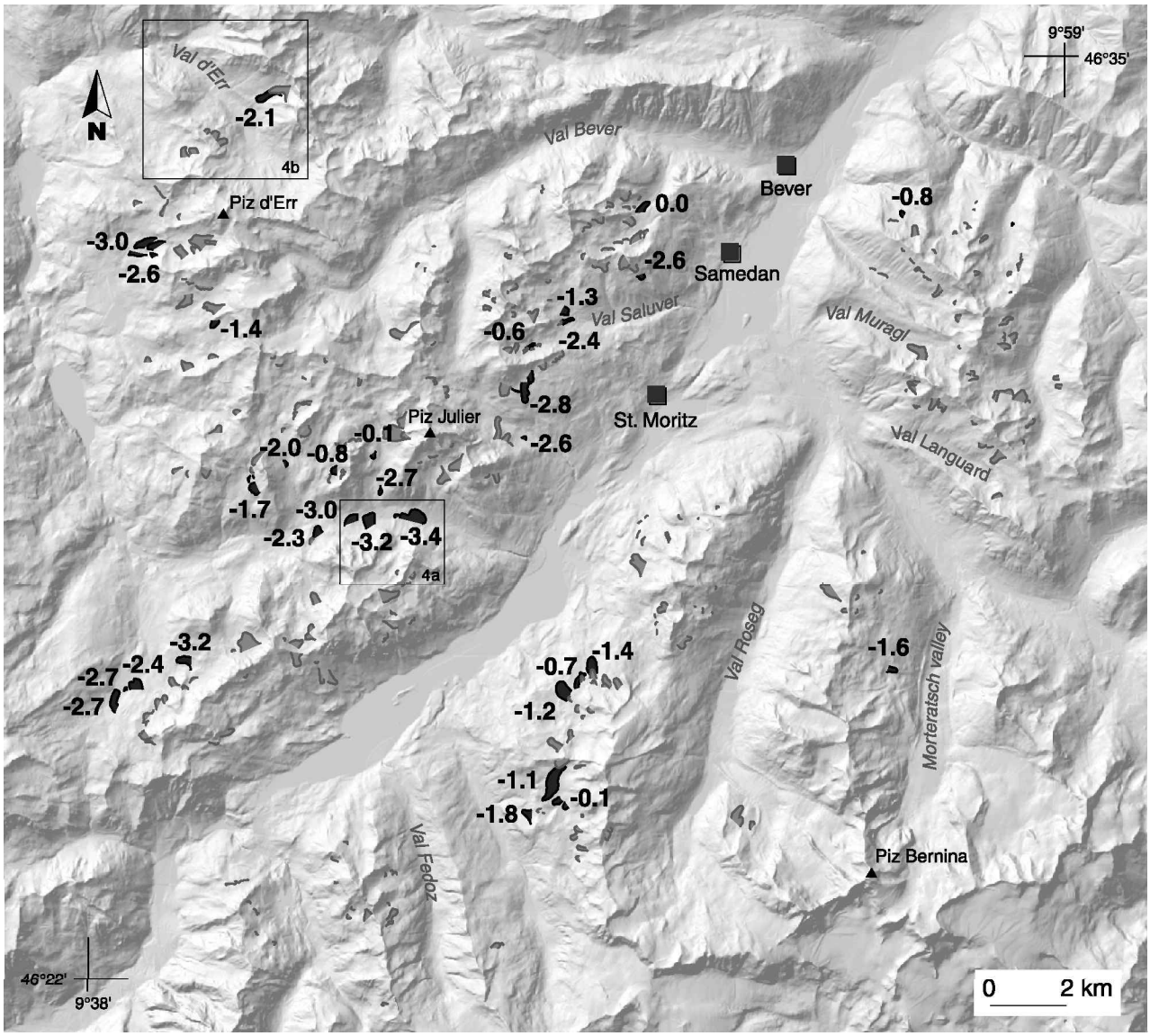

Fig. 3. Locations and ΔT-values of 32 relict rockglacier fronts. Black shaded outlines represent relict rockglaciers, grey shaded outlines represent inactive and active rockglaciers. Background is the shaded digital elevation model DEM25 of Switzerland, on which calculations in the presented study are based. DEM25 reproduced by permission of the Swiss Federal Office of Topography, 23.5.2001, BA013420.

ents. This spatial extrapolation was performed within a GIS environment using again the permafrost distribution model PERMAMAP in ARC/INFO. The modelled results provide evidence that permafrost distribution during the Younger Dryas was abundant in areas free of surface ice and that most of the valley slopes were perennially frozen (Fig. 5). In northern and north-western expositions of higher located side valleys (e.g. Val Bever, Val Roseg, and the valley of the Morteratsch glacier) and in hanging valleys (e.g. Val Fedoz, Val Muragl, Val Languard and Val Saluver) discontinuous permafrost presumably reached down into the foot of the slopes.

Quantitatively, this suggests that permafrost during the Younger Dryas had been present in areas above c. 1950 m a.s.l. in slopes exposed to the north, above 2200 m a.s.l. in easterly exposed areas, above 2450 m a.s.l. on south-faced hillsides, and above 2150 m a.s.l. in west-exposed slopes, i.e. 500 m to 600 m below the present-day limits of discontinuous permafrost in the investigated area.

In order to estimate the range of uncertainty of the reconstruction, a 'hypothetical' former MAAT (T_f) calculated by the model was compared with calculated present-day MAAT (T_p) at the fronts of 100 active rockglacier in the study area (cf. Fig. 3). According to the assumption that active rockglaciers represent the lower limit of discontinuous permafrost, their T_p- and T_f-values should be approximately equal. The comparison of the T_p- and T_f-values ($\Delta T = 0.1°C \pm 0.5°C$) imply that the model works with an

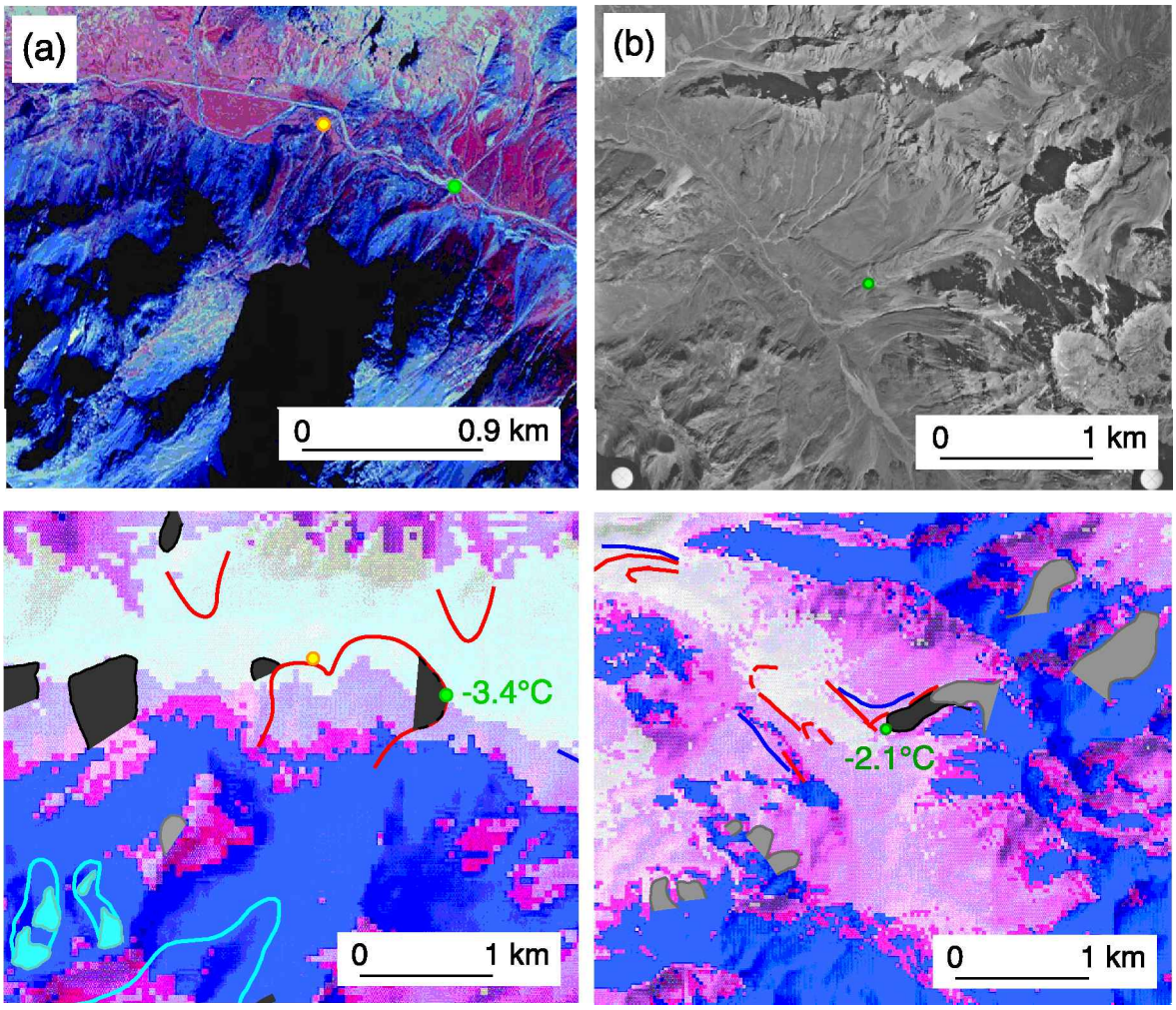

Fig. 4. Comparison of modelling results with independent temporal data: (a, left) according to surface exposure datings on a partially 'rockglacierized' Younger Dryas (Egesen I) moraine at Julierpass by Ivy-Ochs et al. (1996), and (b, right) according to the position of a relict rockglacier relative to moraines from a late Younger Dryas advance (most presumably Egesen III) of a former cirque glacier (O. Schlosser, unpublished data). The yellow dot (only on 4a) marks the approximate location of the exposure datings, the green dots (on a and b) assign the location for which the temperature shifts ΔT between the Younger Dryas and today have been calculated. The corresponding values of ΔT at these locations are also given in green. Rockglaciers are represented in the same way as in Fig. 3. Present-day permafrost distribution is depicted in dark blue, permafrost distribution during the Little Ice Age (LIA) in dark pink and permafrost distribution during the Younger Dryas in light pink. Present-day glacier extents are shaded in turquoise, glacier advance stages of the LIA are outlined with thin lines in turquoise. Palaeo-reconstructions for the Older Dryas (Daun) glacier stages are given in dark blue, and the Younger Dryas (Egesen I– III) advance stages are marked with red lines. Sources: moraines in (a) after Gamper-Schollenberger & Suter (1982) and in (b) after Schlosser (O. Schlosser, unpublished data), infrared aerial photograph of the Swiss Federal Office of Topography, 7.9.1988, Flight-line 061 160, Image-No. 4724, black-and-white aerial photograph of the Swiss Federal Office of Topography, 9.9.1959, Flight-line 175A, Image-No. 3429. Both aerial photographs are not rectified and, therefore, distorted compared to the GIS-based maps.

average accuracy of some tenths of a degree Celsius. This uncertainty corresponds to a mean error in the calculated displacement of the permafrost limit of a few tens of metres only. However, it has to be taken into account that effects of long-persisting snow at the foot of slopes (e.g. due to repeated avalanching) can depress the local lower limit of the permafrost distribution remarkably but that these effects are not accounted for in the model.

The findings suggest that, indeed, most of the relict rockglaciers considered here may have developed during the Younger Dryas. Relict rockglaciers with modelled ΔT-values around -3°C (corresponding to a lower permafrost limit which was depressed by roughly 500 to 600 m as compared to today) possibly formed during early stages of the Younger Dryas, relict rockglaciers with smaller ΔT-values more presumably during the final stages of the Younger Dryas cold phase, or even reaching preboreal time.

Discussion

Analysis of relict rockglaciers as a basis for GIS-modelling of the Younger Dryas permafrost distribution in the Err-Julier Area (eastern Swiss Alps), indicates that mean annual

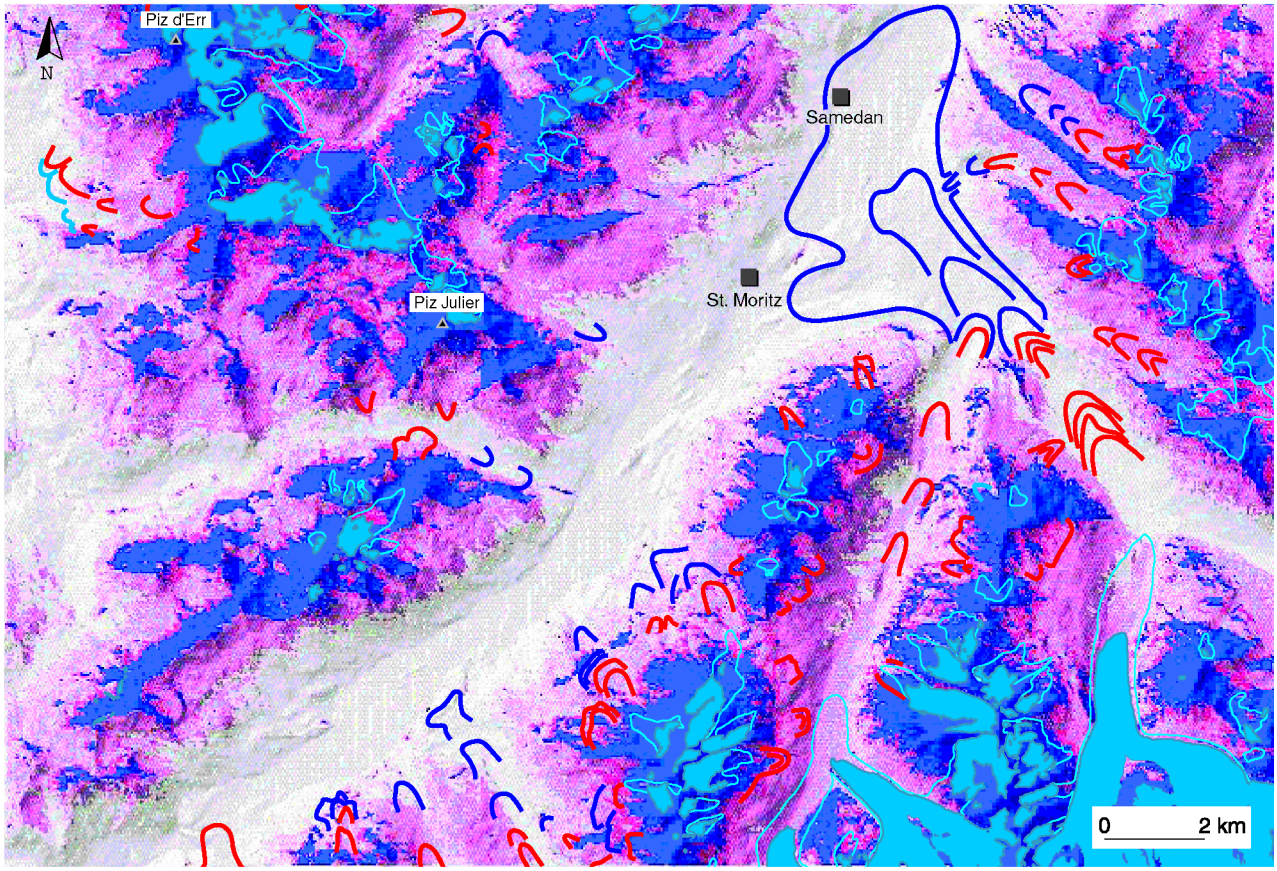

Fig. 5. Present-day permafrost and palaeo-permafrost distributions in the Err-Julier area according to modelling results, overlain by digitised outlines of present and past glacier extents. Glacier and permafrost representation as in Fig. 4. *Sources*: Glacier reconstructions after Gamper-Schollenberger & Suter (1982), DEM25 reproduced by permission of the Swiss Federal Office of Topography, 23.5.2001, BA013420.

air temperature at that time was at least 3°C lower than today. The corresponding lowering in glacier equilibrium line altitudes (ELA) in the eastern Swiss Alps has been estimated at 200 m with respect to the Little Ice Age and some 300 m between the early Younger Dryas and today (Maisch 1992, 1995). Our modelling results (lowering of the permafrost distribution by 500 m to 600 m) suggest that, during the Younger Dryas, the lower limit of permafrost occurrence had thus been depressed considerably more than glacier equilibrium lines. This indicates strongly reduced precipitation and much larger abundance of mountain permafrost at that time, results which correspond well with calculations carried out by Haeberli (1982) and Kerschner (1985), suggesting a precipitation reduction during the later phases of the Younger Dryas (Egesen II) by up to 30%–40%. Sailer & Kerschner (1998) found similar values in their study area in the Ferwall group in western Tyrol, Austria. Analyses of ELA depression in relation to precipitation change by Kerschner et al. (2000) give a more detailed and slightly different picture; still, they are broadly consistent with the implication of the here-presented model results. Temperature reconstructions from other disciplines, for example ∂^{18}O-measurements and pollen analyses on lake sediments (e.g. Eicher 1994) point to temperature depression values for the Younger Dryas in the same order of magnitude as our results. Furthermore, such conditions are also in broad agreement with AOGCM (Atmosphere-Ocean General Circulation Models) modelling and proxy evidence relating to northern and central Europe, indicating strong meridional gradients in temperature depression for the area between the remaining Scandinavian ice sheet and the Alps during the Younger Dryas (Renssen et al. 2000).

From Fig. 5 it appears that the Younger Dryas glaciers (delineated in red) were mostly surrounded by permafrost. With MAAT values at the equilibrium line around −5°C to −6°C, these glaciers may have had a polythermal structure of englacial temperature with temperate firn in accumulation areas but slightly cold near-surface ice in the ablation areas and margins which were frozen to the bed (Hooke et al. 1983).

Relict rockglaciers with modelled ΔT-values around −3°C were probably still active during the Younger Dryas and presumably disintegrated by the end of the Alpine Lateglacial transition to the Holocene. However, investigations by Gamper-Schollenberger & Suter (1982) show that most of the areas where rockglaciers potentially could have developed, i.e. areas above the lower limit of discontinuous permafrost distribution, were still glacierized during the

early Younger Dryas (Egesen I). Only in the stages of the late Younger Dryas (Egesen II and III), were glaciers limited to an extent which would have allowed for rockglacier development. This observation is also in close agreement with results from Sailer & Kerschner (1998).

This means that the investigated rockglaciers would have had to develop (1) either within very short time, or (2) during an extended stage of reduced glacierization before the early Younger Dryas (Egesen I) with subsequent reactivation thereafter, or (3) in glacier-free areas during the later phases of the Younger Dryas (Egesen II and III), or (4) from morainic debris material brought down relatively close to their front by small glaciers, or (5) by a combination of cases (2) to (4). The occurrence of case (1) is of low probability according to present knowledge and modern measurements. In cases like the Val d'Err rockglacier which is clearly confined within late Younger Dryas (Egesen III) moraines, scenario (2) can be excluded. Yet, in other cases, where topographic circumstances are not that clear, it is difficult to assess the probability of such a scenario (i.e. 2). The knowledge about the involved processes and timescales is clearly incomplete. Possible examples for case (3) can be found in the present study area as well as in other regions of the Alps. Modern examples of case (4) can, for instance, be seen on debris-covered glacier tongues in the permafrost areas of Svalbard. It may, thus, be reasonable to assume that permafrost creep had involved debris originally transported by polythermal glaciers in many cases and that a combination of processes as implied in scenario (5) seems to be highly probable. In any case, a combined consideration of glacial and periglacial processes in an environment of discontinuous mountain permafrost constitutes the key to a better understanding of lateglacial landscape dynamics.

Conclusion

The presented approach of a GIS-based quantitative reconstruction and modelling of the Younger Dryas permafrost distribution provides interesting possibilities for palaeoclimatic and palaeo-glaciological analyses. A depression of *c*. 500 m to 600 m of the lower permafrost limit, of *c*. 3°C to 4°C of the mean annual air temperature and *c*. 30% to 40% of annual precipitation is likely to have occurred during the Younger Dryas. Glaciers in the region at that time were mostly surrounded by discontinuous permafrost and probably had a polythermal structure. The derived reduction in precipitation and, hence, changes in snow cover characteristics are likely to have had a marked influence on ground thermal conditions. Such effects must be investigated by more process-oriented energy-balance models currently under development (Hoelzle et al. 2001).

To obtain more conclusive information on actual rockglacier ages, dating of such surfaces using a combination of absolute and relative age determination methods (such as radiocarbon dating, optically stimulated luminescence, cosmogenic exposure dating, lichenometry, Schmidt-Hammer measurements, and weathering-rind mapping) is presently being explored.

Acknowledgements. – This study was financially supported by a research grant of the 'Stiftung zur Förderung der wissenschaftlichen Forschung' at the University of Zurich. Meteorological data was provided by the MeteoSwiss (former Swiss Meteorological Service), Zurich. We thank Dr. A. Kääb, University of Zurich, and two anonymous referees for their constructive comments on the manuscript.

Manuscript submitted 15 May 2001; accepted 15 August 2001

References

Barsch, D. 1996. *Rockglaciers. Indicators for the Present and Former Geoecology in High Mountain Environments*. Springer Series in Physical Environment 16. Springer-Verlag, Berlin. 331 pp.

Eicher, U. 1994. Sauerstoffisotopenanalysen durchgeführt an spät- sowie frühpostglazialen Seekreiden. Lotter, A. F. & Amman, B. (eds) *Festschrift Gerhard Lang*, 277–286. Verlag J. Cramer, Berlin.

Frauenfelder, R. & Kääb, A. 2000. Towards a palaeoclimatic model of rockglacier formation in the Swiss Alps. *Annals of Glaciology* 31, 281–286.

Funk, M. & Hoelzle, M. 1992. Application of a potential direct solar radiation model for investigating occurrences of mountain permafrost. *Permafrost and Periglacial Processes* 3:2, 139–142.

Gamper-Schollenberger, B. & Suter, J. 1982. Karte der spätglazialen Gletscherstände im Oberengadin. Maisch, M. & Suter, J. (eds) *Exkursionsführer Teil A: Ostschweiz (Hauptversammlung DEUQUA)*, Zürich. Department of Geography, University of Zurich. *Physische Geographie* 6, 15.

Gensler, G. A. 1978. *Das Klima von Graubünden*. Habilitations-Schrift, Schweizerische Meteorologische Anstalt, Zürich. 125 pp.

Gorbunov, A. P. 1983. Rockglaciers of the mountains of middle Asia. *Fourth International Permafrost Conference, Proceedings*, 359–362. National Academy Press, Washington D.C.

Haeberli, W. 1982. Klimarekonstruktionen mit Gletscher-Permafrost-Beziehungen. *Materialen zur Physiogeographie* 4, 9–17.

Haeberli, W. 1983. Permafrost–glacier relationships in the Swiss Alps today and in the past. *Fourth International Conference on Permafrost, Proceedings*, 415–420. National Academy Press, Washington D.C.

Haeberli, W. 1985. Creep of mountain permafrost: internal structure and flow of Alpine rockglaciers. *Mitteilung der VAW ETH Zürich*, 77. 142 pp.

Haeberli, W. & Vonder Mühll, D. 1996. On the characteristics and possible origins of ice in rockglacier permafrost. *Zeitschrift für Geomorphologie* 104, 43–57.

Haeberli, W., Kääb, A., Wagner, S., Vonder Mühll, D., Geissler, P., Haas, J. N., Glatzel-Mattheier, H. & Wagenbach, D. 1999. Pollen analysis and ^{14}C age of moss remains in a permafrost core recovered from the active rockglacier Murtèl-Corvatsch, Swiss Alps: geomorphological and glaciological implications. *Journal of Glaciology* 45:149, 1–8.

Hoelzle, M. 1998. Rockglaciers, Upper Engadin, Switzerland. IPA Data and Information Working Group, *comp. Circumpolar Active-layer Permafrost System (CAPS), version 1.0*. Boulder, CO, Colorado, National Snow and Ice Data Center (NSIDC). International Permafrost Association, CD-ROM.

Hoelzle, M. & Haeberli, W. 1995. Simulating the effects of mean annual air-temperature changes on permafrost distribution and glacier size: an example from the Upper Engadin, Swiss Alps. *Annals of Glaciology* 21, 399–405.

Hoelzle, M., Haeberli, W. & Keller, F. 1993. Application of BTS-measurements for modelling mountain permafrost distribution. *Sixth International Conference on Permafrost, Proceedings*, 272–277. South China University of Technology Press, Beijing.

Hoelzle, M., Mittaz, C., Etzelmüller, B. & Haeberli, W. 2001. Surface energy fluxes and distribution models relating to permafrost in European mountain permafrost areas: an overview of current developments. *Permafrost and Periglacial Processes* 12:1, 53–68.

Hooke, R. L., Gould, J. E. & Brzozowski, J. 1983. Near-surface temperatures near and below the equilibrium line on polar and subpolar glaciers. *Zeitschrift für Gletscherkunde und Glazialgeologie* 19, 1–25.

Ivy-Ochs, S., Schlüchter, C., Kubik, P. W., Synal, H.-A., Beer, J. & Kerschner, H. 1996. The exposure age of an Egesen moraine at Julier Pass,

Switzerland, measured with the cosmogenic radionuclides ^{10}Be, ^{26}Al and ^{36}Cl. *Eclogae geol. Helv.* 89:3, 1049–1063.

Kääb A. 2000. Photogrammetry for early recognition of high mountain hazards: new techniques and applications. *Physics and Chemistry of the Earth* 25:9, 765–770.

Kääb, A., Haeberli W. & Gudmundsson, G. H. 1997. Analysing the creep of mountain permafrost using high precision aerial photogrammetry: 25 years of monitoring Gruben rockglacier, Swiss Alps. *Permafrost and Periglacial Processes* 8:4, 409–426.

Kääb, A., Gudmundsson, G. H. & Hoelzle, M. 1998. Surface deformation of creeping mountain permafrost. Photogrammetric investigations on rock-glacier Murtèl, Swiss Alps. Lewkovicz, A. G. & Allard, M. (eds.) *7th International Conference on Permafrost (Yellowknife, 23–27 June 1998)*, Collection Nordicana 57, 531–537. Centre d'Études Nordiques, Université Laval, Québec.

Kaufmann, V. 1998. Deformation analysis of the Doesen rockglacier (Austrian Alps, Europe). Lewkovicz, A. G. & Allard, M. (eds.) *7th International Conference on Permafrost (Yellowknife, 23–27 June 1998)*, Collection Nordicana 57, 551–556. Centre d'Études Nordiques, Université Laval, Québec.

Keller, F. & Gubler, H. U. 1993. Interaction between snow cover and high mountain permafrost, Murtèl-Corvatsch, Swiss Alps. *Sixth International Conference on Permafrost, Proceedings*, 332–337. South China University of Technology Press, Beijing.

Kerschner, H. 1983. Lateglacial paleotemperatures and paleoprecipitation as derived from permafrost-glacier relationships in the Tyrolean Alps, Austria. *Fourth International Permafrost Conference, Proceedings*, 589–594. National Academy Press, Washington D.C.

Kerschner, H. 1985. Quantitative paleoclimatic inferences from lateglacial snowline, timberline and rockglacier data, Tyrolean Alps, Austria. *Zeitschrift für Gletscherkunde und Glazialgeologie* 21, 363–369.

Kerschner, H., Kaser, G. & Sailer, R. 2000. Alpine Younger Dryas glaciers as palaeo-precipitation gauges. *Annals of Glaciology* 31, 80–84.

Konrad, S. K., Humphrey, N. F., Steig, E. J., Clark, D. H., Potter, N. Jr & Pfeffer, W. T. 1999. Rockglacier dynamics and paleoclimatic implications. *Geology* 27:12, 1131–1134.

Maisch, M. 1992. Die Gletscher Graubündens: Rekonstruktionen und Auswertung der Gletscher und deren Veränderungen seit dem Hochstand von 1850 im Gebiet der östlichen Schweizer Alpen (Bündnerland und angrenzende Regionen). Department of Geography, University of Zurich. *Physische Geographie* 33A/B. 324 pp./128 pp.

Maisch, M. 1995. Gletscherschwundphasen im Zeitraum des ausgehenden Spätglazials (Egesen-Stadium) und seit dem Hochstand von 1850, sowie Prognosen zum künftigen Eisrückgang in den Alpen. In *Gletscher im ständigen Wandel*, Jubiläums-Symposium der Schweizerischen Gletscherkommission 1993 Verbier (VS), *Publikationen der SANW/ASSN* 6, 47–63. vdf-Hochschulverlag, Zurich.

Mittaz, C., Hoelzle, M. & Haeberli, W. 2000. First results and interpretation of energy-flux measurements of Alpine permafrost. *Annals of Glaciology* 31, 275–280.

NFP31. 1998. *Glaziologische Karte Julier-Bernina (Oberengadin)*. Synthesekarte, Publikation im Rahmen des Nationalen Forschungsprogrammes 'Klimaänderungen und Naturkatastrophen' NFP 31. vdf-Hochschulverlag, Zurich.

Renssen, H., Isarin, R. F. B., Vandenberghe, J., Lautenschlager, M. & Schlese, U. 2000. Permafrost as a critical factor in paleoclimate modeling: the Younger Dryas case in Europe. *Earth and Planetary Science Letters* 176, 1–5.

Sailer, R. & Kerschner, H. 1998. Equilibrium line altitudes and rockglaciers in the Ferwall-Group (western Tyrol, Austria) during the Younger Dryas cooling event. *Annals of Glaciology* 28, 141–145.

Schwarb, M., Frei, C., Schär, C. & Daly, C. 2000. Mean annual precipitation throughout the European Alps 1971–1990. *Hydrological Atlas of Switzerland*, Plate 2.6.

Suter, J. 1981. Gletschergeschichte des Oberengadins: Untersuchung von Gletscherschwankungen in der Err-Julier-Gruppe. *Physische Geographie* 2. 147 pp.

White, S. E. 1971. Rockglacier studies in the Colorado Front Range, 1961 to 1968. *Arctic and Alpine Research* 3, 43–64.